SR00-260-6

THE UNIVERSITY OF MICHIGAN

COLLEGE OF ENGINEERING
Department of Mechanical Engineering
Heat Transfer Laboratory

Final Technical Report

LOW HEAT-FLUX BOILING OUTSIDE VERTICAL AND HORIZONTAL TUBES

John A. Clark
Herman Merte, Jr.
William C. Elrod
Edward R. Lady

ORA Project 04653

under contract with:

U. S. ATOMIC ENERGY COMMISSION
SAVANNAH RIVER OPERATIONS OFFICE
CONTRACT NO. AT(38-1)-260
AIKEN, SOUTH CAROLINA

administered through:

OFFICE OF RESEARCH ADMINISTRATION ANN ARBOR

March 1965

This report was also a dissertation submitted by the third author in partial fulfillment of the requirements for the degree of Doctor of Philosophy in The University of Michigan, 1965.

ACKNOWLEDGMENTS

The authors wish to express their appreciation to Professors Joseph E. Shigley and Richard E. Balzhiser for their interest and cooperation in serving as members of the Doctoral Thesis Advisory Committee.

The contribution of Professor Wen-Jei Yang in performing a literature survey for this research program is gratefully acknowledged. Sincere appreciation is expressed for the untiring assistance of Mr. Ying S. Kao in the experimental effort, the assistance of Mr. Jaring Vander Veen in design and Mr. Thomas Mackey in construction, and the excellent work of Mr. Frank Kartje in the fabrication of components and in operation and maintenance of the low heat flux boiling system.

Grateful acknowledgment is made for the sincere interest and valuable assistance of Mr. Robert H. Renshaw, technical monitor of this research program for the Atomic Energy Commission Limited of Canada. Gratitude is extended to Mr. Al Bancroft of the Atomic Energy Commission Limited for assistance in handling water chemistry problems.

The support provided by Mr. H. A. Pearson of the Melrath Pump Company in solving a difficult pumping problem is appreciated.

This research program was supported by the United States Atomic Energy Commission under Contract AT(38-1)-260.

TABLE OF CONTENTS

TABLE OF CONTENTS (Continued)

TABLE OF CONTENTS (Concluded)

LIST OF TABLES

LIST OF FIGURES

LIST OF FIGURES (Continued)

LIST OF FIGURES (Continued)

LIST OF FIGURES (Continued)

LIST OF FIGURES (Continued)

LIST OF FIGURES (Concluded)

NOMENCLATURE

Other nomenclature is defined locally as necessary.

A	heat transfer area, ft^2
C_p	specific heat, Btu/lbm-^oF
C	constant
D	characteristic diameter, ft
g	gravitational acceleration, ft/sec^2
Gr	Grashof number, $\frac{\rho^2 g\beta \Delta T D_o^3}{\mu^2}$ or $\frac{\rho^2 g\beta \Delta T x^3}{\mu^2}$
G	mass velocity, ρV, $lb/hr\text{-}ft^2$
h	heat transfer coefficient, Btu/hr-ft^2-^oF
$\bar{h}_c$	average convection heat transfer coefficient, Btu/hr-ft^2-^oF
i	electrical current per unit area, amp/ft^2
I	total current, amp
k	thermal conductivity, Btu/hr-ft-^oF
N	number of bubbles
n	exponent
Nu	Nusselt number, $\frac{hD}{k}$ or $\frac{hx}{k}$
PPB	parts per billion
p	pressure, lbf/ft^2 or $lbf/in.^2$, as specified
Pr	Prandtl number, $\frac{C_p \mu}{k}$

q	rate of heat transfer, Btu/hr
Re	Reynolds number, $\frac{D_o G}{\mu}$ or $\frac{V_\infty x}{\mu}$
r	tube radius, ft
T	temperature, ^oF
TC	thermocouple
T	temperature difference, ^oF
V	velocity
μ	viscosity, lbm/hr-ft
ρ	density, lbm/ft^3
ρe	electrical resistivity, ohm-cm or ohm-ft, as specified
ν	kinematic viscosity, μ/ρ, ft^2/sec
β	temperature coefficient of volume expansion, $1/^oF$

Subscripts

b	boiling
B	bulk water
c	convection or critical
i	inside
o	outside
sat	saturation
w	wall = heating surface
∞	symbol for infinity

ABSTRACT

An investigation was made of the heat transfer from the outside surface of single 3/4 in. diameter tube to high purity saturated water in the pressure range from 535 to 1550 psia. Heat transfer characteristics were examined under natural convection conditions and at a velocity of 4.7 ft/sec with the tube oriented horizontally (in cross flow) and vertically (with flow parallel to the axis). The heat flux range of interest extends from the non-boiling region through incipient boiling to a low heat flux in the nucleate boiling region. Three commercial heat exchanger tube materials were considered to examine the effects of variation of material properties and surface condition on the boiling characteristic curve.

It is shown that close control of water chemistry is required to assure attainment of reproducible boiling data in the pressure range of this investigation. The dissolved oxygen content and level of suspended solid material in the boiling fluid are important parameters which must be maintained as nearly zero as practicable. The water pH does not have a direct effect on the boiling heat transfer characteristics but is important, especially in ferrous metal systems, in the control of oxidation.

Non-boiling forced convection heat transfer from the outside surface of horizontal tubes to high pressure saturated water are correlated by the generally accepted equation for flow normal to a cylinder. For flow parallel with a vertical tube the equation for heat transfer from a flat plate may be used. In this study of the vertical tube the heat transfer coefficient did not vary with axial position since fully developed turbulent flow conditions existed. Natural convection non-boiling data may be represented by an equation of the following type:

$$Nu = C\,(Gr\ Pr)^{\frac{1}{4}}$$

The value of the constant C required in this equation for heat transfer to high pressure saturated water is approximately four times that reported by other investigators for studies at atmospheric pressure.

Equations given which represent the natural convection nucleate boiling data obtained are of the form:

$$q/A = f(P)\,(T_w - T_{sat})^n$$

The coefficients, f(P), and exponents, n, of these equations are affected by the pressure, tube material and tube orientation.

It is concluded that the non-boiling heat transfer characteristics are independent of material properties and for forced convection conditions may be predicted by generally accepted correlation equations. Incipient boiling points and nucleate boiling heat transfer are affected by pressure, velocity, tube orientation, and tube material. The more corrosion resistant materials support higher surface superheat without boiling than do those more susceptible to corrosion. In the nucleate boiling region the variation of $T_o - T_{sat}$ for Monel, Inconel, and carbon steel is small at a given heat flux but the slope of the characteristic curve is so steep that a large variation in heat flux results at a given value of $T_o - T_{sat}$. Hence, a single boiling characteristic curve cannot be used to represent the nucleate boiling region for various materials under the conditions of this investigation without introducing large error.

This is the final report on the University of Michigan ORA Project 04653. A complete description of the experimental apparatus and procedure is included. The results given herein for a horizontal Monel tube supersede those reported previously in Ref. 50.

I. INTRODUCTION

A. PURPOSE

In recent years great emphasis has been placed on boiling heat transfer since the very large heat flux which can be realized is of primary importance in the operation of nuclear reactors and in cooling large rocket engine nozzles. The major interest and effort has been placed on investigation of heat transfer at very high values of heat flux. This is not unexpected in view of the severe cooling problems in the applications cited. The conditions which lead to failure of the heat transfer surface must be well known in order to avoid catastrophe. Advancements in the performance of these systems depend to a large measure on the development of suitable materials to withstand the operating conditions. However, from a thorough understanding of the heat transfer processes involved, the material requirements may be more fully understood and made less severe.

The economical factors of initial cost and cost of operation must be considered also. In the pressurized water reactor which utilizes a primary reactor coolant loop and a secondary power generation loop, the amount of energy transferred per pound of water in the primary loop may be relatively small. A thorough knowledge of all boiling heat transfer phenomena up to the burnout point is necessary to effect

the most economical design of the primary loop to secondary loop heat exchanger within the limits of operational safety requirements.

The purpose of this investigation is to study heat transfer to saturated, pressurized water at low heat flux in the regime from non-boiling through incipient boiling to low values of boiling heat flux. The pressure range of interest is 535 to 1550 psia. The range of heat flux covered is from 100 to 100,000 Btu/hr-ft^2. Boiling of distilled, degassed and deionized water takes place on the outside surface of a horizontal or vertical tube immersed in a pool of water. Tube materials include Monel, Inconel, and carbon steel. Attention is given to the control of pH, electrical resistivity, dissolved oxygen content and quantity of suspended solids in the boiling medium. The study considers saturated pool boiling and boiling with forced convection at a velocity of 4.7 ft/sec.

The heat transfer regime of interest in this study can best be illustrated by reference to a typical boiling curve, Fig. 1. The curve is divided into regions which result from differences in the heat transfer phenomena that occur as the level of heat flux or temperature difference is varied. The location of the curve may shift for various liquids and for a given liquid is affected by pressure, velocity, boiling surface condition, orientation, dissolved gases in the liquid, and various additives which affect the surface tension of the liquid at the heated surface, among others. It is found in this research that the

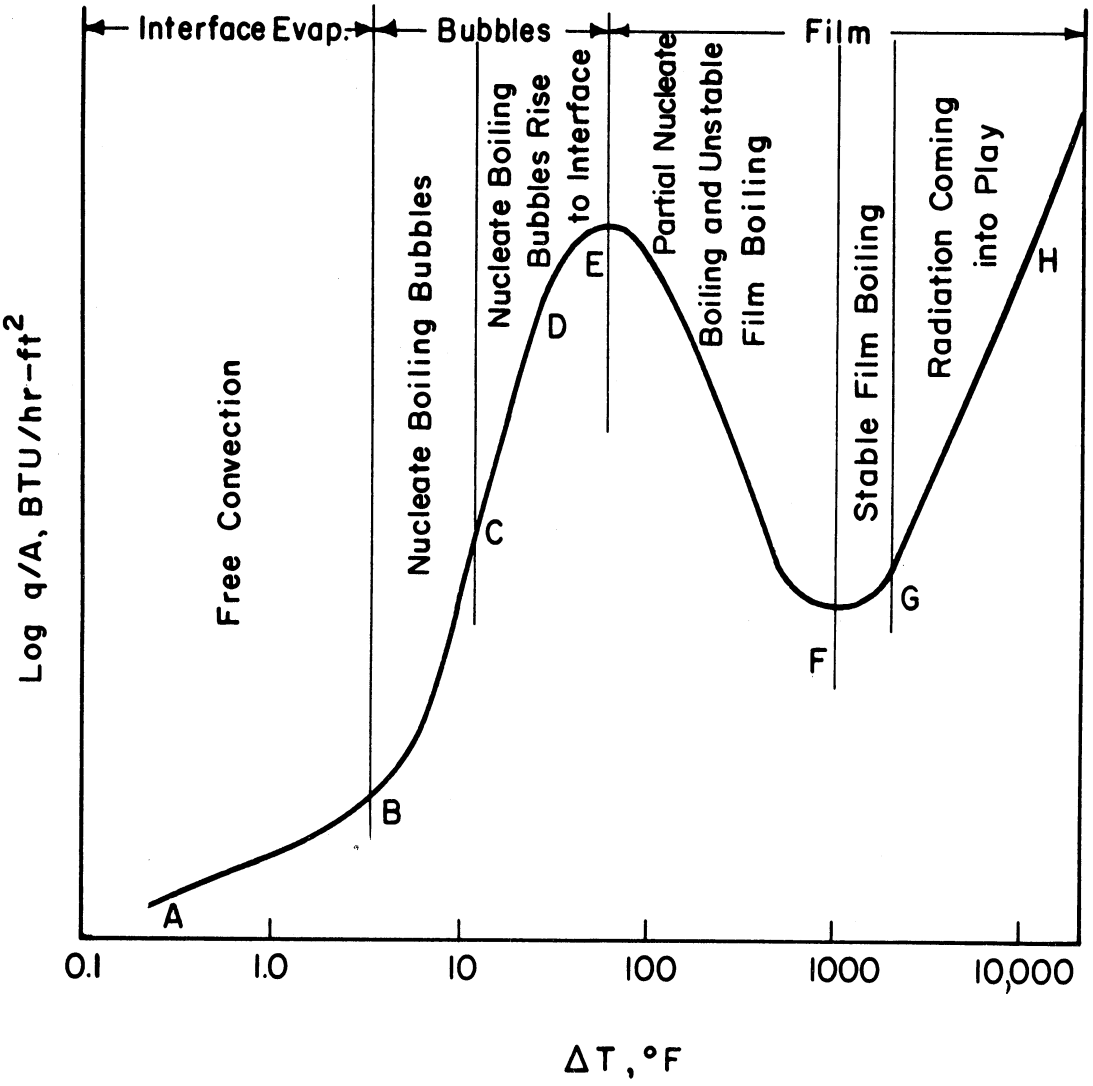

Fig. 1. Typical boiling-characteristic curve.

amount of suspended solids in the liquid also affects the boiling characteristic. However, the general shape of the curve and characteristics of boiling are similar for all liquids.

The region from A to B represents heat transfer without boiling. Inasmuch as the liquid is considered to be saturated, heat transfer to the liquid increases the temperature above the saturation temperature and results in superheated liquid. The warmer, less dense liquid rises from the hot surface to the liquid-vapor interface where evaporation takes place. In a pure liquid no bubbles appear in the region.

The appearance of bubbles marks the second major region of the boiling characteristic curve. This is shown as the portion of the curve from B to E. This may be subdivided into three sections which are labeled B-C, C-D, and D-E. The region from B to C is distinguished by small bubbles on the hot surface, which grow from discrete sites or nuclei and then collapse as heat is transferred from them to the bulk of the liquid. As the temperature of the hot surface is increased, the bubbles are detached from the heated surface and rise to the liquid-vapor interface. With increasing temperature difference more and more nucleation sites are activated, resulting in a very rapid increase in the heat flux. This portion of the curve is nearly a straight line and is labeled C-D. Point D is sometimes referred to as the point of departure from nucleate boiling (DNB). As the

temperature difference increases beyond point D the heat flux increases less steeply, as shown by the portion of the curve from D to E. This change in slope may be due to interference between the bubbles. This interference increases until the peak heat flux in nucleate boiling, point E, is reached. This is known as the "burnout point" or point of maximum heat flux because an increase in heat flux causes a large increase in the temperature difference (from E to H) which will probably cause the melting of the surface.

At temperature differences greater than that at point E, the physical appearance again changes. With electrical resistance heating the EFGH portion of the curve is difficult to obtain due to the step change E to H described above. It is readily obtained if the surface is heated by a condensing vapor. In the region from E to F the heat transfer surface is in transition from nucleate boiling to film boiling. Both nucleate boiling and film boiling are observed. The film boiling is unstable with patches of vapor appearing and disappearing in random fashion over the heated surface. The patches of film insulate the heating surface and as the ΔT is increased a decrease in heat flux results. At higher values of ΔT, the amount of heating surface affected by film patches is greater. At point F stable film boiling is observed with the entire heating surface covered by a film of vapor. From F to G, heat is transferred primarily by conduction and convection through the vapor film and as the ΔT is increased the

heat flux again rises. At point G with the temperature about 1000°F, radiation begins to have pronounced effect. The slope of the curve becomes steeper with rising ΔT until the point at which failure of the heat transfer surface is reached.

This study is concerned with the non-boiling and nucleate boiling characteristics of the boiling process in the region of the point of incipient boiling. The effects of water chemistry including pH, dissolved oxygen content, electrical resistivity and amount of suspended solids in the boiling medium are considered.

B. LITERATURE REVIEW

In boiling heat transfer research considerable attention has been given to the effects on the heat transfer coefficient produced by variation of pressure, surface roughness, surface contamination, dissolved gases, and additives to promote wetting the surface. These and other factors were covered in a literature survey by Clark et al.[1,2] A brief review of previous work pertinent to this investigation is given here.

It has been generally established that nucleation takes place from small pits and scratches in a heated surface. However, a large amount of scatter exists in the data from different sources and differences of opinion exist concerning the conditions necessary for nucleation from solid surfaces. Bankoff[3] suggests that ebullition

proceeds from small quantities of vapor or gas trapped in cavities in the solid surface. It is probable that even with the most rigorous precautions to remove entrapped gas, some will remain for nucleation sites. In a paper on the fracture of liquids, Fisher[4] states that no finite pressure can force liquid all the way to the top of a sharp apex cone, thus a nucleation source remains. Mead, Romie and Guibert[5] indicate that air entrapped in surface crevices markedly decreases the degree of liquid superheat attainable at a liquid-solid interface.

Corty and Faust[6] investigated the nucleate boiling of ethyl ether and n-pentane on horizontal nickel and copper surfaces with varying degree of roughness. They found that a very high value of liquid superheat could be attained when increasing the heat flux from a low value. When boiling started, the superheat reduced to the normal value for nucleate boiling for that heat flux. Curve abed of Fig. 2 illustrates this phenomenon. Bubbling started at a random point and spread concentrically around the point. As the heat flux was decreased from a high value, the nucleation sites diminished in activity then disappeared forming a hysteresis abedcdb. The hysteresis was established again on immediately repeating the cycle but with less initial superheat as shown by curve abfcdb. Nucleation sites which were recently active are easily reactivated indicating the superheat required to activate sites for the second cycle was not as great as that for the first. The last remaining nuclei on decreasing heat flux were

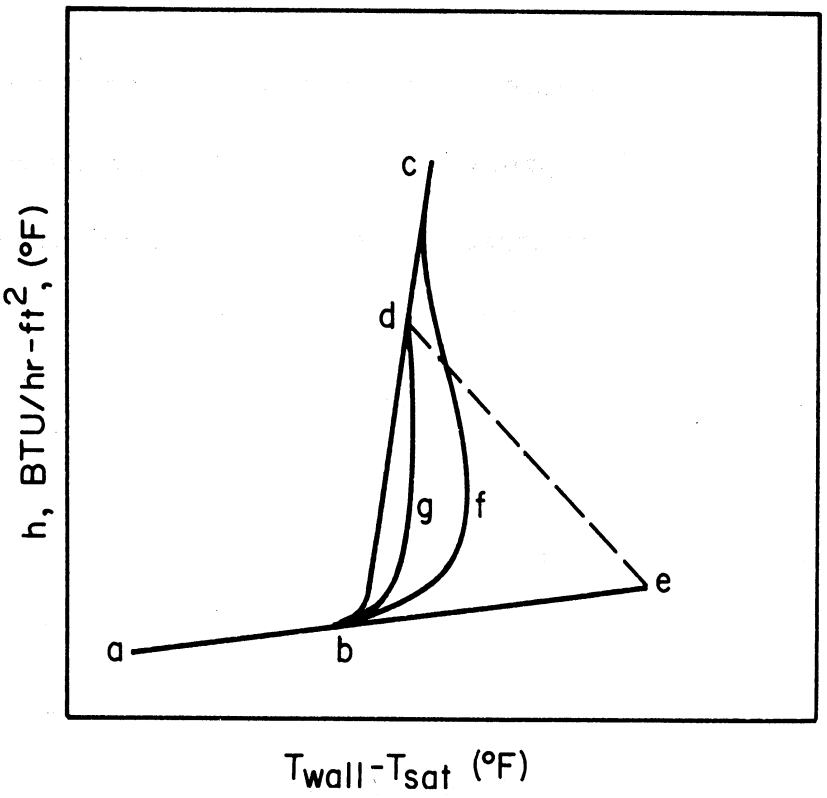

Fig. 2. Hysteresis effect in nucleate boiling.

the first to be reactivated if the heat input was immediately increased. On further increase of heat flux, these sites became centers for patches of nucleate boiling. At about 40,000 Btu/hr-ft^2 the surface was again completely covered with bubbles and the hysteresis effect vanished. It was observed that the surface temperature of the patch boiling area was considerably lower than that of the bare surface. Griffith and Wallis[7] also found that the mean surface temperature is not equal to the temperature of an active cavity. They conclude that the wall superheat at which nucleation will begin at a pre-existing gas filled cavity is fixed by surface tension and other known fluid properties.

Lady[8] also observed the hysteresis effect in nucleate boiling on the outside surface of a horizontal tube at 535-1550 psia but its nature was somewhat different. Starting at a low heat flux and increasing the heat input, a higher ΔT at a given heat flux was required when increasing the heat input than was obtained when it was decreased. For a cycle starting at high heat flux to low flux and back to the starting value only a slight hysteresis was observed. However, if the heat input was shut-off and then restarted the hysteresis returned approximately to the one established on initial start-up. Large values of superheat were not obtained.

In a photographic study of nucleation sites, Clark, Strenge, and Westwater[9] determined that pits and scratches are effective sites.

Pits are more effective than scratches since the scratches are more easily flooded. The size of active pits observed ranged from 0.0003 to 0.003 in. diameter.

Attempts have been made to establish a relation between the number of active nucleation sites and the heat flux by several investigators. Jakob[10] counted two active sites per square inch at a heat flux of 18,000 Btu/hr-ft^2 and concluded that a linear relationship exists between the heat flux and the number of sites. For boiling water on a smooth brass surface, Nishikawa, et al.[11] counted up to eight active sites per square inch at a value of heat flux up to 13,600 Btu/hr-ft^2. They found that $h \sim (N/A)^{1/3}$ and that this relation was not affected by surface contamination, surface-active agents, dissolved salts, or degree of surface roughness. Kurihara and Meyers[12] counted up to 28 active sites per square inch at heat flux up to 19,000 Btu/hr-ft^2. They verified Nishikawa's relationship and stated that neither nature of fluid nor degree of microroughness affect the relationship. Corty and Faust[6] counted up to 60 active sites per square inch for pentane boiling on nickel at a heat flux up to 25,000 Btu/hr-ft^2.

All the preceding studies involved a visual count of the number of active sites and were necessarily limited to low values of heat flux. Gaertner and Westwater[13] counted active sites after plating a thin layer of nickel on a copper plate while boiling from the copper surface. The heat flux range extended from 7,680 to 535,000 Btu/hr-ft^2 and

the ΔT from 17.3 to 218°F. The number of sites ranged from zero to a maximum of 1130 at 317,000 Btu/hr-ft^2. The boiling liquid was an aqueous solution of nickel salts containing 20% solids.

The present investigation shows an influence of suspended solids on the position of the heat flux versus ΔT curve. It is possible that the suspended solids may have affected the number of active sites during the plating process investigated by Gaertner and Westwater.

When ebullition begins the slope of the heat flux versus ΔT curve becomes much greater than for the non-boiling regime. Thus for a small increment in the difference between the wall temperature and water saturation temperature there is a large change in the heat flux. Very large values of heat flux are thus attainable with nucleate boiling at modest temperatures.

An investigation was made of the energy transferred from a heated surface to water in the form of latent heat in bubbles by Rohsenow and Clark.[15] It was found that the amount of energy transferred to the colder water by condensing bubbles is negligible. They state that the bubbles act as agitators which cause violent agitation of the quiescent layers of liquid adjacent to the heated surface. This violent motion in the superheated liquid at the heated surface is said to be responsible for the very high rate of heat flux attainable in nucleate boiling. Other researchers, Jakob,[16] Chang and Snyder,[17]

Gunther and Kreith[18], agree that agitation caused by the bubbles effects a large increase in the rate of heat transfer.

Recent experiments by Moore and Mesler[19] and others indicate that latent heat transport in the region of low heat flux is more important than previously realized and should be considered as a significant part of the heat transfer mechanism. Rallis, et al.[20] found that the mean volume of the bubbles averaged over the entire surface remained constant, essentially independent of heat flux or average active site population, while the bubble frequency increased with heat flux. Moore and Messler attributed the high rate of heat transfer in nucleate boiling to evaporation of liquid at the heated surface and simultaneous condensation at the opposite side of the bubble in communication with the colder fluid.

A number of parameters influence the heat flux versus temperature difference curve in the nucleate boiling region. These include pressure, velocity, finely dispersed gas particles in the fluid, surface roughness and surface contamination. It is shown in the present investigation that another parameter, suspended solids, must also be considered.

Many investigators[8, 16, 22, 24, 37, 38] have obtained data which shows the effect of pressure on heat transfer with nucleate boiling. The effect of increased pressure is to reduce the temperature difference required at a given value of boiling heat flux. Correlations

for experimental heat transfer data are available which include a pressure dependent term. Jakob[16] recommends graphs developed by Cichelli and Bonilla[21] for alcohol, propane and water. For other substances Jakob recommended an equation by Insinger and Bliss[22] with empirical pressure factor.

Velocity has an appreciable effect on convection heat transfer. This is treated in any text which considers natural and forced convection heat transfer. Clark and Rohsenow[23] and Rohsenow[24] present data for boiling inside tubes. They indicate that the effect of velocity in nucleate boiling is small and disappears as the heat flux is increased. The vanishing point occurs at higher values of heat flux as the velocity is increased. Data are presented herein for very low values of heat flux for boiling saturated water on the outside of a tube which agrees with their finding. However, the value of heat flux at which velocity effect disappears is much lower than the data of Clark and Rohsenow. The difference is probably due to the high degree of subcooling of the liquid used in obtaining their data.

Surface condition can affect boiling heat transfer data significantly. Two situations are considered: roughness and contamination of the surface. Corty and Faust[6] investigated nucleate boiling with n-pentane and ethyl ether on nickel and copper surfaces with various degrees of roughness. The roughness was established by polishing the surface with emery cloth from grade 3 through 4/0. It was found

that as the surface roughness increased a lower temperature difference was required for a given value of heat flux in nucleate boiling. However, as the roughness was increased, a higher initial superheat was required to initiate ebullition. Jakob and Fritz[25] observed the effect of roughness on nucleate boiling. Surfaces were roughened by sand blasting which produced a rougher surface than investigated by Corty and Faust. For these surfaces the effect on boiling due to roughness decreased with time of emersion in water which had been thoroughly degassed by boiling. The effect returned upon subsequent exposure of the surface to air. Jakob[16] indicates that air adsorbed by the freshly roughened surface probably decreased during boiling and while exposed to thoroughly degassed water accounting for the change in heat transfer performance. On a smoother surface with smaller cavities for nucleation sites, the removal of trapped gas or vapor would not be as readily accomplished.

Contamination of the heated surface is recognized as an uncontrollable parameter. Researchers avoid conflict by insisting on a clean surface for establishing heat transfer characteristics for a given experimental setup. This has been acceptable for boiler design since the resistance to heat flow is much greater on the gas side than on the liquid side and errors in liquid side heat transfer coefficient have only a minor effect on the overall heat transfer performance. McAdams, et al.[26] present some data to show that surface

contamination results in an increase in the metal surface to water temperature difference at a given heat flux. A deposit on the surface forms an insulating layer which then causes the metal surface temperature to rise in order to maintain a given rate of heat transfer. Lady[8] presents data to show the effect on a heat transfer system with internal heat generation. A similar situation would occur for an insulating layer deposited on the fuel plates of a nuclear reactor. Cleanliness in the heat transfer fluid and close control of corrosion are necessary if surface contamination is to be avoided.

Foreign matter in the fluid may act as nucleation sites and reduce the temperature difference required for boiling at a given heat flux. Vigorous boiling for a period sufficient to reduce the gas content in the liquid to a desired low level is a practice common to all researchers. The gas content is usually measured by the level of dissolved oxygen present as determined by a Winkler technique. This technique is described in reference 27. An oxygen content in the range of 0.3 to 1 cc/liter (0.43 to 1.43 PPM) is normally accepted for adequate control of atmospheric gases. It is found in this research that this level is much too high for control of corrosion in ferrous metal systems and that more attention should be given to this factor.

Suspended solid material in the boiling liquid has not been investigated with respect to its effect on the nucleate boiling characteristics. King[28] mentioned the presence of dissolved gases or small

particles in the fluid among other factors which govern the superheating of a liquid prior to ebullition. Larson[29] noted the lack of information in this area and speculated that a suspended solid ebullator might have the same effect as a volatile component. In a photographic study of nucleation sites, Clark, Strenge and Westwater[9] observed a speck on the heated surface which supported nucleation momentarily and then disappeared. In the present study it has been determined that solid material even in very small amount has an effect on the nucleate boiling characteristics and should be considered if reproducible data are to be obtained.

II. EXPERIMENTAL APPARATUS AND INSTRUMENTATION

A. SUMMARY

The system utilized in this investigation was designed to study the boiling of distilled and degassified water external to round tubes. The design conditions are:

Heat flux:	0-400,000 Btu/hr-ft^2
Pressure:	500-2,000 psia
Saturation Temperature:	467-635°F
Velocity:	pool boiling to 5 ft/sec
Tube Orientation:	horizontal and vertical

The system was designed sufficiently large to accommodate small bundles of tubes, up to 5 in. in overall diameter oriented either horizontally or vertically. This size is adequate for a tube bundle of 13 tubes, 3/4 in. O.D. on a normal triangular pitch of 1.5 times the outside diameter.

In this study the following ranges of independent variables are investigated for a single tube:

Heat flux:	62 to 118,500 Btu/hr-ft^2
Pressure:	535-1550 psia
Velocity:	pool boiling to 4.7 ft/sec
Tube Orientation:	horizontal and vertical
Tube Material:	Monel, Inconel, carbon steel
Tube Diameter:	3/4 in. O.D.

The experimental apparatus consists of a stainless steel pressure vessel, 12-3/4 in. O.D. by 36 in. long in which the test section

(Monel, Inconel, or carbon steel tube) is placed in a horizontal or vertical plane. The tube is heated by the dissipation of direct current electrical energy. The vessel is partially filled with distilled water so that the tube is immersed to a depth of approximately 18 in. Means of heating the water, controlling the pressure, creating and measuring the flow of water upward parallel with or normal to the axis of the tube, deionizing, degassing and controlling the level of suspended solids and dissolved oxygen in the fluid are provided. These are discussed in detail in following sections.

The experimental apparatus is located in the Heat Transfer Laboratory of the Department of Mechanical Engineering of The University of Michigan. Facilities supplied by the laboratory include the following:

(1) 12 volt, 3,000 ampere direct current

(2) 460 volt, 3-phase, 60-cycle power--50 kw

(3) 110 volt, 1-phase, 60-cycle power--2 kw

(4) compressed air, 90 psig, 100 std cfm

(5) cooling water, 50 psig, 10 gal/min

A photograph of the experimental apparatus is shown in Fig. 3. This photograph was taken before thermal insulation was applied to the vessel and pipes which have elevated temperatures during operation.

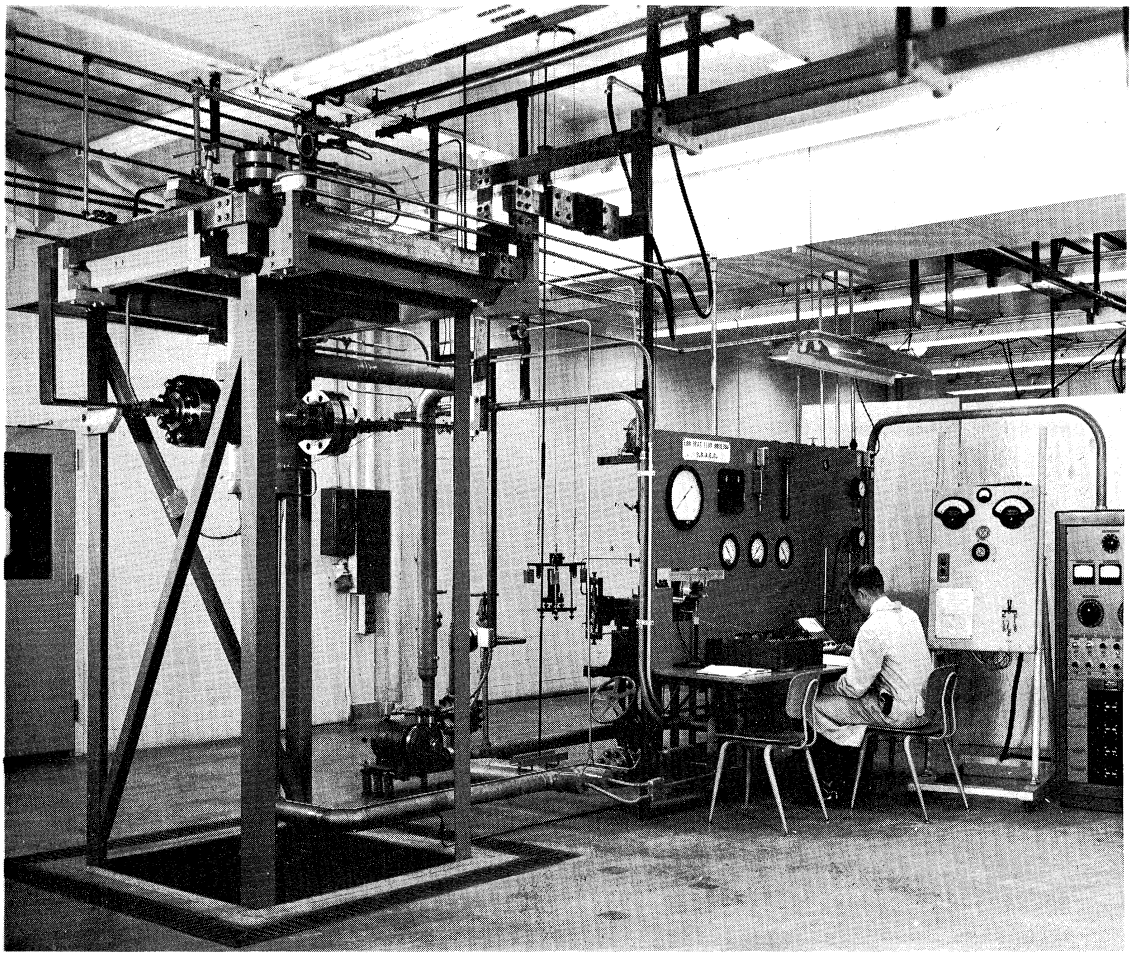

Fig. 3. Low heat flux boiling experimental apparatus.

B. TEST SECTION

The test section is a 7 in. long Monel, Inconel or carbon steel tube, nominally 3/4 in. O.D. by .049 in. wall, silver soldered to nickel and chrome plated copper electrodes which protrude through flanges of the stainless steel pressure vessel. Tables I, II, and III provide information on the tube materials used. The laboratory direct current power source is connected to the electrode just outside the vessel flanges as can be seen in Fig. 3. The electrode diameter is increased to 1 in. where it passes through the flanges in order to minimize the current density and resultant Joulean heating of the copper.

TABLE I

MONEL TEST SECTION SPECIFICATIONS

Supplier	Wolverine Tube Division Calumet and Hecla, Inc.	
A.S.T.M. Specification	B-163	
Physical Condition	Seamless, cold drawn, bright annealed	
Chemical Analysis (by supplier)	Nickel	64.2%
	Copper	33.0%
	Iron	1.44%
	Manganese	1.12%
	Silicon	.07%
Mechanical Properties (by supplier)	Tensile strength	81,000 psi
	Yield strength	47,400 psi
	Elongation, 2 in.	48%
	Hardness, Rockwell B	74-75

TABLE II

INCONEL TEST SECTION SPECIFICATIONS

Supplier	Huntington Alloy Products Division The International Nickel Company	
A.S.T.M. Specification	B-167-58T	
Physical Condition	Seamless, cold drawn, annealed, pickled, and ground	
Chemical Analysis (by supplier)	Nickel	76.53%
	Chromium	15.73%
	Iron	6.83%
	Copper	0.38%
	Silicon	0.25%
	Manganese	0.21%
	Carbon	0.04%
	Sulfur	0.007%
Mechanical Properties (typical data sheet values)	Tensile strength	80-100,000 psi
	Yield strength	30-50,000 psi
	Elongation, 2"	55-35%
	Hardness, Rockwell B	88 max

TABLE III

CARBON STEEL TEST SECTION SPECIFICATIONS

Supplier	The Michigan Seamless Tube Company	
A.S.T.M. Specification	A-106, Grade B	
Physical Condition	Seamless, cold drawn, annealed	
Chemical Analysis (by supplier)	Manganese	0.50%
	Carbon	0.24%
	Silicon	0.21%
	Sulfur	0.028%
	Phosphorous	0.011%
	Iron	Balance
Mechanical Properties (by supplier)	Tensile strength	70,400 psi
	Yield strength	46,700 psi
	Elongation, 2 in.	43.7%

A cross sectional view of the test section is shown in Fig. 4. Temperature measurements of the inside adiabatic wall are made by 12 chromel-constantan thermocouples, 30 gauge, with glass and high temperature varnish insulation. In the drawing only six thermocouples are shown. At each of the positions shown there are four thermocouples, oriented at 0^{o}, 90^{o}, 180^{o}, and 270^{o}. This provides a measure of the variations in temperature in the circumferential direction. A sheet of mica of 0.003 in. thickness is inserted in the tube before the thermocouple assembly is installed. This provides electrical insulation of the thermocouples from the test section, thereby eliminating the problem of direct current pickup in the thermocouple emf measurement. The resistance between the thermocouple and the tube exceeds one megohm. Each thermocouple junction is silver soldered and held in position by a ceramic bead fastened by cement to an Inconel spring. This spring forces each thermocouple junction against the mica sheet with a force of about 1 lb. The 12 pairs of thermocouple leads pass from the test section through an axial hole, 1/4 in. diam. in one end of the copper electrode.

The electrode must be electrically insulated from the test vessel at the gland through the flange. A special stuffing box was designed to utilize high temperature steam packing which is electrically non-conducting. The packing arrangement consists of alternate layers of Garlock 900 asbestos sheet packing and John Crane Superseal 4-J

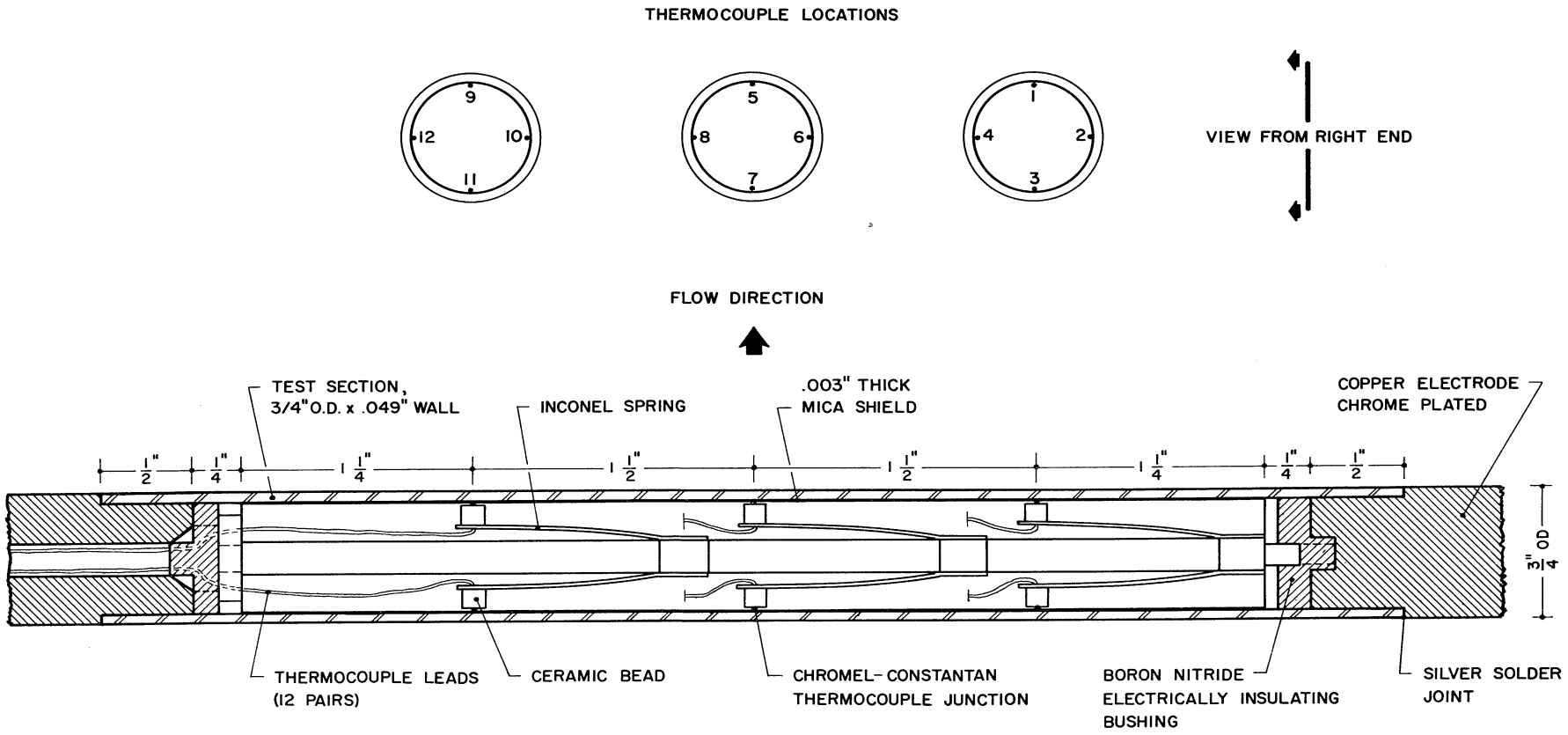

Fig. 4. Test section.

braided asbestos, mica lubricated packing. The sheet packing is machined into the solid rings 1-5/8 in. O. D. by 1 in. I. D. by 1/4 in. thick. These rings center the electrode in the gland and resist extrusion of the softer braided packing. The braided packing is supplied in a continuous roll, 5/16 in. square in cross section. Single rings with overlapping beveled ends are formed and placed between the layers of sheet packing. The softer braided packing makes the seal pressure tight. A stainless steel gland is used to tighten the packing initially and while in service. The gland has a larger than normal inside diameter in order to avoid accidental short circuiting of the electrode. The gland is tightened by a follower plate which is pulled by three studs fastened to the vessel flange. The electrical resistance between the electrode and the vessel is about 10,000 ohms without water in the vessel. The resistance is approximately 100 ohms when the vessel is filled with water to the normal operating level. Since the vessel is grounded and the maximum voltage on the electrode is about 1.5 volts above ground, the current leakage to ground is 0.015 ampere. This is negligibly small compared to the electrode current of 28 to 2500 amperes.

C. TEST VESSEL

The boiling studies are carried out in a test vessel, designed and fabricated in accordance with the ASME Pressure Vessel Code,

Section VIII. The maximum working conditions are 2,000 psig and 650°F. The shell consists of 1 in. thick, type 347 stainless steel, ASME Specification A 312 T 347. Its length is 38 in. and the outside diameter is 12-3/4 in. The heads are flat T 347 forgings, 4 in. thick. The vessel is oriented with its axis vertical and is supported approximately 8 ft above the floor by two lugs bolted to a structural steel framework.

Cross sectional views of the test vessel and its assembled components are shown in Figs. 5 and 6. The horizontal test section, Fig. 5, or vertical test section, Fig. 6, is held in the center of the vessel by the electrodes, which in turn are held rigidly in place by the electrically insulated packing gland. All flanges are type 347 stainless steel, 1500 lb ring joint type, with a welding neck connection.

The free surface of the water, about 18 in. above the test section, is shown in the figures. Above the free surface is a steam space. All air is vented from the steam space by vigorous boiling of the water for 2 hr prior to each series of runs. During this time the pressure is held to about 30 psig and a continuous venting of steam and air is permitted. Steam passes out of the test vessel to the condenser and the condensate is returned by gravity flow counter-current to the steam. The steam space temperature and bulk water temperature are measured by calibrated chromel-constantan thermocouples encased in stainless steel sheaths.

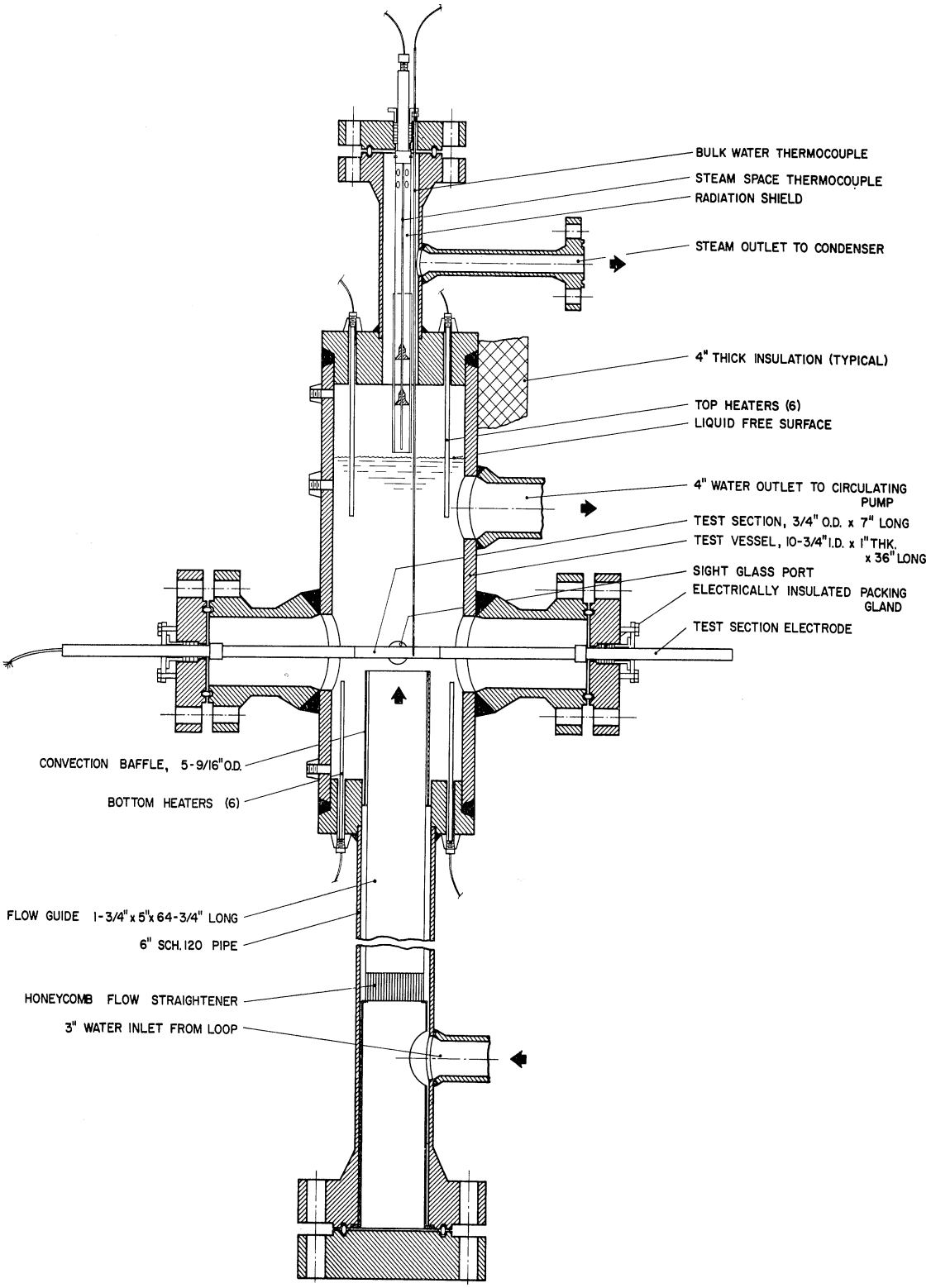

Fig. 5. Test vessel assembly, horizontal test section.

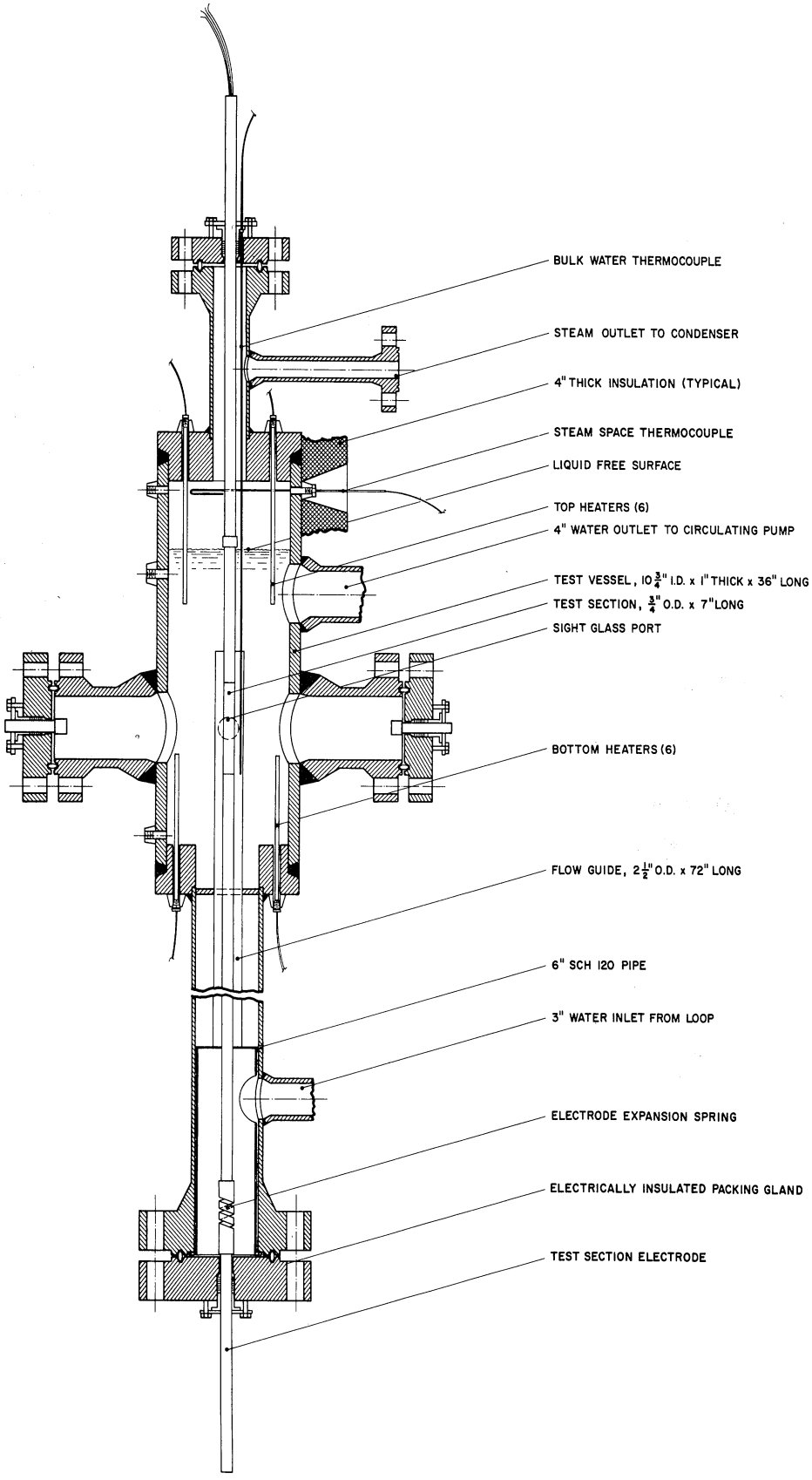

Fig. 6. Test vessel assembly, vertical test section.

Forced convection of water upward parallel with or normal to the test section is caused by a circulating pump which is mounted in the main flow loop external to the test vessel. Water from the vessel is conducted to the pump suction by a 4 in. schedule 80 outlet pipe. The water is returned through a 3 in. schedule 80 pipe and enters a 6 in. schedule 120 pipe 13 in. above the bottom flange. Inside the 6 in. pipe is a stainless steel flow guide. Baffles prevent water from flowing upward between the inside wall of the 6 in. pipe and the flow guide. The effect of the flow guide is to provide a fully developed turbulent flow profile 1 in. in front of the test section. The maximum average velocity in the flow guide is approximately 5 ft/sec for the forced convection tests with a horizontal test section and 10 ft/sec with a vertical test section.

The water in the test vessel is brought up to and maintained at the required test temperature by 12 immersion heaters which are threaded into fittings on the top and bottom heads. The six bottom heaters are rated at 650 watts each at 230 volts. The six top heaters are rated at 1000 watts each at 230 volts, with all of the resistance heating wire being concentrated in the 3 in. length at the end away from the threaded fitting. The ends of the top heaters are always immersed below the water surface, thus insuring adequate heat removal from the top immersion heaters. Each set of six heaters is wired in three phase, delta connection to the 460 volt supply, with

two heaters being in series on each leg of the connection. The immersion heaters have an Inconel sheath. They are supplied by the Watlow Manufacturing Company.

The liquid level in the test vessel is measured by a Minneapolis-Honeywell indicating bellows meter, rated at 2500 psi static pressure with a full scale range of 0-25 in. water. The pressure connections are shown at the left side of the vessel in Figs. 5 and 6. The connection immediately below the top head is connected to the high pressure side of the meter because this leg of the pressure transmitting line is always filled with liquid due to condensation. The connection immediately above the bottom head is connected to the low pressure side of the meter. The meter was calibrated against a U-tube manometer at atmospheric pressure and found to indicate well within the specified accuracy of $\pm$ 1-1/4% full scale.

A low level shut-down switch is incorporated as a safety feature. A well is inserted in the connection shown in Figs. 5 and 6, somewhat below the liquid free surface. Into this well is inserted a 3/8 in. diam heater, rated at 130 watts and 80 volts. Also in the well and adjacent to the heater is a thermocouple which generates an emf in opposition to another thermocouple positioned in the water. The differential emf is sensed by a sensitive relay manufactured by Assembly Products, Inc. If the differential emf exceeds 5 millivolts, the relay shuts off all power to the system. Due to the high heat

transfer coefficient between a heated surface and boiling water, the temperature of the well remains nearly that of the boiling water and of the steam. If the water level drops and the well is exposed to steam, the temperature rises due to the lower heat transfer coefficient. This in turn actuates the safety shut-down. The low level shut-down has a time lag of approximately 1 min when the liquid level falls below the well.

The test vessel and the 6 in. inlet section were covered with 4 in. of calcium silicate insulation. The piping loop was covered with a 2 in. layer of the same material. Flanges were covered by 2 in. thick molded Fiberglas sections held by insulation straps. This provides ready access to the flange studs and nuts. The insulated vessel and piping are shown in Fig. 7.

D. SYSTEM FLOW CIRCUITS

The test vessel is connected with three circuits which serve the functions of providing the circulation necessary for forced convection studies, of maintaining the water at a specified purity, and of controlling the pressure. The complete flow diagram is shown in Fig. 8. Referring to the figure, the test section (2) is shown in the test vessel (1) on the left. These items have been described in previous sections. The remainder of the system will be described in the following sub-sections:

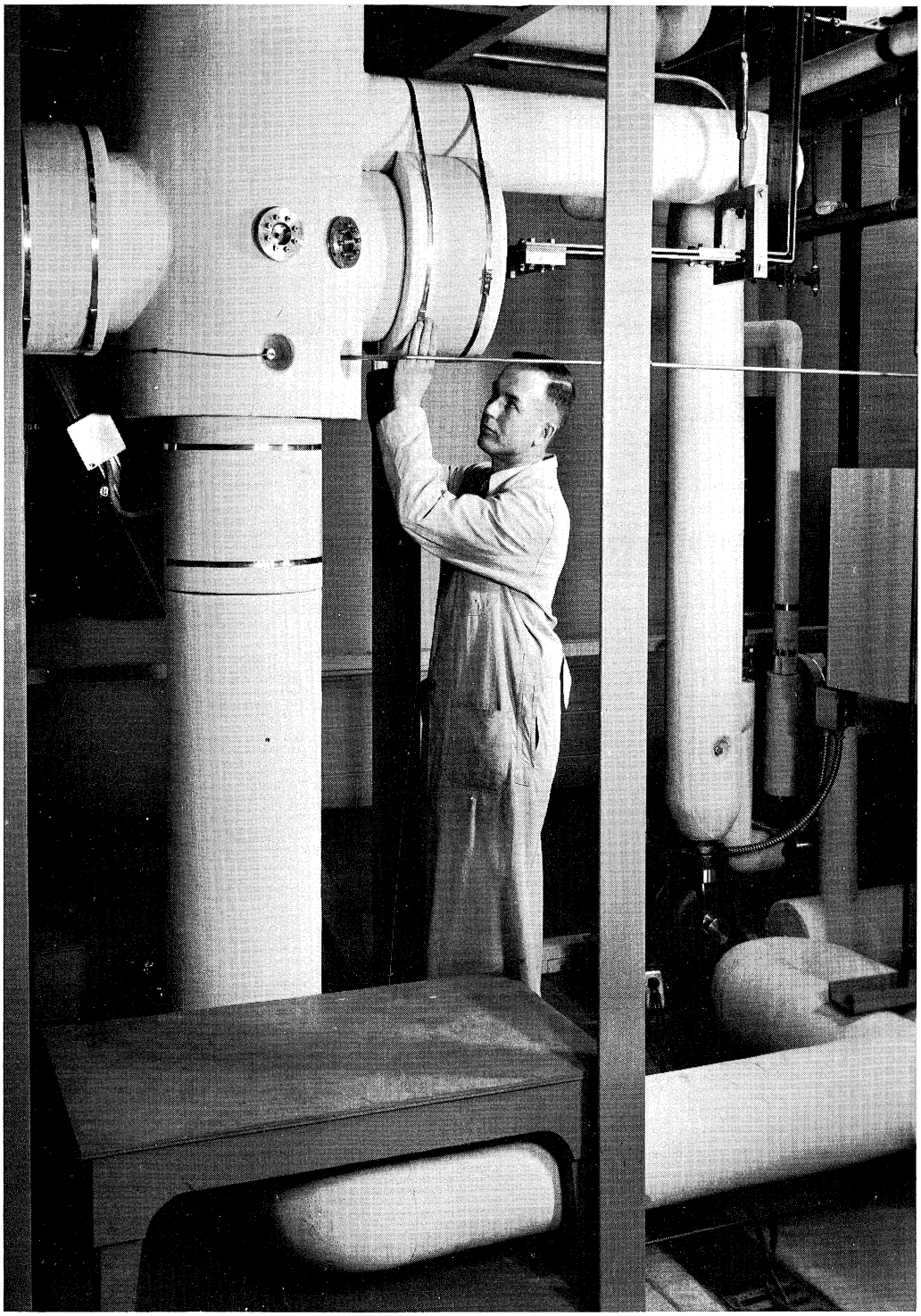

Fig. 7. Insulated vessel and piping.

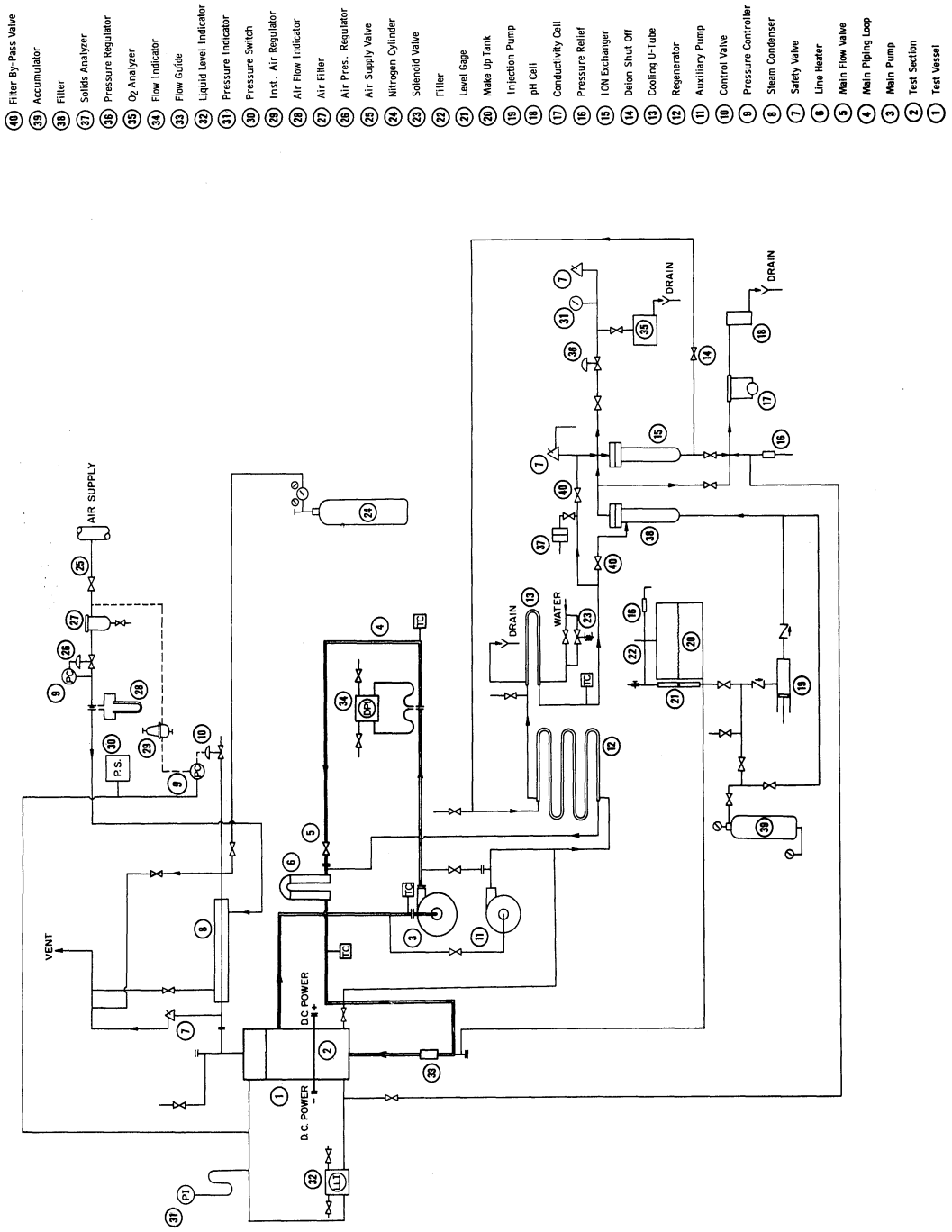

Fig. 8. System flow diagram.

1. Primary Flow Loop

The primary flow loop (4) consists of a 4 in. schedule 80 stainless steel pipe leading from the upper portion of the test vessel to a circulating pump, whence it flows in 3 in. schedule 80 stainless steel pipe through the flow metering section, the control valve, heater, and back to the inlet at the bottom of the test vessel. The range of velocities normal to a horizontal test section which can be achieved is from 0 to 5 ft/sec, the range parallel to a vertical test section is from 0 to 10 ft/sec.

a. Circulating Pump.--The circulating pump (3) is supplied by Melrath Canned Pumps, Inc. to the following specifications:

Capacity - 140 gal/min water
Discharge head - 40 ft
Net positive suction head - 4 ft
Static pressure - 2000 psig
Materials - All wetted parts of 300 series stainless steel
Drive - Direct connected electric motor
Power - 440 volts, 60-cycle, 3-phase

The most stringent requirements which this pump must meet are the pressure and temperature associated with boiling water at 2000 psig and the very low available net positive suction head (NPSH). The static head on the pump is approximately 7 ft. Due to the flow resistance of the suction piping, the NPSH is less than the 7 ft available due to elevation of the free surface above the pump. Since it is not feasible to increase the available NPSH by cooling the water as it

flows to the pump, due to the very large heat exchange requirements, the pump must operate at the low value of 4 ft NPSH. The circulating pump performs this service as specified. It was found that with circulation at atmospheric pressure the pump becomes quite noisy at about 200°F, apparently due to cavitation. This noise disappears at lower flow rates and at a pressure of about 30 psig. However, another noise of a similar nature is encountered in the pressure range from 60 to 120 psig. To avoid these problems the auxiliary circulating pump (11) is used until the pressure reaches at least 150 psig.

The pump and totally enclosed motor (3) have no thermal insulation or cooling. The pump, therefore, operates at nearly saturation temperature (467-600°F). The 5 hp induction motor operates at nearly these temperatures, since it is cooled only by natural convection of the ambient air. The pump has operated continuously for 612 hours with saturated water at temperatures from 400 to 600°F, predominately at approximately 475°F. The service life of the original motor bearings (carbon graphite) averaged about 150 hours. A new bearing material (silver impregnated graphite) gave greatly improved service.

b. Flow Measurement. --The pump discharges into a 60 in. long section of 3 in. schedule 80 stainless steel pipe. This length of 20 diameters precedes a sharp-edge orifice designed to ASME standards.

The orifice diameter is 2.000 ± .001 in. This orifice was installed in its piping system and calibrated by weigh tank measurements.

The pressure differential across the orifice flange taps is indicated by two Minneapolis-Honeywell indicating bellows meters, similar to the test vessel liquid level indicator (32). One of these meters (34) is shown in Fig. 8. It has a range of 0-100 in. of water. A similar meter with a range of 0-25 in. of water is installed in parallel with the first in order to permit more accurate flow measurements for low velocity runs, when the orifice differential is less than 25 in. water. The temperature of the water flowing through the orifice is measured by a thermocouple (TC) installed in an elbow downstream of the meter. This temperature is needed to make the density correction to the orifice reading.

c. Flow Control.--The flow through the primary loop is controlled by manually throttling on a 2 in. "Y" valve (5). This valve is similar to a globe valve but has a lower pressure drop when fully open. The valve has a Type 316 stainless steel body and is a Powell No. 1314 A. For 600°F service the Teflon valve packing was removed and replaced with mica impregnated asbestos rings.

d. Temperature Control.--Following the flow control valve the water passes through a line heater (6). This consists of a "U" tube of 3-in. schedule 80 stainless steel pipe with three immersion heaters in each leg. The six heaters are wired in three pairs so that the

same amount of heat is put into each leg. The total rating of the immersion heaters is 18.2 kw. One pair of heaters is controlled by a variable voltage transformer which permits power variations of 0-4.6 kw. A second pair of heaters is rated at 4.6 kw and has ON-OFF control. The third pair of heaters is rated at 9.0 kw and has ON-OFF control. This control arrangement permits infinite variation of the power inputs from 0-18.2 kw but uses a small size variable transformer.

The temperature of the water following the line heater is measured by another thermocouple (TC). The flow enters the bottom of the test vessel through the 6 in. pipe in which is inserted a flow straightener and guide (33).

e. Installation.--The entire primary flow loop is fabricated from Type 347 stainless steel pipe and flanges. With the exception of the pump suction line, the loop is in a horizontal plane, 8 in. above the floor. The entire loop and pump baseplate is spring mounted to permit thermal expansion without creating excessive stresses due to restraints of fixed supports. Portions of the loop before and after the calcium silicate insulation was applied may be seen in Figs. 3 and 7.

2. Water Purification Loop

Provision is made for continuous purification of the water by means of the filtration and deionizing of a small stream which

by-passes the primary flow loop. Referring to Fig. 8, the main pump (3) or the auxiliary circulating pump (11) creates the pressure necessary to force approximately 1 gal/min through the purification loop. This hot water (470-600°F) is cooled in a counter-current flow heat exchange or regenerator (12) which reduces the temperature to 150°F. It is further cooled by heat exchange with cooling water in a thermostatically controlled U-tube type exchanger (13). The flow rate in the purification loop may be controlled by throttling the deion shut-off valve (14). The cooled water passes through a line filter (38) with a 1-3 micron pore size to remove suspended solids and then through the ion exchanger (15) which controls the effluent resistivity and pH. The deionized and filtered water is returned to the primary loop ahead of the line heaters, having been warmed to within 50°F of the saturation temperature by the regenerator (12).

The total quantity of water in the system is approximately 50 gal. If the assumptions are made of perfect mixing, and complete deionizing in the bed, then the purification flow of 1 gal/min would reduce the ion concentration by 1/e every 50 min. In actual service the clean-up is considerably slower, due to the incomplete deionizing and the creation of new ions from the walls of the system. By circulating through the ion exchanger continuously, the water resistivity and pH can be maintained at the values specified for the ion exchange resin employed.

a. Auxiliary Circulating Pump.--An auxiliary circulating pump, similar to but smaller than the main pump, permits the deionizing loop to be operated independently of the main loop. The pump is Chempump Model CFT-3/4-3/4-S. It is also a canned rotor pump and has a water cooled stator.

b. Regenerator.--The regenerator consists of 60 ft of 1/2 in. O.D. by .065 in. wall tubing inside of an equal length of 1/2 in. schedule 10 pipe (.840 in. O.D. by .083 in. wall). All material is Type 347 stainless steel. The 60 ft length is formed into a multiple S-shape, consisting of six lengths each 10 ft long. The tubing and pipe size were chosen such that high velocities, and resulting high heat transfer coefficients, would exist on both the tube and shell side at the rated flow of 1 gal/min. The regenerator is hung from the ceiling in a vertical plane and can be seen at the upper left of Fig. 3.

c. U-Tube Exchanger.--The U-tube exchanger consists of 20 ft of Type 304 stainless steel tubing, 1/2 in. O.D. by .065 in. wall, inside of a jacket of 3/4 in. O.D. copper tubing. The high pressure water passes counter-current to a flow of cooling water in the jacket. The cooling water flow may be controlled manually or thermostatically. For thermostatic control, a solenoid valve is actuated by a Thermo Electric Co. Type 80025 electronic controller which senses the temperature of the high pressure distilled water. This exchanger

insures that the water entering the ion exchanger and that used for sample analysis is maintained at the desired temperature.

d. Ion Exchanger.--The ion exchanger is a stainless steel pressure vessel containing approximately 7 lbs of ion exchange resin. Two types of resin were used in conducting this research. Rohm and Haas Amberlite MB-1 resin is capable of increasing the electrical resistivity from 500,000 ohm-cm to 4 megohm-cm at a flow rate of 1 gal/min. This maintains the system water resistivity above 2 megohm-cm and the pH at about 7.4. Rohm and Haas IRN-170 resin maintains the system water at approximately 200,000 ohm-cm with a pH value of about 9.5.

e. Line Filter.--Suspended solids are removed from the water by a 1-3 micron pore size filter element in the line ahead of the ion exchanger. A large surface area is provided by two stacked Cuno Type ACSA filter elements enclosed in a stainless steel pressure vessel. This allows control of the suspended solids level in the system and prevents clogging of the ion exchanger which would reduce its effectiveness. Provision is made for agitating the water at the bottom of the pressure vessel to keep solid material in suspension to be filtered out.

f. Water Analysis.--Sample taps are provided for water analysis to determine resistivity, pH, dissolved oxygen content and level of suspended solids. In addition to the sample taps, a tap is provided

through which hydrazine may be added for control of the dissolved oxygen level.

A sample for determining pH and resistivity may be taken before or after the ion exchanger or directly from the test vessel at the lower liquid level connection. The sample is passed through an electrolytic conductivity flow cell. This cell is connected to an Industrial Instruments Solu Bridge, Type RD-32, which indicates the specific resistance of the water. The range of the bridge is 20,000 to 4,000,000 ohm-cm, with an accuracy of 5% of the indicated reading. After leaving the conductivity cell, the water sample is passed through the cell of a Leeds and Northrup Model 7401 pH indicator, then discarded.

The suspended solids sample tap is located ahead of the line filter. A one liter sample is passed through a 0.45 micron pore size disc filter element (Millipore Type HA or Gelman Type GM-6) and discarded. Suspended solids analysis during pool boiling tests may be accomplished by taking a sample directly from the bottom of the vessel at the lower liquid level connection.

A Hays Dissolved Oxygen Analyzer is used to determined the level of dissolved oxygen in the water. The sample is taken at the inlet to the ion exchanger, passed through a pressure reducer-regulator, flow control valve and dosing tank to the analyzer and discarded. The analyzer is calibrated to indicate dissolved oxygen content based

on an oxidation-reduction reaction which occurs in a zinc-silver galvanic cell. An electric current is produced in an external load circuit which is proportional to the amount of dissolved oxygen present in the water. Fig. 9 shows the arrangement of the components used for water chemistry control and analysis.

3. Pressure Control Loop

The pressure in the system is generated and maintained by boiling the water in the test vessel. Pressure may be controlled by (a) adjustment of the power input to the system, (b) removing energy in the condenser (8), or (c) venting steam through a manually operated needle valve or through a Research Controls diaphram operated control valve (10). This valve may be operated manually or automatically by a Fisher pressure controller (9). All three methods of control are used initially in degassing. This is done by vigorous boiling at about 30 psig, operating the condenser as a reflux condenser, and permitting the noncondensable gases to escape along with some steam through vents at the highest part of the system. The pressure on the system is indicated by a Heise precision gage (31), having a range of 0-2500 psig and 2.5 psi scale divisions. It was calibrated to read correctly to within 0.1%.

a. Steam Condenser.--The steam condenser consists of a Type 347 stainless steel tube, 1-1/8 in. O.D. by 0.120 in. wall by 6 ft long, positioned centrally within a copper tube of 1-5/8 in. O.D.

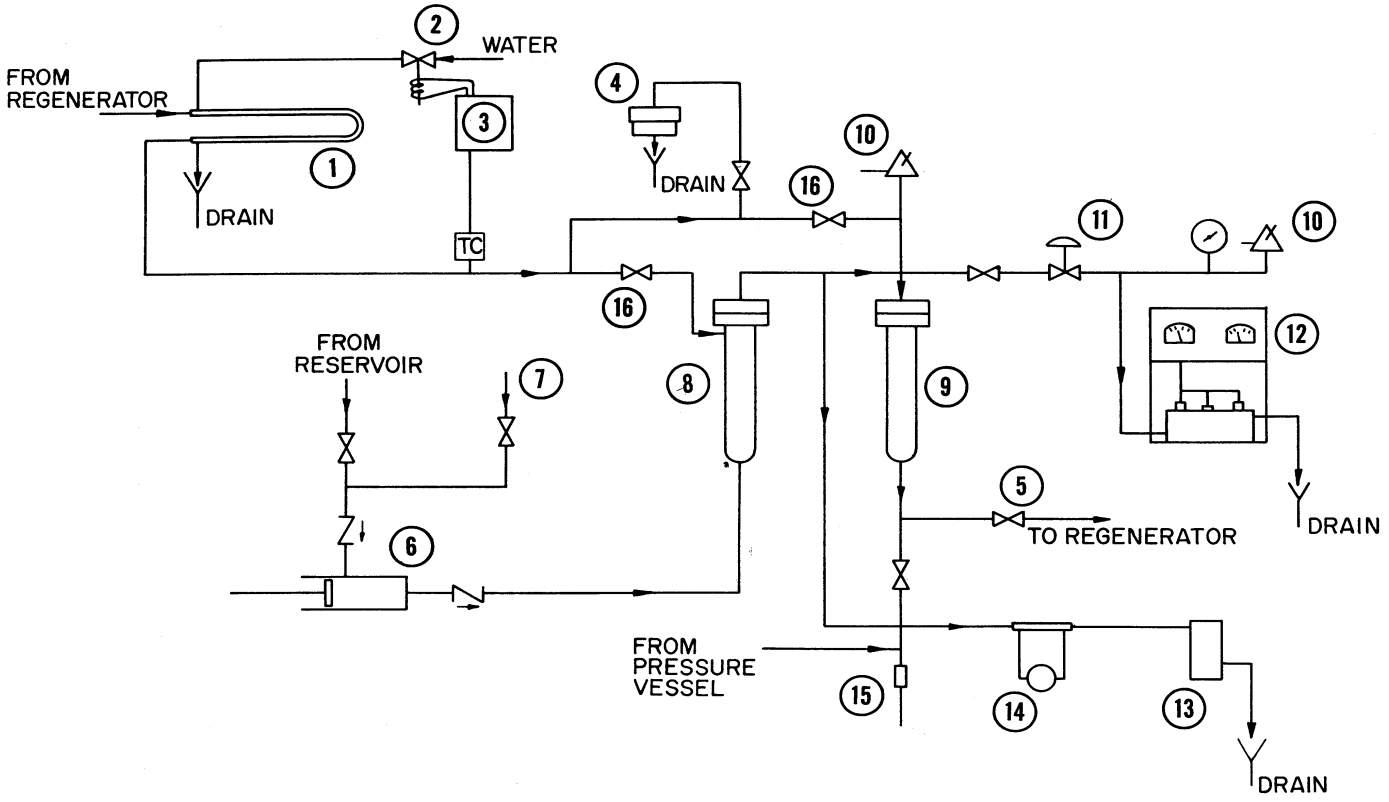

16 Filter By-Pass Valve
15 Pressure Relief
14 Conductivity Cell
13 pH Cell
12 Dissolved Oxygen Analyzer
11 Pressure Regulator
10 Safety Valve
9 ION Exchanger
8 Filter
7 Hydazine Inlet
6 Injection Pump
5 Deion Shut Off
4 Suspended Solids Sample Filter
3 Signaling Controller
2 Solenoid Valve
1 Cooling U-Tube

Fig. 9. Water chemistry control and analysis loop.

by 0.072 in. wall. The assembly is inclined from the horizontal with a pitch of 1 in./ft. The steam enters the lower end and the condensate drains counter-current to the steam flow. The upper vent is connected to the noncondensable gas bleed. The copper jacket has a Crane No. 404 expansion joint to permit differential thermal expansion of the stainless tube and the copper jacket. The jacket is silver soldered to the stainless tube by copper heat exchanger tees. In operation the cooling air flows counter-current to the steam flow. The condensing capacity of the unit is regulated by adjustment of the cooling air flow rate and pressure. The design rating is 20,000 Btu/hr.

b. Steam Bleed System.--Provision is made to bleed automatically excess steam from the system by a Research Controls needle valve, actuated by a Fisher controller. The minimum band on the controller is 2% of full range, or 60 psi. It was found in operation that manual control of the heat input to the immersion heaters and heat rejection in the air cooled condenser permitted such precise pressure control that fluctuations could not be observed on the Heise pressure gage. This control was achieved by semi-continuous observation of the steam space thermocouple emf. Variations of one microvolt could be observed. This corresponds to $0.025^{\circ}F$ or approximately 0.25 psi change in saturation pressure at a level of 1,000 psia. During tests the steam temperature was held constant to $\pm 0.1^{\circ}F$ ($\pm$ 1 psi) for periods of several hours at a time.

4. Water Make-up System

The water make-up system consists of means of storing, injecting and draining the distilled water used in the system. Referring to Fig. 8, distilled water is supplied to the 55 gal stainless steel make-up drum (20) through the filler connection (22). A vertical Tygon tube serves as the level gage (21). The make-up tank may be purged with nitrogen from a cylinder (24). Excess pressure on the tank is prevented by a relief valve (23). Water is injected into the system by an injection pump (19). This water is fed to the inlet side of the filter (38) before the ion exchanger (15) so that the make-up water is filtered and deionized before it reaches the test vessel. The system may be drained back into the make-up drum through a line connected to the low point of the system. Nitrogen from the cylinder is used to break the vacuum and pressurize the test vessel for complete drainage. Up to 5 gal of high purity water may be stored in the accumulator for addition to the system when needed.

a. Make-up Drum.--The make-up drum is a 55 gal drum of Type 304 stainless steel. It is mounted horizontally on a table above the main piping loop at the rear of the control panel. The drum is seen at the left of Fig. 10.

b. Injection Pump.--The injection pump is a Wallace and Tiernan Metering Pump - Series 200. It has a single stainless steel plunger of 1/2 in. diam. The speed is fixed at 83 strokes per min

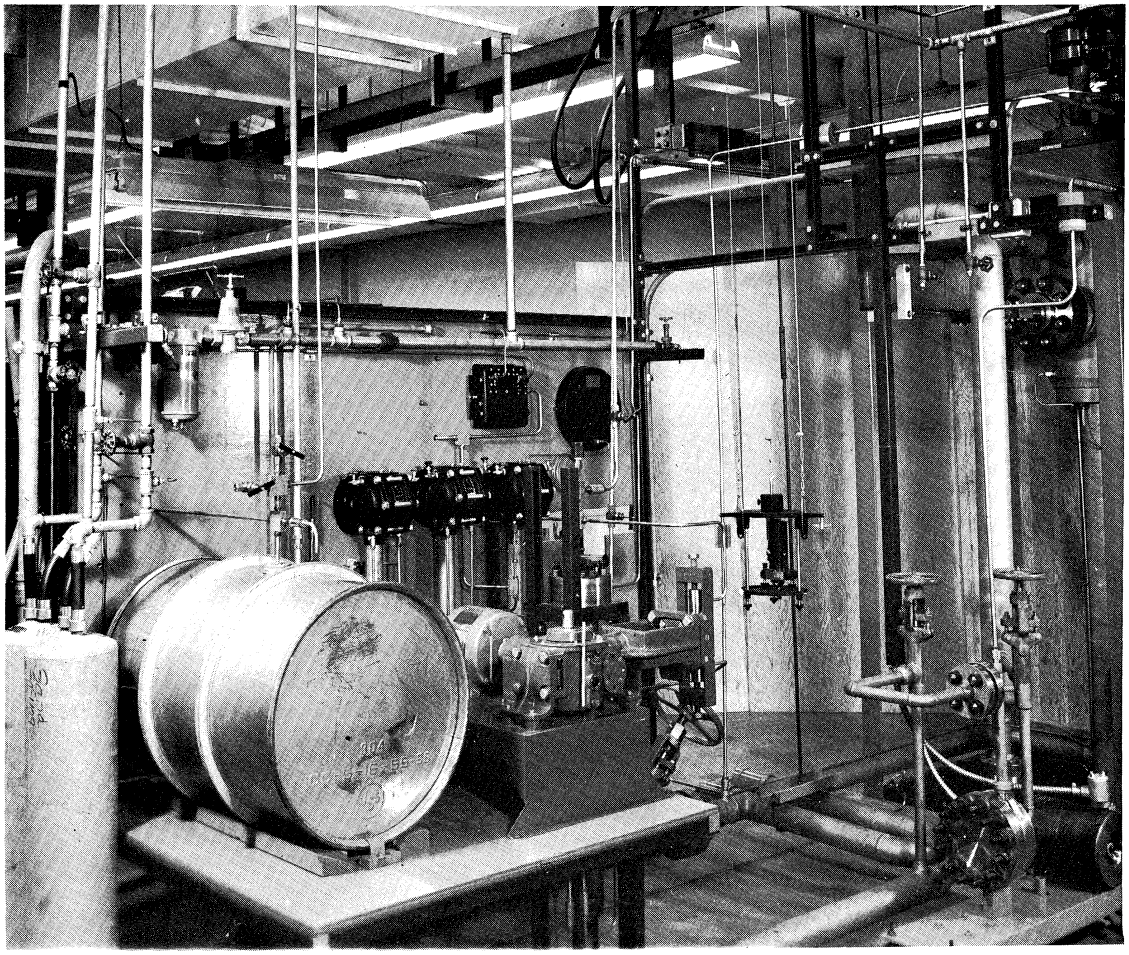

Fig. 10. Rear view of system, before insulation.

but the stroke is adjustable from 0-100%. The maximum rating is 5.9 gph at 2,000 psi. The pump is driven through a worm gear by a one horsepower electric motor which is controlled manually from the 440 volt control panel. The pump is shown in the foreground of Fig. 10 mounted on the same table as the make-up drum.

5. Safety Devices

The system is protected from excessive pressure by two Farris safety valves, set to relieve at the maximum design pressure of 2,000 psig. One valve is connected directly to the steam space of the test vessel and discharges to a vent pipe which exhausts into the suction of a large building roof ventilator. The second valve is on the ion exchanger and is installed to prevent excessive pressure in the exchanger and line filter in the event that the purification loop shut-off valves are closed when the injection pump is started. Despite every reasonable care in operation, this situation occurred several times during test runs and the safety valve functioned as required.

A pressure switch is also installed on the system. This is a Barksdale Catalog No. B2T-A32SS. It has two independent contacts adjustable between 160 and 3200 psig. One contact is used as a high pressure shut-off and is set at 1775 psig. It shuts off all 440 volt power to the system on excessive pressure. The other contact is set at 420 psig. It shuts off all 440 volt power to the system if the

pressure drops below the set point. This serves to protect the pumps and heaters in the event of a line break and sudden loss of water from the system.

E. CONTROL PANELS AND POWER SUPPLIES

The operation of the low heat-flux boiling apparatus is monitored and controlled from a control panel along with the a-c electrical control and power distribution panel and direct current generator control panel. In the right half of Fig. 3 the process panel is at the left, the d-c generator control panel in the center, and the a-c panel on the right.

1. Process Control Panel

On the process control panel are mounted the following instruments:

Name	Details
1. Differential Pressure Indicator, Minneapolis-Honeywell	0-25 in. water range, 1-1/4% full scale accuracy, to indicate liquid level in test vessel
2. Differential Pressure Indicator, Minneapolis-Honeywell	0-25 in. water range, 1-1/4% full scale accuracy, to indicate orifice differential, low flow
3. Differential Pressure Indicator, Minneapolis-Honeywell	0-100 in. water range, 1% full scale accuracy, to indicate orifice differential, high flow

4. Pressure Gauge, Heise	2500 psi range, 0.1% full scale accuracy, to indicate pressure of system
5. Pressure Controller, Fisher	0-3000 psi range, to control valve bleeding steam from the system
6. Pressure Switch, Barksdale	160-3200 psi range, to provide electrical shut-down on high or low pressure
7. U-Type Manometer, King	0-10 in. range, to indicate flow of cooling air to condenser
8. pH Indicator, Leeds and Northrup	Model 7401, to indicate pH of water
9. Conductivity Cell, Industrial Instruments	Range 20,000 to 4,000,000 ohm-cm, to indicate electrical conductivity of water
10. Galvanometer, Leeds and Northrup	Type 2284, to indicate thermocouple null balance
11. Potentiometer, Leeds and Northrup	Type K-3, to measure thermocouple emf
12. Pressure Gauges	0-100 psig, 3 gauges, to indicate cooling water pressures
13. Air Regulator, Wilkerson	0-20 psig, to regulate cooling air flow
14. Dissolved Oxygen Analyzer, Hays	0-100 PPB with built in calibrating system

2. Alternating Current Panel

An alternating current electrical control and power distribution panel was designed and fabricated to supply and control the 440 volt,

60 cycle, 3 phase power required for the immersion heaters and pump motors. The electrical schematic diagram of this panel is seen in Fig. 11. On the left of the figure is a 110 volt control circuit with interlocking safety relays actuated by the low level switch and the pressure switches. On the right is shown the heater and pump circuits. The immersion heaters total 28.1 kw rating. The Chempump, supplied from surplus stock, was wired for 220 volt, 3 phase power and requires a separate circuit. All circuits are protected against overload and equipped with indicating lights and meters.

3. Direct Current Panel

Direct-current resistance heating of the test section is caused by the passage of currents up to 3000 amp at 12 volts, produced by a Hanson-Van Winkle-Munning motor-generator set of 36 kw rating. This current is distributed throughout the laboratory by copper bus bars of 3 sq in. cross-sectional area. The voltage from the generator may be varied from 0.5 volts minimum to an overload of 15 volts. The control panel for this m-g set is seen in the right center of Fig. 3.

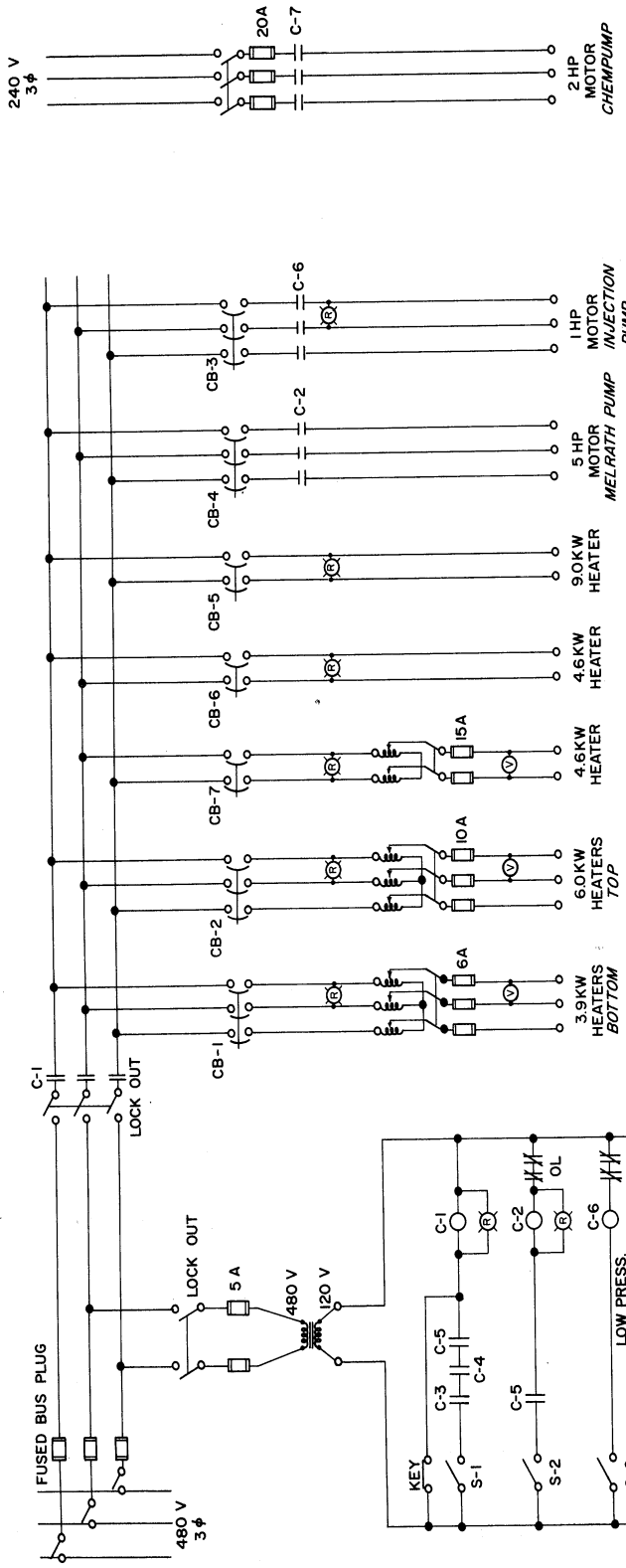

Fig. 11. a-c distribution schematic.

III. TEST PROCEDURES

A. MATERIALS CONSIDERED AND TEST SECTION ORIENTATION

Heat transfer characteristics were investigated for Inconel, Carbon steel, and Monel tubes. Monel, Inconel, and carbon steel tubes were oriented horizontally in the pressure vessel, Fig. 5, and a Monel tube was oriented vertically, Fig. 6. All test sections were instrumented as shown in Fig. 4. The dimensions of the individual tubes, surface roughness, electrical resistivity and thermal conductivity are given in Tables IV through VII below.

B. TEMPERATURE MEASUREMENT

The measurement of temperature is a matter of fundamental importance in any heat transfer research. In this study all temperatures are measured by the use of chromel-constantan thermocouples, calibrated against a platinum resistance thermometer as described in Appendix A.

All thermocouples have silver soldered or welded hot junctions. The wires are brought directly to distilled-water ice reference junctions, without intermediate junctions. The emf from the reference junctions is measured through shielded copper leads by a Type K-3 Universal Potentiometer (Leeds and Northrup) used with a Model 2284d moving coil galvanometer, mounted in a Julius suspension hung from the roof of the laboratory building.

TABLE IV

DIAMETER AND WALL THICKNESS OF TEST SECTIONS[a]

Material	Inconel	Inconel	Carbon steel	Monel	Monel
Test Section Designation	HI1	HI2	HS	HM	VM
Run Numbers[b]	HI1-1 through HI1-29	HI2-1 through HI2-20	HS-1 through HS-14	HM2-1 through HM2-20	VM-1 through VM-13
Average OD,[c] inches	0.7500	0.7505	0.7540	0.751	0.7511
Average Wall Thickness,[d] inches	0.0511	0.0501	0.0490	0.0535	0.0526
Max. Wall Thickness, inches	0.0520	0.0515	0.0496	0.055	0.0540
Min. Wall Thickness, inches	0.0504	0.0483	0.0483	0.052	0.0510

[a]Readings were made with a point micrometer, calibrated with gage blocks.

[b]HI1-1 represents the first test run for the No. 1 horizontal Inconel test section, VM-1 represents the first run for the vertical Monel test section, etc.

[c]Based on four measurements at two axial positions, two perpendicular readings at each position.

[d]Based on eight measurements, four at each end of tube.

TABLE V

SURFACE ROUGHNESS OF TEST SECTIONS[d]
(μ-in. RMS)

Material	Inconel	Carbon steel[c]	Monel
Axial Traces[a]			
Max.Reading	68	52	40
Min.Reading	57	27	5
Average	62	35	15
Circumferential Traces[b]			
Max.Reading	35		16
Min.Reading	20		5
Average	27		10

[a]Average of eight traces

[b]Average of three traces

[c]Readings taken on two samples after exposure to high temperatures. One sample used for electrical resistivity measurements, the other used for boiling studies. Two other samples not exposed to high temperature gave lower readings. The two samples used for these data gave very nearly the same results.

[d]Readings are in μ in. (RMS). Measurements made with a Type Q Profilometer Amplifier, Model 1, manufactured by the Micrometrical Co. Traces made with a Type MA Stylus.

TABLE VI

ELECTRICAL RESISTIVITY

Temperature, °F	Resistivity,[a] μohm-cm		
	Inconel	Carbon steel	Monel
100	105.2		49.4
200	105.8		50.6
300	106.4		51.6
400	107.0	30.0	52.5
500	107.7	34.5	53.2
600	108.3	39.5	53.8
700		45.2	

[a]Measured as a function of temperature by passing a small known electrical current through a sample of the tube and measuring the voltage drop across a known length.

TABLE VII

THERMAL CONDUCTIVITY

Temperature, °F	Thermal Conductivity,[a] Btu/hr-ft °F		
	Inconel	Carbon steel	Monel
450	9.6	27.4	16.4
500	9.8	27.3	16.9
550	10.0	27.2	17.3
600	10.2	26.9	17.8
650	10.4	26.3	18.3

[a]Measured with a comparison technique by the Dynatech Corp., Cambridge, Mass.

1. Steam Temperature

The steam temperature thermocouple is encased in and insulated from a stainless steel sheath of 1/8 in. diameter. Two arrangements were used as shown in Figs. 5 and 6. For the horizontal test sections, Fig. 5, the thermocouple protrudes downward from the top flange with its tip being from 1 to 3 in. above the liquid level. Although a radiation shield was provided, careful examination indicated that it was not necessary. For the vertical test section, Fig. 6, the thermocouple extends through the side of the vessel at the top and is looped to obtain the desired depth of immersion, as discussed in Appendix A.

The steam space thermocouple was used to hold the system test conditions constant since this allowed much closer control than could be maintained by observing the pressure gage. By periodic observation of the steam space temperature the conditions were held to within $\pm$ 0.1 ^{o}F which corresponds to approximately $\pm$ 0.5 psi at 535 psia and $\pm$ 1.2 psi at 1550 psia. The pressure gage accuracy is $\pm$ 2.5 psi. A smaller incremental change can be observed but the sensitivity cannot compare with that of the thermocouple-potentiometer combination.

2. Bulk Water Temperature

The bulk water thermocouple is encased in and insulated from a 1/16 in. diameter stainless steel sheath. This thermocouple protrudes

downward from the top flange with its tip being about level with the bottom of the test section, Figs. 5 and 6. The immersion depth of this and the steam space thermocouple is sufficient to insure negligibly small conduction error.

3. Test Section Temperatures

As described earlier, the test section has 12 thermocouples pressed against but insulated from the inside wall. The data reported reflect the readings of all 12 thermocouples. Zero readings were taken at the beginning and end of each run to "calibrate" the system as indicated in Appendix A. Some readings fluctuated with time, a few as much as $\pm$ 12 μv or $\pm$ 0.3°F. For all readings a time-average of the fluctuations was recorded from observation over a number of cycles. The inside wall of the test section is an adiabatic surface. This eliminates a temperature gradient through the .003 in. thick mica insulator and, hence, the measured temperature is the same as that of the inside surface of the metal test section.

4. Wall Temperature Drop

The temperature at the outside of the test section is required in order to determine the temperature difference between the heat transfer surface and the saturation temperature of the water or the bulk water temperature. The temperature drop across the wall at a heat flux of 100,000 Btu/hr-ft^2 is less than 25° for Monel, Inconel,

and carbon steel tubes. Hence, the temperature variation of thermal conductivity and electrical resistivity for Monel and Inconel is sufficiently small to permit an assumption of constant physical properties. However, for carbon steel the variation of electrical resistivity with temperature required a two step calculation in order to keep the error in electrical resistivity to less than 1%. In this case, two equations were established and the appropriate one for the temperature range was employed.

The expression for wall temperature drop is

$$T_i - T_o = \Delta T_{wall} = \frac{q'''}{2k}\left[\frac{r_o^2 - r_i^2}{2} - r_i^2 \ln\left(\frac{r_o}{r_i}\right)\right] \qquad (1)$$

where q''' is the heat generation per unit volume. The heat generation rate, q''', Btu/hr-ft^3, is found from the product of the resistivity, ρ_e, ohm-ft, and the square of the current density, i, amp/ft^2;

$$q''' = i^2 \rho_e C_1 \qquad (2)$$

where C_1 is a conversion factor equal to 3.413 Btu/watt-hr. Based on the total cross-section of the test section, A_{tube}, ft^2, and the total current, I, amperes this is

$$q''' = \frac{I^2 \rho_e C_1}{(A_{tube})^2} \qquad (3)$$

The tube wall temperature drop, to the nearest 0.1°F, except at very low flux, is subtracted from the average reading of the twelve

thermocouples in the horizontal test sections to give an average outside tube surface temperature. For the vertical test section, each group of four thermocouples is used for a separate calculation although in the same manner as previously stated. The use of average temperatures and a total tube cross-sectional area renders unnecessary a consideration of slight variations in tube wall thickness around the circumference in computing the wall temperature drop.

C. POWER MEASUREMENT

The total current which passes through the test section is determined by measuring the voltage drop across a shunt of 10^{-5} ohm resistance. An L & N, Type 8662, potentiometer is used to measure the voltage drop across the shunt and indicate the current to within 0.1%.

D. ELECTRICAL RESISTIVITY MEASUREMENT

As noted above, the electrical resistivity, ρe, is required to calculate the heat generation term, q'''. This property was measured as a function of temperature by passing a small known electrical current through a sample of the tube and measuring the voltage drop across a known length. This gives the resistivity of the material as drawn in tubular form. Values obtained are given in Table VI.

E. THERMAL CONDUCTIVITY MEASUREMENT

The thermal conductivity, k, used to calculate the wall temperature drop was measured by using plates of the tube material machined from the thick wall shell from which the tubes were drawn. The shell size was $2\frac{1}{2}$ in. O. D. by 0. 312 in. wall. This was split, flattened, annealed, and machined into a flat plate approximately 0. 3 in. thick by $2\frac{1}{2}$ in. square. The thermal conductivity of these samples was measured with a comparison technique by the Dynatech Corp., Cambridge, Mass. Results are presented in Table VII.

F. PHOTOGRAPHIC STUDY OF NUCLEATE BOILING

Photographs of the boiling on the outside surface of the test section were made using a Crown Graphic camera and Polaroid Type 47 film, ASA 3000, 0. 5 millisecond exposure at f/32. Front lighting was provided by a Heiland Strobonar III electronic flash held against the sight glass port which is 35° from the normal to the test section. The viewing port, through which the camera was focused, is normal to the test section. Back lighting, through the port 180° from the camera port, was not used. The sight glass consists of a 2 in. thick fused quartz lens backed by a relatively clear mica disc to prevent etching of the quartz by the high temperature water.

The design of the sight glass assemblies is described in reference 1. At the operating conditions of this investigation glass is

etched rapidly by the high temperature water. This is potentially dangerous with tempered glass. Consequently, the lens assembly was changed from the original design incorporating two discs of tempered soda-lime glass, each 1 in. thick by 2-3/16 in. diameter, to a single disc of fused quartz, 2 in. thick by 2-3/16 in. diameter.

The quartz lens proved to be about an order of magnitude less susceptible to etching than those made of glass. However, visibility through this lens was unsuitable after approximately 25 hours exposure to water at 473°F and 535 psia. A thin mica disc placed between the water and the lens eliminated the etching and provided good visibility up to the maximum test condition of 600°F and 1550 psia.

G. SYSTEM PREPARATION AND OPERATION PROCEDURE

The control of water chemistry requires special operating procedures in preparation for a series of test runs, for each run, and in performing maintenance on the system. The need for control of water chemistry in this investigation and the levels required are outlined in Section IV.

Special attention is given to keeping oxygen out of the system at all times. Nitrogen is introduced as the water is drained for maintenance purposes and the nitrogen is forced out again as the system is refilled with water. Oxygen is primarily responsible for surface contamination and the suspended solids.

All components are washed with methlene chloride solvent and rinsed with distilled water prior to installation in the system. The system is rinsed with distilled water when shut down to remove solid material which is broken from the metal surface by thermal contraction during cool-down. Water added to the system is passed through the filter and ion exchanger to insure it to be of high purity.

Before each series of runs the water in the system is degassed while circulating and boiling vigorously for a period of two hours. While degassing, the system is held at approximately 30 psig and a small bleed of steam and non-condensable gases is permitted from two high points of the system. Hydrazine is added when the system is cold to act as an oxygen scavenger. Upon completion of degassing the dissolved oxygen level is less than 20 PPB. The final oxygen level reduction is accomplished while the system pressure is less than 200 psig by a small addition of hydrazine as required.

Even with rinsing the system as described above, the suspended solids level in the water is very high when the system is brought up to operating conditions at 535 psia. Heater voltages and flow velocity are set to hold the system at the desired test condition and it is operated continuously for about 48 hours while filtering suspended solids until the level remained constant. The filter is in a by-pass loop just upstream of the ion exchanger, Figs. 8 and 9. Hence, suspended solids are removed and dissolved solids treated to control water pH

and resistivity simultaneously. No power is supplied to the test section until a constant suspended solids level is reached and the dissolved oxygen level is below 7 PPB.

The level of water in the system must be kept within narrow limits for proper operation. To do so water must be drained as the pressure is increased. This provides water for frequent samples of oxygen, suspended solids, pH and resistivity. Excess water is stored in an accumulator to be reintroduced when the pressure is reduced.

Changes in system temperature result in an increase in suspended solids level as described in Section IV. After a change it is operated at the new test condition while filtering until the suspended solids are at a constant low level prior to heating the test section. During pool boiling runs when only the main vessel is heated and no circulation is provided, the solids level remains approximately constant at a satisfactory low level. Water samples are removed directly from the vessel for analysis during the series of pool boiling runs.

Test runs are made first under forced convection conditions at 535, 1015, and 1550 psia. Recheck runs are made and then the circulation is stopped to allow pool boiling studies. Operation in this manner is required to minimize the temperature changes for suspended solids control. The system pressure is maintained above 500 psia until a series of runs is completed. The series includes both

forced convection and pool boiling runs with check runs to determine repeatability of data. A series normally consists of 12 to 15 runs and requires from $1\frac{1}{2}$ to 2 weeks to complete.

H. ATTAINMENT OF STEADY STATE CONDITIONS

At the beginning of a run, or after making a change of heat flux in the test section, sufficient time was allowed for the attainment of steady state conditions before data were taken. This ranged from 10 minutes to 1 hour depending on the steadiness of the steam space temperature and test operation considerations. For example, the maximum heat flux of 100,000 Btu/hr-ft^2 was maintained for 1 hour before taking data to allow for stabilization of the test surface temperatures. At other test conditions the time required for stabilization was much less.

The heat balance of the system was manually adjusted so that the steam space temperature did not vary by more than $\pm$ 0.1°F over any series of readings. Usually an entire run, lasting from 4 to 6 hr was made without the temperature varying by more than $\pm$ 0.2°F. The thermocouple-potentiometer method of control proved to be much more sensitive than control by use of the pressure gage.

At a specified test condition, readings were made of the various thermocouple emfs, pressure, flow rate, liquid level, power input to test section, and power to system heaters. For each test condition,

data were recorded in the same sequence. The steam space thermocouple emf was recorded just before and after reading the test section thermocouples. It was also read at intermediate points to insure steady conditions while the twelve test section thermocouples were read. If a difference in steam space readings was noted, an average was taken. However, if the difference exceeded $0.1^{\circ}F$ another complete set of readings were taken. This did not occur often. Several measurements were made of the electrical current through the test section and an average value recorded.

Data were taken by two observers, one reading the K-3 potentiometer and the other taking and recording the remaining data. The two observers frequently swtiched roles to minimize the effect of personal bias in reading.

IV. WATER CHEMISTRY

The effect of a dissolved gas in a boiling liquid on the initiation of ebullition and on the nucleate boiling curve has long been recognized. All researchers degas the system by vigorous boiling and exhausting the non-condensable gases. Corrosion has been avoided insofar as the heated test surface is concerned since this introduces an uncontrollable parameter in the definition of the test surface. Corrosion may also affect the nucleation characteristics of the heated surface and prevent the attainment of reproducible data.

In boiling systems it may be necessary to control the oxidation of the heated surface under investigation and all of the components of the system which are exposed to the high temperature boiling fluid. Such was the case in the present investigation.

The experimental apparatus, as already mentioned, was fabricated with type 347 or type 304 stainless steel. When gaseous oxygen is present in the boiling medium (distilled water) the hot surface is oxidized readily at high temperature. This results in the formation of a layer of black magnetic iron oxide (magnetite, Fe_3O_4) on the metal surface. The magnetite layer, when properly controlled, aids in reducing the corrosion rate of the system components. This is of importance in a steam power plant in reducing maintenance problems.

In a research system such as described herein corrosion control has a more fundamental importance, that of insuring reproducibility of the test results.

The layer of magnetite is very brittle and is broken from the surface with thermal expansion or contraction, thus exposing the bare metal for further oxidation to continue the process. Magnetite which is removed from the surface becomes suspended solid material in the water. As the level of solid material in the water is increased deposits will be found at various points in the system and on the heated test surface. This forms an insulating layer on the test surface and causes a change in the nucleate boiling curve as shown in Fig. 12. The curve for HI1-9 was obtained with a clean heat transfer surface. The curve for run HI1-14 shows the change of slope and increased ΔT which results with a thin (approximately 0.0005 in. thick) insulating layer on the test surface.

Operational procedures were adopted to minimize the temperature changes in the system while taking a series of experimental runs and steps were taken to reduce the dissolved oxygen level to minimize the rate of corrosion in the system. Recommended levels for dissolved oxygen for high pressure steam generating boilers are given by Hamer, Jackson, and Thurston[30] as follows.

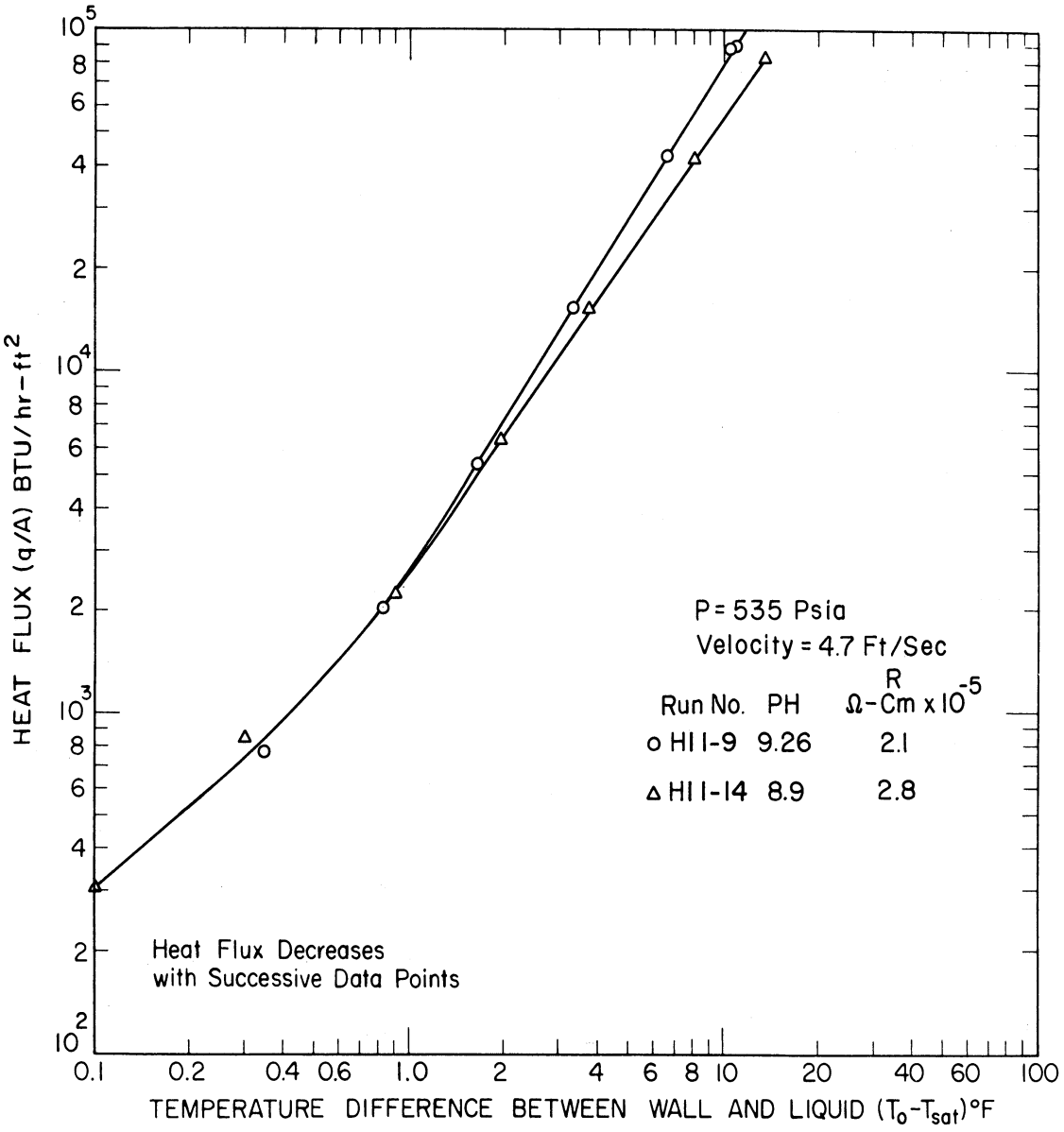

Fig. 12. Effect of surface contamination on boiling characteristics.

Pressure, psia	Recommended Dissolved O_2 Level
> 500	30 PPB
>1500	5 PPB

The above levels cannot be reached simply by vigorous boiling to degas the system. For example, degassing to a level of 0.3 cc/liter dissolved oxygen corresponds to 429 PPB. In the research reported herein, the dissolved oxygen was controlled by circulating the water and vigorous boiling for a period of two hours as well as using a chemical scavenger to reach the desired level. Hydrazine, which reacts as follows with no solid by-product, was used as the scavenging agent. The nitrogen gas was vented from the system.

$$N_2H_4 + O_2 \rightarrow N_2 + 2H_2O$$

A Hays dissolved oxygen analyzer with a range of 0 to 100 PPB was used to monitor the oxygen level. Initial investigation of oxygen concentration was accomplished by means of the Winkler test. The sensitivity of this test proved to be inadequate for measurement after thoroughly degassing for two hours and it could not be used for measuring the low oxygen levels required. The level of dissolved oxygen was controlled to less than 30 PPB for all tests and less than 7 PPB for most of the tests.

Pocock[31] recommends that the oxygen level be maintained as near to zero as possible for high pressure steam boilers. In

supercritical boilers corrosion control is very important for obvious reasons. Water treatment problems for large power plants are much more complex than for a closed loop boiling distilled water. However, the recommendation to maintain dissolved oxygen level as near zero as possible is considered appropriate in a research system of the type used for this investigation.

With control of dissolved oxygen level and minimizing temperature changes, the problem of an insulating layer depositing on the test surface can be avoided. However, suspended solid material will still be present in the water and this presents another problem. Fig. 13 shows a series of test runs made after beginning control of oxygen level, except for run HI1-2. A progressive shift of the data to higher values of ΔT at a given value of heat flux was obtained. All data presented are for a clean test section surface. The shift reflects an apparent change in test section nucleation characteristics. Since no change in slope of the curves is noted the effect is not that of an insulating layer of contamination, as is shown in Fig. 12. The water pH was changed from 9.5 to 7.4 after run HI1-8 and back to 9.5 after run HI1-24 with no apparent effect on the shifts. Only the pool boiling runs at 535 psia are shown on Fig. 13. The forced convection runs at 535 psia are shown on Fig. 14. A similar shift of the data is evident though of less magnitude.

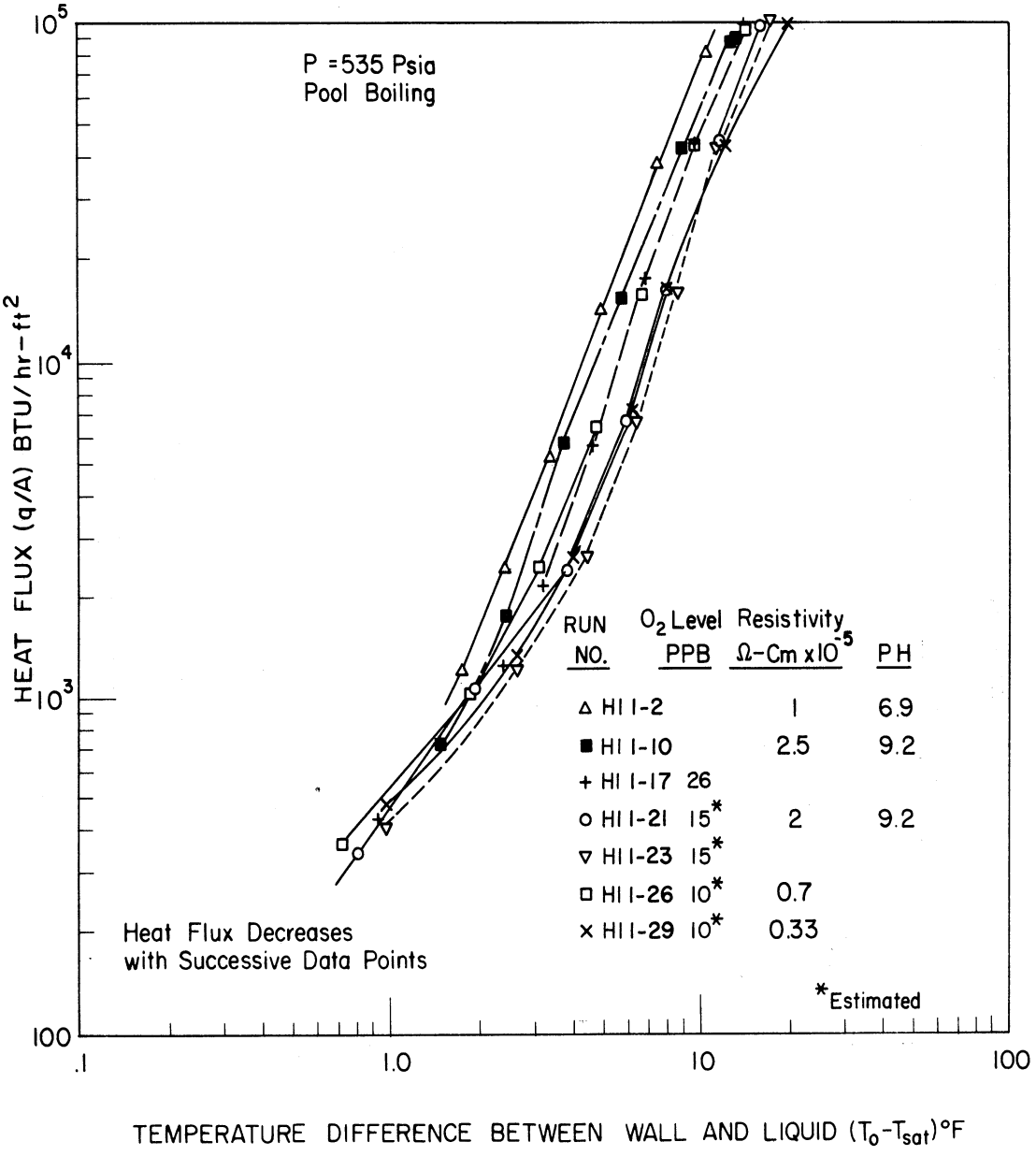

Fig. 13. Pool boiling of saturated distilled water at 535 psia, runs taken while developing water chemistry requirements.

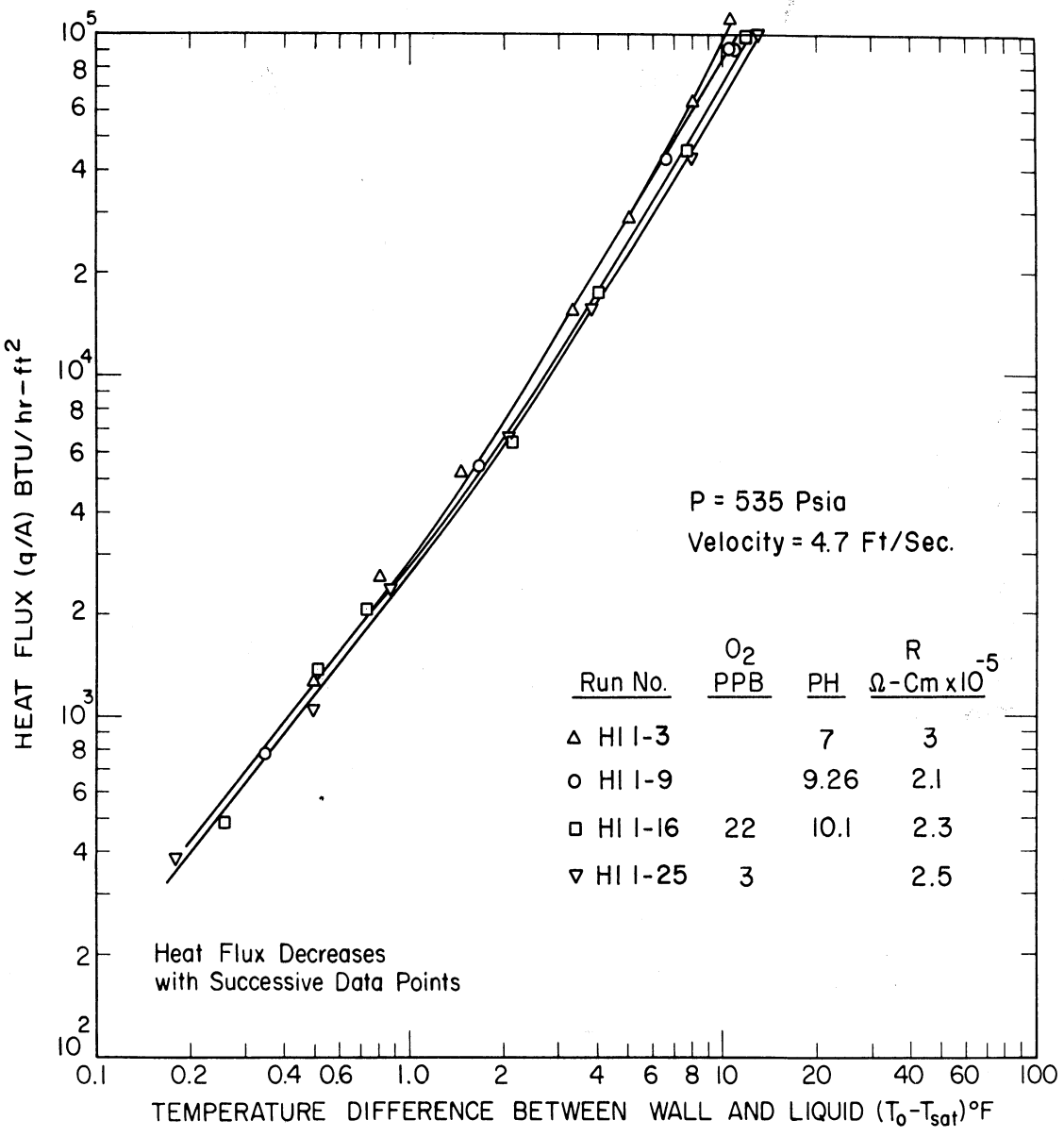

Fig. 14. Heat transfer to saturated distilled water flowing at 4.7 ft/sec and 535 psia, runs taken while developing water chemistry requirements.

The history of operation which resulted in Figs. 13 and 14 is such that a gradual reduction of the suspended solids level in the water was probable. Subsequent to the taking of these data a by-pass filter was installed and arrangements were made to sample the water to determine the quantitative level of suspended solids. With continuous circulation of the water at the desired test condition and filtering the flow in the by-pass loop it was possible to maintain the solids level at less than 40 PPB for the horizontal test sections and less than 70 PPB for the vertical test section.

The sampling filter is a 0.45 micron pore size disc element manufactured by Millipore or Gelman. The level of suspended solids is determined from a one-liter water sample passed through the filter. Two techniques were employed to evaluate the solids level from the filter sample. First, a weighing technique was used in which the weight of the dry filter element was determined before and after accumulating the sample. The accuracy of this technique using a chemical balance was poor with a small sample and it was abandoned. Second, a color comparison chart introduced by Mr. Fred Pocock of the Babcock and Wilcox Research Department, Alliance, Ohio, was used for direct comparison with the filter element.

The level of suspended solids was reduced to about 40 PPB at 535 psia and about 10 to 15 PPB at 1015 and 1550 psia. The dissolved oxygen level and pH were maintained at about 5 PPB and 9.5

respectively. Under these conditions good repeatability of the data has been established as will be shown in Section V, Test Results. With a "clean" system the lack of repeatability in the data as evidenced by the shift shown in Figs. 13 and 14 has not been encountered.

Tests were made to determine the effect of suspended solids level on the nucleate boiling characteristic curve. The results are shown in Figs. 15 and 16. It was not possible to establish and maintain as wide a range in suspended solids level as desired. However, the results show that as the solids level is increased the curve shifts to lower values of ΔT at a given flux.

This suggests the possibility of either bulk phase nucleation or surface nucleation or both existing as a consequence of a low level of suspended solids in the fluid. Should bulk phase nucleation exist it doubtless occurs in the superheated liquid in the boundary-layer near the surface. Some evidence of this occurrence was obtained from visual (photographic) observations made during one run, Fig. 63. In this instance thousands of small vapor bubbles were observed near and downstream from the heated surface. The liquid had been thoroughly degassed and subsequent tests disclosed that electrolysis was not responsible for the bubbles. While the results are somewhat inconclusive, it does seem reasonable to point to the possibility of suspended solids as the source of the bubbles.

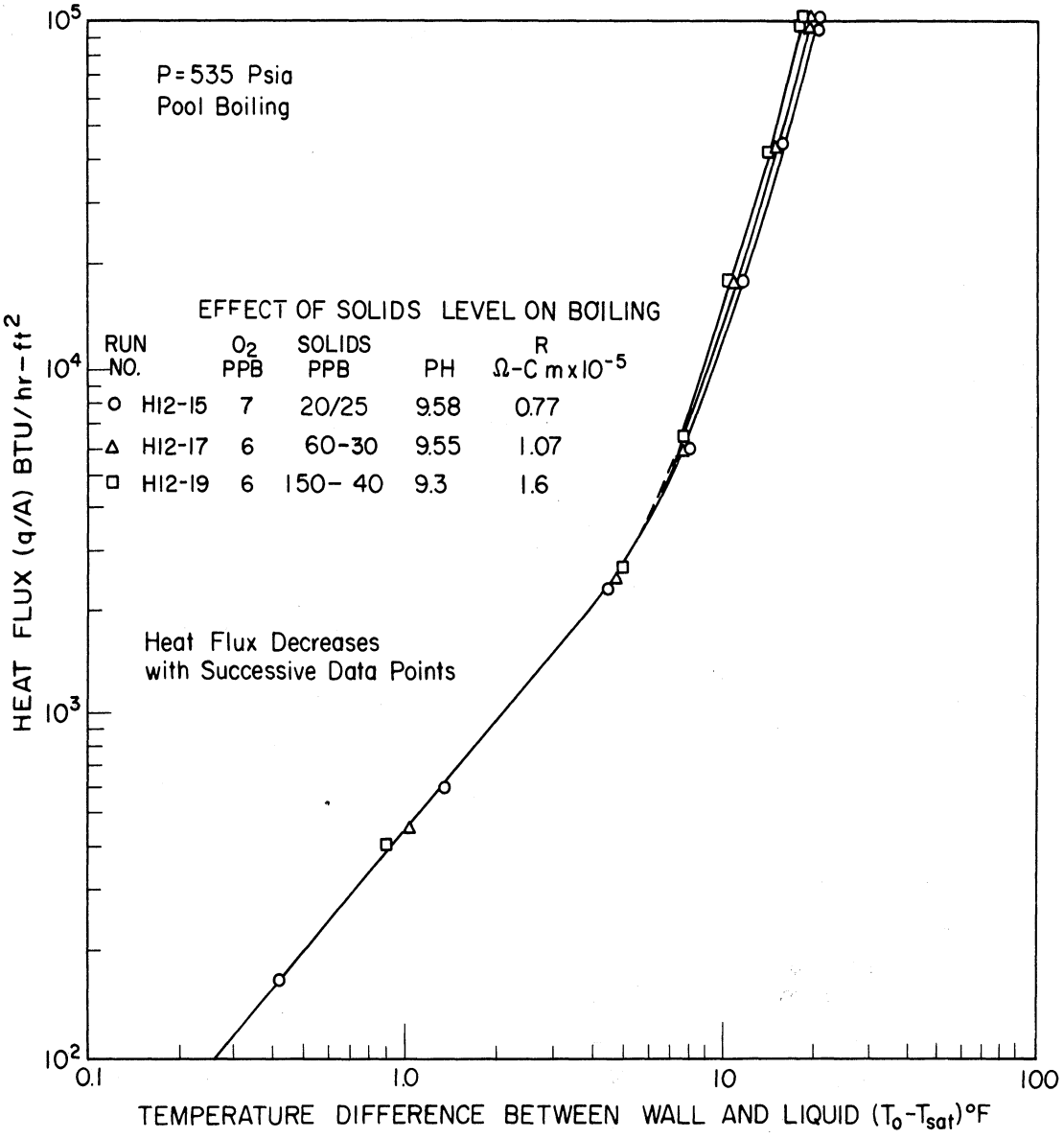

Fig. 15. Effect of suspended solids level on pool boiling saturated distilled water at 535 psia.

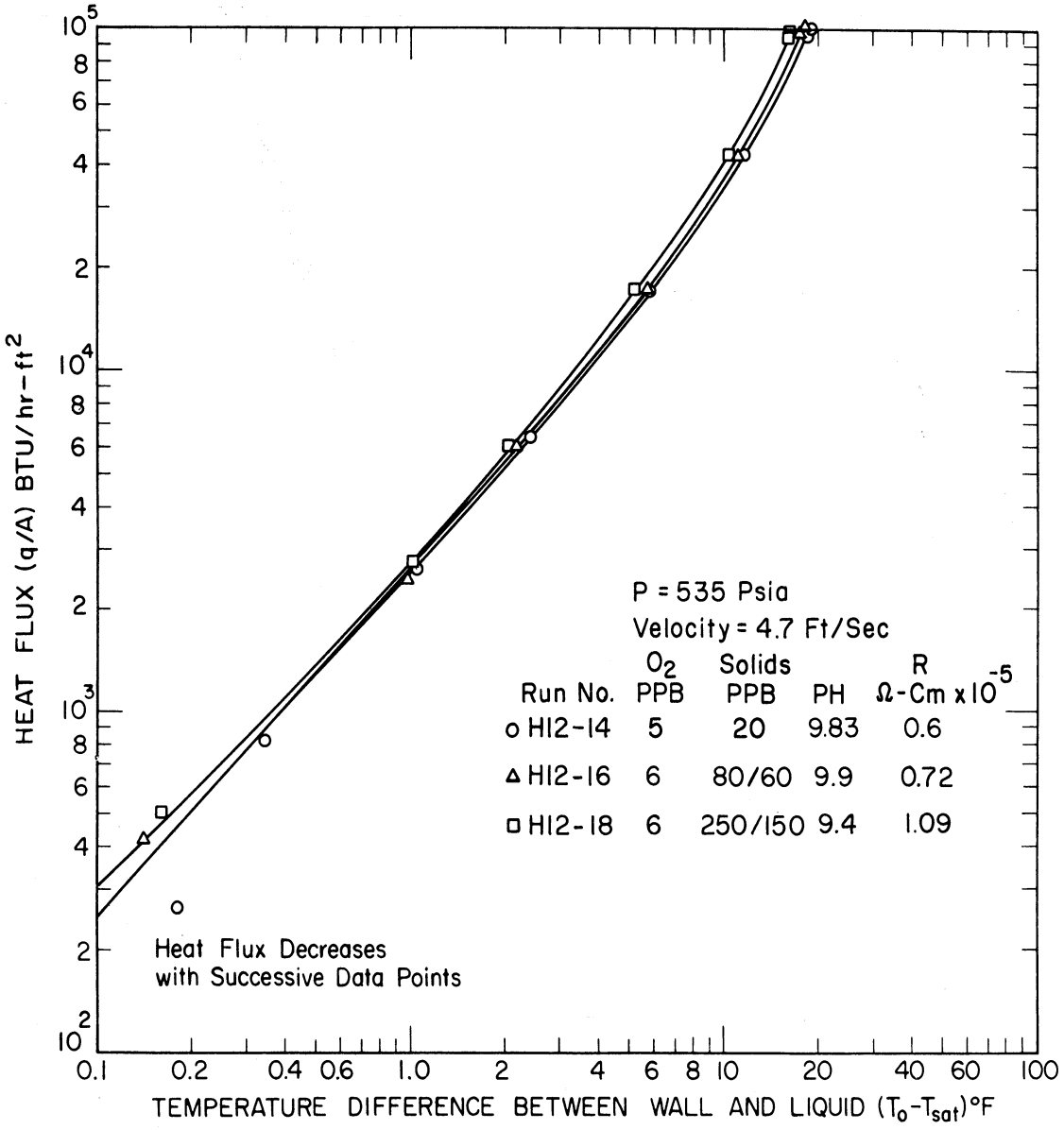

Fig. 16. Effect of suspended solids level on forced convection boiling saturated distilled water at 535 psia and 4.7 ft/sec velocity normal to test section.

There appears also the strong possibility that a "critical" level of suspended solids exists below which nucleation, and thus heat transfer rate, is promoted but above which surface contamination occurs. If this is true, the role of solids in the fluid introduces a new dimension into the problem of boiling heat transfer and cavitation.

V. TEST RESULTS

An experimental investigation was made of boiling high purity distilled water on the outside surface of a single 3/4 in. diameter tube. The heat flux range extends from the non-boiling convective heating region through incipient boiling to low values of heat flux in the nucleate boiling region. Experimental results are presented in the form of curves with heat flux plotted versus the difference between outside wall temperature and water saturation temperature. The investigation includes horizontal and vertical orientation of the tube. Tube materials were Monel, Inconel, and carbon steel with commercial finish as would be utilized in heat exchanger manufacture (See Table IV). Photographs were made of the boiling surface to provide a better understanding of the heat transfer mechanisms involved in low heat flux boiling. The data for the curves shown are included in Appendix C.

A difference in wall superheat has been noted[6, 8] at a given value of heat flux depending on whether the boiling condition is approached from a lower heat flux or from a higher heat flux. Hence, by starting at a low heat flux, increasing the heat flux progressively to the maximum value, then decreasing the heat flux in a like manner, a hysteresis is established as shown in Fig. 17. The position of the increasing heat flux curve depends on the prior history of the test

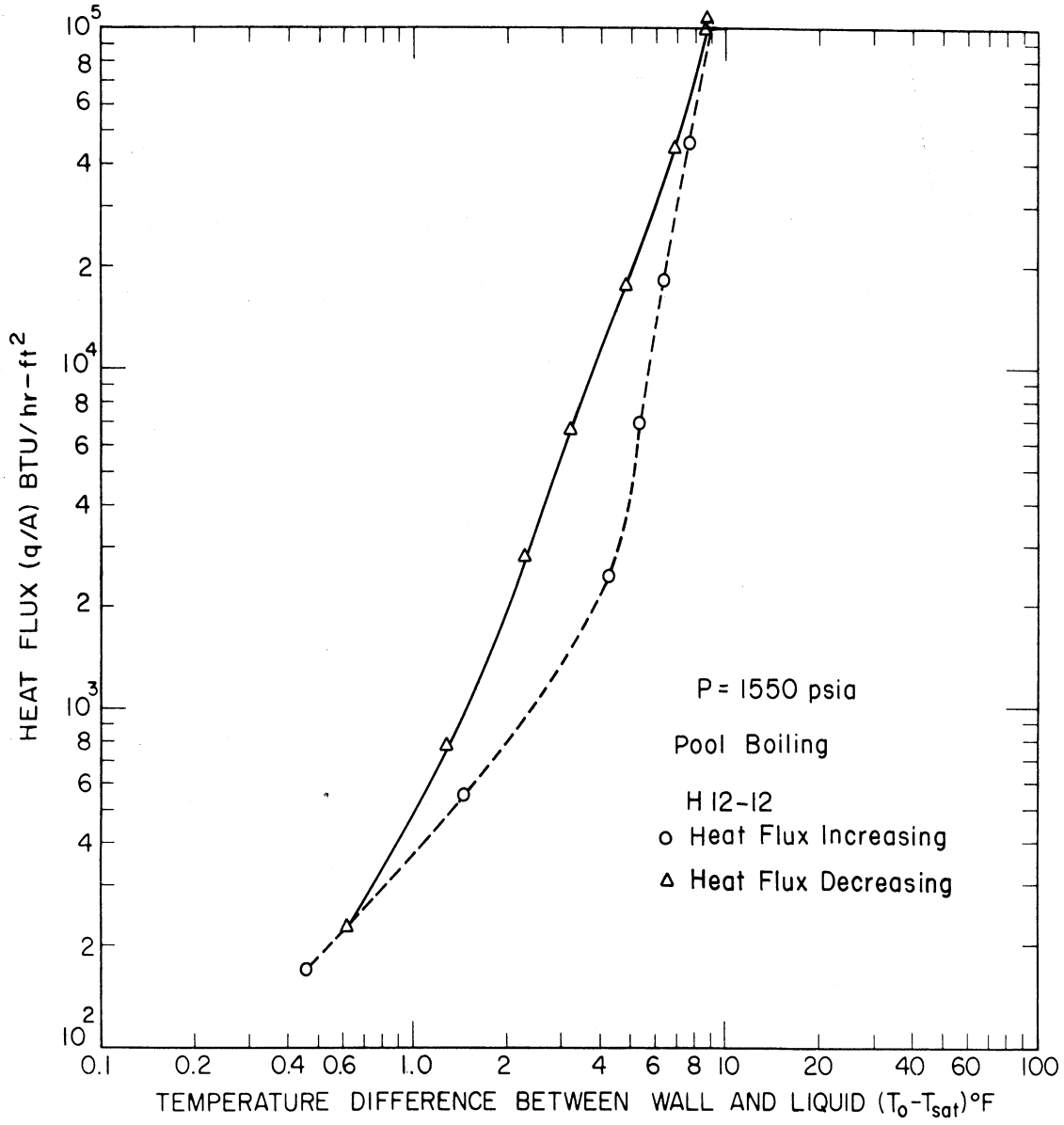

Fig. 17. Hysteresis effect in saturated pool boiling from horizontal Inconel tube at 1550 psia.

surface, whereas the position of the decreasing heat flux curve is stable for boiling water of high purity, as discussed in Section IV. All data used in the summary curves were taken when approached from a higher heat flux. Steady-state conditions were established at each test point prior to the recording of data.

In each series of test runs reproducibility of the data was established by repeating the conditions of most of the runs. The re-check runs were generally made two or more days later than the first run with runs at other test conditions in between. In one case, a repeat run was made immediately after the first run and a third run at the same condition was made two days later after an intervening run at another test condition. These runs, HI2-10, 11, 13, show very good repeatability (see Fig. 19).

A. HORIZONTAL TEST SECTIONS

1. Inconel

Two Inconel test sections were investigated. The first was used for the tests described in Section IV while establishing the water chemistry requirements to insure good reproducibility of test results. The thermocouple leads were damaged as it was being removed for examination so a second test section was used for the test runs described below.

The heat transfer characteristics of the Inconel tube under forced convection conditions are shown in Fig. 18. The effect of pressure is shown with two runs each at 535, 1015, and 1550 psia. As the pressure is increased, the position of the curve shifts to a lower value of ΔT as has been found by others. The curves converge to a single curve in the non-boiling range as would be expected. Nucleation appears to begin at lower values of q/A and ΔT as the pressure is increased. This is indicated by the increase in slope of the curves at lower ΔT as the pressure is increased.

The results of pool boiling studies with the Inconel test section are summarized in Fig. 19. The effect of pressure is shown to be greater than in the case with forced convection. However, as in forced convection, the curves converge to a single curve in the non-boiling region. The point of incipient boiling is more clearly defined for pool boiling, and also occurs at lower ΔT for increased pressure.

A comparison of forced convection and pool boiling heat transfer characteristics is given in Figs. 20, 21, and 22, each figure for a different pressure. The data from Figs. 18 and 19 were used for these figures. The effect of forced convection in increasing the heat flux at a given temperature difference is apparent. The steeper slope of the pool boiling curve in the non-boiling region is more clearly evident in Fig. 20. The pool boiling curve retains a steeper slope

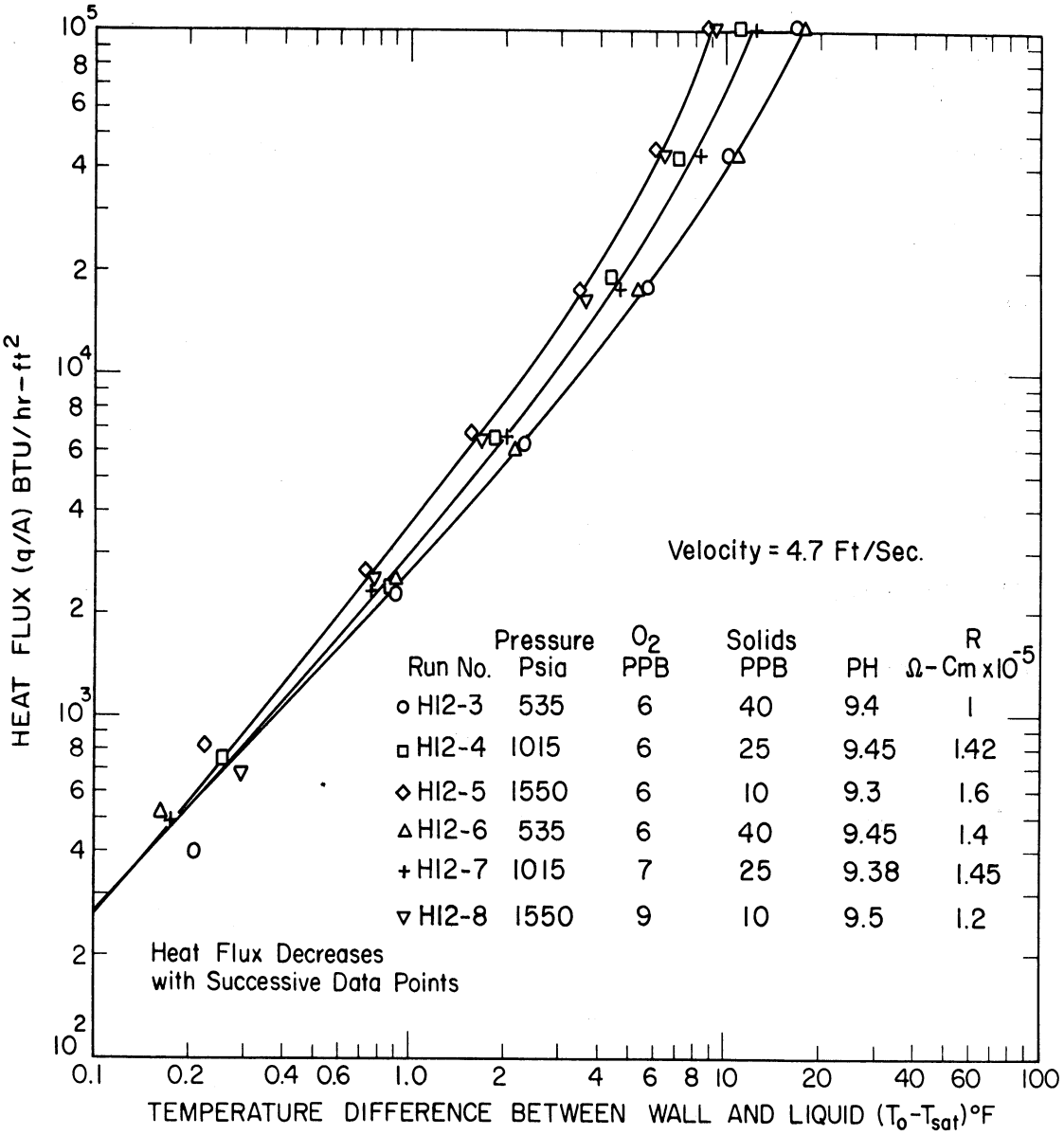

Fig. 18. Boiling of saturated distilled water flowing at 4.7 ft/sec normal to 3/4 in. O.D. Inconel tube, showing effect of pressure.

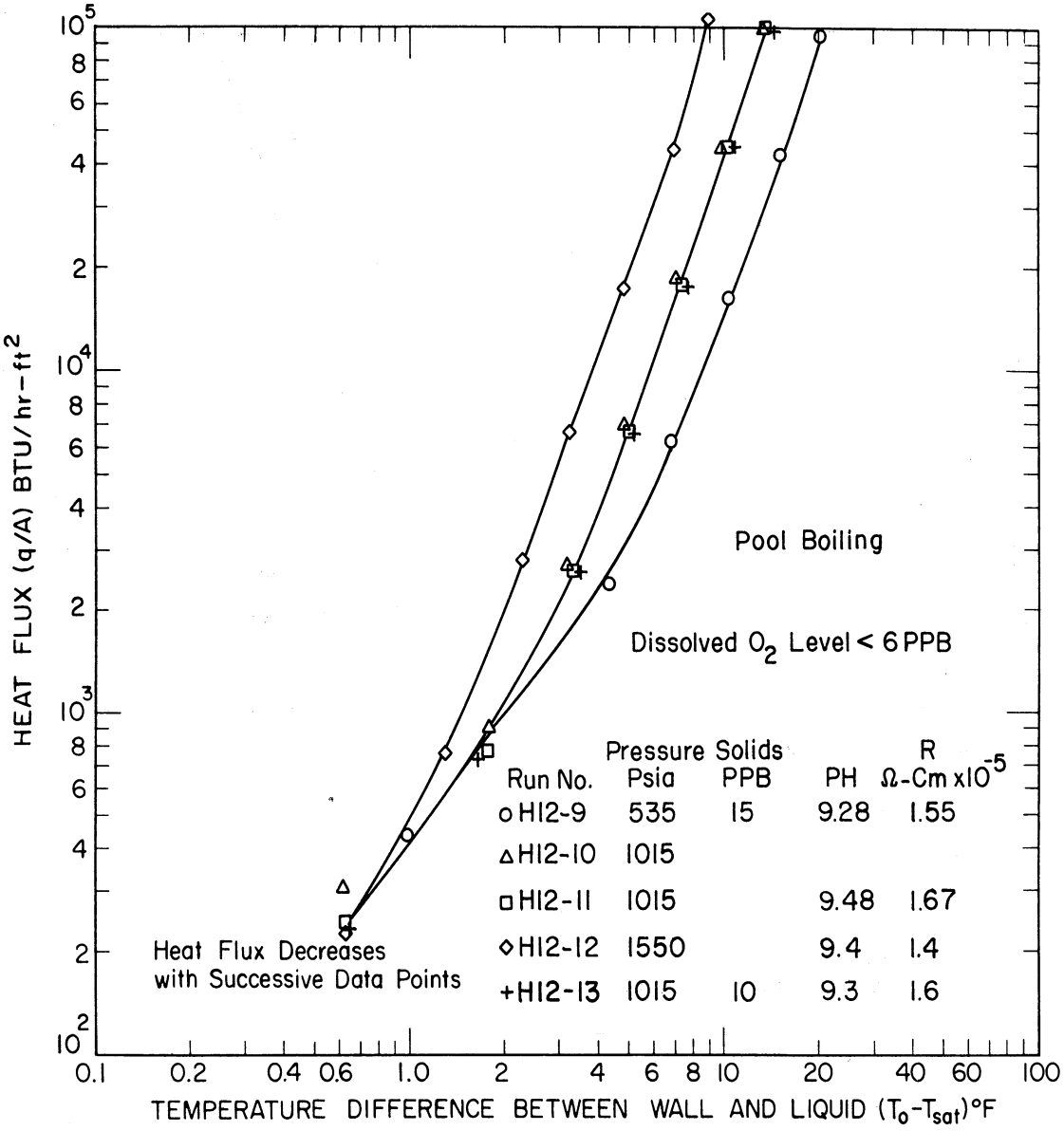

Fig. 19. Pool boiling of saturated distilled water on outside surface of 3/4 O.D. Inconel tube, showing effect of pressure.

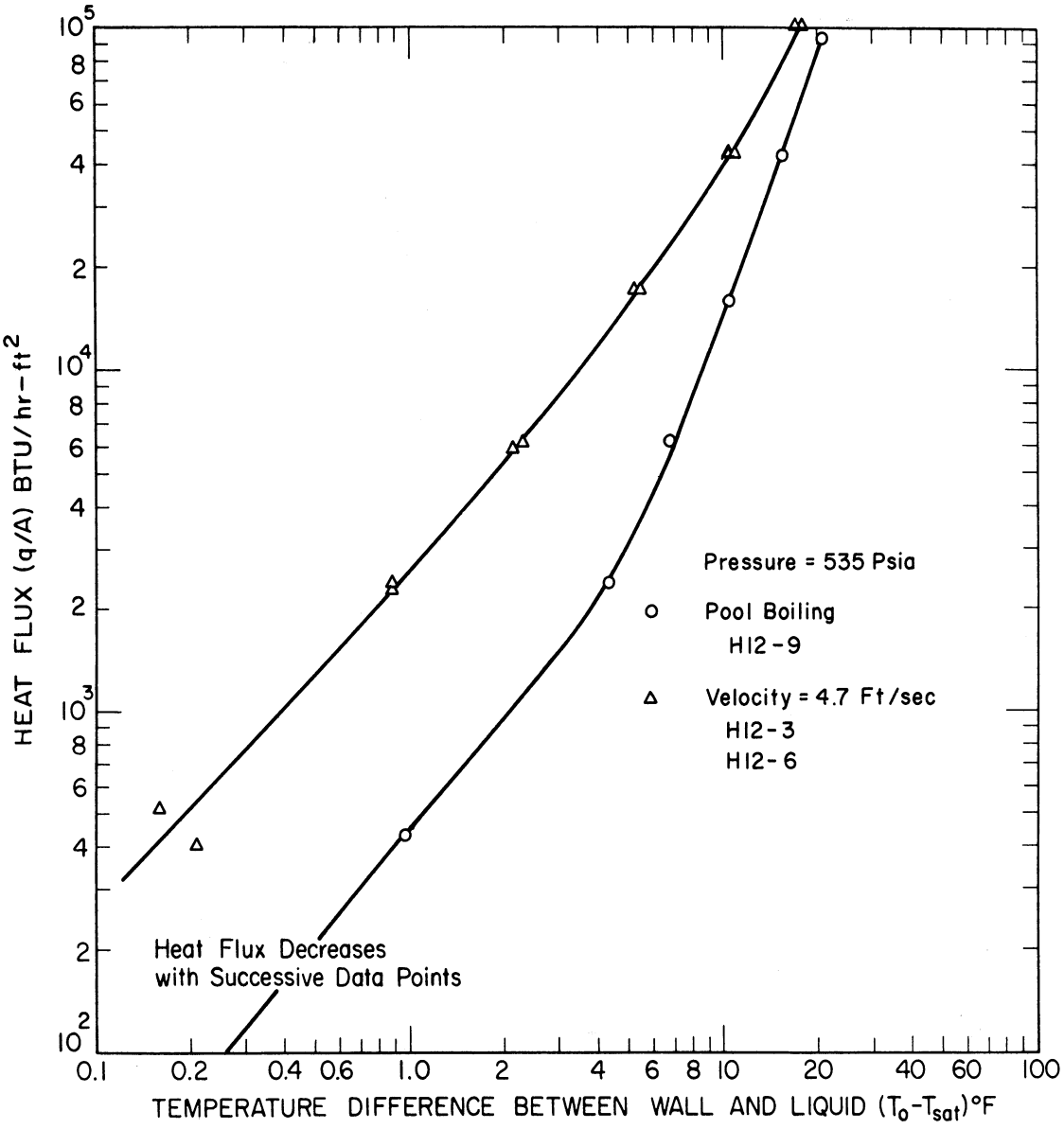

Fig. 20. Comparison of forced convection and pool boiling saturated distilled water at 535 psia, horizontal Inconel tube.

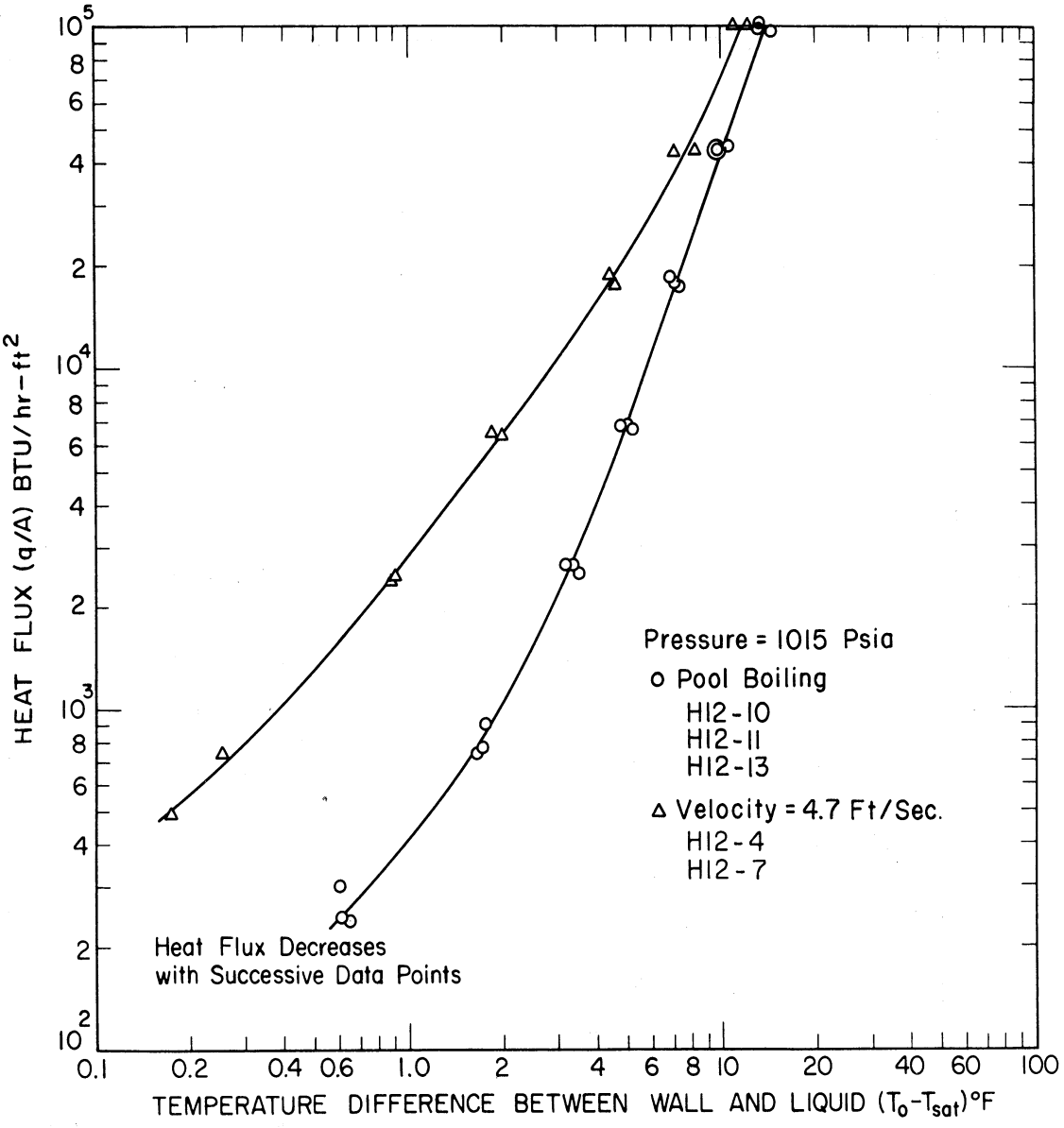

Fig. 21. Comparison of forced convection and pool boiling saturated distilled water at 1,015 psia, horizontal Inconel tube.

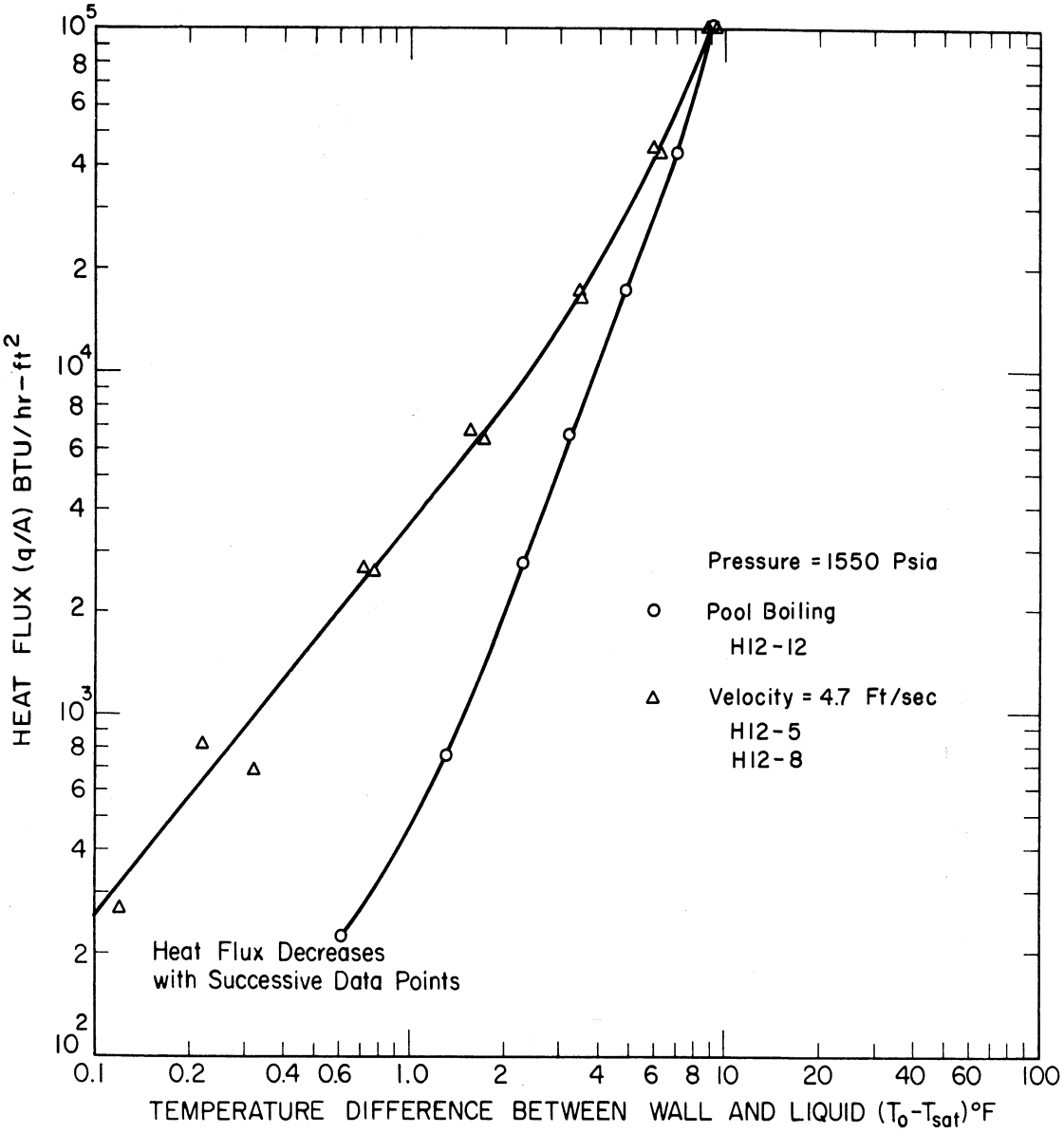

Fig. 22. Comparison of forced convection and pool boiling of saturated distilled water at 1,500 psia, horizontal Inconel tube.

than the forced convection curve in the nucleate boiling region up to the highest heat flux investigated. As the pressure increases the influence of forced convection on the relative position of the characteristic curve becomes less. At 1550 psia the curves converge at 100,000 Btu/hr-ft^2. The effect of varying forced convection velocity on the convergence was not investigated but from the work of others,[15] the point of convergence for a fixed pressure would occur at successively higher heat flux as the velocity is increased.

2. Carbon Steel

A summary of forced convection studies with a carbon steel test section is presented in Fig. 23. The seven test runs include good repeatability checks. A single curve would represent the three pressures in the non-boiling region very well and within the accuracy of the data. The slight shift of data to higher ΔT at a given heat flux as the suspended solids level is reduced is evident in the nucleate boiling region for 535 and 1550 psia. As for the Inconel test section, the beginning of nucleation occurs at lower ΔT as the pressure increases and the pressure effect continues to the maximum heat flux investigated.

The pool boiling characteristics established for a carbon steel test section are shown in Fig. 24. The repeatability for recheck runs is very good. The curves converge in the non-boiling region and the pressure effect on incipient nucleation is shown.

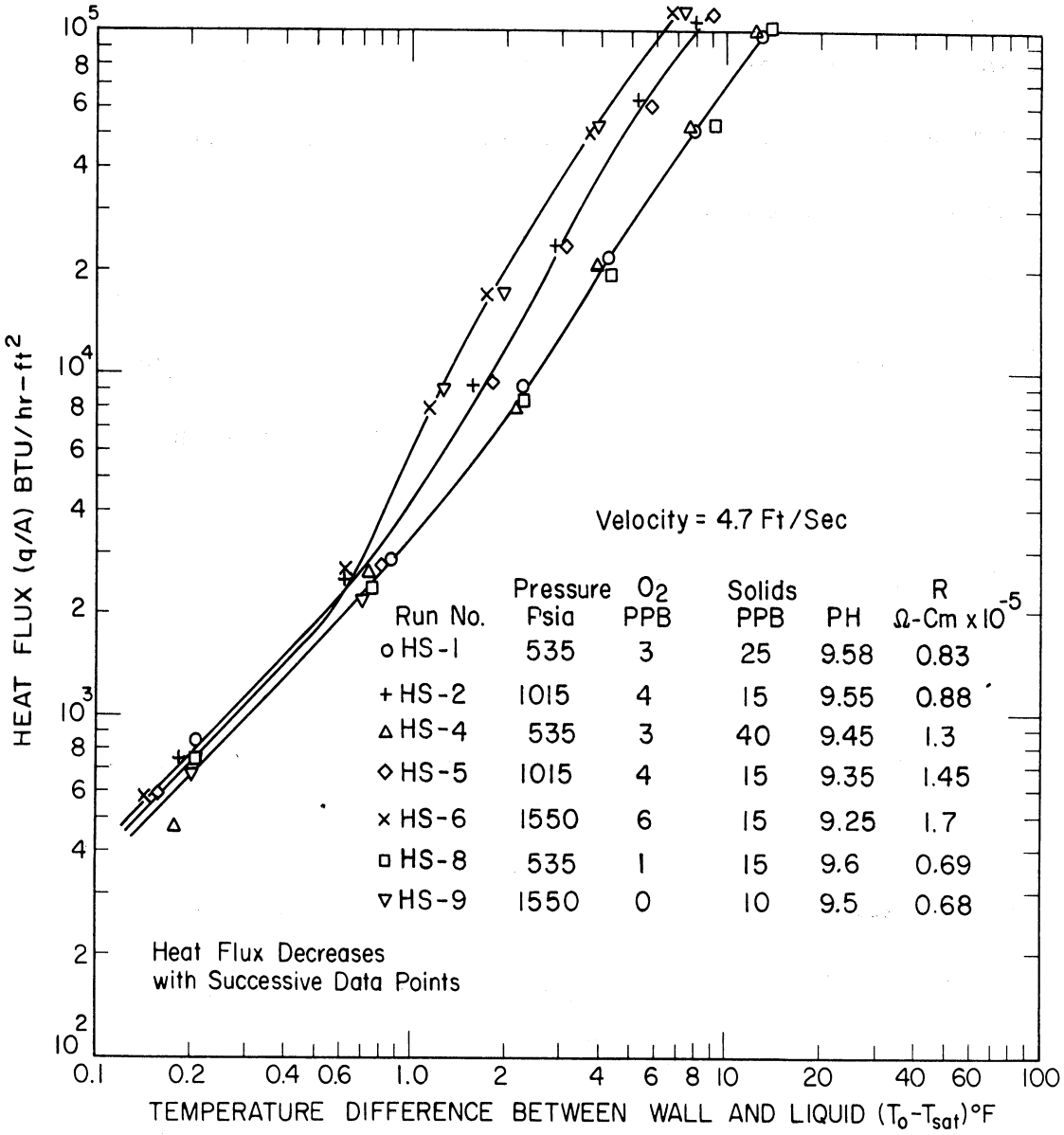

Fig. 23. Boiling of saturated distilled water flowing at 4.7 ft/sec normal to 3/4 in. O.D. carbon steel tube, showing effect of pressure.

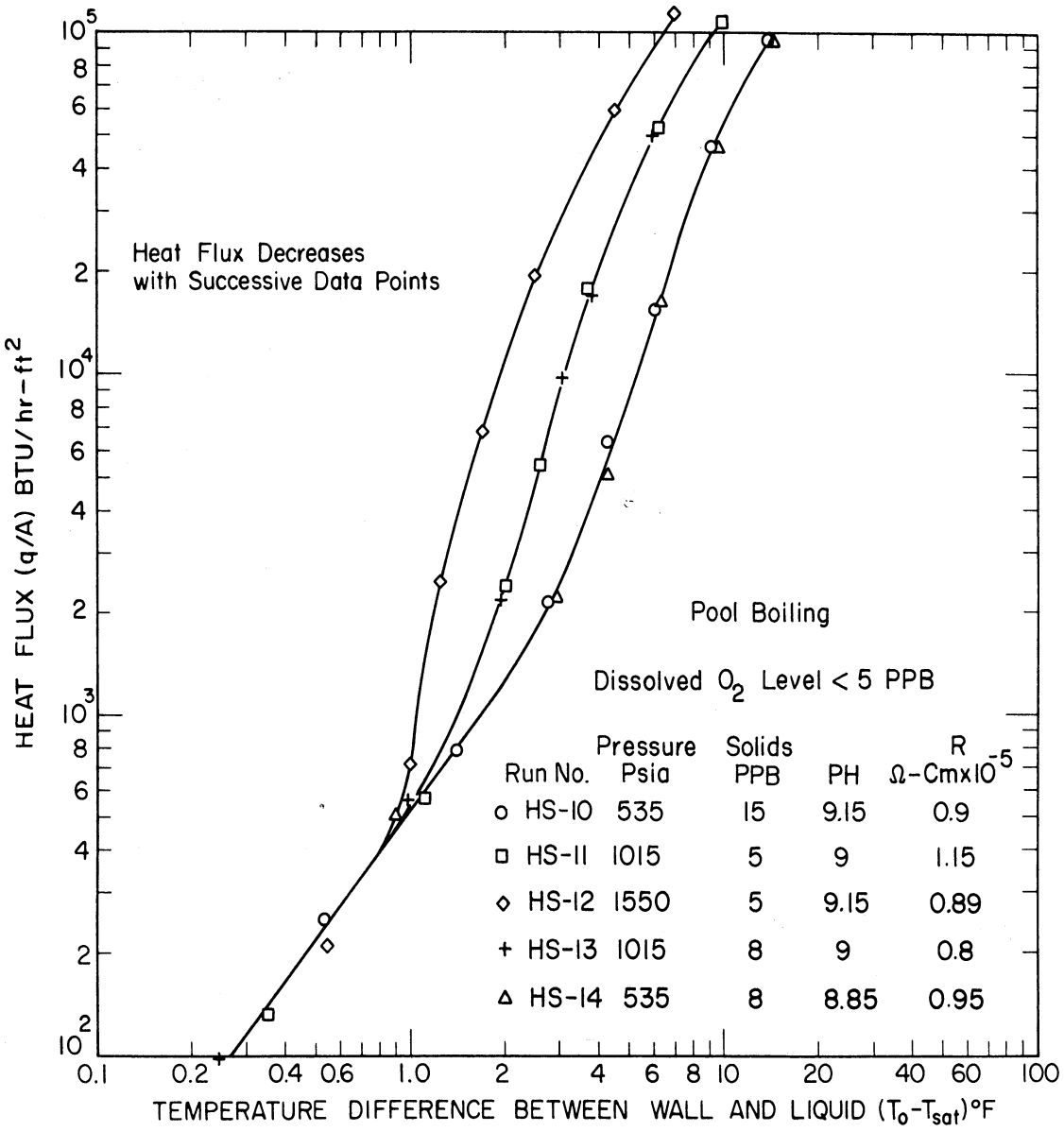

Fig. 24. Pool boiling of saturated distilled water on outside surface of 3/4 in. O.D. carbon steel tube, showing effect of pressure.

Forced convection and pool boiling effects are compared at pressures of 535, 1015, and 1550 psia in Figs. 25, 26, and 27, respectively. The data from Figs. 23 and 24 were used to establish these curves. These curves, like those for Inconel, show the steeper slope for pool boiling in both the non-boiling free convection region and the nucleate boiling region up to the highest flux investigated. They also converge in the vicinity of 100,000 Btu/hr-ft^2.

3. Monel

Heat transfer characteristics for a horizontal Monel test section under forced convection conditions are summarized in Fig. 28. An increase of pressure has a pronounced effect on the relative position of characteristic curve in the nucleate boiling region. However, in the non-boiling region a single curve represents the data for the pressure range from 535 to 1550 psia as expected. The incipient boiling point appears to shift to lower values of ΔT as the pressure is increased and the transition from non-boiling to boiling occurs gradually. Reproducibility of the data at each pressure is seen to be very good.

Pool boiling heat transfer characteristics are summarized in Fig. 29. Pressure has a marked influence on the relative position of the nucleate boiling curve as was found with forced convection. A single curve represents the data for the entire pressure range in the

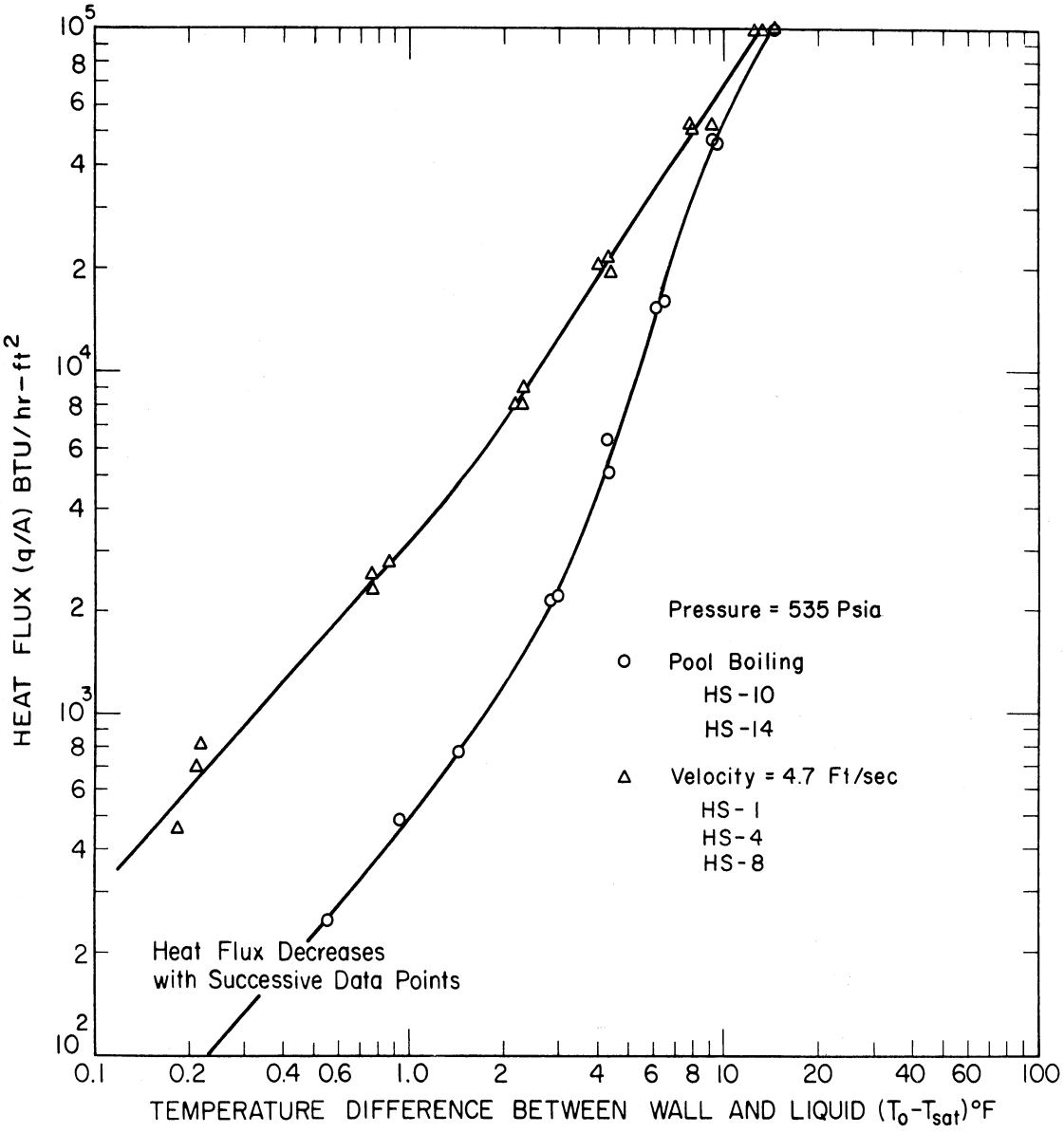

Fig. 25. Comparison of forced convection and pool boiling saturated distilled water at 535 psia, horizontal carbon steel tube.

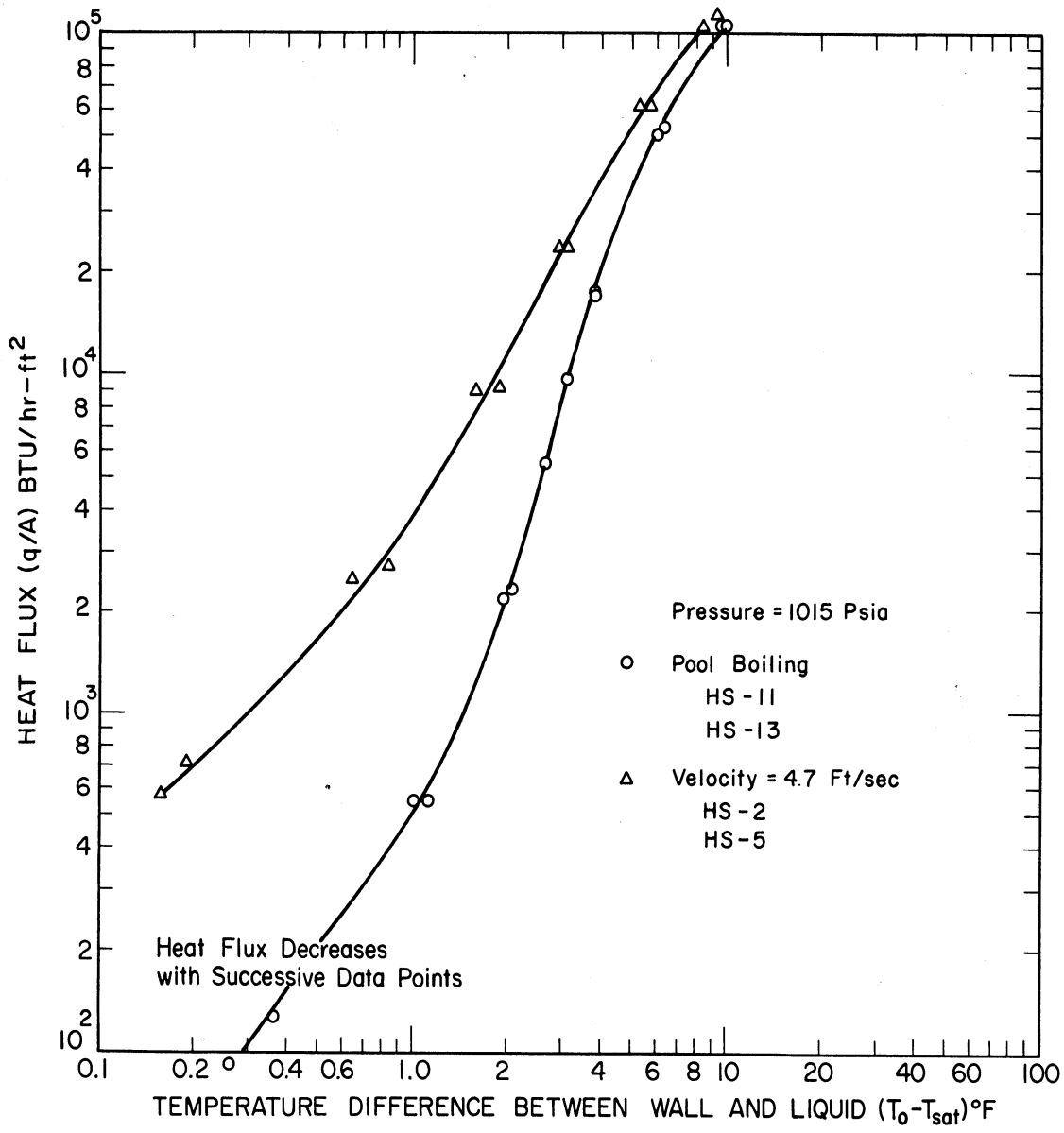

Fig. 26. Comparison of forced convection and pool boiling saturated distilled water at 1,015 psia, horizontal carbon steel tube.

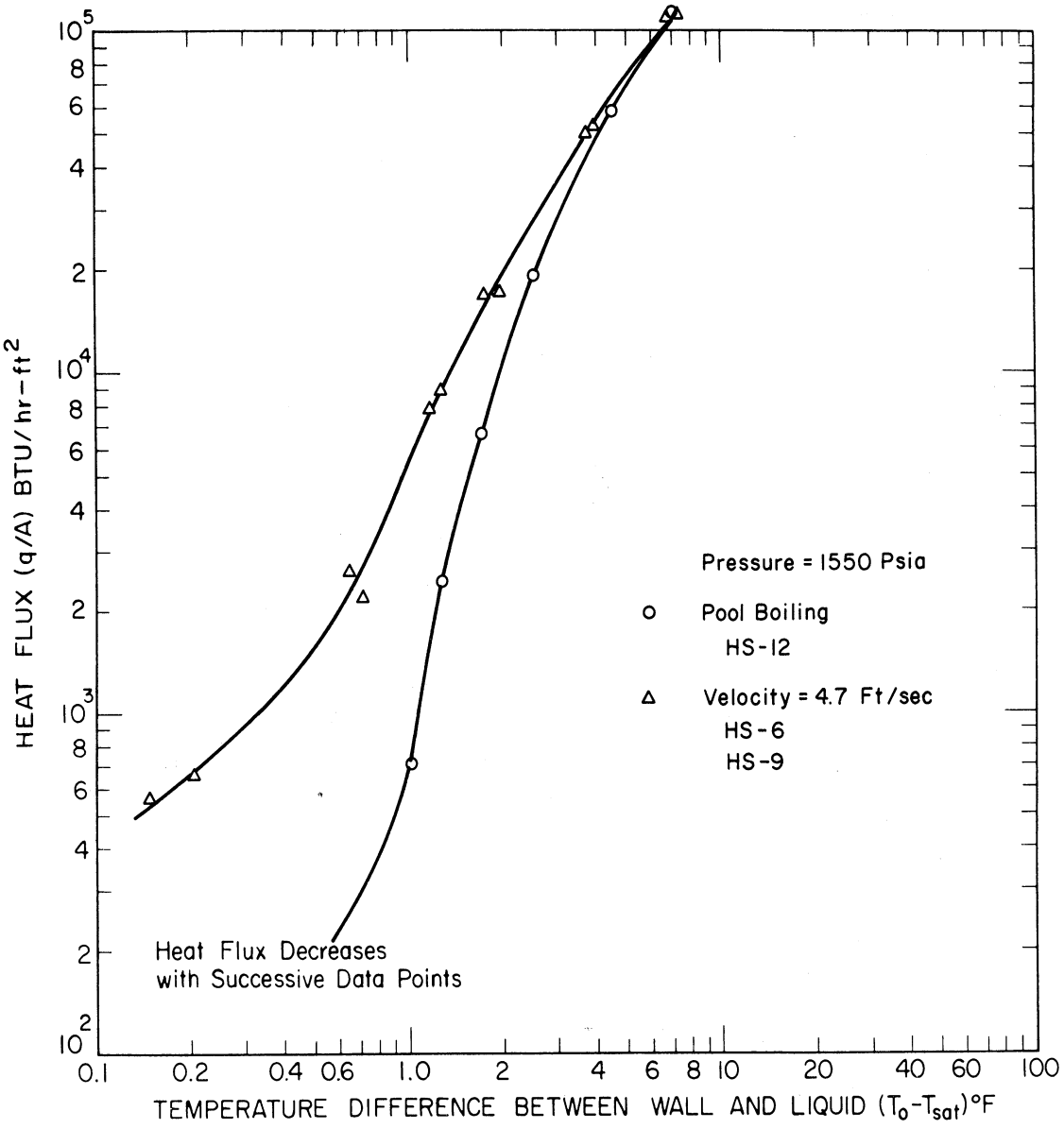

Fig. 27. Comparison of forced convection and pool boiling saturated distilled water at 1,550 psia, horizontal carbon steel tube.

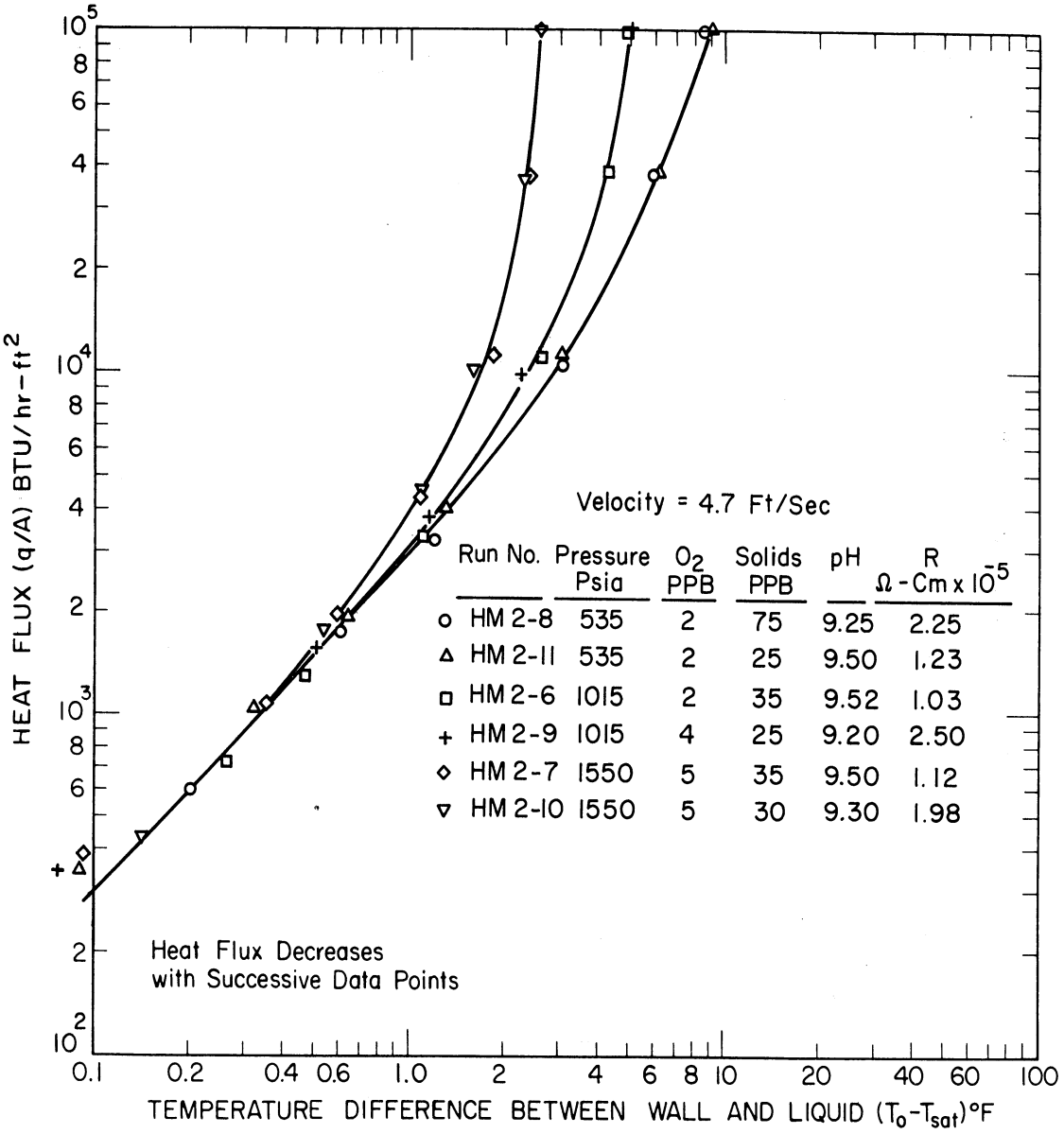

Fig. 28. Effect of pressure on boiling of saturated distilled water flowing at 4.7 ft/sec normal to 3/4 in. O.D. Monel tube.

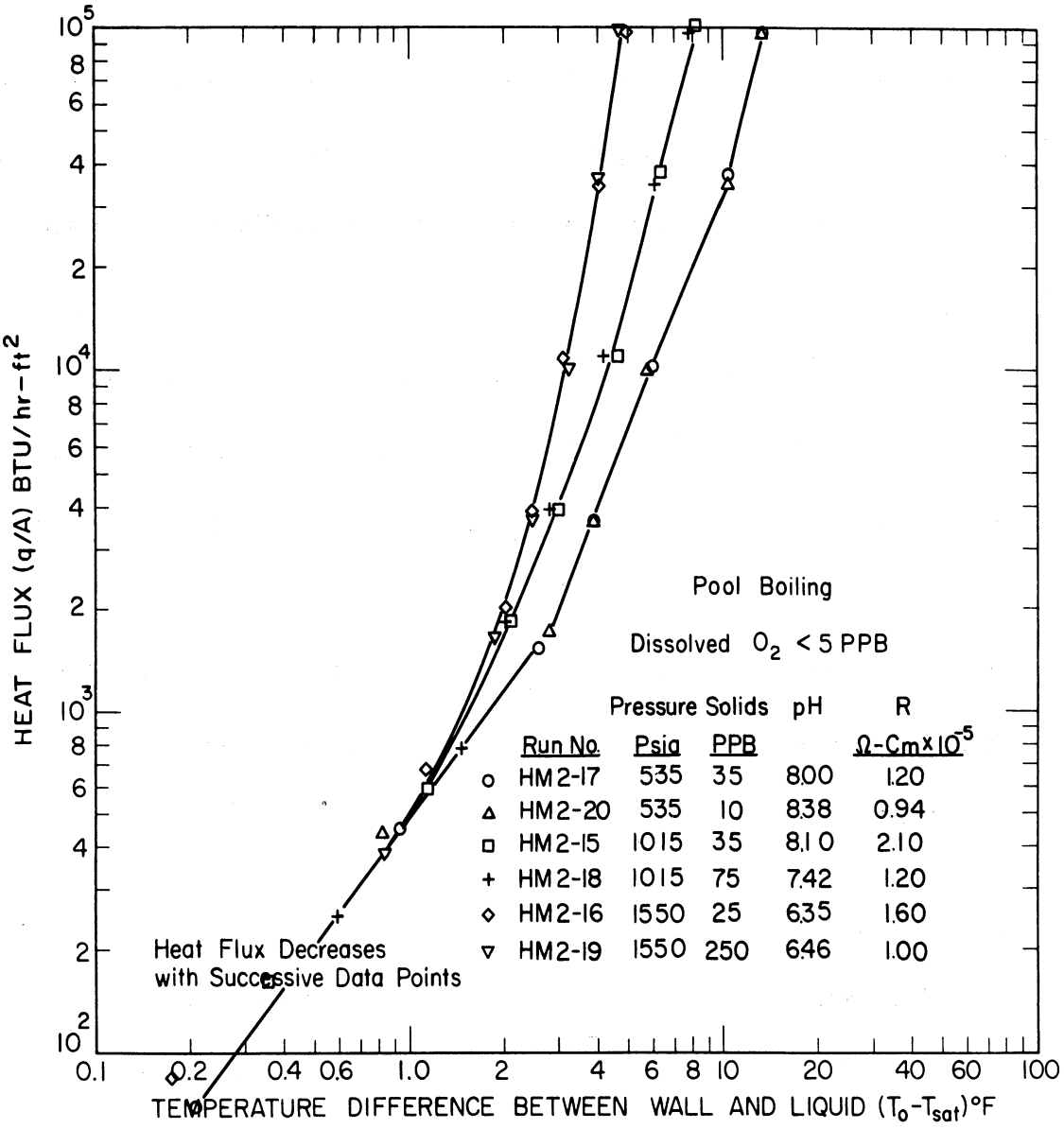

Fig. 29. Effect of pressure on pool boiling saturated distilled water on outside surface of 3/4 in. O.D. Monel tube.

non-boiling region. Transition from non-boiling to boiling appears to occur within a smaller range of heat flux than in the forced convection case. Reproducibility of the data is good, especially so at 535 and 1015 psia.

The effect of velocity on the heat transfer data for the Monel tube at 535, 1015, and 1550 psia is shown in Figs. 30, 31, and 32, respectively. The result of forced convection is to shift the curve to a higher heat flux at a given ΔT as found for Inconel and carbon steel. However, contrary to the results for the other materials, the influence of forced convection does not diminish as the pressure is increased.

4. Comparison of Materials

A comparison can be made of the heat transfer characteristics of horizontal Monel, Inconel, and carbon steel test sections. A vertical test section was investigated for only the Monel material but it is expected that the material comparison would be about the same if it were based on vertical tube data. As indicated in Appendix B, some error is possible in the curves due to instrumentation accuracy and uncertainties in material properties. However, the total error is less than the difference between the curves so a comparison is considered appropriate.

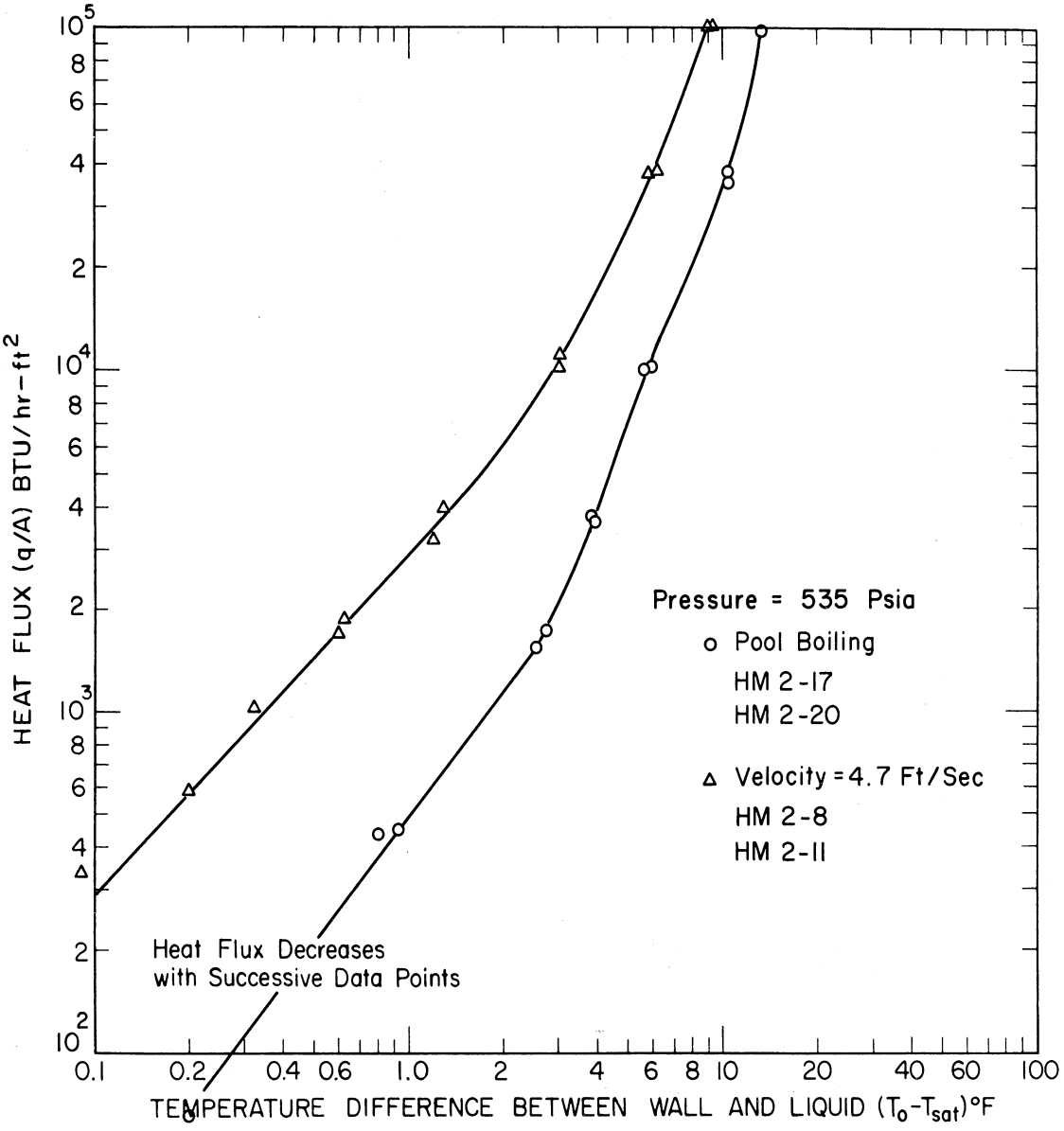

Fig. 30. Comparison of forced convection and pool boiling saturated distilled water at 535 psia, horizontal Monel tube.

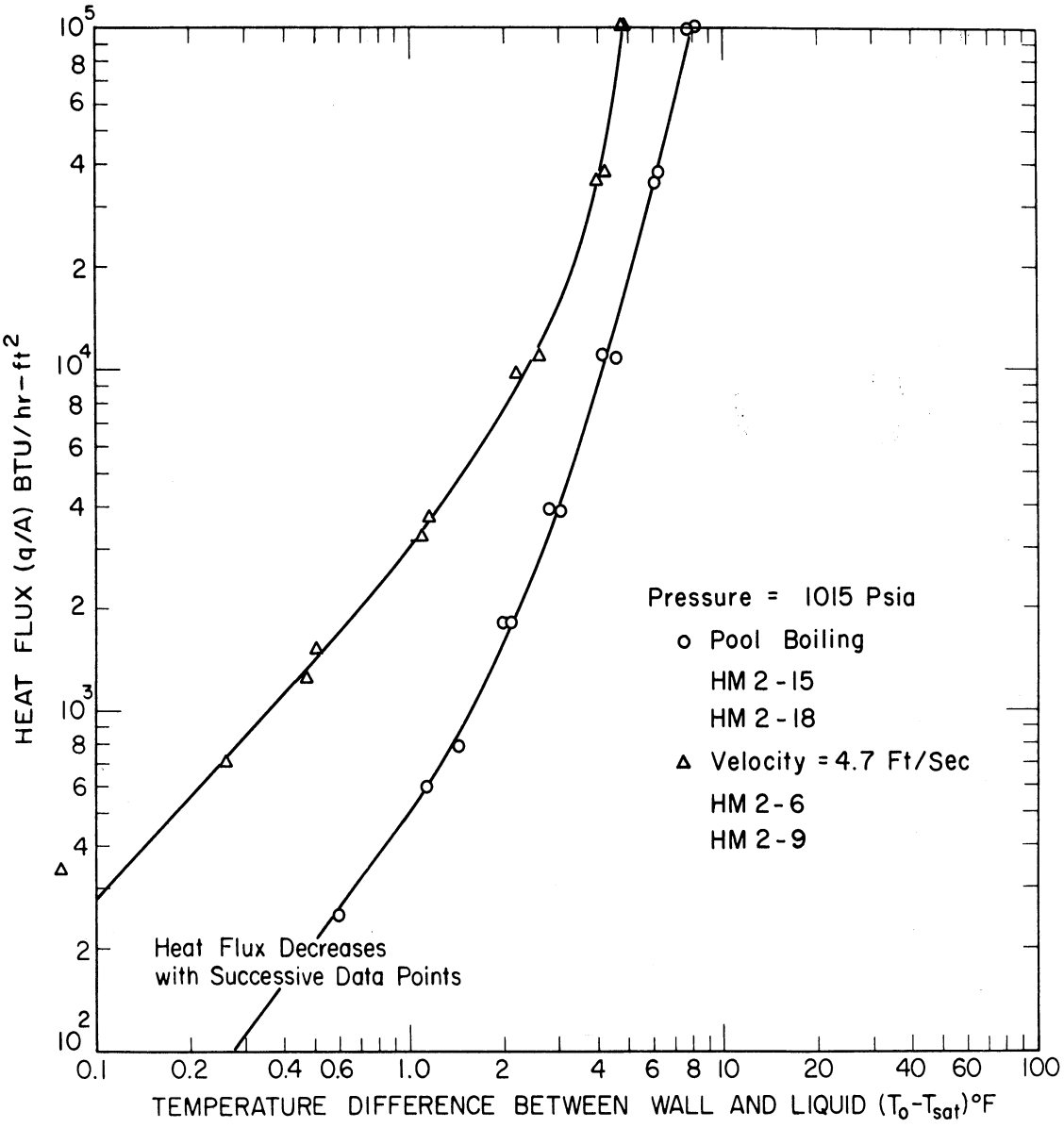

Fig. 31. Comparison of forced convection and pool boiling saturated distilled water at 1,015 psia, horizontal Monel tube.

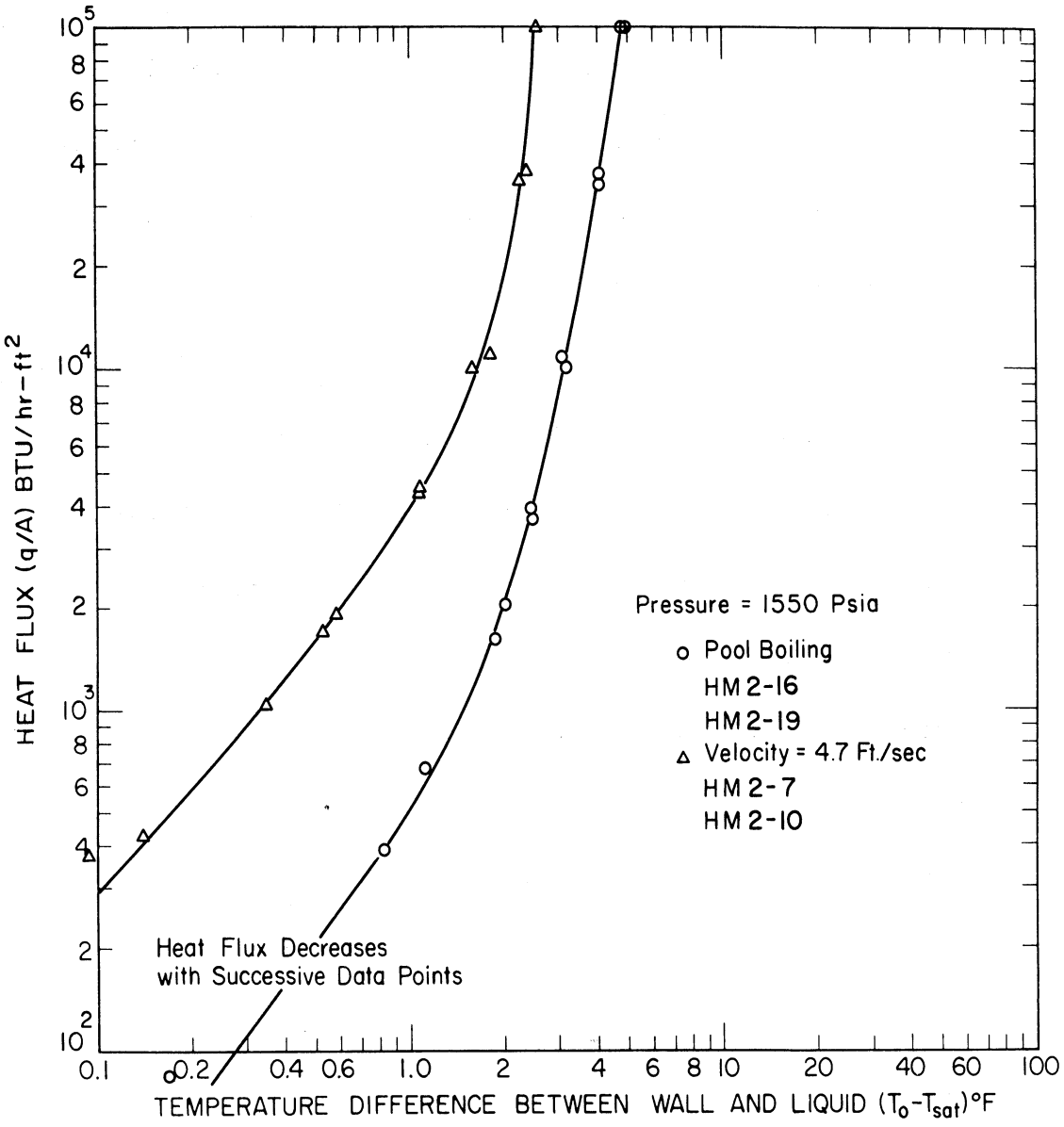

Fig. 32. Comparison of forced convection and pool boiling saturated distilled water at 1,550 psia, horizontal Monel tube.

The characteristic curves for forced convection conditions are presented in Figs. 33, 34, and 35 at 535, 1015, and 1550 psia, respectively. The general appearance of the curves is the same at different pressures so they are discussed as a group.

Some variation of heat flux at a given ΔT exists in the non-boiling region, the data for carbon steel being slightly higher than that for Monel and Inconel. The variation diminishes with pressure increase and disappears at 1550 psia. A single curve could replace the three individual curves with an accuracy of $\pm$ 10%. The slope of the curves is about the same and nearly equal to 1, as would be expected for high Reynolds numbers.

Incipient nucleation is seen at progressively higher ΔT and heat flux for carbon steel, Monel, and Inconel in that order. In the nucleate boiling region the slopes of the curves for the materials are quite different. The slope of the Inconel curves gradually increases with increased heat flux. The Monel curves have a much larger increase of slope as the heat flux is increased but their general shape is similar to those for Inconel. The curves for carbon steel, however, have an opposite curvature; the slope of the curves decreases with increase of heat flux. These effects are accentuated with increase in pressure.

The pool boiling characteristics of the materials are compared in Figs. 36, 37, and 38 at 535, 1015, and 1550 psia. They will be

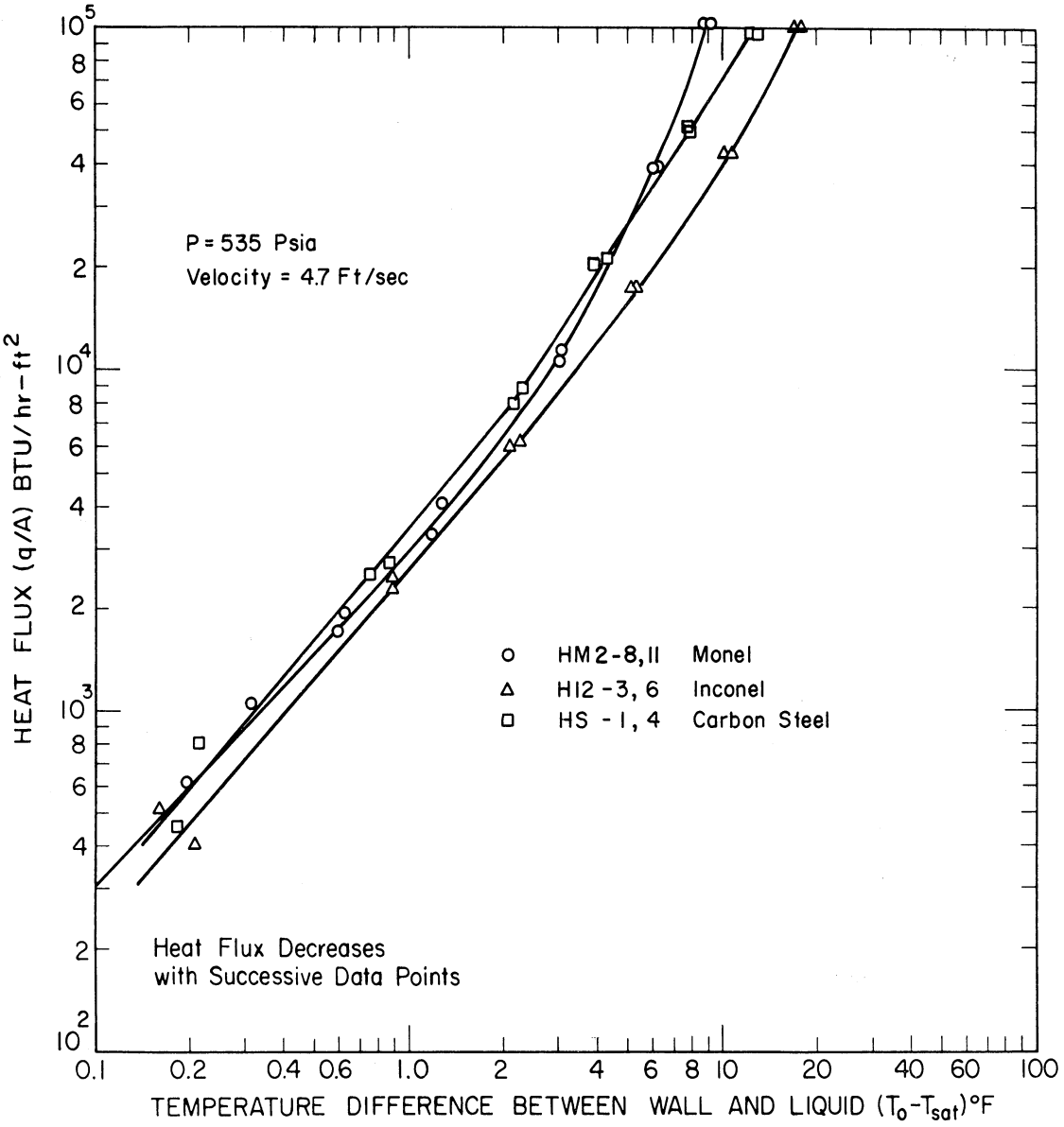

Fig. 33. Forced convection boiling of saturated distilled water from outside surface of horizontal Inconel, carbon steel and Monel tubes at 535 psia, 4.7 ft/sec.

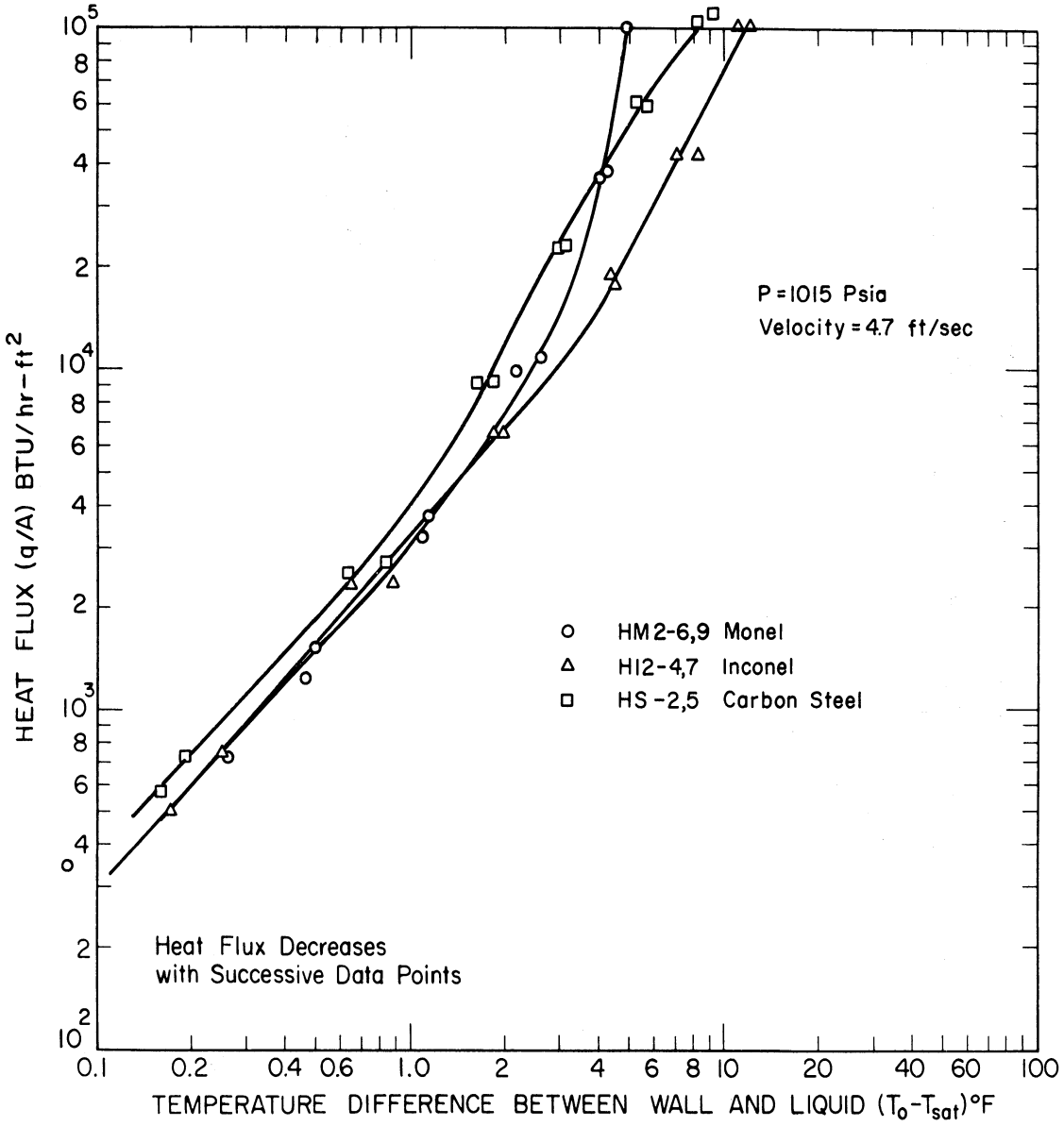

Fig. 34. Forced convection boiling of saturated distilled water from outside surface of horizontal Inconel, carbon steel and Monel tubes at 1,015 psia, 4.7 ft/sec.

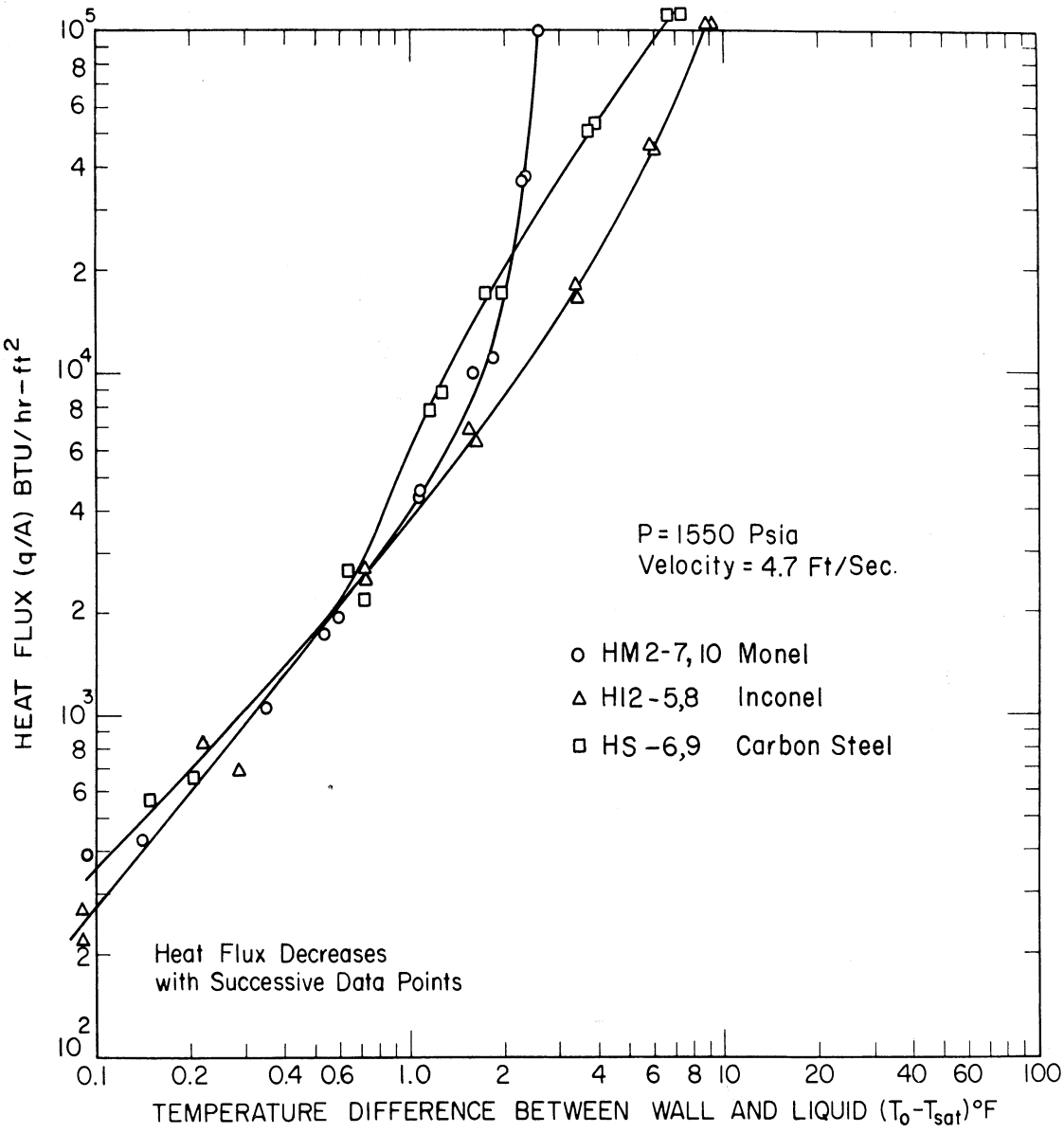

Fig. 35. Forced convection boiling of saturated distilled water from outside surface of horizontal Inconel, carbon steel and Monel tubes at 1,550 psia, 4.7 ft/sec.

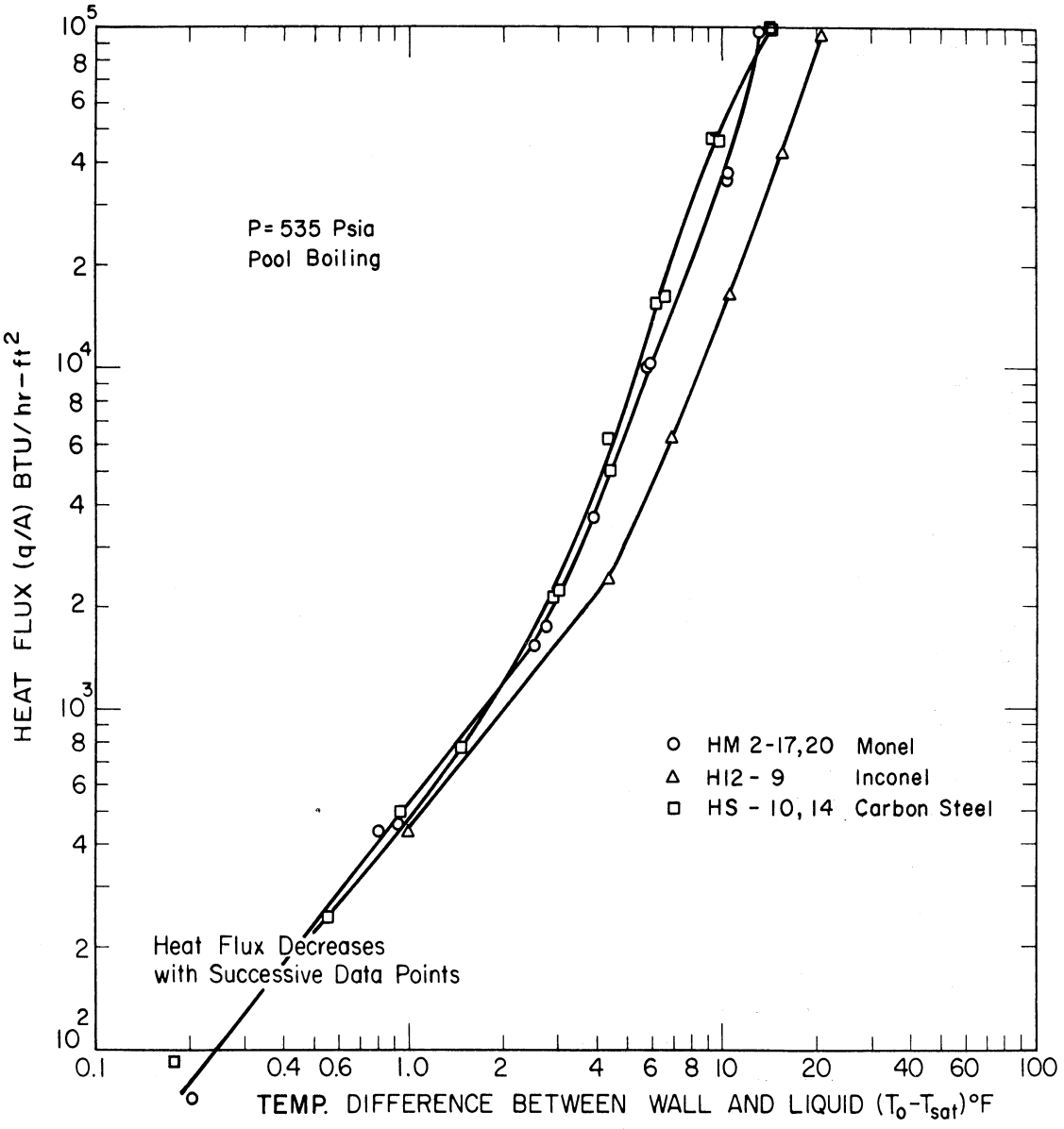

Fig. 36. Pool boiling of saturated distilled water from outside surface of horizontal Inconel, carbon steel and Monel tubes at 535 psia.

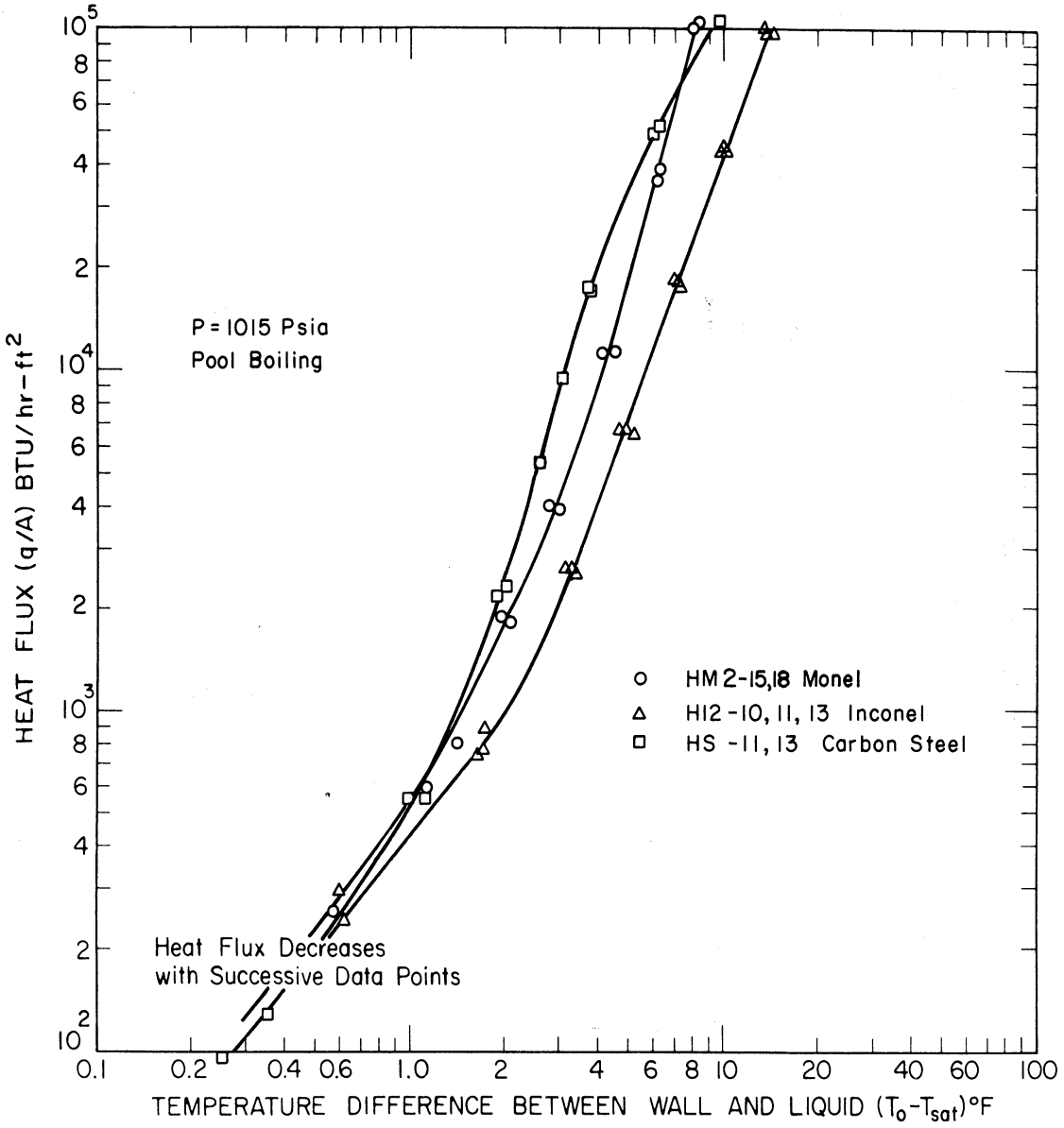

Fig. 37. Pool boiling of saturated distilled water from outside surface of horizontal Inconel, carbon steel, and Monel tubes at 1,015 psia.

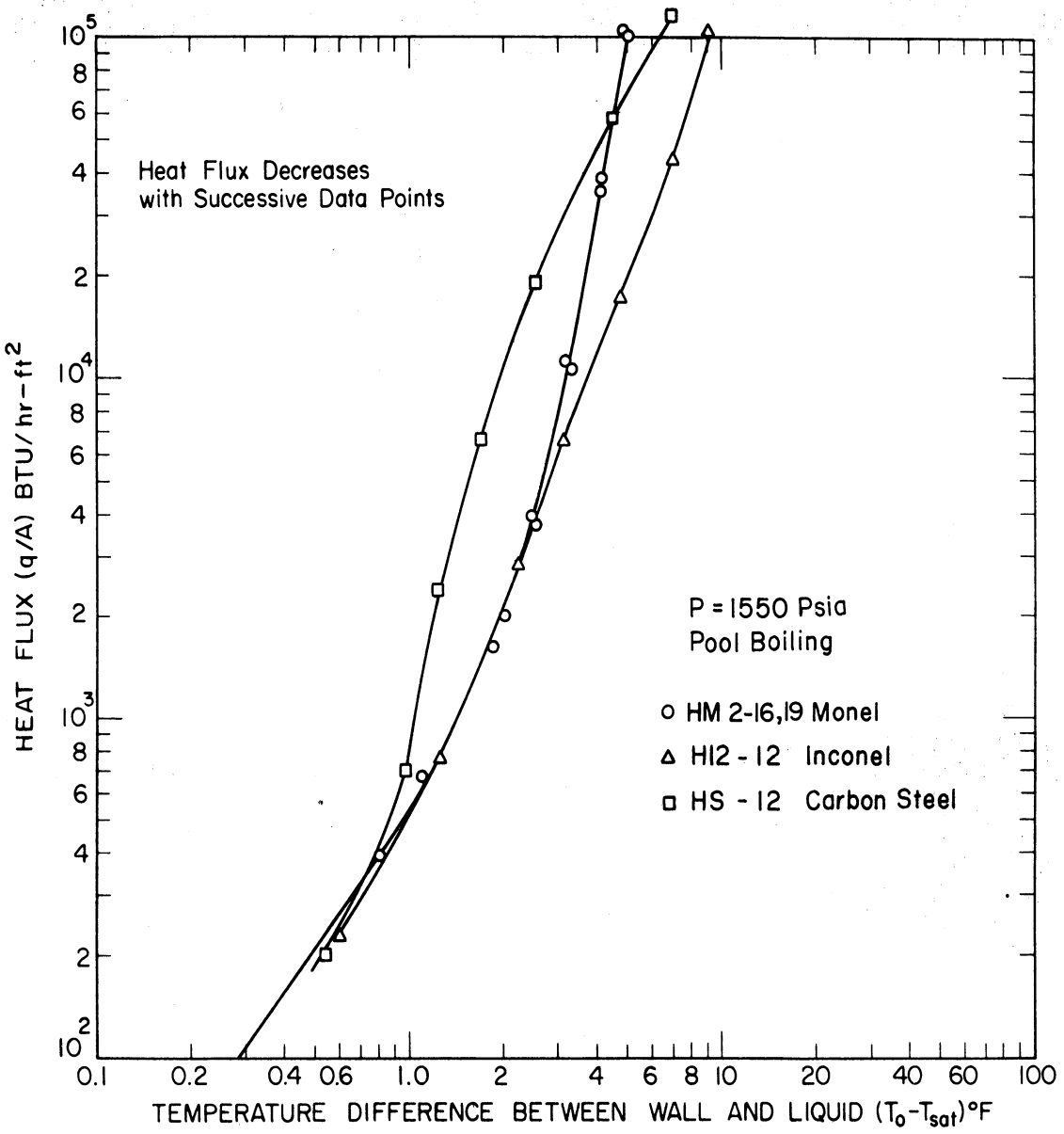

Fig. 38. Pool boiling of saturated distilled water from outside surface of horizontal Inconel, carbon steel, and Monel tubes at 1,550 psia.

discussed as a group as was done for forced convection. Examination of the three figures indicates that all of the curves regardless of material or pressure converge to a single curve in the non-boiling region. A curve with slope of 1.25 (i.e. $q/A \sim \Delta T^{1.25}$) could represent all curves shown in this region. This is characteristic of laminar free convection.

As for the forced convection case, incipient nucleation appears at progressively higher heat flux and ΔT for carbon steel, Monel, and Inconel in that order. However, at 1550 psia the incipient boiling point for Monel and Inconel is approximately the same.

In the nucleate boiling region the slope of the Inconel curves is independent of pressure. The Monel curves are similar in shape to those for Inconel, however, an increase in slope occurs with increase in pressure. The carbon steel curves again exhibit an opposite curvature which in this case also is accentuated with increase in pressure.

B. VERTICAL TEST SECTION

The heat transfer characteristics for a vertical tube were investigated with a Monel test section. The 3/4 in. diameter tube was located in the center of the pressure vessel inside a 2.43 in. ID flow guide as shown in Fig. 6. The location of thermocouples is the same as for the horizontal test sections, as given in Fig. 4. The

data obtained for all twelve thermocuples for each run are tabulated in Appendix C. Summary curves of the vertical test section data are presented in Figs. 39 through 47 and data for the individual test runs are presented in Figs. 48 through 58.

The results of forced convection tests are shown in Figs. 39, 41, and 43 for the bottom, center, and top thermocouple positions respectively. Water flows into the pressure vessel through the bottom flange and leaves at a point above the test section. Hence, a fluid element passes the bottom, center, and top instrumentation positions successively in that order. The similarity of the summary curves for the three positions is evident. The reproducibility of the data on repeat runs is shown to be good, especially so at 535 and 1550 psia. The effect of pressure increase is to shift the nucleate boiling section of the curve to lower ΔT at a given value of heat flux as occurs with a horizontal test section. Nucleation appears to begin at lower ΔT, and the slope of the nucleate boiling curve increases as the pressure is increased.

Figs. 40, 42, and 44 present the results of pool boiling tests at the bottom, center, and top thermocouple locations respectively. Repeatability is shown to be very good at 535 and 1015 psia. An increase of pressure produces the expected reduction of ΔT at a given heat flux. The nucleate boiling curves remain approximately parallel throughout the heat flux range investigated. As was the case for

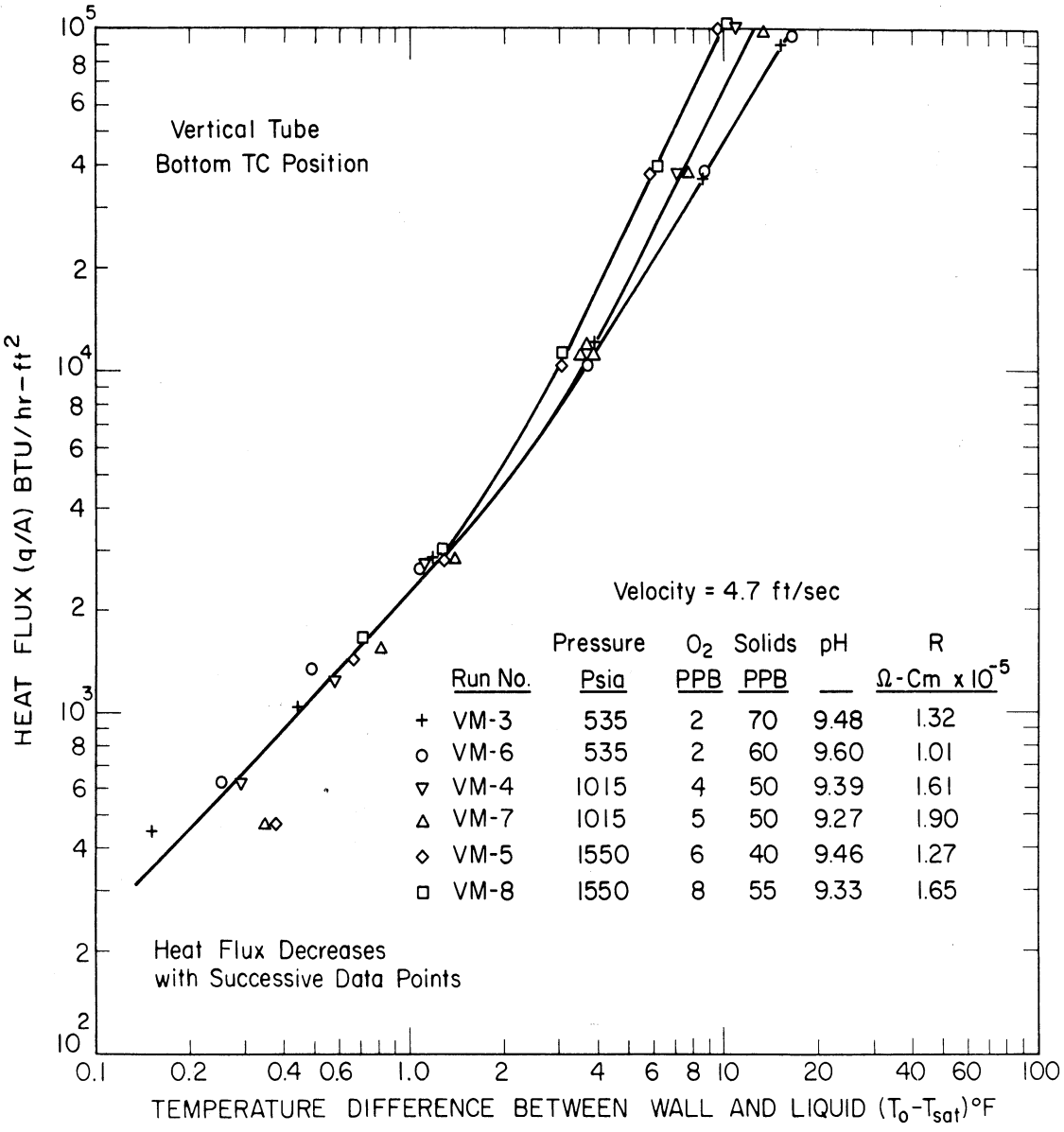

Fig. 39. Boiling of saturated distilled water flowing at 4.7 ft/sec parallel with 3/4 in. O.D. Monel tube, pressure effect at bottom TC position.

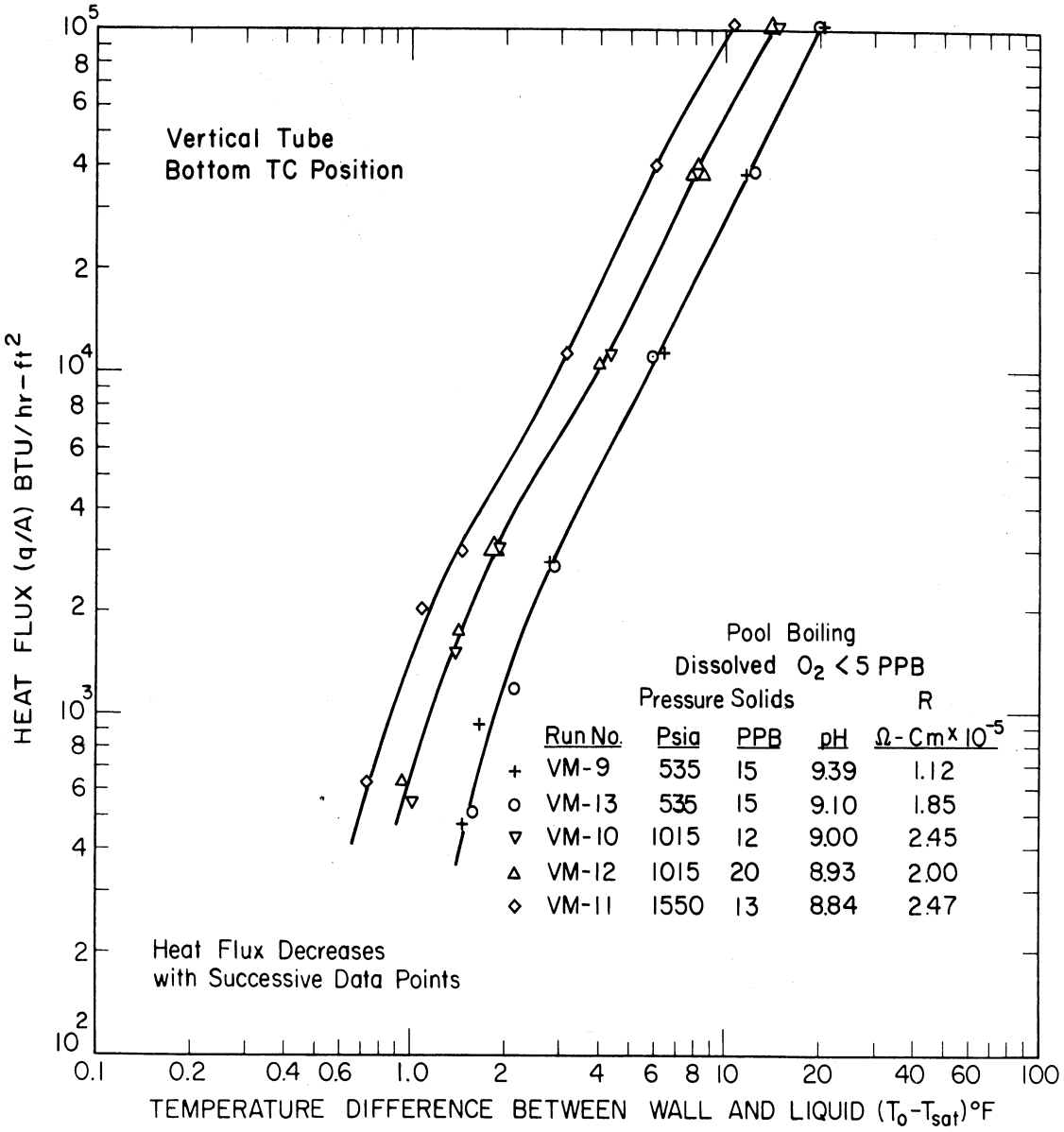

Fig. 40. Pool boiling of saturated distilled water from outside surface of vertical 3/4 in. O.D. Monel tube, pressure effect at bottom TC position.

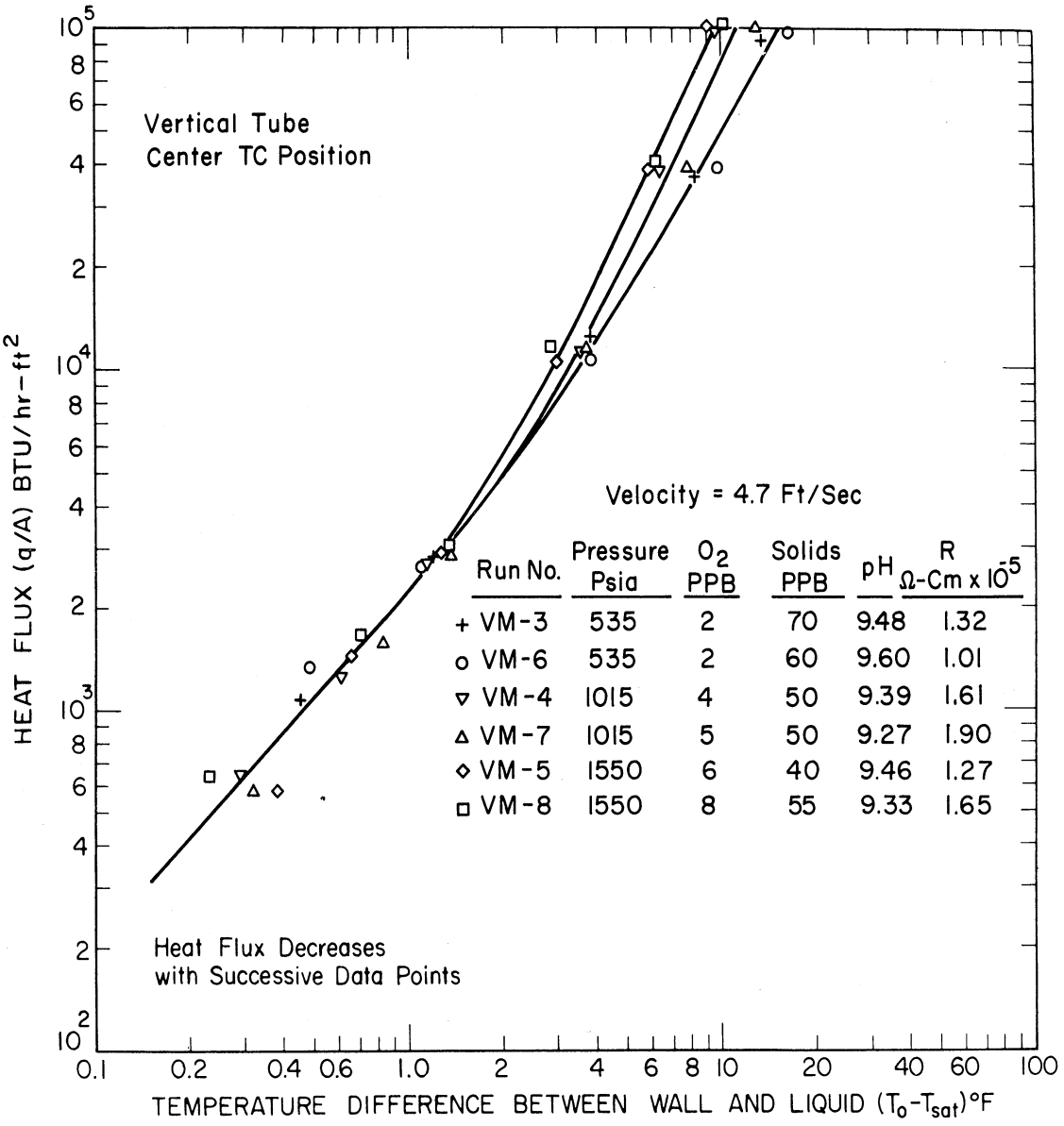

Fig. 41. Boiling of saturated distilled water flowing at 4.7 ft/sec parallel with 3/4 in. O.D. Monel tube, pressure effect at center TC position.

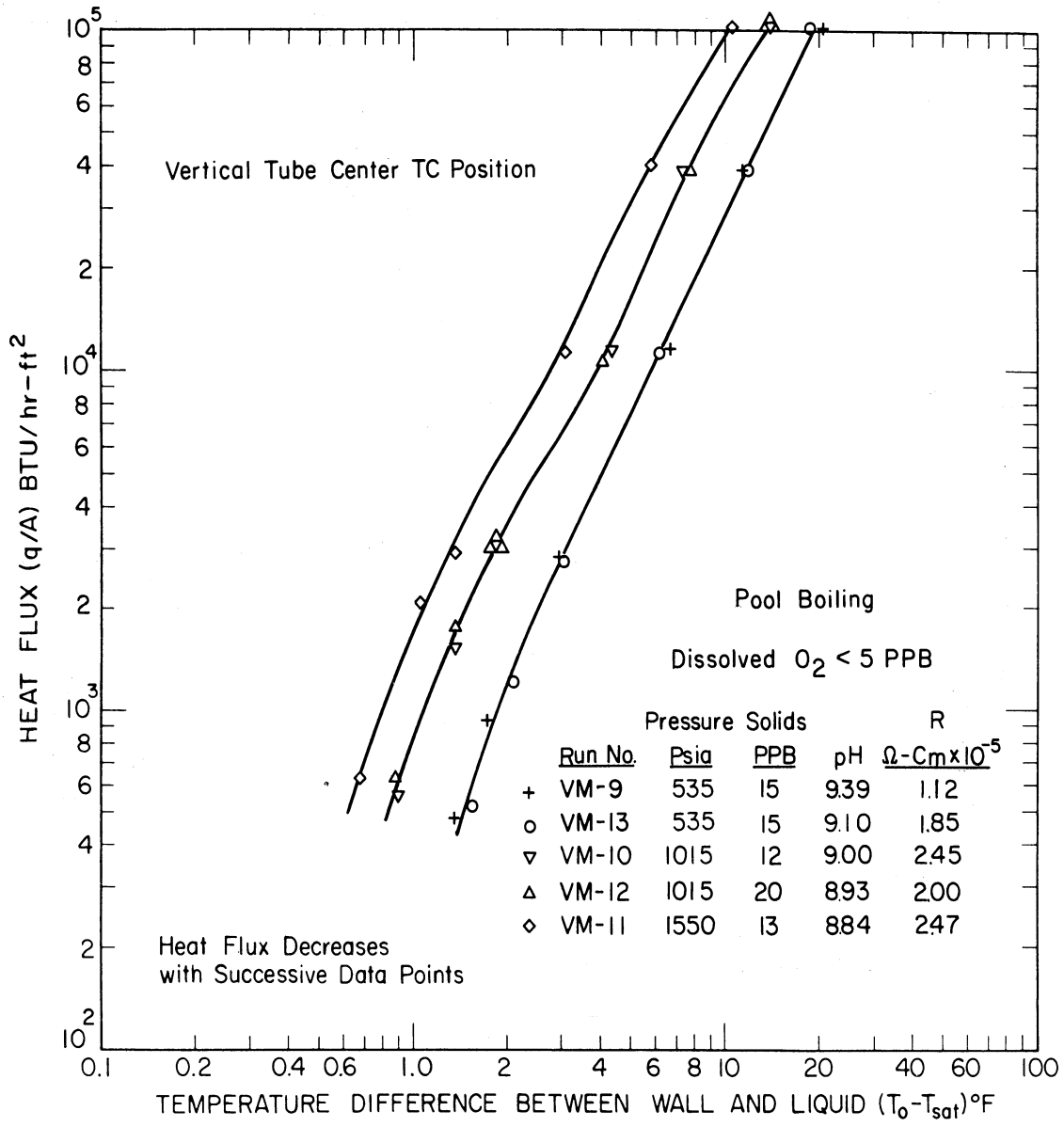

Fig. 42. Pool boiling of saturated distilled water from outside surface of vertical 3/4 in. O.D. Monel tube, pressure effect at center TC position.

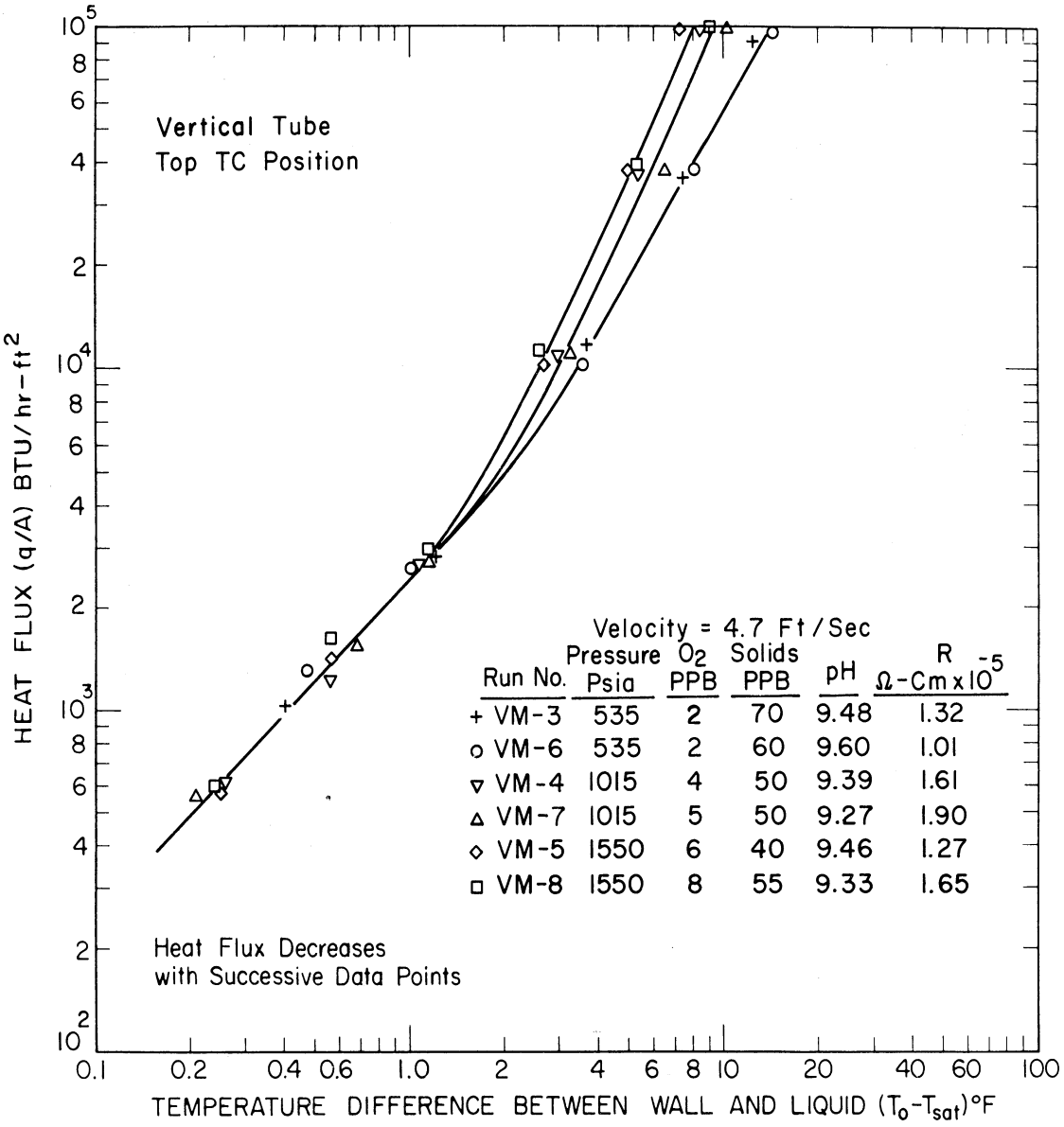

Fig. 43. Boiling of saturated distilled water flowing at 4.7 ft/sec parallel with 3/4 in. O.D. Monel tube, pressure effect at top TC position.

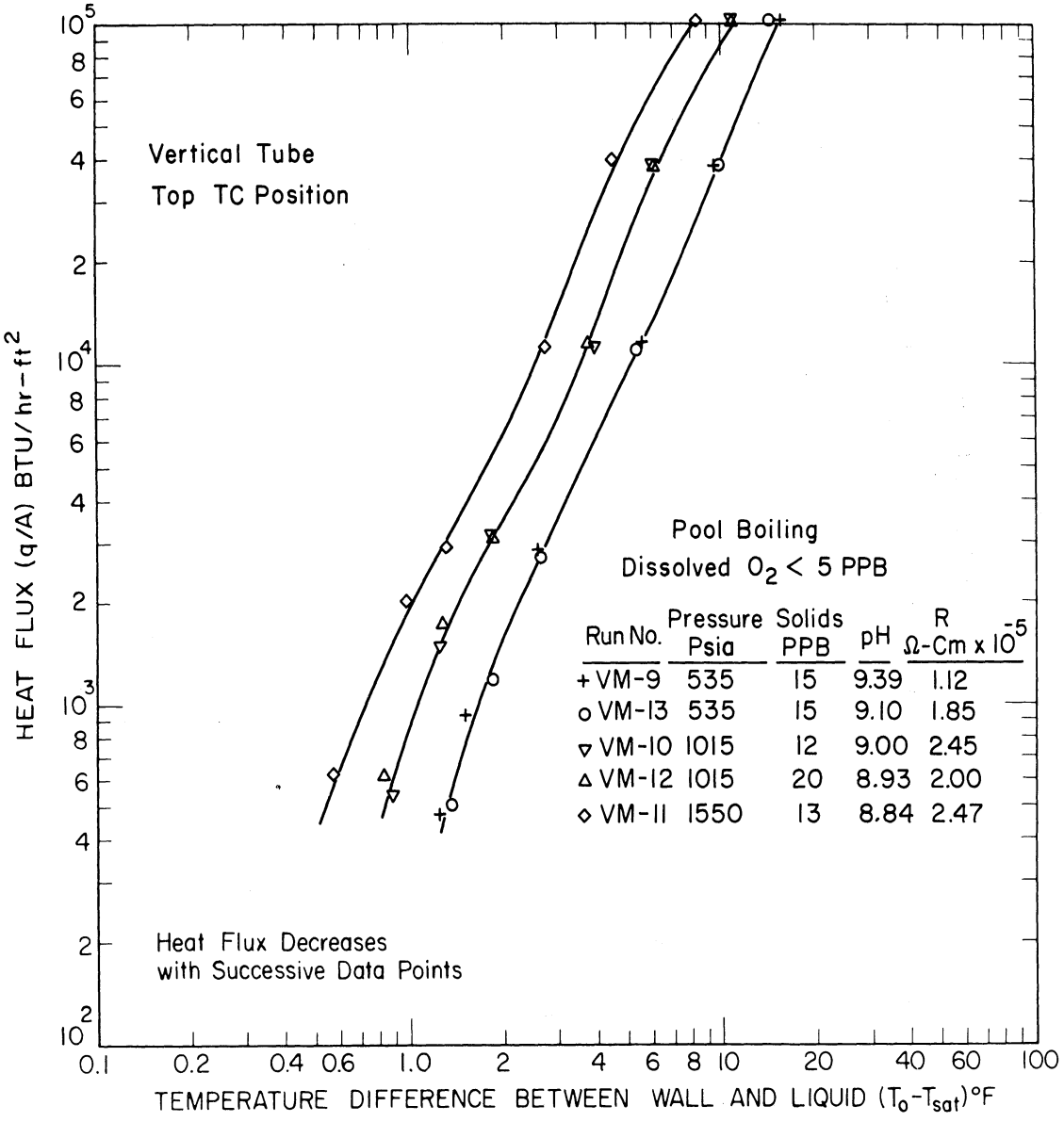

Fig. 44. Pool boiling of saturated distilled water from outside surface of vertical 3/4 in. O.D. Monel tube, pressure effect at top TC position.

forced convection, the summary curves for pool boiling are similar for the three instrumentation positions. Non-boiling conditions were not obtained even for a ΔT as low as $0.7^{\circ}F$.

A comparison of forced convection and pool boiling is given in Figs. 45, 46, and 47 for the bottom thermocouple position. The effect of forced convection diminishes with increased pressure. At 1550 psia, Fig. 47, the effect vanishes when nucleate boiling begins in forced convection and results in a single curve for both forced convection and pool boiling from there to the highest heat flux investigated. Similar curves could be established for the center and top thermocouple positions. Examination of Figs. 41 and 42 and Figs. 43 and 44 indicates that the effect of forced convection diminishes with increased pressure and disappears at 1550 psia for these positions also.

Complete data for the individual test runs are given in Figs. 48 through 58. The variation of heat transfer characteristics over a short axial distance is shown by plotting data for the bottom, center, and top thermocouple positions independently on each of these figures.

For the forced convection runs, Figs. 48 through 53, it is seen that data for the three axial positions are approximately the same at low heat flux. Above a heat flux of 10,000 Btu/hr-ft^2, the data for the top instrumentation position show a shift to lower ΔT than that for the lower instrumentation position at a given heat flux. In two

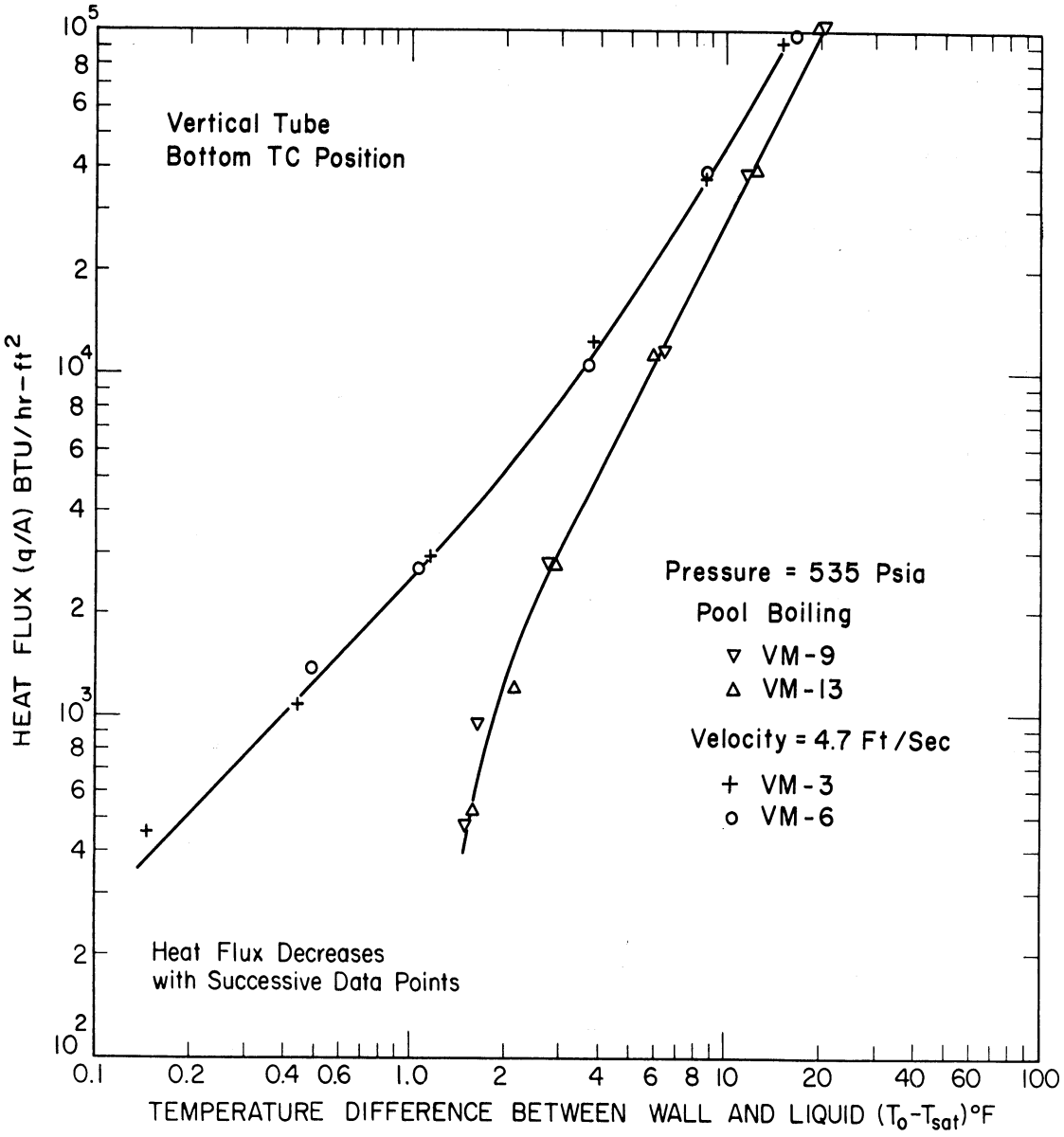

Fig. 45. Comparison of forced convection and pool boiling saturated distilled water at 535 psia, vertical Monel tube.

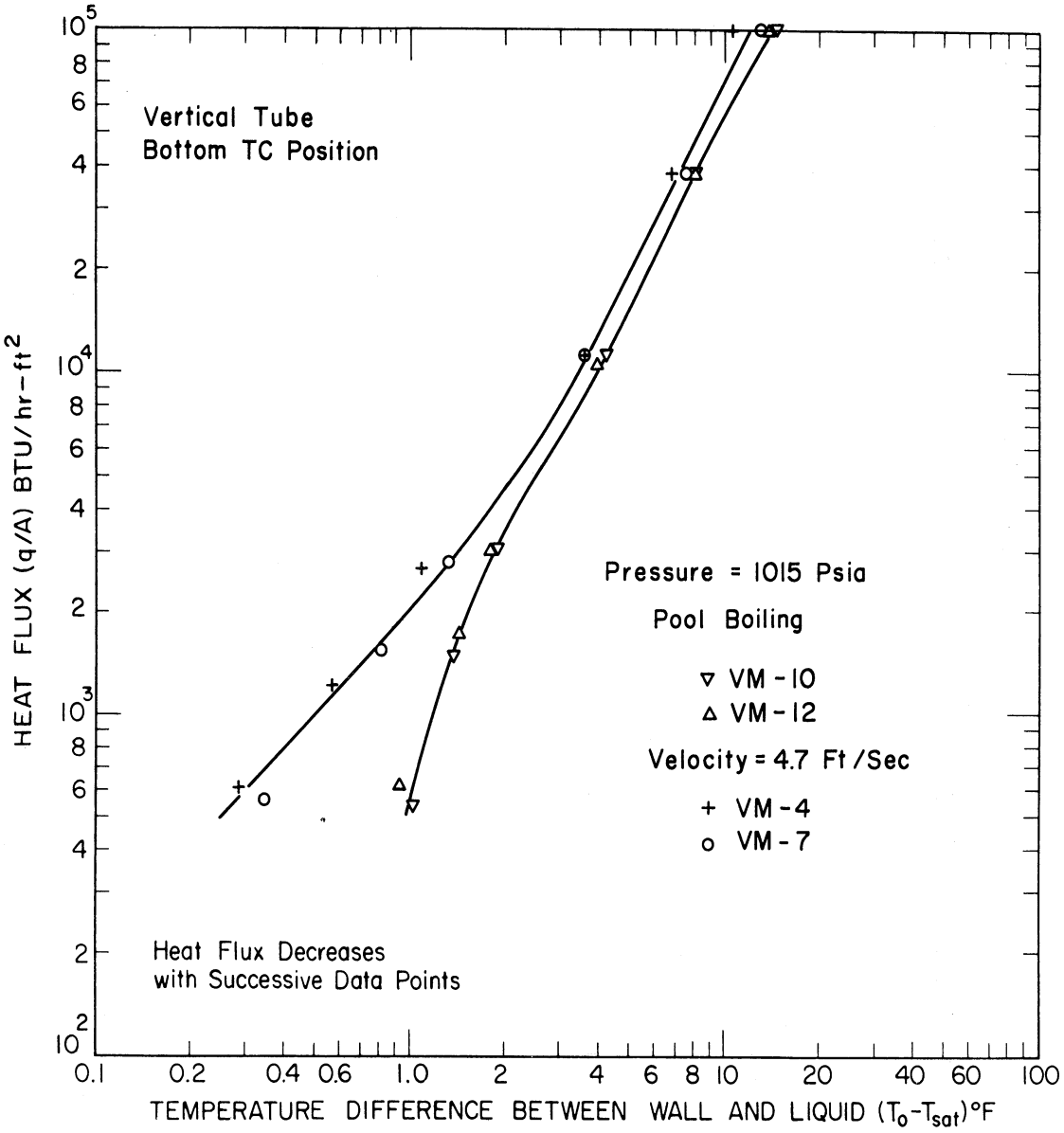

Fig. 46. Comparison of forced convection and pool boiling saturated distilled water at 1,015 psia, vertical Monel tube.

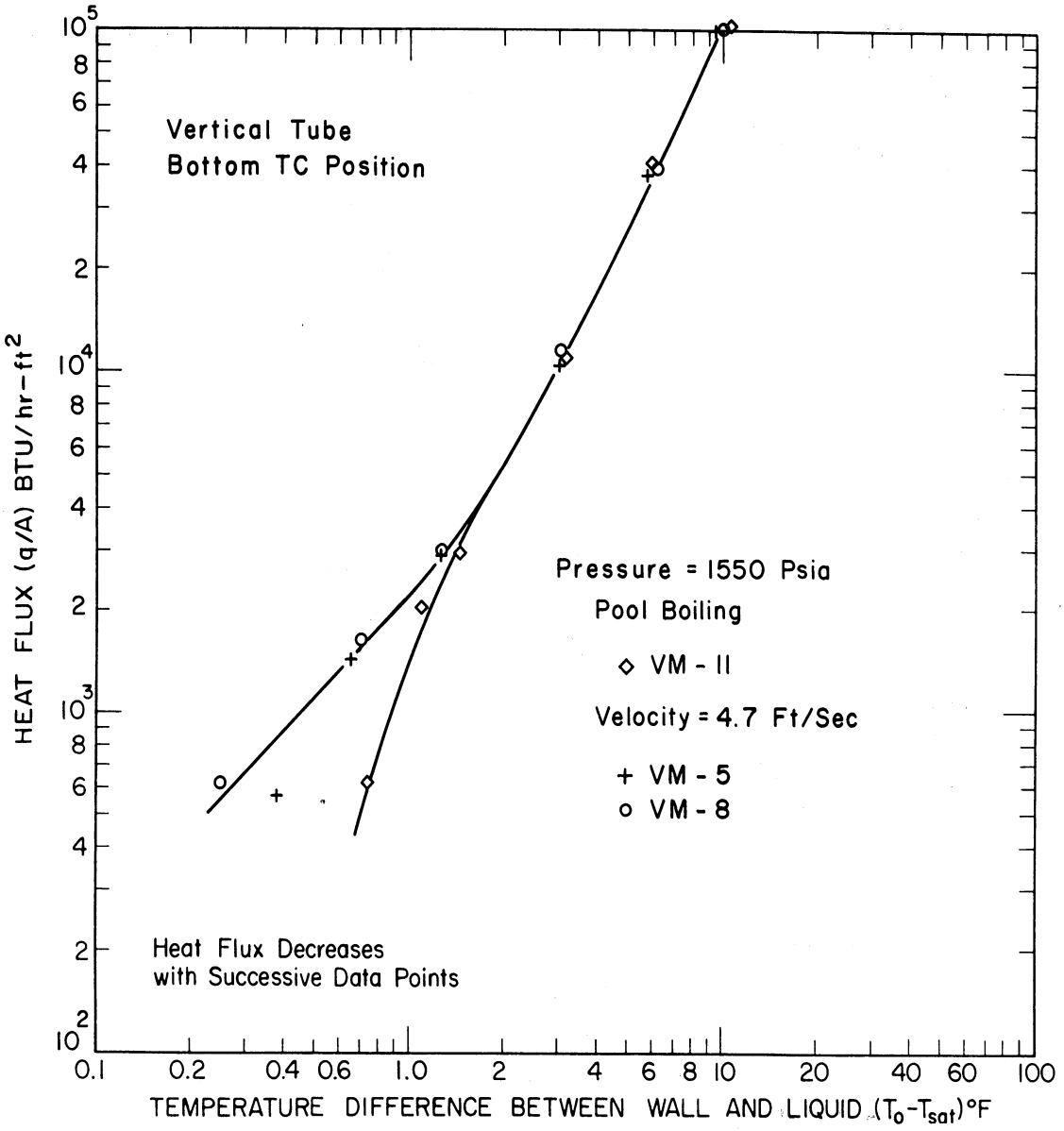

Fig. 47. Comparison of forced convection and pool boiling saturated distilled water at 1,550 psia, vertical Monel tube.

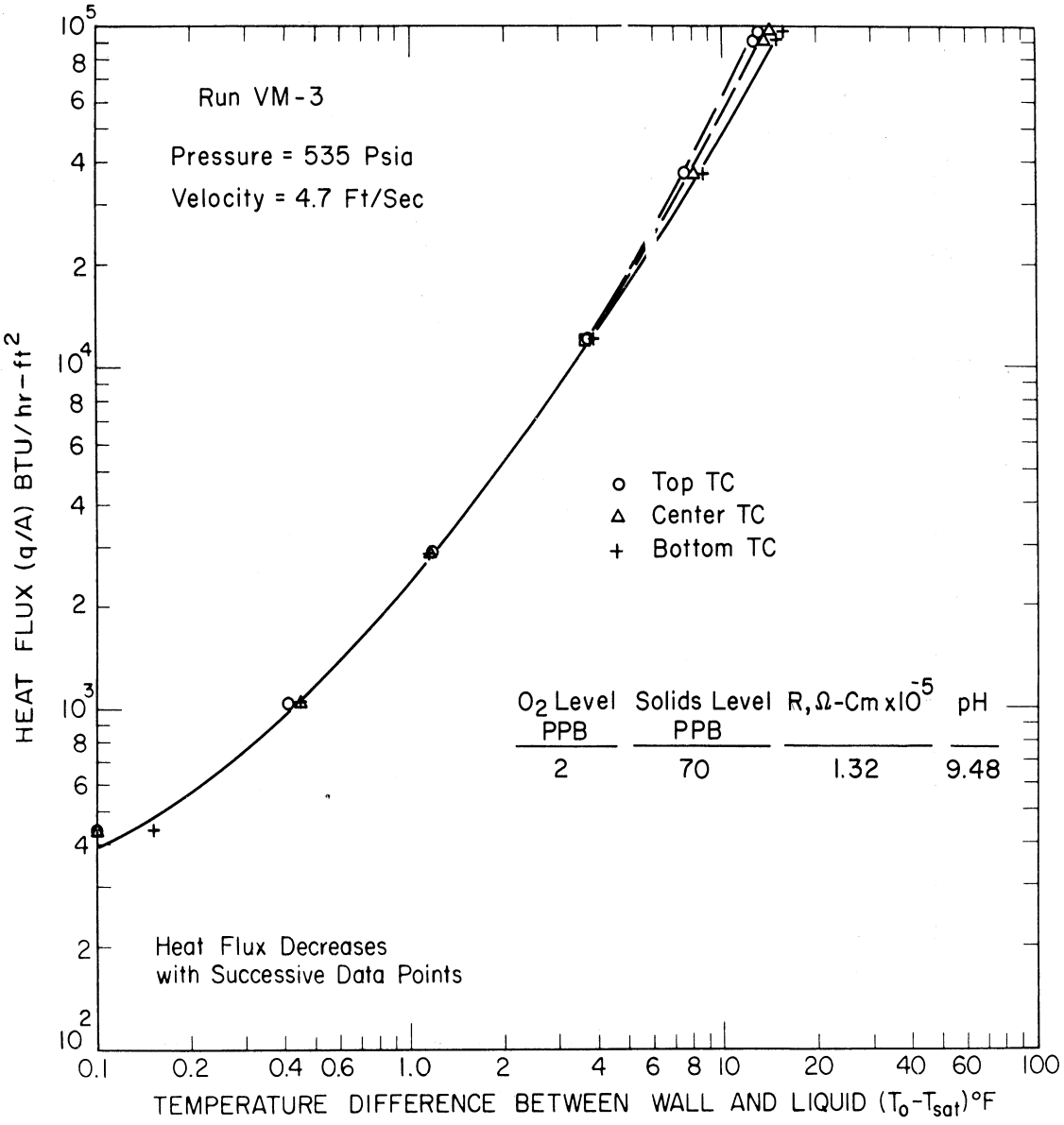

Fig. 48. Heat transfer at three axial positions for boiling saturated distilled water flowing at 4.7 ft/sec parallel with 3/4 in. O.D. Monel tube at 535 psia.

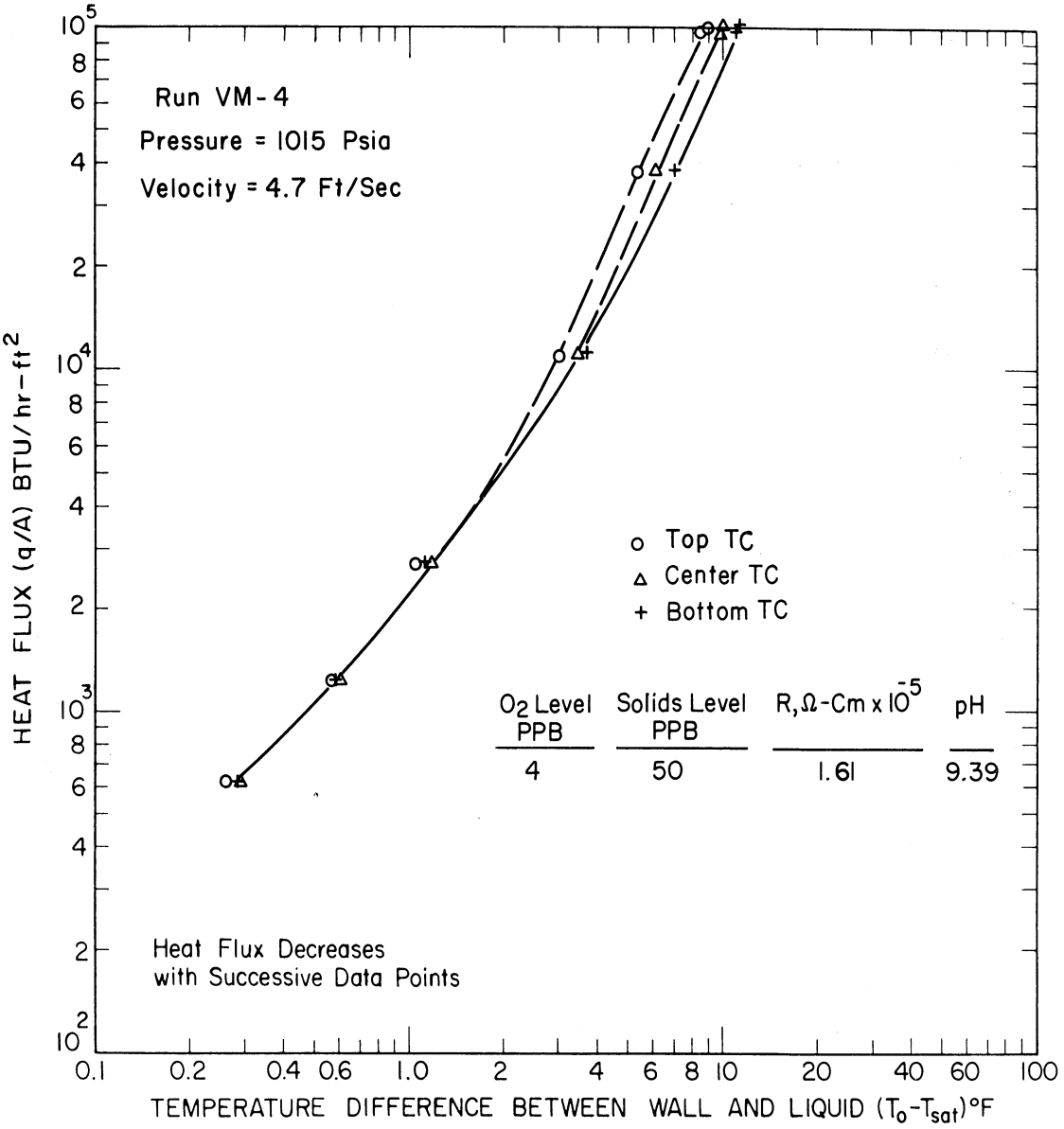

Fig. 49. Heat transfer at three axial positions for boiling saturated distilled water flowing at 4.7 ft/sec parallel with 3/4 in. O.D. Monel tube at 1,015 psia.

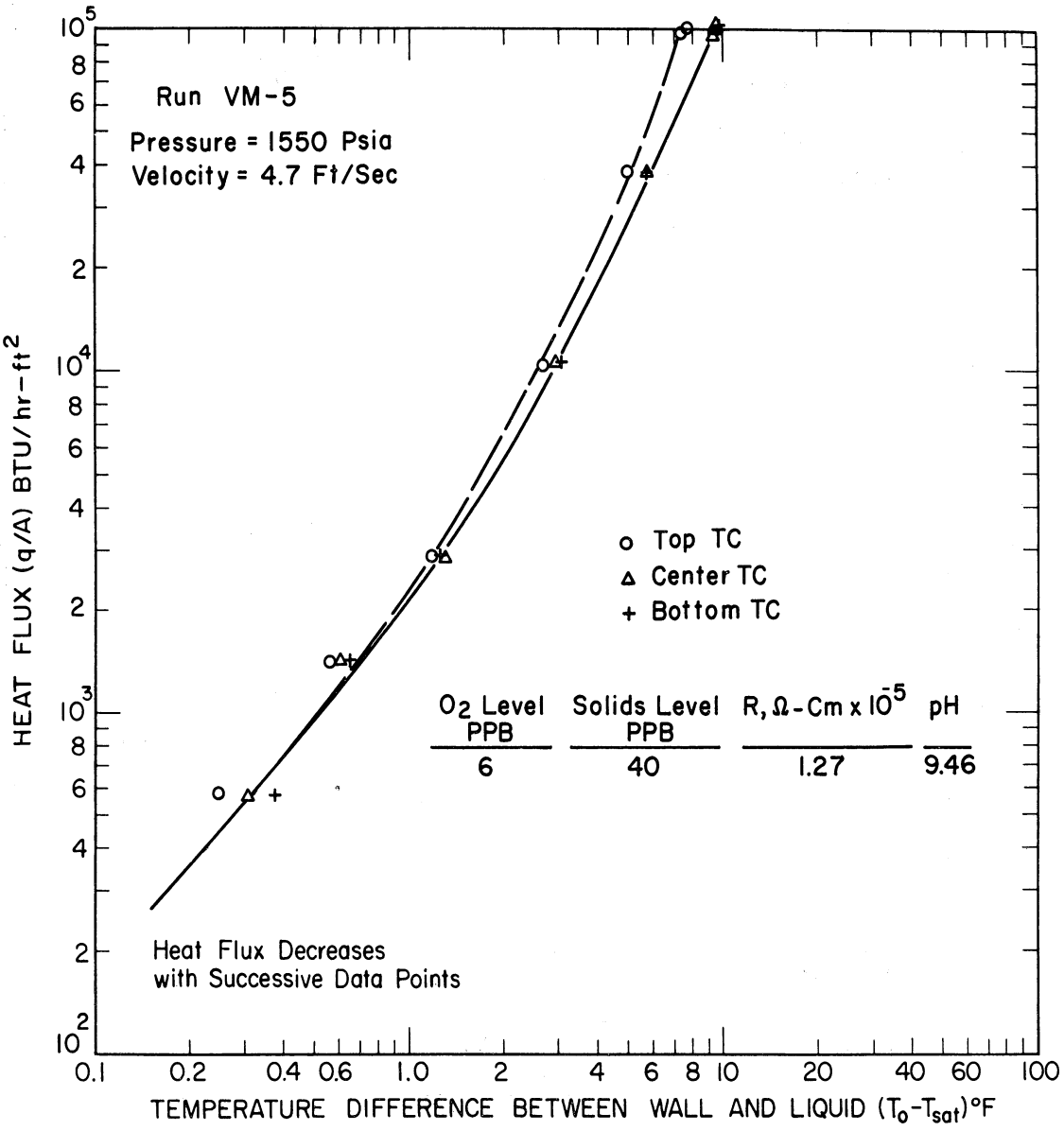

Fig. 50. Heat transfer at three axial positions for boiling saturated distilled water flowing at 4.7 ft/sec parallel with 3/4 in. O.D. Monel tube at 1,550 psia.

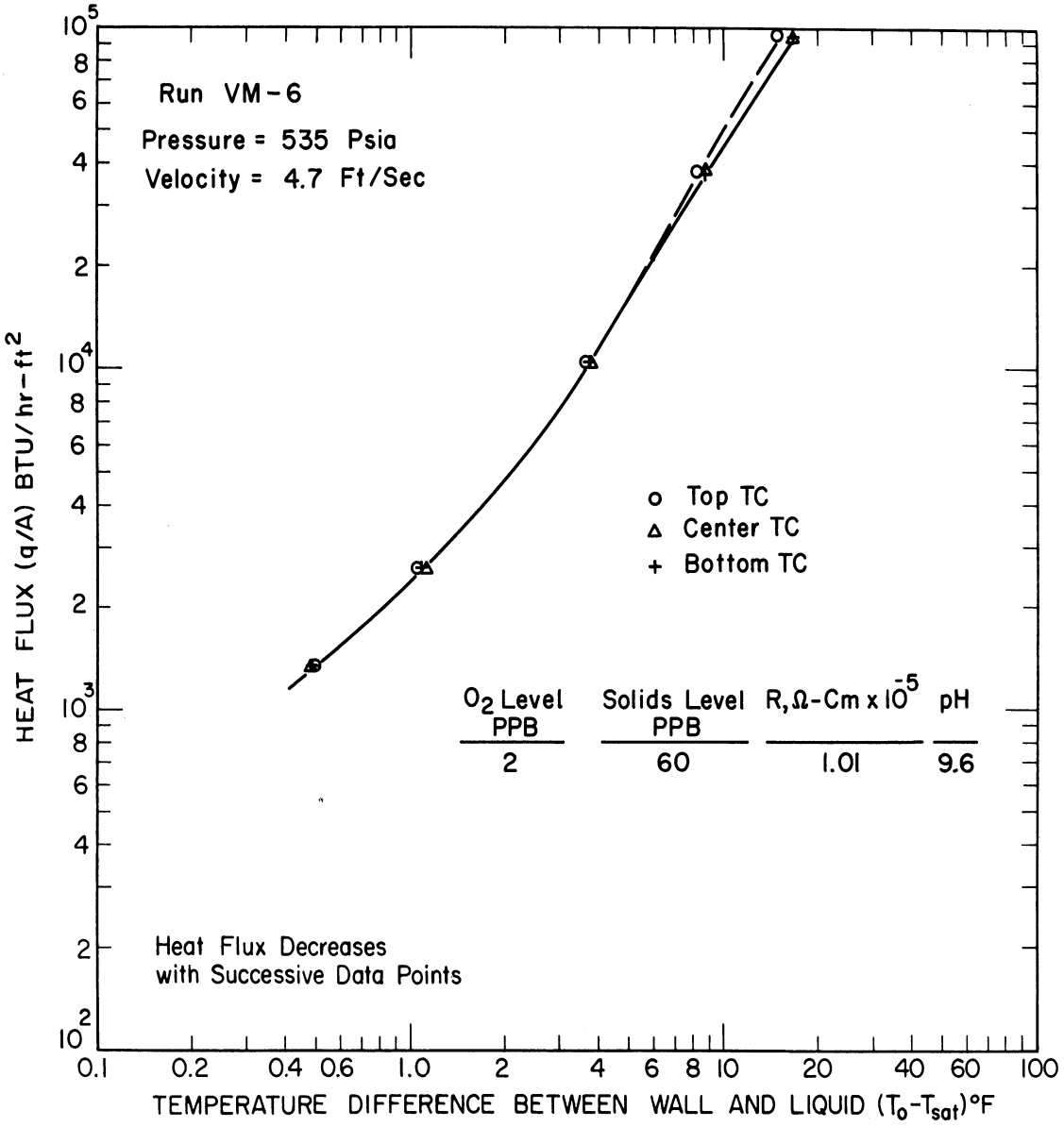

Fig. 51. Heat transfer at three axial positions for boiling saturated distilled water flowing at 4.7 ft/sec parallel with 3/4 in. O.D. Monel tube at 535 psia.

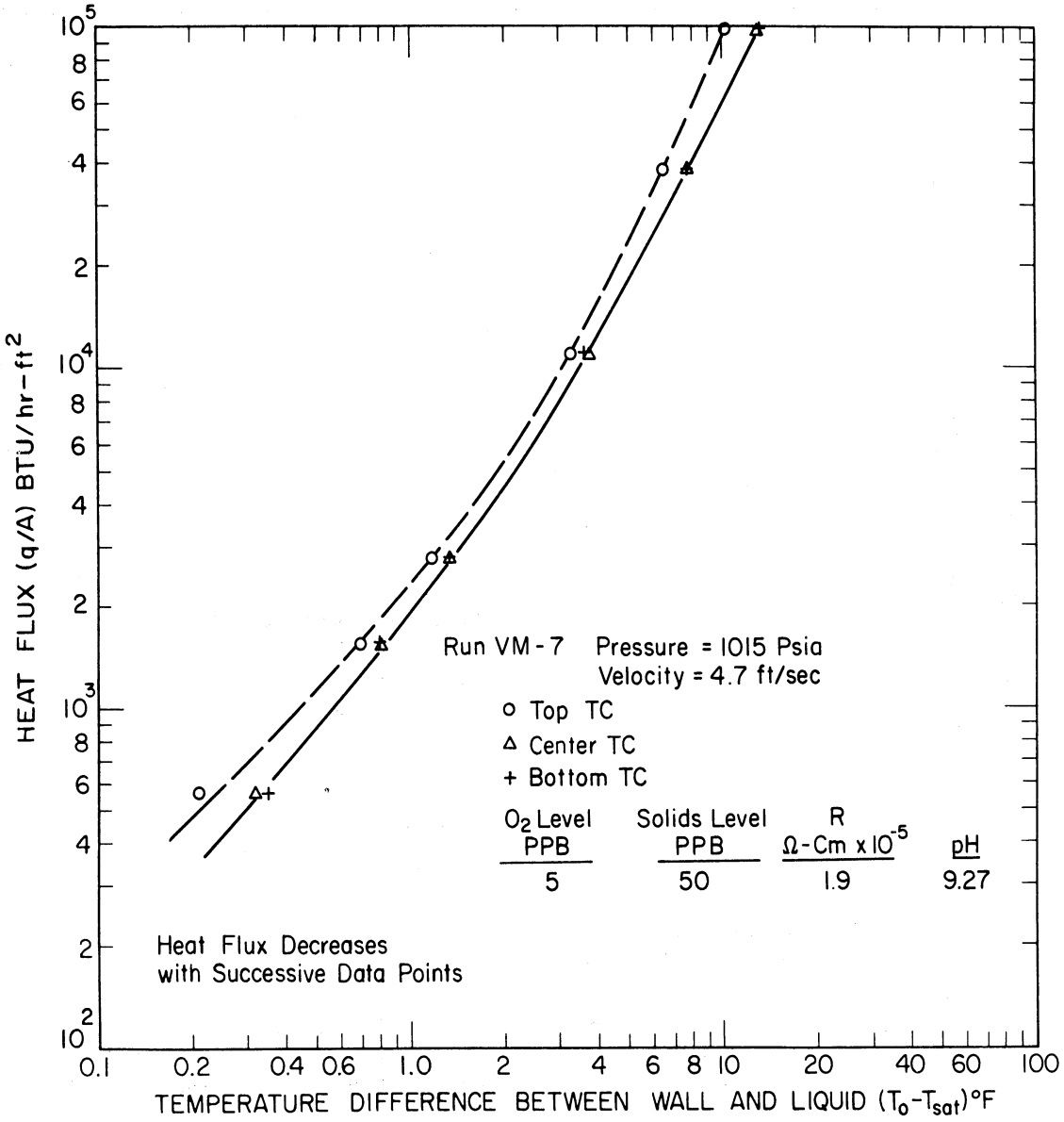

Fig. 52. Heat transfer at three axial positions for boiling saturated distilled water flowing at 4.7 ft/sec parallel with 3/4 in. O.D. Monel tube at 1,015 psia.

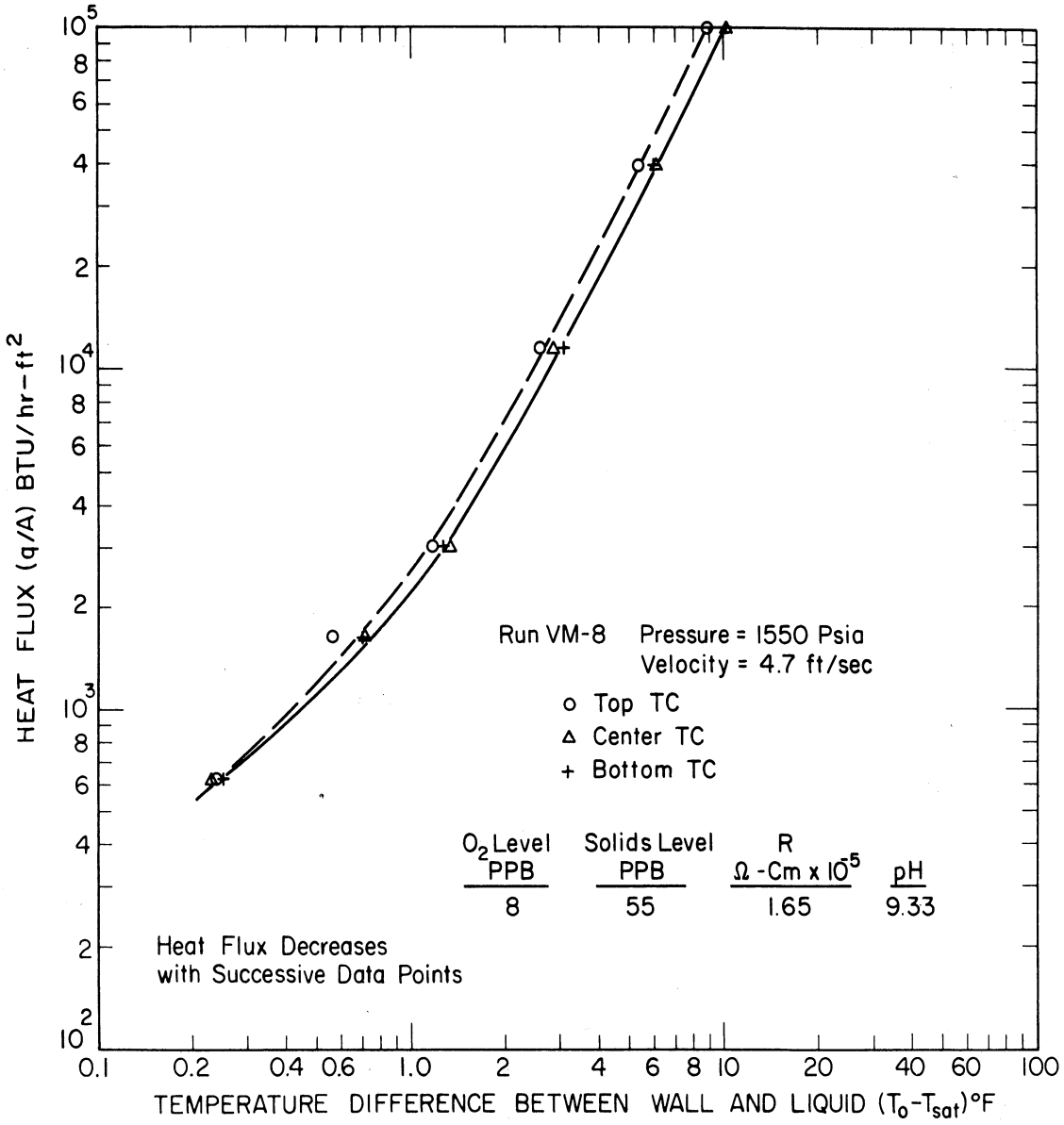

Fig. 53. Heat transfer at three axial positions for boiling saturated distilled water flowing at 4.7 ft/sec parallel with 3/4 in. O.D. Monel tube at 1,550 psia.

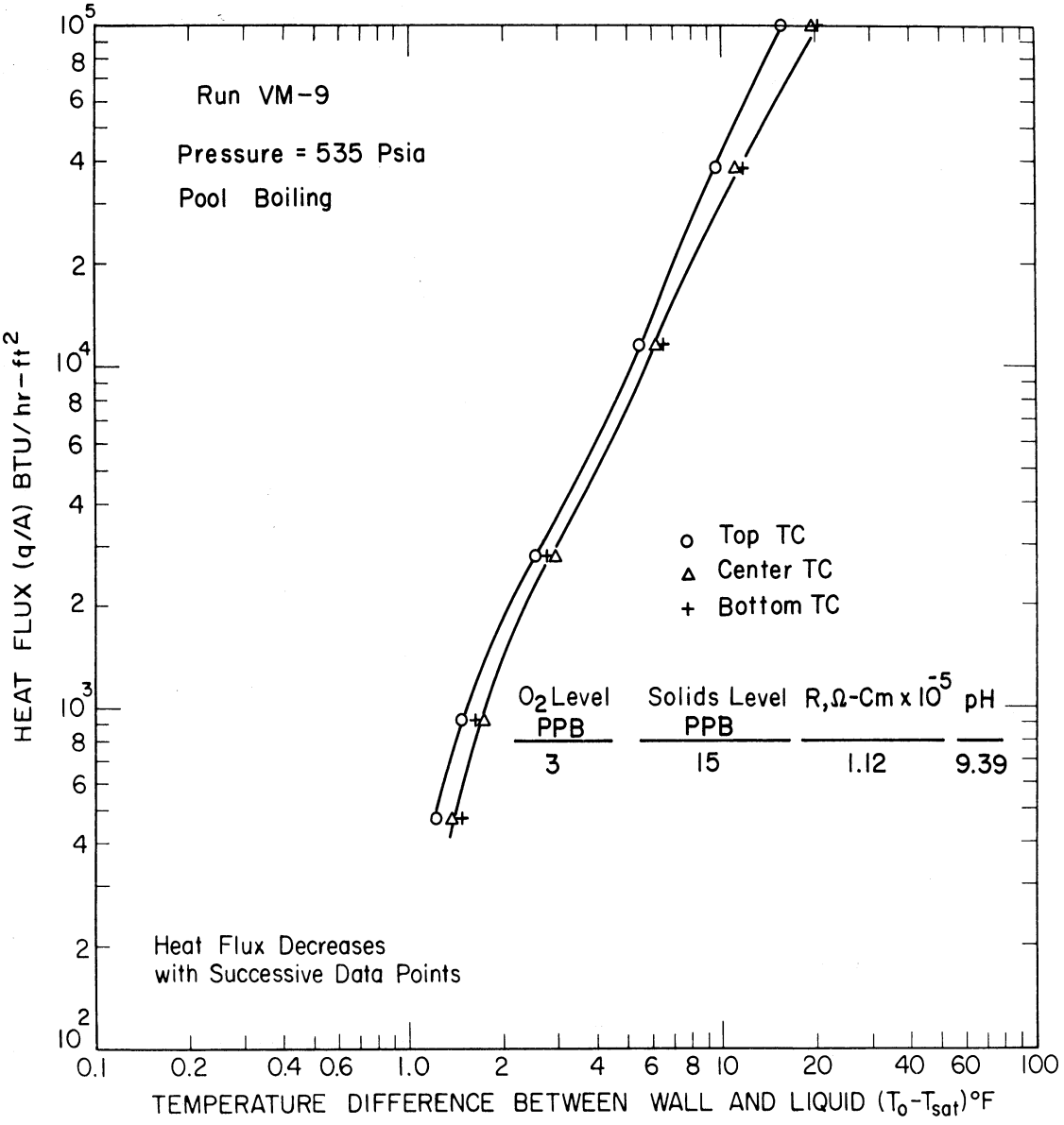

Fig. 54. Heat transfer at three axial positions for pool boiling saturated distilled water from outside surface of 3/4 in. O.D. Monel tube at 535 psia.

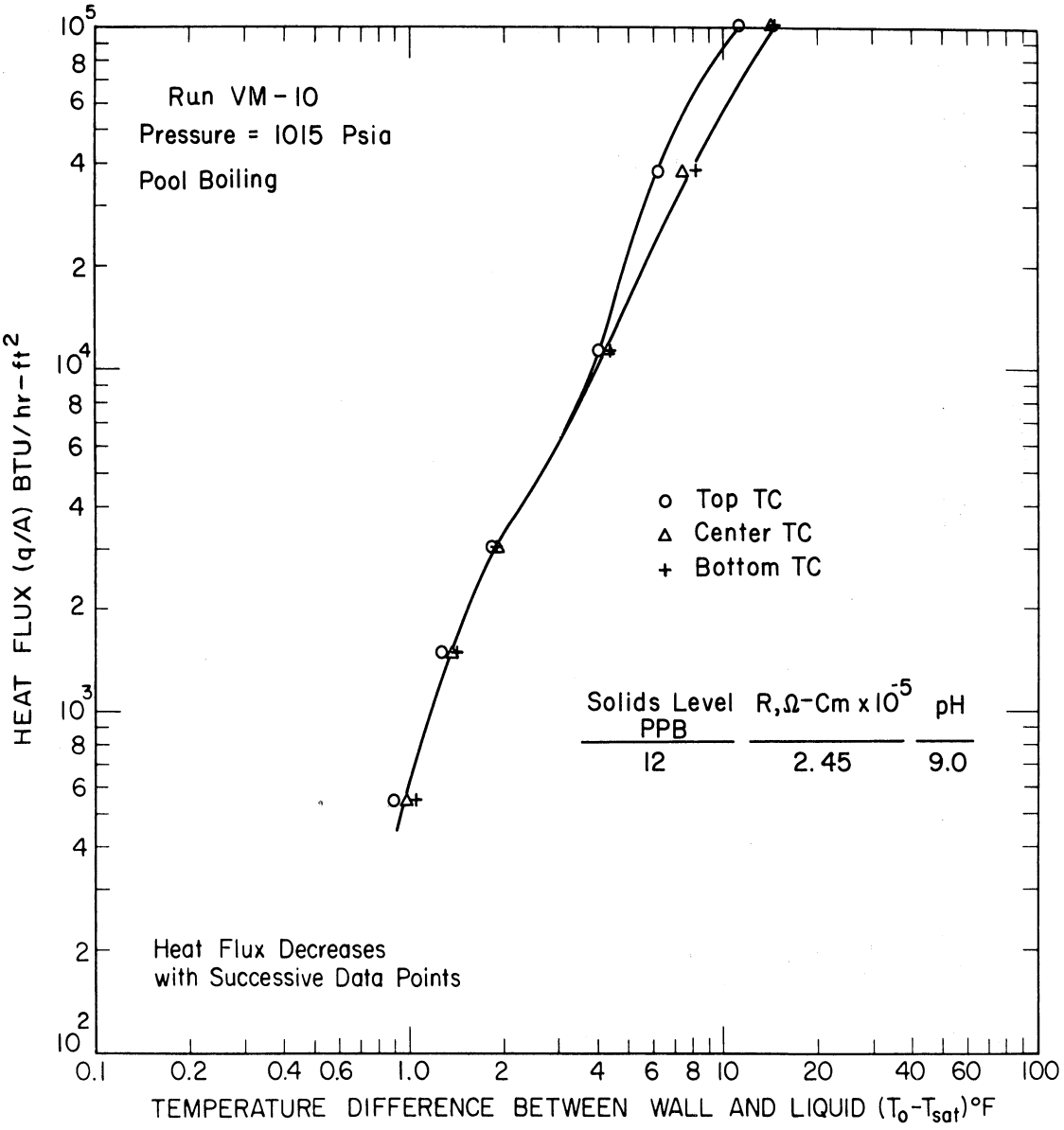

Fig. 55. Heat transfer at three axial positions for pool boiling saturated distilled water from outside surface of 3/4 in. O.D. Monel tube at 1,015 psia.

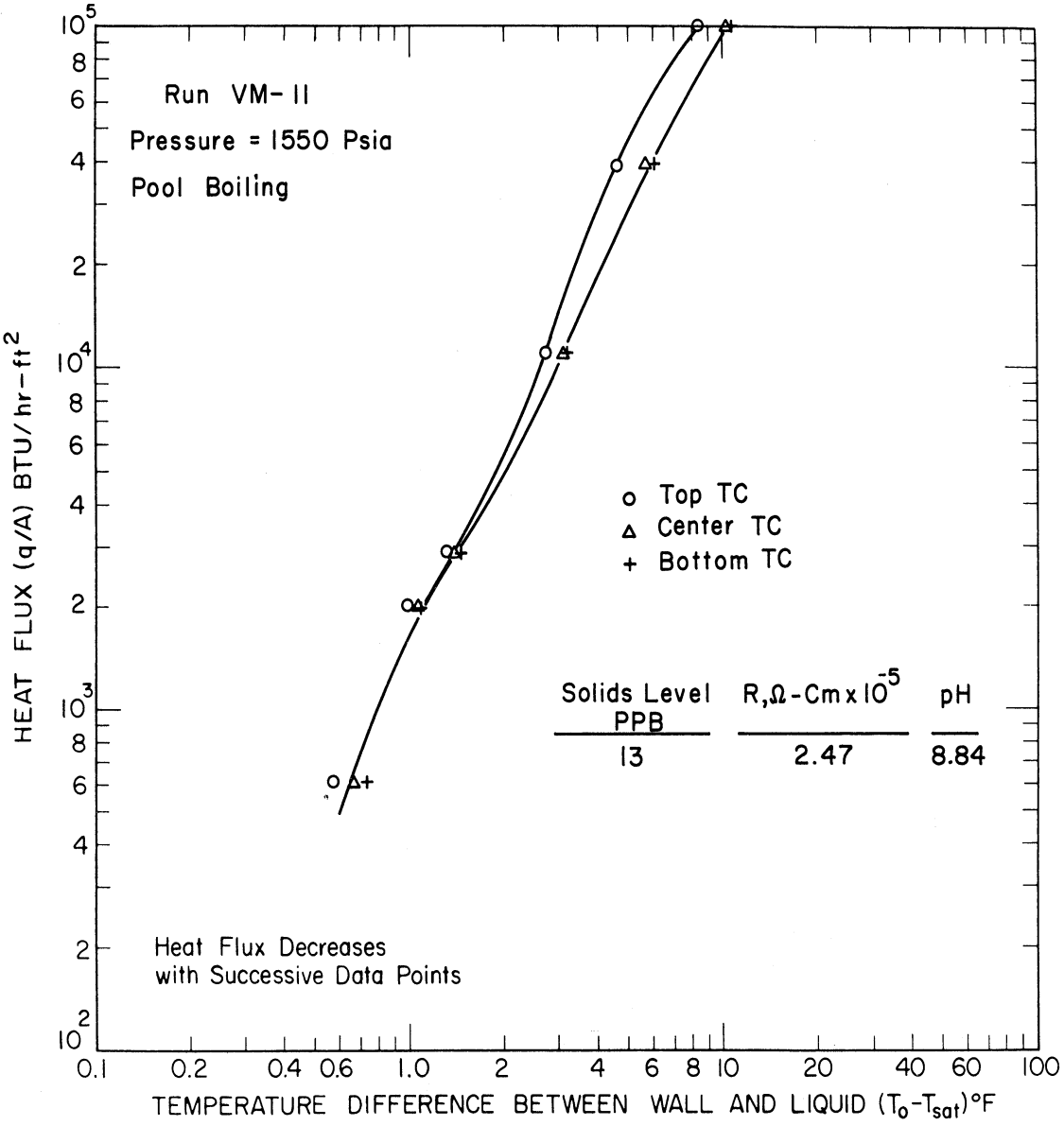

Fig. 56. Heat transfer at three axial positions for pool boiling saturated distilled water from outside surface of 3/4 in. O.D. Monel tube at 1,550 psia.

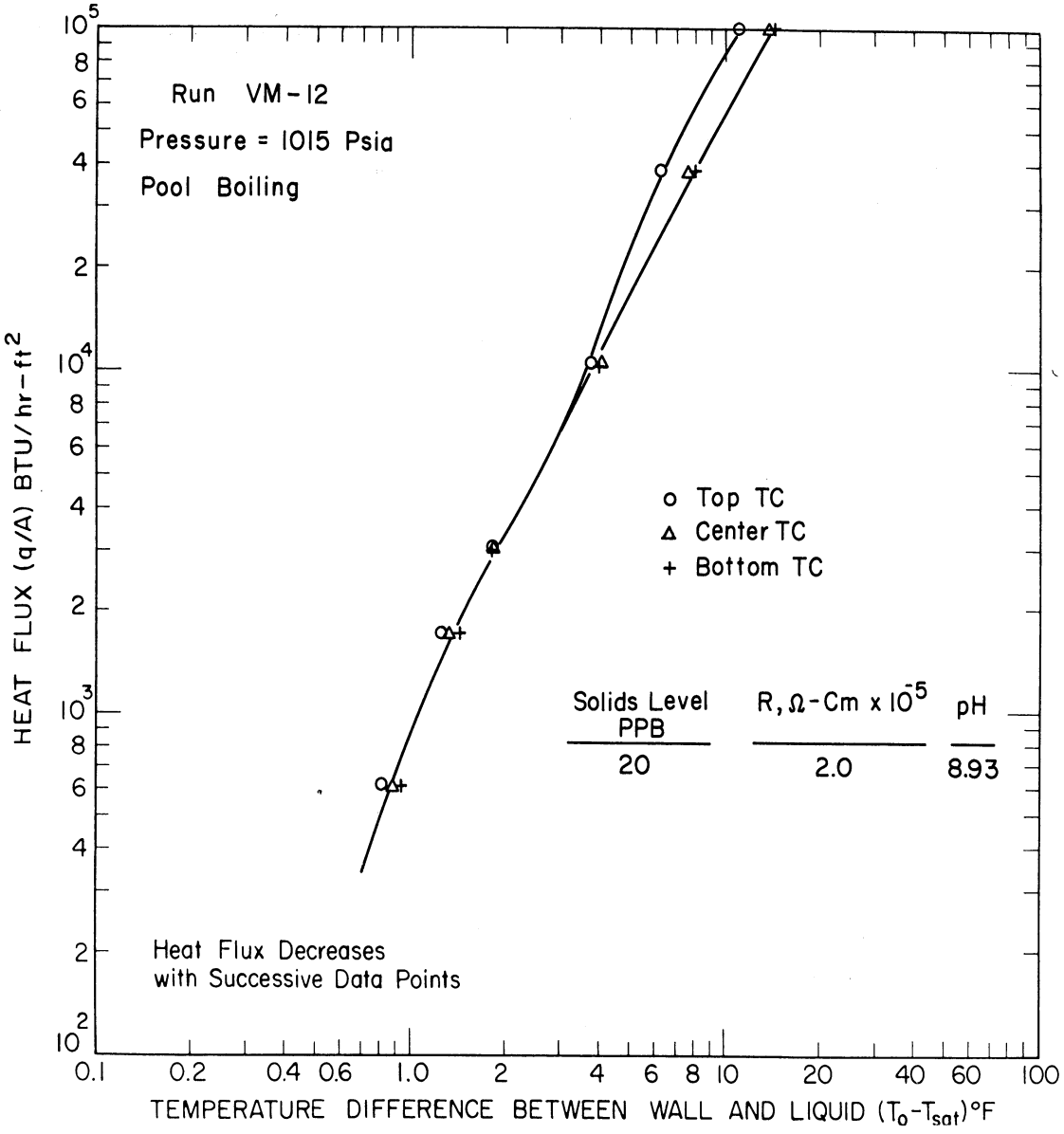

Fig. 57. Heat transfer at three axial positions for pool boiling saturated distilled water from outside surface of 3/4 in. O.D. Monel tube at 1,015 psia.

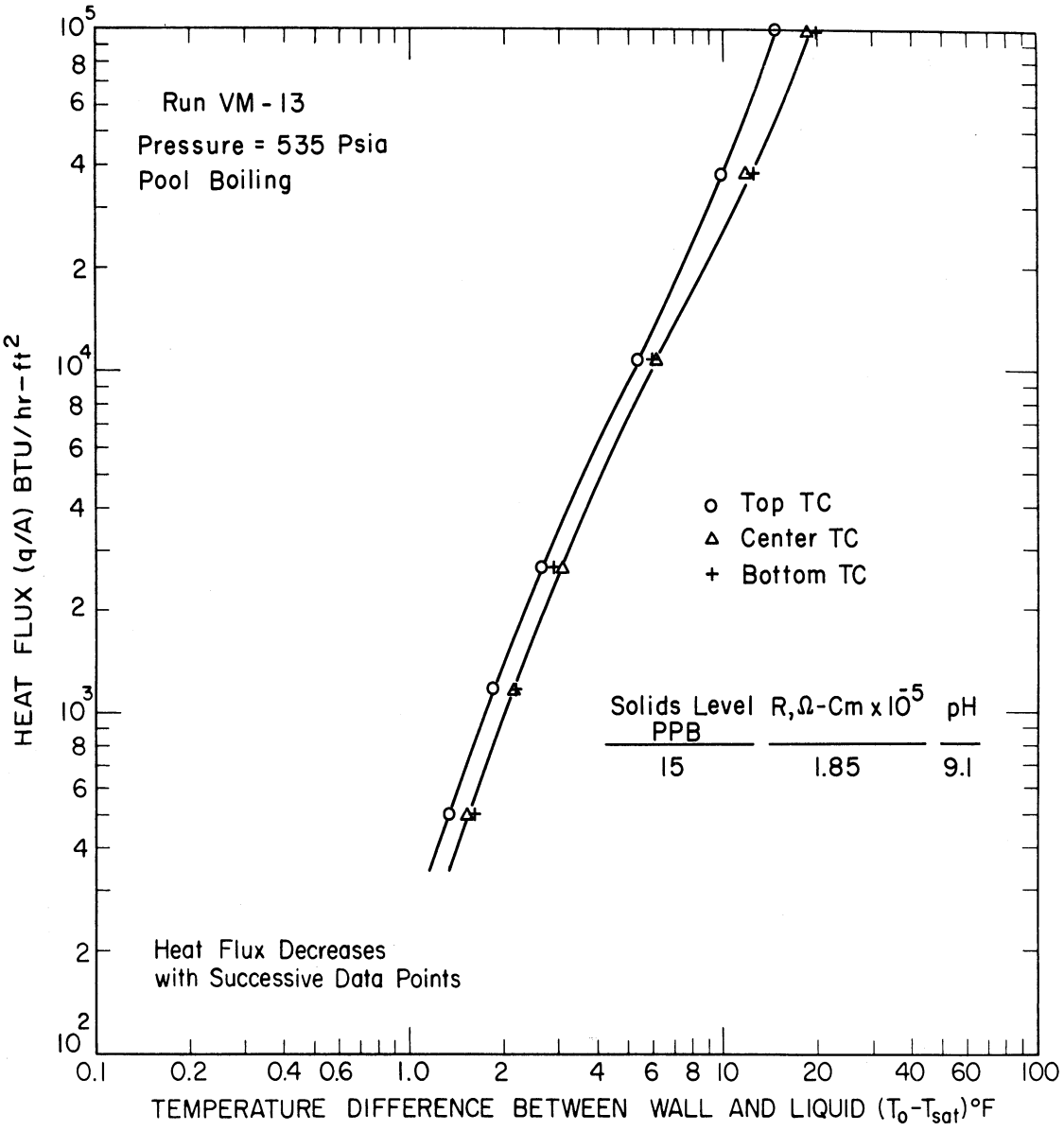

Fig. 58. Heat transfer at three axial positions for pool boiling saturated distilled water from outside surface of 3/4 in. O.D. Monel tube at 535 psia.

runs, Figs. 48 and 49, the data for the center position also shift to lower ΔT above 10,000 Btu/hr-ft^2.

In the pool boiling runs, Figs. 55 through 58, data for the bottom and center thermocouple positions are the same throughout the heat flux range investigated. However, the data for the top thermocouple position indicate a lower ΔT at a given heat flux than that for the other two positions over the same heat flux range.

C. VERTICAL VS. HORIZONTAL ORIENTATION

Two Monel test sections were investigated. One Monel tube was installed vertically in the pressure vessel as shown in Fig. 6 and the other horizontally as shown in Fig. 5. Heat transfer characteristics for these tests are presented in sub-sections A and B above.

Summary curves for the vertical and horizontal test sections under forced convection conditions are given in Fig. 59. The data for the bottom thermocouple position of the vertical test section are used for this comparison. Similar sets of curves could be establishe by using the center and top thermocouple data for the vertical test section.

At a given ΔT the heat flux for the horizontal tube is greater than that for the vertical tube throughout the entire heat flux range investigated. In the non-boiling region, the horizontal tube data is approximately 30 percent higher than that for the vertical tube, but

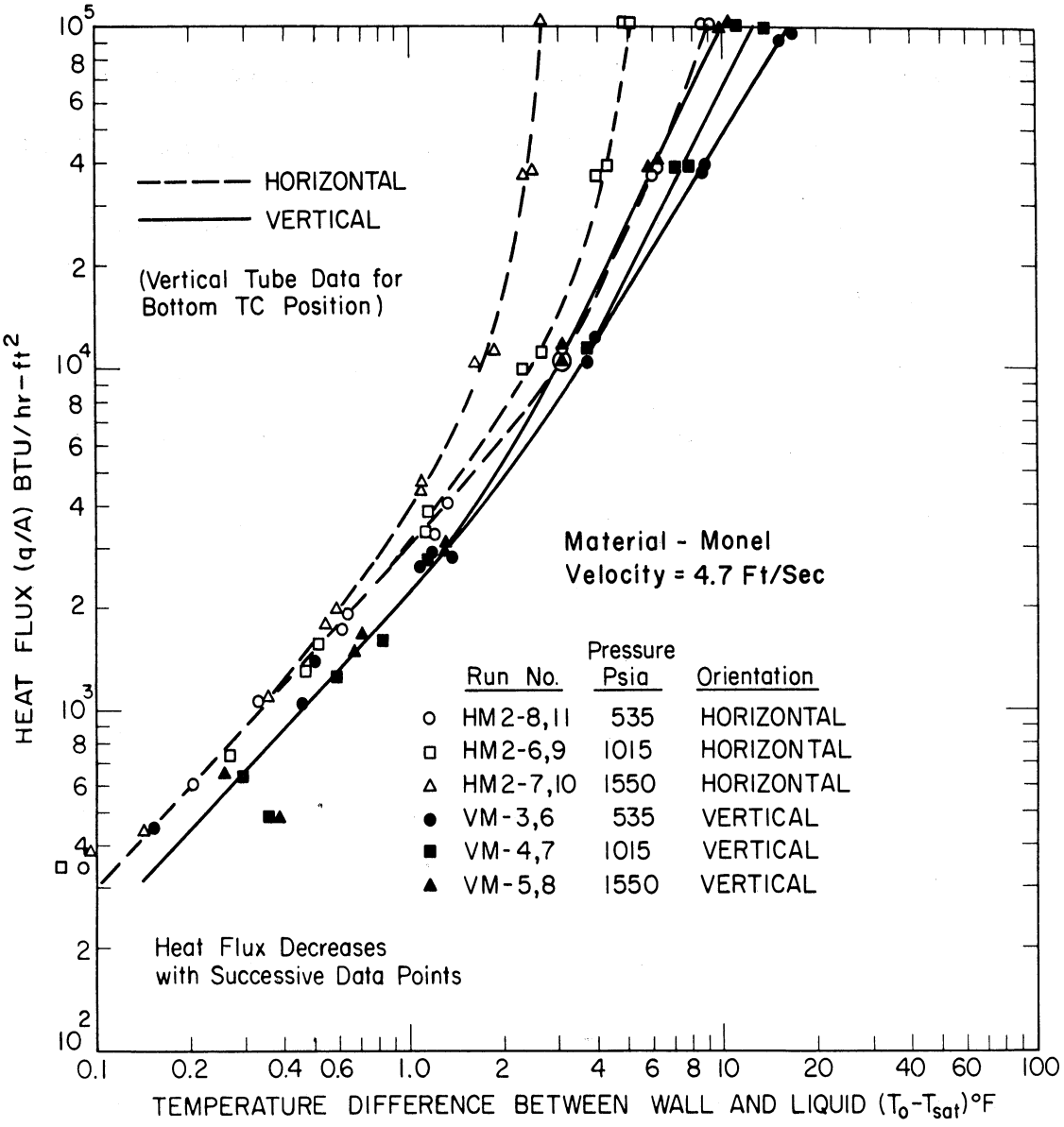

Fig. 59. Heat transfer characteristics for horizontal and vertical Monel tubes with forced convection at 4.7 ft/sec.

the slope of the two curves is the same. In the nucleate boiling region the slope of the curves for the vertical tube increases slightly with pressure increase, whereas for the horizontal tube data, a large increase in slope occurs.

The pool boiling heat transfer characteristics for the vertical and horizontal Monel tubes are compared in Fig. 60. Data in the non-boiling region was not obtained for the vertical test section so comparison can only be made for the nucleate pool boiling region. The slopes of the curves for the horizontal test section are higher than those for the vertical test section. At a given heat flux level less than 15,000 Btu/hr-ft^2 in the nucleate boiling region a higher ΔT is required for the horizontal tube than for the vertical tube. Above 15,000 Btu/hr-ft^2 the vertical tube requires a higher ΔT.

A comparison between the data for the horizontal test section and that for the center and top thermocouple positions of the vertical test section in the nucleate pool boiling region would be the same as described above. The point of intersection of the two sets of curves (vertical and horizontal) occurs as approximately 15,000 Btu/hr-ft^2 at all pressures for the center and bottom thermocouple positions. However, for the data of the top thermocouple location, the point of intersection would occur at from 30,000 to 60,000 Btu/hr-ft^2 depending on the test pressure.

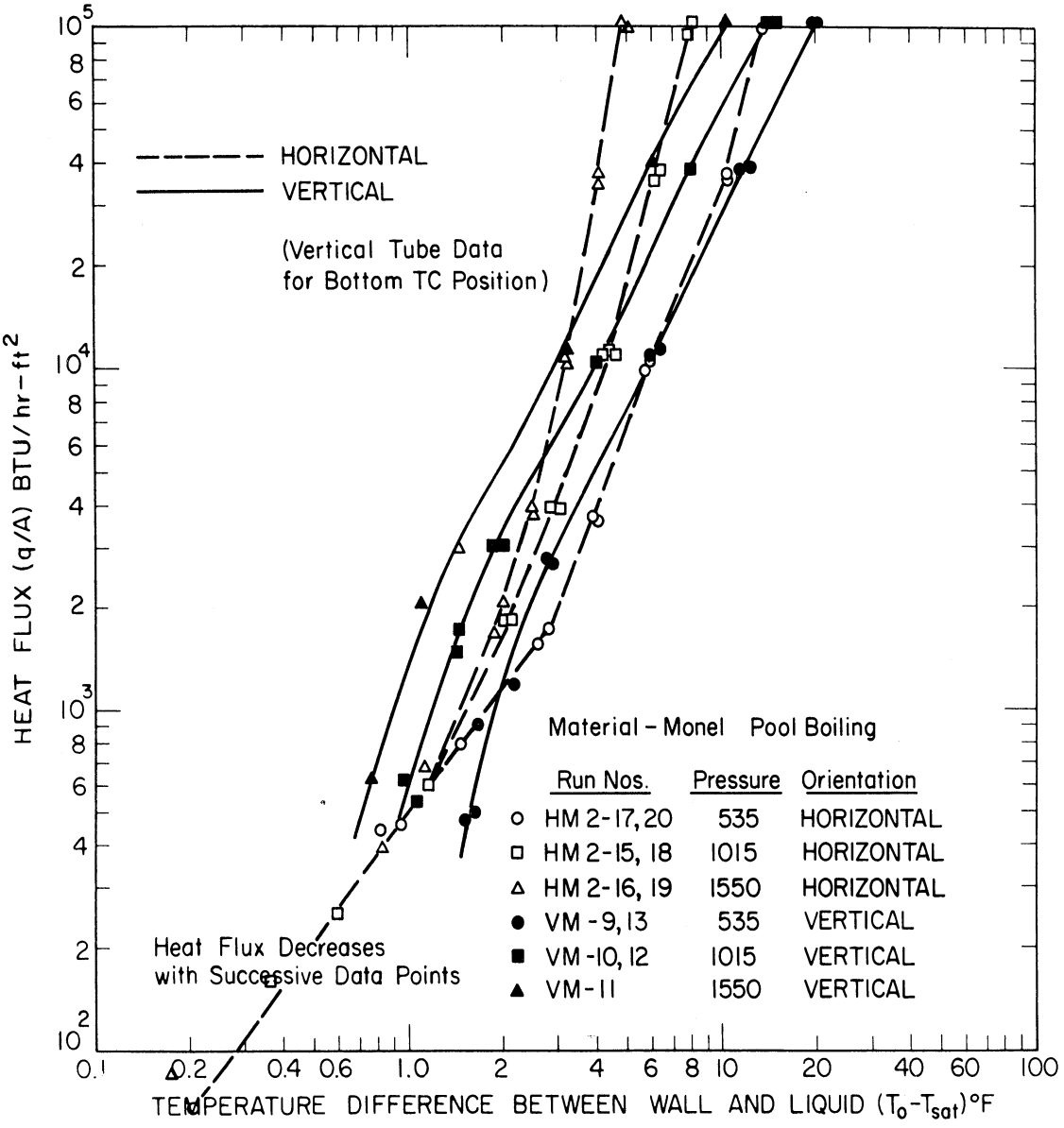

Fig. 60. Pool boiling heat transfer characteristics for horizontal and vertical Monel tubes.

D. PHOTOGRAPHIC RESULTS

In order to provide a better understanding of the heat transfer mechanisms involved in low heat flux boiling, photographs were taken during a number of runs. The details of the camera, film, and lighting were given in Section III - F above. Three sets of pictures are included with varying pressure and convection conditions.

The pictures were made during the test runs described in Section IV and do not correspond to the data presented in the summary curves. Visual observations during the Inconel test runs for which summary curves are presented indicated that the photographic results would be qualitatively the same. However, since increasing the water purity caused a shift of the characteristic curve to higher ΔT at a given heat flux in the nucleate boiling regime, the incipient boiling point and the first appearance of bubbles occur at a higher value of heat flux. Difficulty in maintaining optical clarity with the sight glass assemblies under the high temperature, high pressure conditions of the tests prevented photographic study in later tests.

Six photographs taken during run HI1-16 are shown on Fig. 61. The conditions throughout this run were 535 psia pressure and a forced convection velocity of 4.7 ft/sec upward and normal to the tube. The heat transfer data are included on Fig. 14. The photographs are arranged in order of decreasing heat flux, from the initial test

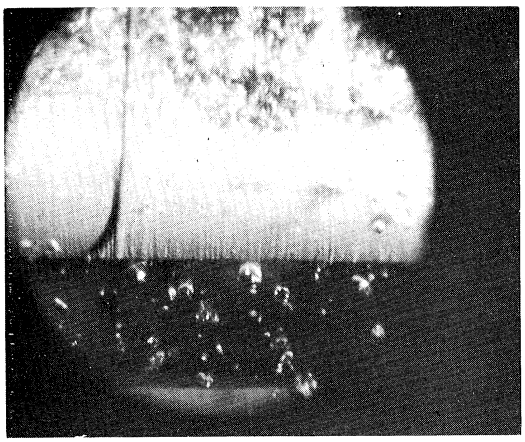

Heat Flux = 99,300 Btu/hr-ft^2

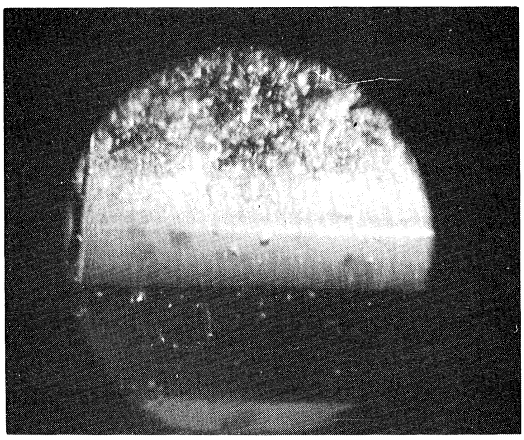

Heat Flux = 45,600 Btu/hr-ft^2

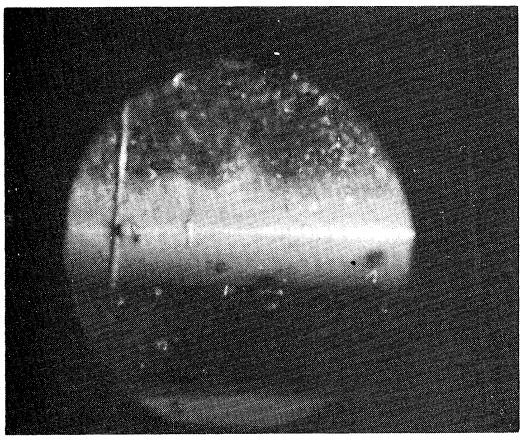

Heat Flux = 17,540 Btu/hr-ft^2

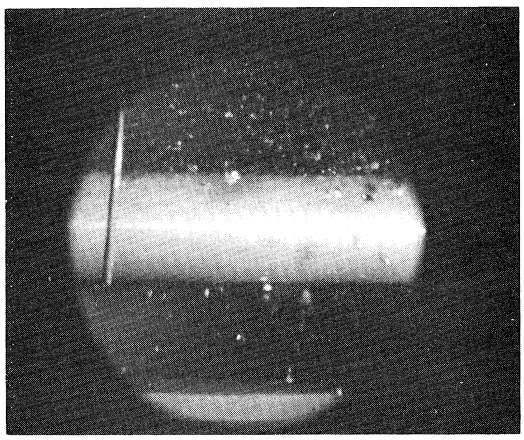

Heat Flux = 6,300 Btu/hr-ft^2

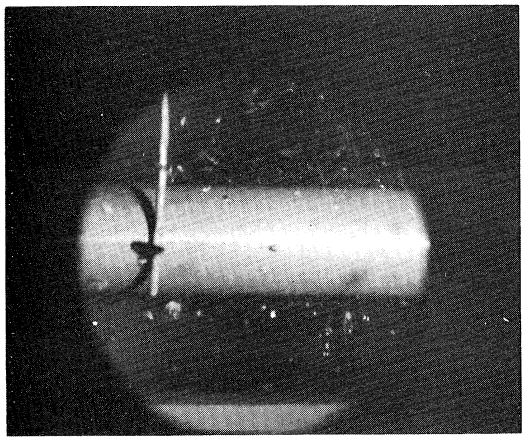

Heat Flux = 2,016 Btu/hr-ft^2

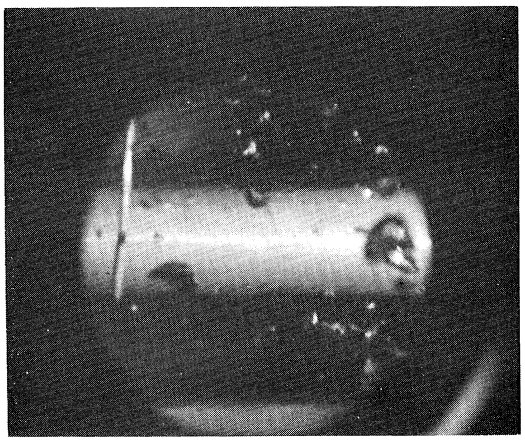

Heat Flux = 1,330 Btu/hr-ft^2

Fig. 61. Photographs of saturated forced convection boiling from outside surface of horizontal Inconel tube at 535 psia, 4.7 ft/sec (Run HI1-16).

condition of 99,300 Btu/hr-ft^2 and decreasing to a heat flux of 1330 Btu/hr-ft^2.

The large bubbles seen below the horizontal test section are formed by the electrical heaters in the circulation loop. The presence of vapor bubbles in the free stream indicates that the degassed water is saturated. The water temperature is measured by a thermocouple inclosed in a 1/16 in. diameter sheath, seen at the left of the pictures. Virtually no bubbles can be seen on the last two pictures, for which the heat flux is 2016 and 1330 Btu/hr-ft^2, respectively.

Photographs taken during run HI1-17 are shown on Fig. 62. The conditions throughout this run were 535 psia and pool boiling. Heat transfer data for this run are included on Fig. 13. The photographs are arranged in order of decreasing heat flux, from the initial test condition of 99,300 Btu/hr-ft^2 to the final condition of 437 Btu/hr-ft^2. No bubbles are evident at the very lowest heat flux, and the visible bubble population is very sparce at a flux of 1250 Btu/hr-ft^2.

The photographs of run HI1-20, shown on Fig. 63, were taken under conditions of 1550 psia and pool boiling. The heat transfer data for this run are tabulated in Appendix C. The heat flux range is from 101,000 to 446 Btu/hr-ft^2.

Of particular interest in Fig. 63 is the cloudy appearance thought to result from thousands of small bubbles in the two photographs of the intermediate heat flux condition. The cause of this is

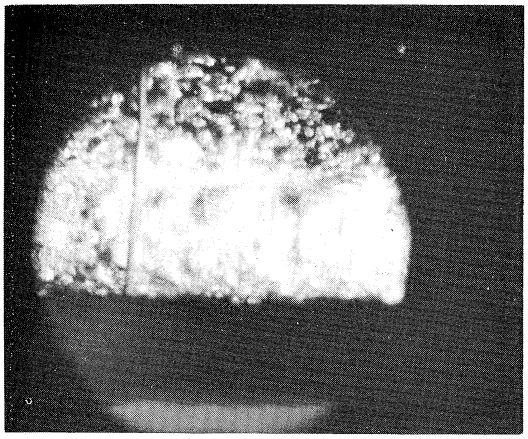

Heat Flux = 99,300 Btu/hr-ft^2

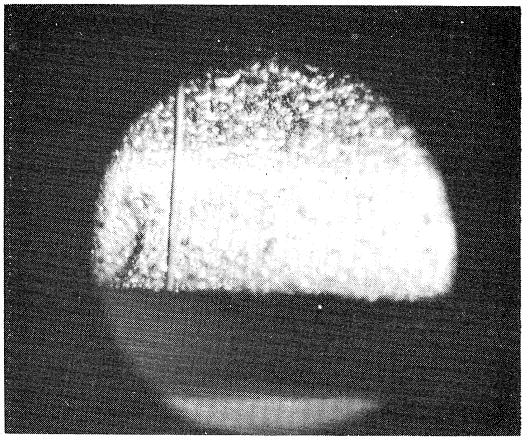

Heat Flux = 43,800 Btu/hr-ft^2

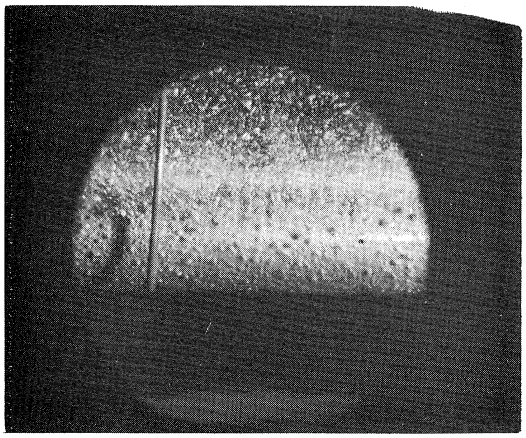

Heat Flux = 17,390 Btu/hr-ft^2

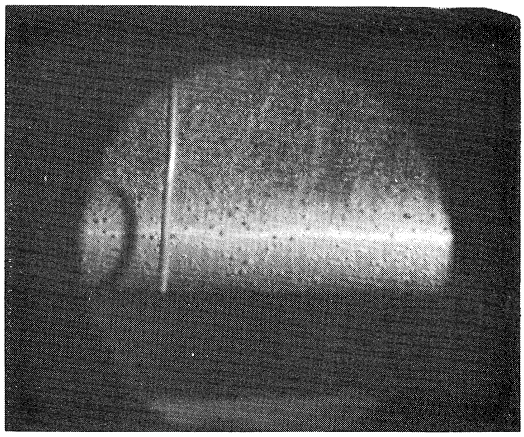

Heat Flux = 5,655 Btu/hr-ft^2

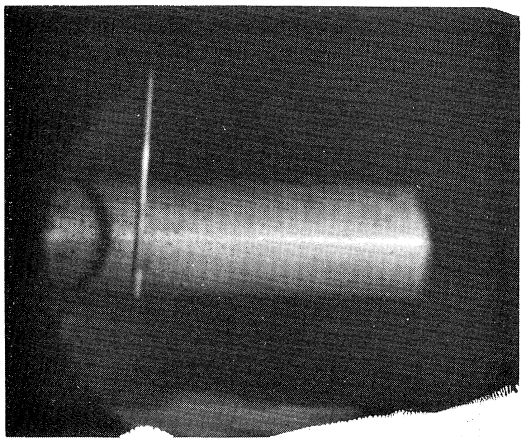

Heat Flux = 1,250 Btu/hr-ft^2

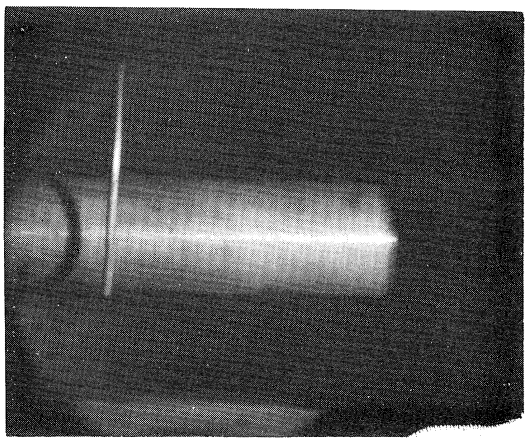

Heat Flux = 437 Btu/hr-ft^2

Fig. 62. Photographs of saturated pool boiling from outside surface of horizontal Inconel tube at 535 psia (Run HI1-17).

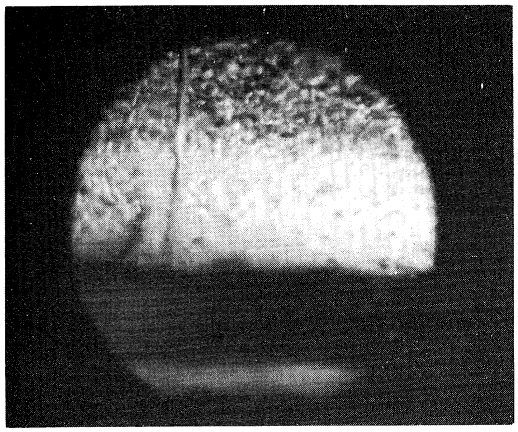

Heat Flux = 101,650 Btu/hr^2

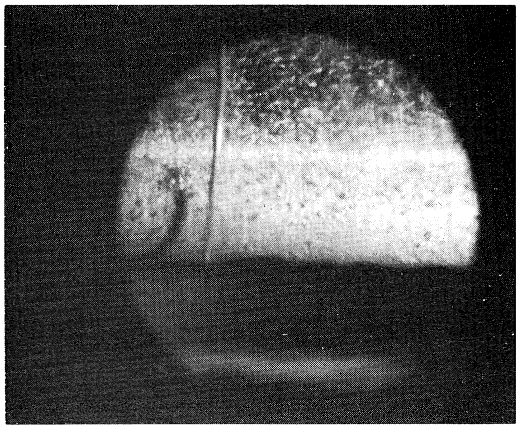

Heat Flux = 43,440 Btu/hr-ft^2

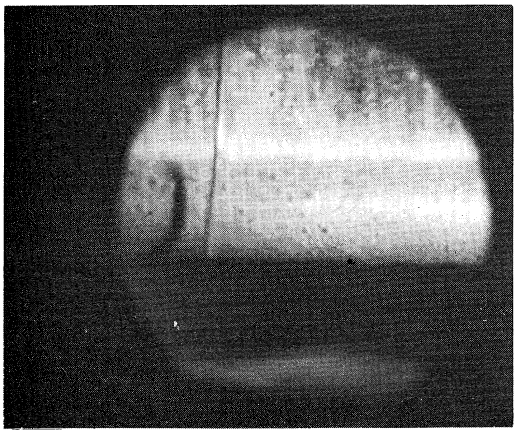

Heat Flux = 16,530 Btu/hr-ft^2

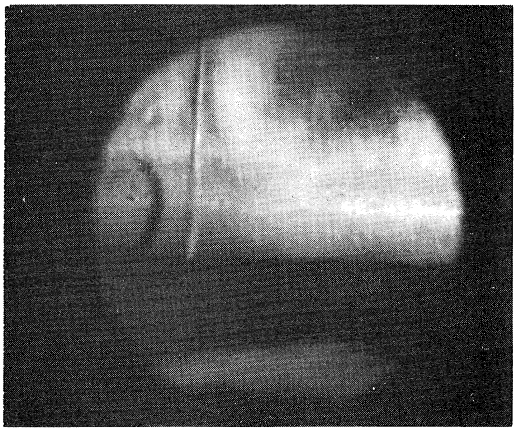

Heat Flux = 6,625 Btu/hr-ft^2

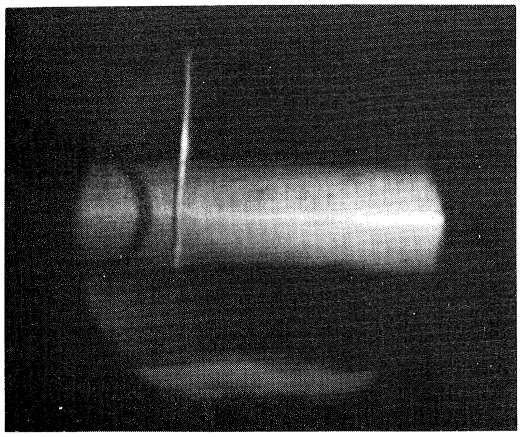

Heat Flux = 1,280 Btu/hr-ft^2

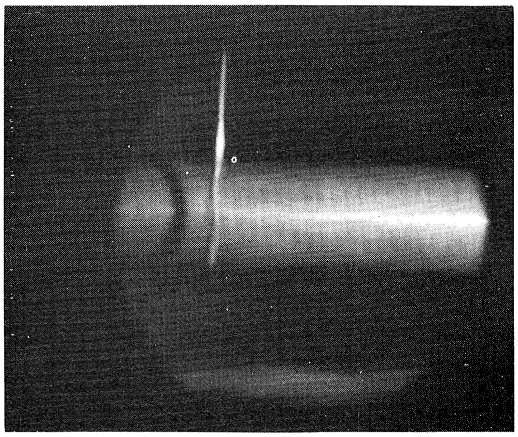

Heat Flux = 446 Btu/hr-ft^2

Fig. 63. Photographs of saturated pool boiling from outside surface of horizontal Inconel tube at 1,550 psia (Run HIl-20).

unknown, although it may result from the influence of suspended solids material on the nucleation process as discussed in Section VI. The possibility of electrolysis causing a fine mist of bubbles which form the clouds was examined. To investigate this the electrical bus was disconnected at one end of the test section and connected to the test vessel. Under saturated pool conditions at 535, 1015, and 1550 psia a voltage was impressed between the test section and the vessel with the water for electrolyte to determine whether electrolysis would occur and produce the observed bubbles. At voltage values from 0 to 15 VDC no bubbles were visible and no electric current could be measured during the tests.

VI. DISCUSSION OF RESULTS

A. HEAT TRANSFER CHARACTERISTICS

The heat transfer characteristics for boiling from the outside surface of 3/4 in. diameter horizontal and vertical tubes to high purity saturated water are presented. The investigation covers low heat flux boiling at high pressure with natural and forced convection. The range of heat flux extends from the non-boiling region through incipient boiling to a heat flux of 100,000 Btu/hr-ft^2 in the nucleate boiling region.

1. Non-Boiling Region

At low values of wall superheat, heat is transferred by convection from the heated surface to the water. In natural convection the heated fluid rises to the liquid-vapor surface where evaporation takes place. With forced convection, evaporation also occurs at the liquid-vapor interface but forced circulation increases the heat transfer as compared to that for gravity circulation at a given temperature difference between the liquid and the heated surface.

a. Forced Convection. --The horizontal test section data obtained for forced convection non-boiling heating are correlated very well by the following equation given by Kreith[32] for a cylinder in crossflow:

$$\frac{\bar{h}_c D_o}{k} = 1.1\, C \left(\frac{V_\infty D_o}{\nu} \right)^n Pr^{0.31} \qquad (4)$$

In this equation C and n are constants which are dependent on the Reynolds number. Table X in Appendix A gives a comparison of measured ΔT for Inconel and carbon steel test sections and the ΔT calculated from Eq. (4). Agreement between measured and calculated values is good at low heat flux. Deviation occurs as the effects of boiling begin to influence the heat transfer characteristics. This is evident at lower values of heat flux as the pressure is increased as seen in Figs. 18 and 23. The characteristic curves for individual pressures converge in the non-boiling region. A common curve with a slope of 1 fits the data for the pressure range from 535 to 1550 psia very well in this region.

The forced convection non-boiling data for the vertical Monel test section may be correlated by the following equation given by Kreith for flow parallel to a flat plate:

$$Nu_x = \frac{hx}{k} = 0.0288\, Pr^{1/3} \left(\frac{V_\infty x}{\nu} \right)^{0.8} \qquad (5)$$

With x based on test section heated length, this equation fits the data at the bottom thermocouple position closely. However, the reduction in heat flux at a given ΔT predicted by Eq. (5) for the center and top thermocouple locations does not occur in the test data as seen in Figs. 48 through 53.

In reference (45) the following expression for boundary layer thickness is developed for turbulent flow over a flat plate by assuming $V/V_\infty = (y/\delta)^{1/7}$ and $\tau_o = 0.0225\,(\nu/V_\infty\delta)^{\frac{1}{4}}$:

$$\delta = 0.37\,(\nu/V_\infty x)^{1/5}\,x \qquad (6)$$

Applying this relation for the flow conditions at 535 psia the turbulent boundary layer would completely fill the annulus about 1 ft from the entrance to the flow guide. Thus fully developed turbulent flow would exist in the unheated approach section ahead of the test section. With fully developed turbulent flow, the convective heat transfer coefficient remains constant for almost the entire heated length. The exception is a short distance from the point of beginning heating in which the thermal laminar sublayer is developed. Hence, the forced convection non-boiling data for a vertical Monel test section under the flow conditions of this investigation may be represented by:

$$q/A = 2300\,(T_w - T_{sat}) \qquad (7)$$

for: $T_w - T_{sat} < 2^oF$ at 535 psia

$T_w - T_{sat} < 1^oF$ in 535 to 1550 psia range.

b. Natural Convection.--The non-boiling natural convection data at 535, 1015, and 1550 psia fit a single curve as indicated by Figs. 19, 24, and 29 for the horizontal test sections. As indicated above, natural convection non-boiling data were not obtained for the vertical

test section. A correlation, given by McAdams,[33] of heat transfer with natural convection for conditions when the product of Grashof and Prandtl numbers is between 10^3 and 10^9 is:

$$Nu = 0.53\,(Gr\ Pr)^{0.25} \tag{8}$$

Under the test conditions of this investigation, the product of Grashof and Prandtl numbers ranges from 10^6 to 10^7. Hence, the correlation expressed by Eq. (8) should be applicable for the non-boiling region.

Since the heat transfer rate can be written:

$$q = hA(T_w - T_B) = \mu A \Delta T, \tag{9}$$

we can express q as:

$$q/A = 0.53\,\frac{k}{D_o}\left(\frac{\rho^2 g\beta D_o^{\,3} C_p}{\mu k}\right)^{0.25} \Delta T^{1.25} \tag{10}$$

which illustrates that the heat flux, q/A, is proportional to the temperature difference, ΔT, raised to the 1.25 power. For saturation conditions Eq. (10) reduced to:

$$q/A = 125.5\,\Delta T^{1.25} \quad \text{at } 535 \text{ psia}$$

$$q/A = 123\,\Delta T^{1.25} \quad \text{at } 1015 \text{ psia}$$

$$q/A = 120\,\Delta T^{1.25} \quad \text{at } 1550 \text{ psia}$$

A single equation:

$$q/A = 123\,\Delta T^{1.25} \tag{11}$$

could be used for the pressure range from 535 to 1550 psia under the conditions of this investigation.

The data obtained for the horizontal Monel, Inconel, and carbon steel test sections in the non-boiling region (reference Figs. 19, 24, and 29) may be represented by the following equations:

For Monel, $q/A = 500\,\Delta T^{1.2}$

For Inconel, $q/A = 420\,\Delta T^{1.23}$

For carbon steel, $q/A = 500\,\Delta T^{1.27}$

The non-boiling data for all three materials may be represented to within $\pm$ 10% by the equation:

$$q/A = 460\,\Delta T^{1.25} \qquad (12)$$

The experimental data for Monel, Inconel, and carbon steel tubes are approximately four times that predicted by Eq. (11). The literature contains very little non-boiling natural convection data for saturated water at elevated pressures. McAdams[33] presents curves of Addoms and Rinaldo for saturated pool boiling at atmospheric pressure which include the non-boiling region. The correlation of Addoms' curve for a 0.048 in. diameter wire with Eq. (10) is good. Rinaldo's data is presented to show the effect of reducing the wire diameter.

From Eq. (10) it can be seen that at a given ΔT the heat flux is proportional to $D_o^{-\frac{1}{4}}$. The variation of Rinaldo's data from that of Addoms is considerably greater than would be predicted by the change of diameter. For a wire diameter of 0.024 in. Rinaldo's data are 1.3 times that predicted by Eq. (10), for a 0.004 in. diameter the data are 2.6 times the predicted value.

The data of Farber and Scorah[38] for pressure from 0 to 100 psig also are not correlated by Eq. (10). A change of exponent would be required to fit the data. Their method of welding thermocouples to the surface of the wire which was heated by the passage of an electric current probably introduced error in temperature measurement. Thus their non-boiling data is questionable.

Hyman, Bonilla and Ehrlich[47] present data for heating water and other fluids at atmospheric pressure from the surface of horizontal cylinders which are correlated by Eq. (10). However, the fluid temperatures were less than saturation temperature for the pressure. A large increase in heat flux was noted with relatively small increase in ΔT at conditions slightly below the point for boiling to begin. This was attributed to turbulence in the wake which increased until it affected almost the entire upper half of the cylinder. They indicate that turbulence is initiated at:

$$\log_{10}\left(\frac{Gr\ Pr}{D_o^3}\right) = 11.2 \pm 0.2$$

The maximum value of this logarithmic function for the non-boiling data in the present research is 10.759 which indicates that turbulence was not a factor.

Further investigation appears to be necessary to determine the factors which affect the non-boiling natural convection of saturated water at elevated pressures. The results of this investigation are considered valid even though they are not correlated by Eq. (10).

2. Incipient Boiling Point

The location of the incipient boiling point for the horizontal Monel, Inconel, and carbon steel test sections under saturated pool boiling conditions was determined by examination of Figs. 19, 24, and 29. It is taken as the point of intersection of the non-boiling curve and the fully developed boiling curve as suggested by McAdams, et al.[36] Similarly, the incipient boiling point for these test sections under forced convection conditions was determined from Figs. 18, 23, and 28. Below 6000 Btu/hr-ft^2 the effect of nucleation on the position of the boiling curve for the Inconel tube is weak at each test pressure, Fig. 18.

The forced convection test data for the vertical Monel test section exhibit a little more scatter in the non-boiling region than was encountered for the horizontal test sections. The effect of nucleation on the boiling curve below 10,000 Btu/hr-ft^2 is weak. Incipient

boiling points were established from Figs. 39, 41, and 43. These data are included with those for Inconel and carbon steel in Table VIII. From Figs. 39, 41, and 43 it can be seen that the ΔT at incipient boiling increases slightly in the direction of flow; average values for the three positions were tabulated. The range of heat flux for pool boiling with the vertical Monel tube did not extend to low enough value to establish the incipient boiling point.

Bankoff[34] presents data of several investigators on the incipient boiling point for various surface-fluid combinations. The data of Addoms[35] for boiling water from the surface of a 0.024 in. diameter platinum wire are in the pressure range of this investigation. By interpolation, values were determined at 535, 1015, and 1550 psia and included in Table VIII for comparison. General agreement exists among the saturated pool boiling data although some variation which may be attributable to material or surface condition is evident.

3. Nucleate Boiling

In the nucleate boiling region the heat transfer by natural or forced convection is very greatly amplified by small but very intense convective currents which result from the formation and collapse of bubbles at discrete nucleation sites. As a result a large increase in heat flux results from a relatively small increase in the temperature difference between the heated surface and the fluid. It has been found useful to correlate boiling data by an equation in the form:

TABLE VIII

$(T_o - T_{sat})$ - °F AT INCIPIENT BOILING POINT[a]

Pressure Psia	Test Sections							Addoms' Data (0.024 in. dia. wire)
	Horizontal						Vertical	
	Inconel		Carbon steel		Monel		Monel	Platinum
	Pool	4.7 Ft/sec	Pool	4.7 Ft/sec	Pool	4.7 Ft/sec	4.7 Ft/sec	Pool
535	4.8	1.9	2.7	1.4	2.7	2.6	2.5	3.4
1015	2.7	0.7	1.3	0.9	2.0	2.3	2.0	2.3
1550	1.1	0.27	0.95	0.6	1.6	1.5	1.0	1.85

[a]All data are for boiling saturated water.

$$q/A = C\,(T_w - T_{sat})^n \qquad (13)$$

On a plot of heat flux versus temperature difference as shown in Sections IV and V, the value of n in Eq. (13) is the slope of the characteristic curve in the nucleate boiling regime.

The slope of the characteristic curve in the nucleate boiling region is greater than that in the non-boiling region. A gradual change of slope occurs under forced convection conditions when progressing from the non-boiling region to the nucleate boiling region, Figs. 18, 23, 28, and 39. However, a more abrupt change in slope is noted for the case of pool boiling, Figs. 19, 24, and 29. The slopes in the nucleate boiling region for the test sections investigated are shown in Table IX. Where considerable curvature exists in the curves, a best straight line fit for the data was used to determine slope. A variation in slope is apparent, ranging from 1.81 to 4.7 for pool boiling and from 1.4 to 9.17 for forced convection.

A large variation exists in the values of heat flux at a given surface superheat in the nucleate boiling region for the four test sections, which includes the horizontal Monel, Inconel, and carbon steel test sections and the vertical Monel test section. Figs. 33 through 38 give a comparison of the data for the horizontal test sections. The heat transfer characteristics of the horizontal Monel and vertical Monel test sections are compared in Figs. 59 and 60. The

TABLE IX

SLOPE n OF NUCLEATE BOILING CHARACTERISTIC CURVE[a]
FOR INCONEL, CARBON STEEL, AND MONEL TUBES

Pressure Psia	Horizontal						Vertical	
	Inconel		Carbon steel		Monel		Monel	
	Pool	4.7 Ft/sec	Pool	4.7 Ft/sec	Pool	4.7 Ft/sec	Pool	4.7 Ft/sec
535	2.40	1.68	2.64	1.40	2.50	2.22	1.81	1.49
1015	2.58	1.95	2.96	1.56	3.52	5.32	1.81	1.81
1550	2.55	2.07	3.22	1.71	4.70	9.17	1.81	1.81

[a]The nucleate boiling characteristic curve may be represented by an equation in the form $q/A = C (T_w - T_{sat})^n$ where C is a constant and n is the slope of the characteristic curve plotted on log-log paper.

probable reasons for the variations among the horizontal test sections are surface conditions which affect nucleation site size and distribution, and material properties. The tube orientation is seen to have a significant effect on the nucleate boiling characteristics.

As indicated in Section III, the surface roughness is greater for Inconel than for Monel or carbon steel. Corty and Faust[6] found that, in the range from 4 to 25 μ in. RMS, as the surface roughness is increased the temperature difference required at a given heat flux is reduced. They also found that this relationship did not necessarily hold at higher values of surface roughness. Hence, the Inconel and carbon steel tubes investigated do not fall in the range in which surface roughness might be expected to have a predictable effect.

Surface corrosion may produce a more favorable distribution of nucleation sites than would be found for the non-corroded surface. Other factors related to the material properties may influence the position of the nucleate boiling curve. Larson[46] indicated that corrosion resistant materials support greater wall superheat than do non-corrosion resistant materials and thus are not good ebullators. He found that ebullition could be correlated with floatability (or non-wetting). Substances known to be non-wetting proved to be good ebullators. Floatability may be brought about by surface contaminating films due to chemical reaction (oxidation, carbonation, hydration, etc.).

Monel and Inconel materials are considerably more corrosion resistant than carbon steel. From this, and if the floatability (non-wetting) of the carbon steel is increased by its black oxide surface, it would be expected that the ΔT for nucleate boiling for this material would be less than that for Monel or Inconel materials at low heat flux. Figs. 33 through 38 indicate that this is true below a heat flux of 20,000 Btu/hr-ft^2. The heat flux at which the ΔT for Monel becomes less than that for carbon steel depends on the pressure and is lower for forced convection than for pool boiling. Larson's investigation was not performed with a heating surface. Hence, although floatability may reliably indicate the order of ΔT for incipient nucleation, it correlates the relative position of the nucleate boiling curves only at relatively low values of heat flux.

Larson stated that the burnout heat flux is higher for a wetted surface than that for a non-wetted surface. Burnout conditions were not examined in this investigation but in this basis it might be speculated that the carbon steel test section would reach "burnout" at lower heat flux than that for Monel or Inconel test sections.

From the discussion above it appears that the chemical nature of the liquid-surface combination is a significant factor in the variation of data from one investigation to another. This matter is beyond the scope of this research but may prove to be a fruitful area for further investigation. Water chemistry has been found in this study

to be an important factor in attaining reproducible data and should be given due consideration in any investigation of liquid-surface characteristics.

Correlation equations for the natural convection nucleate boiling data of this investigation may be established in the form of Eq. (13):

$$q/A = C\,(T_w - T_{sat})^n \qquad (13)$$

A single correlation equation to represent the horizontal Monel, Inconel, and carbon steel data is not considered practical due to the great difference in the data for the three materials. The variation of temperature difference at a given heat flux is not large but at a given temperature difference the heat flux range may be as much as a factor of five. Hence, correlation equations are given below for each of these materials and the vertical Monel test section which represent the natural convection nucleate boiling data obtained to within $\pm$ 10% except for Eq. (17) which is to within $\pm$ 15%:

For Inconel:

Above 2500 Btu/hr-ft^2

$$q/A = 93.8 \left(\frac{T_{sat}/T_c}{1 - P/P_c} \right)^{2.9} (T_w - T_{sat})^{2.48} \qquad (14)$$

For carbon steel:

From 2000 to 25,000 Btu/hr-ft^2

$$q/A = 58.9\left(\frac{1}{1 - P/P_c}\right)^{4.18} (T_w - T_{sat})^{3.56} (P/P_c)^{1/6} \qquad (15)$$

Above 25,000 Btu/hr-ft^2

$$q/A = 4085\left(\frac{P/P_c}{1 - P/P_c}\right) (T_w - T_{sat})^{1.78} \qquad (16)$$

For Monel (horizontal):

Above 3,000 Btu/hr-ft^2

$$q/A = 155\left[1 - \left(\frac{T_c P}{T_{sat} P_c}\right)^{4.25}\right]^{10} (T_w - T_{sat})^{\frac{1.419}{1-(P/P_c)^{\frac{1}{2}}}} \qquad (17)$$

For Monel (vertical):

Above 1,500 Btu/hr-ft^2

$$q/A = 3580\left(\frac{P}{P_c}\right)^{1.21} (T_w - T_{sat})^{1.82} \qquad (18)$$

The correlation equations are applicable for the pressure range 535 to 1550 psia. The exponent n is constant indicating suitable correlation with a single slope for the horizontal Inconel and Monel data. However, the carbon steel and vertical Monel data required a change of slope with pressure change to maintain the indicated accuracy. Above 25,000 Btu/hr-ft^2 a single slope for the pressure range was suitable for the carbon steel data.

4. Pressure and Velocity Effects

The effect of pressure on the position of the nucleate boiling curves is evident in the summary curves. This effect is incorporated in the above equations by modifying the proportionality constant and, in the case of the carbon steel and vertical Monel equations by modifying the ΔT exponent. Reduced pressure and temperature based on saturation conditions and the critical values for water are used for reference. All tests were made with saturated water.

The effect of pressure increase on the nucleation process for both horizontal and vertical test sections is to reduce the superheat required at a given value of heat flux. This is consistent with the results of other investigators.[8, 16, 22, 24, 37, 38] McAdams, et al.[36] indicated that the pressure effect decreased at high heat flux approaching burnout values. For the heat flux range of this investigation in pool boiling there is no indication of a reduction in pressure effect as heat flux increases. For the forced convection case there appears to be a slight increase in the pressure effect at the highest heat flux investigated for the Monel and Inconel test sections, Figs. 18, 28, and 39.

Forced convection increases the heat flux at a given ΔT as compared to pool boiling conditions. Engelberg-Forster and Greif[39] concluded that in the nucleate boiling regime forced convection has no effect, that nucleation dominates the heat transfer process. The

present investigation shows that a forced convection effect remains up to the maximum heat flux considered. However, the influence of velocity diminishes as the heat flux increases and is affected by the pressure and tube orientation.

For the horizontal Inconel and carbon steel test sections, the forced convection and pool boiling curves at 1550 psia merge at about 100,000 Btu/hr-ft^2, Figs. 22 and 27. At lower pressures the curves converge as heat flux increases and probably merge at a flux a little higher than 100,000 Btu/hr-ft^2. At higher or lower velocities the point of merger would shift up or down accordingly. The curves for the horizontal Monel test section converge at low heat flux but a large velocity effect remains at the maximum heat flux investigated.

The influence of pressure on the velocity effect was more pronounced for the vertical test section, Figs. 45, 46, and 47. The effect is greatly reduced at 1015 psia. At 1550 psia the forced convection and pool boiling curves merge at about the point where nucleate boiling begins in forced convection.

5. Vertical Test Section - Heat Transfer Characteristics Variation with Axial Position

Examination of Figs. 48 through 58 reveals a variation of heat flux at a given ΔT for the three axial thermocouple locations. The variation is small at a heat flux less than 10,000 Btu/hr-ft^2 for forced

convection, Figs. 48 through 53, but in pool boiling it exists at the minimum heat flux investigated. The variation becomes progressively greater in the range from 10,000 to 100,000 Btu/hr-ft^2.

In Figs. 48 through 53, the variation with axial position is negligible until the effect of forced convection on the heat transfer diminishes considerably and the nucleation effect becomes the dominant factor in boiling. The lower ΔT at a given heat flux at the middle and upper thermocouple locations indicates that the metal surface is cooler as the flow progresses upward along the tube. The probable cause of this effect is increased agitation in the boundary layer as a result of the additional bubbles approaching from below or the turbulence level in the flow stream (and boundary layer) increases due to the boiling action upstream. In either case the heat exchange process is more effective and the outside wall temperature decreases in the direction of flow. The axial distance between the thermocouple locations is 1.5 in. (total distance involved is 3 in.). At greater distance downstream when the quantity of bubbles in the flow becomes large enough to interfere with the bubble pumping action the surface temperature would rise again until as a limit the burnout condition is reached.

A similar condition exists for the pool boiling characteristic curves shown in Figs. 54 through 58. In this case it is noted that the bottom and middle thermocouple locations have essentially the same

characteristic curve. However, the characteristic curve for the top measuring station occurs at a lower ΔT at a given heat flux. This condition extends throughout the heat flux range investigated since the entire curve is for nucleate boiling. The non-boiling range was not reached in the vertical test section pool boiling runs. The cause of the shift to lower ΔT in pool boiling (natural convection) is probably due to agitation of the convection flow stream by the bubbles rising from below thus improving the bubble pumping action in exchanging hot fluid for cold fluid at the heated surface. In this case also the surface temperature would again rise further downstream as the quantity of bubbles becomes large enough to interfere with the pumping action.

The possibility of a reduction in T_{sat} in the direction of flow which would cause a reduction in tube surface temperature was considered. The change in elevation between top and bottom thermocouple positions would result in less than $0.02^{o}F$ temperature change under all test conditions. This is negligibly small compared to the measured change in ΔT in the flow direction. A pressure drop due to friction does not exist in natural convection. This pressure drop under the fully developed turbulent flow conditions of this investigation is negligible. Hence, it is concluded that the observed reduction in ΔT in the flow direction results from the agitation effects of nucleate boiling and not from a change in water temperature. This is consistent with

findings of Jakob[49] who noted a reduction of ΔT in the direction of natural convection flow along a vertical heated surface with nucleate boiling at atmospheric pressure. This effect was attributed to increased stirring effect due to boiling action.

B. WATER CHEMISTRY

The influence of dissolved gas in the boiling medium and additives to reduce the surface tension are recognized as factors which affect the nucleate boiling characteristics of a surface - fluid combination. McAdams et al.[36] presents data to show the effect of dissolved gas on the position of the nucleate boiling curve. A substantial increase in the heat flux at a given ΔT results when the amount of dissolved gas is increased. Degassing is practiced by all researchers to avoid this influence on the data.

To control oxidation of the stainless steel system and maintain a clean test section surface, it was found necessary in this investigation to control dissolved oxygen level to values less than could be reached by degassing alone. Ferrous metals oxidize readily at high temperature with small concentrations of dissolved oxygen in the water. Magnetite, Fe_3O_4, formed on the surface breaks loose with changes in system temperature and appears as suspended solid material in the water. This not only exposes the metal for further oxidation but also supplies solid material which may settle out in the system and on the heat transfer surface.

The suspended solid material was found to produce another effect on the nucleation process in addition to that of insulating the test surface when deposited thereon. At suspended solids levels low enough not to settle out on the test surface an increase in this level caused an increase in the heat flux at a given surface superheat as discussed in Section IV. Thus, in order to obtain good repeatability of the heat transfer data, it was necessary to maintain control of the suspended solids level. At comparable levels of solids the repeatability was very good as indicated above.

The level of suspended solids in the water was reduced until it remained constant prior to taking data as discussed in Section III. For pool boiling, the suspended solids level was very low and approximately the same for all test runs. However, the level attained in forced convection runs was somewhat lower for the horizontal test sections than for the vertical test section. This is probably due to a slightly less rigid flow guide installation used with the vertical electrode which allowed a little higher rate of addition of suspended solids to the water.

The method of determining suspended solids level is described in Section IV. In pool boiling, the level attained was from 5 to 20 PPB. In forced convection, the level attained was 10 to 40 PPB for horizontal test sections and 40 to 70 PPB for the vertical test section.

In general, the level attainable reduced as the pressure increased. At a given test condition the variation of level from one run to another was slight.

The absolute level of suspended solid material in the water may not be the controlling factor in its effect on the nucleate boiling process. The size, weight, and/or chemical composition of the particles may have significance in somewhat the same way that cavity size is important to nucleation as discussed by Hsu.[48]

The water pH and electrical resistivity were varied during the series of tests described in Section IV without apparent effect on the reproducibility of the heat transfer data. Maintenance of a high pH (about 9.5 to 11) aids in stabilizing the magnetite layer on ferrous surfaces and thus assists in handling corrosion problems. Pocock[31] indicated that at low pH (near 7), pH itself becomes a factor in the corrosion process. Hence, it is desirable to maintain the pH at about 9 to 11 to reduce corrosion problems and thus assist in controlling level of suspended solid material in the boiling medium.

Electrical resistivity varies as the inverse of the pH. It can be maintained at about 2×10^6 ohm-cm at pH about 7.5 in the system described herein. At a pH of 9.5 the resistivity is from 1 to 2×10^5 ohm-cm which is high enough to prevent conductance problems in systems which use electrical resistance heating of the test surface. A change of ion exchange resin is required to effect the change of pH and resistivity indicated here.

VII. CONCLUSIONS

A. HEAT TRANSFER

Heat transfer from the outside surface of commercial heat exchanger tubes to saturated high purity water at high pressure has been investigated under both forced convection and pool boiling conditions. The results give information on non-boiling heat transfer, incipient boiling, and nucleate boiling at a heat flux up to 100,000 Btu/hr-ft^2 in the pressure range from 535 to 1550 psia.

Forced convection non-boiling heat transfer characteristics may be predicted closely with generally accepted correlation equations for flow normal to a cylinder or parallel with a flat plate, as applicable. Results obtained for natural convection non-boiling heat transfer from a horizontal cylinder to high pressure saturated water show significantly higher heat flux at a given value of $T_w - T_B$ than predicted by the correlation equation given by McAdams.[33] The literature contains very little natural convection non-boiling data at saturation conditions above atmospheric pressure. That which was examined was not correlated by McAdams' equation. It is concluded that a thorough investigation of natural convection non-boiling heat transfer from horizontal cylinders to water at elevated pressure is necessary to determine the limits of applicability of the correlation equation given by McAdams.

The incipient boiling point for natural convection boiling saturated water at high pressure is more clearly indicated than that under the same conditions with forced convection. Incipient boiling occurs at lower values of surface superheat as the pressure is increased.

The natural convection nucleate boiling of high pressure saturated water from the outside surface of a commercial heat exchanger size tube may be correlated by an equation in the form:

$$q/A = f(P)(T_w - T_{sat})^n$$

The value of n, the slope of the nucleate boiling characteristic curve, is in the range from 1.81 to 4.70 under the conditions of this investigation. Its value is affected by the pressure, tube orientation, and tube material.

1. Effect of Pressure

Pressure variation has substantially no effect on non-boiling heat transfer in natural convection or with forced convection. The incipient boiling point occurs at lower value of $T_o - T_{sat}$ and is more clearly defined as the pressure is increased.

In the nucleate boiling region the effect of pressure increase is to greatly increase the heat flux at a given value of $T_o - T_{sat}$. This effect prevails from incipient boiling to a heat flux of 100,000 Btu/hr-ft^2.

2. Effect of Forced Convection

In the non-boiling region the heat flux under forced convection conditions is directly proportional to $T_W - T_B$ and is predicted by the generally accepted correlation equations. The transition from non-boiling to nucleate boiling is gradual, but becomes less so as the pressure is increased. In the nucleate boiling region, forced convection results in a higher heat flux than for pool boiling.

The influence of forced convection in the nucleate boiling region diminishes as the pressure is increased. As the heat flux is increased the influence of nucleation becomes stronger and eventually overshadows the effect of forced convection. This effect disappears at a heat flux which is dependent on the pressure, velocity, and tube orientation.

3. Effect of Tube Orientation

Tube orientation has an effect on heat transfer characteristics in the non-boiling and nucleate boiling regions. In the non-boiling region with forced convection the correlation equations for flow normal to a cylinder or parallel to a flat plate, as appropriate, may be used to estimate heat transfer. For fully developed turbulent flow parallel to the test section (vertical tube) the coefficient of convective heat transfer does not vary with axial position along the tube.

At a given value of $T_o - T_{sat}$ a horizontal tube (in crossflow) has a higher heat flux than does a vertical tube (parallel flow) in forced convection nucleate boiling throughout the pressure range and to the highest heat flux investigated. The slope, n, of the characteristic nucleate boiling curve is greater for a horizontal tube than for a vertical tube.

In natural convection nucleate boiling at a given $T_o - T_{sat}$ a vertical tube has higher heat flux than does a horizontal tube at low flux values. However, as for forced convection, the slope, n, of the boiling characteristic curve is greater for the horizontal than for the vertical tube. Hence, at higher values of temperature difference the heat flux is higher for the horizontal tube than that for the vertical tube.

The temperature difference, $T_o - T_{sat}$, at a given heat flux above 10,000 Btu/hr-ft^2 decreases in the direction of flow for a vertical tube under forced convection conditions. For natural convection nucleate boiling from a vertical heated surface this decrease in $T_o - T_{sat}$ occurs at a heat flux as low as 500 Btu/hr-ft^2. In both cases this results from increased agitation of the fluid adjacent to the heated surface by bubbles rising from below.

4. Effect of Tube Material on Heat Transfer Characteristics

All heat exchanger tube materials may be expected to have approximately the same non-boiling heat transfer characteristics for

heating saturated water from the outside surface at high pressure. This applies to heating with forced convection as well as natural convection.

The tube material has an effect on incipient boiling and on the nucleate boiling characteristic curve. The more corrosion resistant materials support higher surface superheat without boiling than do those more susceptible to corrosion. As indicated by the results of this investigation, incipient boiling occurs for carbon steel at lower values of $T_o - T_{sat}$ throughout the pressure range considered in both natural and forced convection than it does for Inconel and Monel.

In the nucleate boiling of high pressure saturated water from the outside surface of a tube a considerable variation of heat flux may be expected for different materials at a given surface superheat. The variation in $T_o - T_{sat}$ may be small at a given heat flux but the slope of the characteristic curve is so steep that a large variation in heat flux results at a given value of $T_o - T_{sat}$. In this investigation the range of heat flux for Inconel, Monel, and carbon steel at a given $T_o - T_{sat}$ was as much as five fold. The size and distribution of nucleation sites and the chemical nature of the surface-fluid combination are important factors affecting this. Surface roughness of commercial tube materials in the range for the test sections of this investigation does not correlate with nucleate boiling heat transfer performance.

B. WATER CHEMISTRY

Control of water chemistry is an important factor in the attainment of reproducible boiling heat transfer data. Degassing the boiling fluid is the accepted method of eliminating the influence of dissolved gases on the nucleate boiling characteristic curve. Other factors must be considered, particularly for ferrous metal boiling systems, to insure satisfactory results. These include dissolved oxygen level, suspended solids level, pH, and electrical resistivity.

1. Dissolved Oxygen

The level of dissolved oxygen in the water should be maintained less than 5 PPB and preferably as nearly zero as possible. Dissolved oxygen is responsible for the formation of metallic oxides which appear in the boiling medium and influence heat transfer as indicated below. Thus, control of dissolved oxygen level is a vital factor in controlling suspended solids in the water.

2. Suspended Solids

The level of suspended solid material in the boiling fluid must be kept as low as practicable, preferably less than 50 PPB. When the concentration of suspended solids becomes large, the solids begin to settle out in the system and on the heat transfer surface. This forms an insulating layer of oxide material and causes a change in the slope of the nucleate boiling curve. At lower levels of suspended solid

material, contamination of the heat transfer surface can be controlled but suspended solids in the water still influence the nucleate boiling process. Two possible explanations for the enhancement of nucleation are:

a. Nucleation takes place in the superheated boundary layer with the suspended solids acting as nucleation sites, and/or

b. The suspended solids in some manner trigger inactive nucleation sites on the heated surface into active sites at a lower $T_o - T_{sat}$ than would be required in a clean system.

This aspect of water chemistry needs further investigation to determine the exact role and complete effect of suspended solids on nucleation. It is possible that the particle size and density and the chemical nature of the oxide are important factors in this mechanism.

3. pH and Resistivity of the Water

The pH and resistivity of the water are related in an inverse manner in the range of interest for this investigation. At pH values near neutral the resistivity is very high. As the pH is changed from 7.4 to 9.5, the resistivity changes from approximately 2×10^6 to 2×10^5 ohm-cm. The pH as such in this range has no direct effect on the heat transfer process. However, a high pH (9-11) is beneficial in stabilizing the magnetic iron oxide layer on ferrous parts and thus is a factor in controlling oxidation.

An ion exchanger provides a good means of maintaining the pH of the water at the desired level. The ion exchanger resin may also serve as a filter to remove very small suspended solid particles from the water.

APPENDIX A

THERMOCOUPLE CALIBRATION

A. CALIBRATION APPARATUS AND PROCEDURE

Thermocouples are widely used for the measurement of temperature. A thermocouple consists of an electrical circuit created by two dissimilar metals whose junctions are maintained at different temperatures. Under these conditions an electromotive force is generated. This emf is a function of the two metals used, the relative temperature difference between the junctions, and the absolute temperature level. The basic laws of thermoelectric circuits are given by Roeser.[40]

Although the approximate relation between the emf generated and the temperature is well established for the various suitable thermocouple metal combinations, to achieve accurate results, thermocouples must be calibrated to yield temperatures that are in agreement with the International Temperature Scale. This scale is defined by the standard platinum-resistance thermometer in the range of -182.970 to 630.5°C. The platinum-resistance thermometer is calibrated at the primary fixed points (1948 ITS) which, in our range of temperature, are:

1. Temperature of equilibrium between ice and air-saturated water (ice point) -- 0.000°C.

2. Temperature of equilibrium between liquid water and its vapor (steam point) -- 100.000°C.

3. Temperature of equilibrium between sulfur and its vapor (sulfur point) -- 444.600°C.

The Callendar formula is used to express the temperature as a function of resistance of the platinum thermometer.

There are several methods of calibrating thermocouples to yield accurate indications of temperature, as discussed by Roeser and Lonberger.[41] The most direct procedure is to compare the thermocouples directly with the standard platinum-resistance thermometer. To make a comparison, a reservoir is needed whose temperature can be regulated at a steady value and yet periodically varied to cover the desired range. Because it is desired to cover a wide range of temperatures in a single apparatus, a thermostated liquid bath is not suitable. Therefore a solid copper cylinder, 6 in. in diameter by 18 in. long, was selected to be the controlled isothermal medium.

Direct-temperature regulation of the copper cylinder to $\pm$ 0.1°F would be difficult and direct regulation to $\pm$ 0.001°F virtually impossible. Constancy of temperature is necessary to eliminate uncertainties in the calibration. To achieve the desired result, the cylinder is surrounded by, but thermally insulated from, another system having a large thermal inertia. This second system is a copper pipe, capped

at both ends except for access holes to the inner block. The size is approximately 11 in. O.D., with a 3/8 in. wall thickness.

The outer copper cylinder, or pipe, is thermally insulated from the ambient air by a 5 in. layer of insulation. This whole assembly is positioned in an extended 55-gal steel drum. The temperature of the outer pipe is controlled by the action of an electronic controller, using a thermocouple emf signal, which energizes electrical heaters clamped to the outer surface of the pipe. This controller has a $\pm$ 1°F band and the power control is either on or off. In an analysis made by Clark, et al.,[42] it is shown that for the physical system used, a temperature amplitude of 1°F on the pipe will be damped to approximately $\pm$ 0.001°F in the inner cylinder. In operation no measurable temperature cycling could be observed. A picture of the complete apparatus is seen in Fig. 64.

The temperature of the inner block is accurately measured by a Leeds and Northrup Cat. No. 8163-B platinum resistance thermometer. This thermometer was calibrated by determining its resistance at the fixed points listed above and at the temperature of equilibrium between saturated liquid oxygen and its vapor at one atmosphere pressure and certified to be satisfactory for use as a defining standard by the National Bureau of Standards. A table was furnished by the NBS in 1°C increments for determining the temperature corresponding to the thermometer resistance in the range from -183° to +500°C. Linear

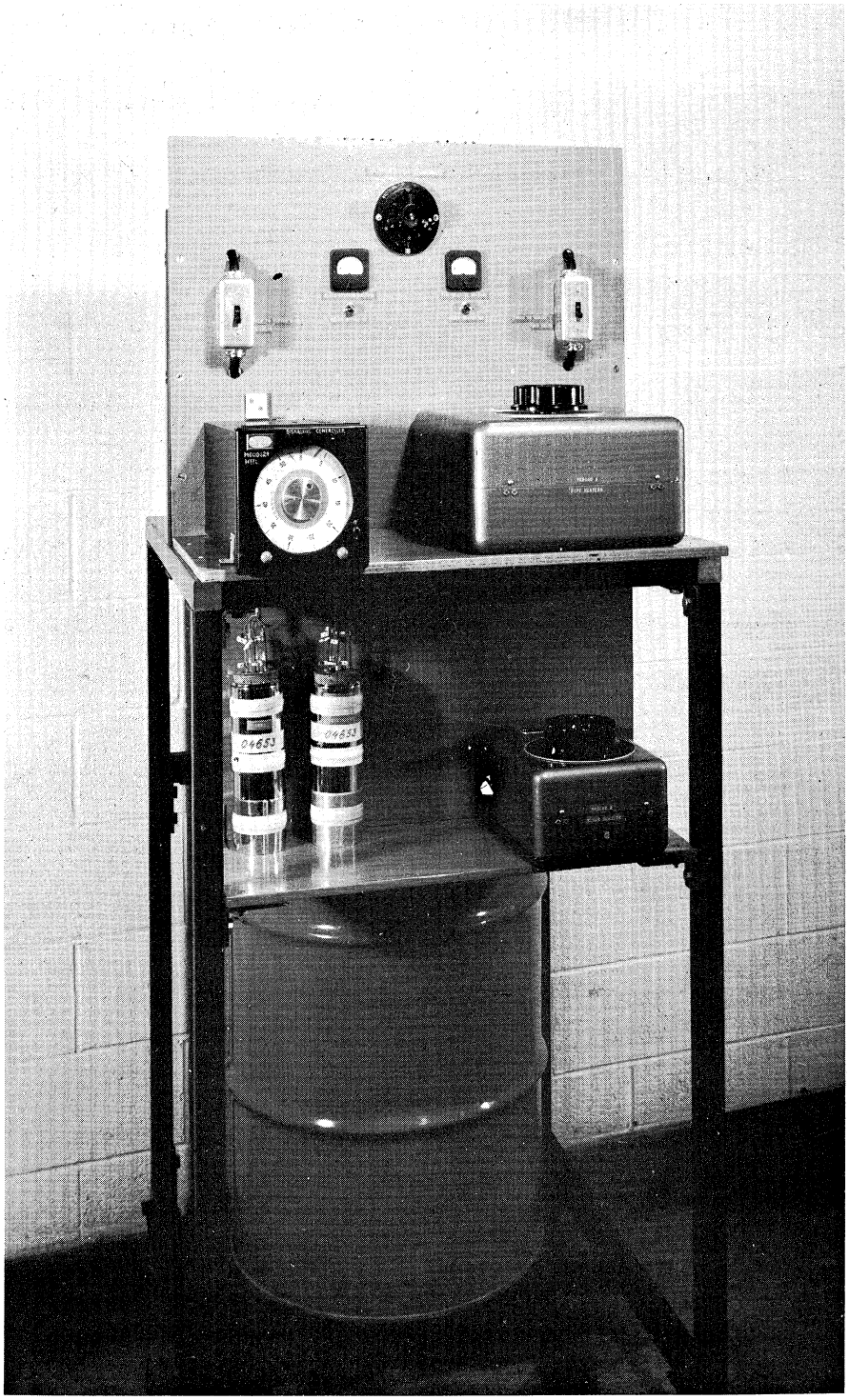

Fig. 64. Thermocouple calibration apparatus.

interpretation is satisfactory between tabulated points. The resistance of the thermometer was measured by a Type G-2 Mueller Bridge and a Model 2284d moving coil galvanometer, manufactured by L & N. The measuring resistors of the bridge are mounted in a special enclosure and held at constant temperature by a thermostat. The precision of the bridge is $\pm$ 0.0003 ohm which corresponds to a temperature variation of $\pm$ 0.003°C. The largest uncertainty in the thermometer calibration was $\pm$ 0.005°C. It is reasonable to consider the combined accuracy of the Mueller Bridge and resistance thermometer to be $\pm$ 0.01°C.

The test section of the low heat flux boiling apparatus consists of a 3/4 in. O.D. tube in which are installed 12 thermocouples made from 30 ga chromel-constantan wire. The tube is 7 in. long and is silver soldered to short sections of the copper electrode. Each thermocouple in the test section was calibrated by measurement of its emf when the whole test section subassembly was inserted into a well in the inner cylinder of the constant temperature apparatus and held at a temperature accurately measured by the platinum resistance thermometer, located in an adjacent well.

Sheathed thermocouples, used to measure the steam and water temperatures, were inserted into other wells in the cylinder and calibrated simultaneously with the test section. The copper cylinder was heated to 750°F and held for 24 hours to stabilize the thermocouples.

Lady[8] found that the chromel-constantan thermocouples emf changed with length of exposure at high temperature. This is consistent with information given by Dahl[43] for other thermocouples utilizing chromel and constantan. By holding the thermocouples at high temperature for 24 hours prior to calibration, the shift in emf output with exposure to temperatures of 650°F and below can be reduced to an acceptable level. The thermocouples were calibrated and then rechecked. If the second calibration agreed with the first within 2 μv the thermocouples were considered satisfactory. Agreement was normally within 1 μv except at 550°F where the output of some of the thermocouples decreased by 2 μv.

Although all 12 thermocouples in the test section were made in similar fashion and from the same spool of wire, the emf-temperature relation differed slightly among them. A Type K-3 Universal Potentiometer (L & N) was used with a Model 2284d moving coil galvanometer to measure the thermocouple emf. The reference junction was held in a distilled water ice bath. According to the manufacturer, the potentiometer-galvanometer combination is accurate to within ± (0.015% of reading plus 2 μv) in the range used. This corresponds to a maximum deviation of ± 5 μv at a level of 550°F, or about ± 0.125° F. Although the absolute accuracy of the instrumentation is as stated, the readings of one thermocouple relative to another are believed to be within ± 2 μv, or ± 0.05°F.

From the calibration of a thermocouple at various known temperatures, a curve of emf versus temperature may be constructed to provide a means of interpolating between the calibration points. It is customary to make use of standard curve and to plot the deviation from the standard curve. A table giving standard, or average, values for chromel-constantan is provided by Shenker, et al.[44] The table is limited to temperatures in $10^{\circ}F$ increments and emf values to 0.1 mv. Thus, if readings are made to 0.001 mv (1 μv), there may be a significant error caused by the round-off of the table. By making use of graphical techniques to insure smooth first and second derivatives, a table of emf versus temperature was generated by the IBM 7090 computer. This table, which, if rounded off, yields the two place table of Shenker, tabulates temperature in increments of $0.1^{\circ}F$ from 30 to $1200^{\circ}F$ and electromotive force to three places (1 μv). Since $0.1^{\circ}F$ represents about 4 μv change in emf, an emf reading accurate to $\pm$ 2 μv may be easily converted to temperature to the nearest $0.1^{\circ}F$.

B. FINAL CALIBRATION IN LOW HEAT FLUX BOILING SYSTEM

The thermocouples were installed in the low heat flux boiling system to a greater depth of immersion than that used for calibration in the constant temperature block assembly. This avoids an error in thermocouple reading due to decreasing the depth of immersion as reported by Dahl.[43] However, it was found that there is also a change in emf for the chromel-constantan thermocouples at a given temperature if the immersion is increased. The change is smaller than that which occurs if the immersion is decreased but it decreases the accuracy of temperature readings and has a serious effect on small temperature differences determined from the readings.

A procedure of calibrating the thermocouples when installed in the system at operating conditions was adopted in order to obtain the desired accuracy in measurements. Thermocouple readings taken with zero electrical current in the tube before and after each test run provide an in-place calibration. This offers the additional advantage that if any change in thermocouple characteristic occurs over a period of time after installation it will be allowed for in each set of data. It is worthy of note that no change in thermocouple characteristics during a series of tests has been observed for these experiments.

Based on the initial calibration of thermocouples in the constant temperature block assembly, typical sets of readings taken with no electrical current passing through the test section are as follows:

Run no.	HI2-3	HI2-5
Steam space	474.0°F	600.2°F
Bulk water	474.4°F	600.6°F
Average of 12 electrode Thermocouples	473.5_5°F	599.6_8°F

Electrode Temperature Distribution

No. of TC's	Temp.	No. of TC's	Temp.
7	473.5	6	599.6
4	473.6	3	599.7
1	473.7	2	599.8
		1	599.9

The above temperature readings indicate an apparent temperature difference of almost 1°F between the test section and water with no electrical current passing through the tube. However, considering one half of the test section as a simple fin of length L with an insulated tip immersed in a fluid at T_B, it can be shown that under the existing flow conditions this temperature difference is negligible as follows:

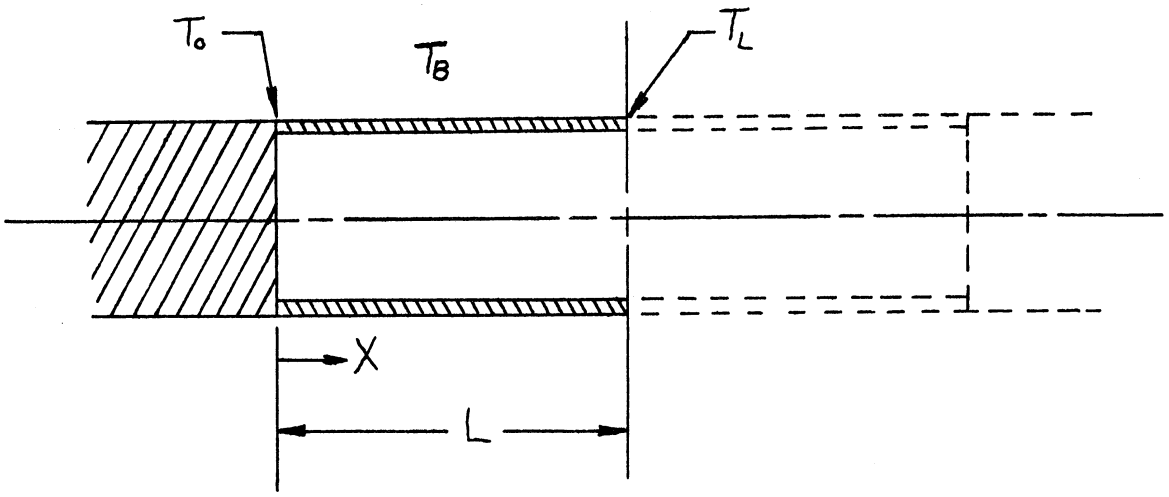

$$\frac{\cosh m(L-X)}{\cosh mL} = \frac{T_B - T}{T_B - T_o} \qquad \text{Ref. Kreith}^{32}\ \text{P. 49} \qquad (19)$$

where L = length of fin = 3 in.

$$m = \sqrt{\frac{\bar{h}_c P}{kS}}$$

P = perimeter of fin = $0.75\,\pi$ in.

S = cross sectional area = 0.1122 in.^{2}

For saturated water at 1550 psia and 4.7 ft/sec velocity, $\bar{h}_c$ can be determined from Eq. (4).

$$Nu = \frac{\bar{h}_c D_o}{k} = 1.1\, C \left(\frac{V_\infty D_o}{\nu}\right)^n Pr^{0.31} \qquad (4)$$

$$\text{For } Re = \frac{V_\infty D_o}{\nu} = 214{,}000$$

$$Pr = 1.075$$

$$C = 0.0239$$

$$n = 0.805$$

$$\bar{h}_c = 2460 \frac{Btu}{hr\text{-}ft^2\text{-}{}^oF}$$

$$m = \sqrt{\frac{\bar{h}_c P}{kS}} = 20.25 \text{ in.}^{-1}$$

$$\text{For } X = L$$

$$\frac{1}{\cosh mL} = \frac{T_B - T_L}{T_B - T_o}$$

$$\cosh mL = \cosh 60.75 = 1.21 \times 10^{26}$$

Hence, $T_B - T_L = \dfrac{T_B - T_o}{1.21 \times 10^{26}}$ which obviously is negligible for any reasonable value of $T_B - T_o$. By the same procedure

$T_B - T = \dfrac{T_B - T_o}{6.42 \times 10^{14}}$ at $X = \dfrac{L}{2}$ which corresponds to the end thermocouple positions.

The calibration-in-place procedure provides a deviation which is applied to the thermocouple readings at each heat flux setting. The deviations determined by the procedure for natural convection

conditions with zero current were the same as those for forced convection so the technique is suitable for both test conditions.

In order to check the calibration-in-place procedure under conditions with an electric current passing through the test section, the temperature difference necessary at various heat flux values was calculated and compared to temperature measurements. From the definition of the average heat transfer coefficient,

$$\bar{h}_c = \frac{q/A}{T_w - T_B} \tag{20}$$

the value of $T_w - T_B$ was calculated for several test runs. As shown in Table X, the calculated values compare very well with measured values at low heat flux. When nucleate boiling begins the calculated and measured values no longer agree as expected.

The beginning of nucleate boiling occurs at higher temperature difference and heat flux as the pressure is reduced. This can be seen in Table X with the correlation between measured and calculated temperature difference being good to higher values of heat flux as the pressure changes from 1550 psia to 535 psia. Data are presented for both Inconel and carbon steel at each pressure. It can be seen that the correlation for Inconel compares favorably to higher heat flux than that for carbon steel, especially at low pressure. This is consistent with the relative position of the boiling characteristic curves for the two materials as seen in Figs. 33-35.

TABLE X

COMPARISON OF CALCULATED AND MEASURED TEMPERATURE DIFFERENCE BASED ON ZERO CALIBRATION

Run. No.	Pressure Psia	Heat Flux Btu/hr-ft^2	Temperature Difference, ^oF Measured	Calculated, Eq.(20)
HI2-5	1550	267	0.09	0.11
		809	0.22	0.33
		2656	0.72	1.08
HI2-8	1550	214	0.09	0.087
		671	0.29	0.273
		2627	0.74	1.07
HS-6	1550	553	0.15	0.225
		2581	0.64	1.05
HI2-4	1015	239	0.056	0.09
		743	0.25	0.273
		2341	0.88	0.84
		6510	1.83	2.45
HS-5	1015	574	0.16	0.216
		2725	0.83	1.02
		9379	1.88	3.52
HS-4	535	475	0.182	0.174
		2528	0.75	0.95
		8030	2.16	3.06
HI2-3	535	62	0.056	0.024
		397	0.207	0.152
		2249	0.88	0.86
		6129	2.24	2.34
		17016	5.40	6.50

The use of calibration with zero current at test conditions gives very consistent and repeatable results. Thus the method is considered not only to be satisfactory but also to permit accuracy in temperature difference measurements consistent with the ability to hold steady state conditions while the measurements are made. The accuracy of temperature differences is considered to be better than $\pm$ 0.1°F.

The accuracy of temperature levels (measured in °F) is probably $\pm$ 0.5°F because of the shift of thermocouple emf at a given temperature which occurred when they were installed in the low heat flux boiling system. By comparison with data given by Shenker,[44] some of the thermocouples would have an error of up to 4°F at 600°F, others an error up to 2°F, if they were not calibrated. This shows that there is a necessity in calibration if an accuracy of about $\pm$ 0.5°F is satisfactory at temperatures up to 600°F. In-place calibration appears to be necessary if more precise results are desired when using chromel-constantan thermocouples.

APPENDIX B

ESTIMATION OF ERRORS

A. TEMPERATURE MEASUREMENT

The thermocouples used for temperature measurement were calibrated as indicated in Appendix A. The initial calibration was found to be in error after the thermocouples were installed in the low heat flux boiling system apparently due to the change of immersion depth. A method of calibration based on zero readings taken before and after each run was employed. The accuracy attained by this method is limited not by the instrumentation capability but by inherent limitations on the ability to maintain steady conditions while taking data.

The instrumentation for temperature measurement consisted of Type K-3 Universal Potentiometer and a Model 2284d moving coil galvanometer. The accuracy of this combination is stated by the manufacturer (Leeds and Northrup) to be $\pm$ (0.015% of reading plus 2 μv) in the range used. However, for temperature differences determined from the readings taken within a short period of time, it is considered that the accuracy attainable is $\pm$ 2 μv, or $\pm$ 0.05^{o}F, for temperatures which are steady.

The variables which affect the ability to maintain steady state conditions include:

a. Line voltage

b. Cooling air temperature and pressure

c. Cooling water pressure and temperature

d. Drafts of air due to fans, doors, windows

e. Generator voltage (test section power supply)

Of the items listed, variation of line voltage is the most serious. A 1 or 2 volt change causes a slow drift of conditions, a 5 volt change must be corrected immediately or the readings of that test condition have to be repeated. The other items, especially drafts, have a noticeable effect on the heat loss from the system.

Even though the accuracy of the potentiometer-galvanometer combination at 550°F is approximately $\pm$ 0.125°F for absolute temperature measurement, variation of temperature as low as 0.025°F can be detected. With constant observation, the conditions could be maintained to very close tolerance. However, while reading the test section thermocouples a drift in system conditions of approximately 0.1°F can occur. By frequent observation of the steam space temperature the amount of drift is minimized. For small changes in the steam space temperature an average temperature is used to minimize the error. A drift exceeding 0.1°F was considered excessive and, after stabilization, another complete set of readings was taken.

The error in temperature measurement including instrumentation error and drift of system conditions is considered to be $\pm$ 0.15°F

relative to the secondary standard. In the zero calibration method the secondary standard is one of the thermocouples which is considered to be correct. The bulk water temperature thermocouple was used as the secondary standard. Absolute accuracy of temperatures is considered to be $\pm$ 0.5°F. Temperature differences will be considered below.

B. CURRENT MEASUREMENT

The current flow through the test section was determined by measuring the voltage drop across a shunt of 10^{-5} ohm resistance. A L & N 8662 potentiometer was used to read the voltage from the shunt. The instrument can be read within 5 μv on the low range scale and within 25 μv on the high scale. The maximum error would be 2% at the lowest readings. Above a current of 100 amperes (1 mv) the error is less than 0.5%. The shunt was calibrated and found to be accurate to within 0.1%.

C. RESISTIVITY MEASUREMENT

The resistivity of the test sections was measured as a function of temperature to within $\pm$ 1%. Values used in the calculations varied less than 1% over the applicable temperature range. On this basis the maximum error in the value of electrical resistivity used could be 1.5%.

D. THERMAL CONDUCTIVITY MEASUREMENT

The thermal conductivity of the tube materials was determined by an outside laboratory. The variation of data was less than $\pm$ 3% from a smooth curve for Monel and carbon steel. For Inconel, two samples were tested with a variation less than $\pm$ 2% from a smooth curve for each but about $\pm$ 7% overall for the two samples. These variations will not affect the comparison of results obtained on repeat runs at a given temperature (and pressure). However, comparison of results with a given test section at different temperatures may have an error of $\pm$ 3%. Comparison of data from one material to another at a given test condition may have an error of $\pm$ 10%. This error would apply directly to the value of temperature difference at a given value of heat flux since thermal conductivity appears in the equation for wall temperature drop.

E. WALL TEMPERATURE DROP

As described in Eqs. 1, 2, and 3, the wall temperature drop is a function of resistivity and thermal conductivity of the tube material, square of the current density, and geometric values which were kept constant throughout the tests. At any given level of temperature, the only variable quantity is the square of the current for a given test section. Therefore all wall temperature drops computed by these equations are precise relative to one another, to within $\pm$ 1% at higher

current values. At low current values the error is insignificant since the wall temperature drop is very small.

When the wall temperature drop is compared in two cases where the temperature is different or for different materials, uncertainties in the thermal conductivity and electrical resistivity affect the total possible error. It is estimated that the relative error in temperature difference for a given test section is $\pm$ 3% in the range from 475 to 600°F. The relative error may be as much as $\pm$ 10% when comparing the different materials at a given test condition.

F. OUTSIDE WALL TEMPERATURE

The average outside wall temperature is obtained by subtracting the wall temperature drop from the average inside wall temperature. The error in the average inside wall temperature relative to the secondary standard is less than that for each thermocouple due to the probability of reduction of error when a large sample is taken. Thus the error in average inside wall temperature is estimated to be less than $\pm$ 0.1°F. At low heat flux (less than about 2000 Btu/hr-ft^2) the error in wall temperature drop is small so the error in outside wall temperature is the same as that of the inside wall temperature. At high heat flux the wall temperature drop reaches 22°F for Inconel, less for Monel and carbon steel. Thus the error in outside wall temperature relative to the secondary standard may be $\pm$ 1°F for Inconel,

and $\pm$ 0.4°F for Monel and carbon steel at 100,000 Btu/hr-ft^2. Relative error in comparing materials could be approximately the sum of the error for the two materials.

G. TEMPERATURE DIFFERENCE BETWEEN WALL AND SATURATION ($T_o - T_{sat}$) OR BETWEEN WALL AND WATER ($T_w - T_B$)

From the above discussion, it is estimated that the possible error in difference between the average outside wall temperature and the saturation temperature varies approximately linearly in the range of heat flux from 10,000 to 100,000 Btu/hr-ft^2. This temperature difference is considered precise to within $\pm$ 0.2°F for Monel and carbon steel and within $\pm$ 0.4°F for Inconel at 10,000 Btu/hr-ft^2. The respective values at 100,000 Btu/hr-ft^2 are $\pm$ 0.4°F and $\pm$ 1.0°F.

In the heat flux range from 0 to 10,000 Btu/hr-ft^2 the difference between the average outside wall temperature and bulk water temperature is important especially if a small amount of subcooling exists. However, no subcooling is evident in the data presented herein. This temperature difference is considered precise to within $\pm$ 0.1°F for all data for a given material below 10,000 Btu/hr-ft^2. The repeatability of the data and the behavior of individual points relative to the curve drawn in the non-boiling region are indicative of accuracy better than that claimed.

H. ABSOLUTE TEMPERATURE MEASUREMENT

As indicated in Appendix A, the characteristics of the calibrated thermocouples changed slightly when installed in the low heat flux boiling system. Based on indications from all thermocouples and the system pressure gage, it is estimated that the absolute temperature measurements under steady state conditions are precise to within $\pm 0.5^{\circ}F$.

I. HEAT FLUX

The uncertainty in the heat flux values computed from the current, resistivity, and tube dimensions is approximately $\pm$ 2.0%.

J. FLOW VELOCITY

The velocity was found by dividing the volumetric flow rate obtained from the orifice pressure drop, by the cross-sectional area of the flow guide. Fluctuations in the orifice differential increase the uncertainty of the measurement, but it is considered to be accurate to within $\pm$ 4% at a velocity of 4.7 ft/sec for the horizontal test section. For the vertical test section, the velocity is considered correct to within $\pm$ 6%.

K. PRESSURE

The system pressure was read from a precision bourdon tube gauge, calibrated to within 0.1% of full scale or 2.5 psi. Agreement

between the pressure reading and the temperature indicated by the steam space and bulk water thermocouples was good at 535 psia. The temperature readings became a little high relative to the pressure reading at 1015 and 1550 psia, the maximum difference being approximately $0.5^{\circ}F$ at 1550 psia. In general, the agreement was satisfactory. Since the temperature readings were used exclusively for control and data reduction, this slight deviation has no effect on the data results presented herein. The difference is within the tolerance on gauge accuracy ($\pm$ 2.5 psi) and atmospheric pressure variation.

APPENDIX C

DATA

Experimental data are presented below for boiling saturated water at high pressure from the outside surface of horizontal and vertical 3/4 inch diameter tubes. Materials considered are Monel, Inconel, and carbon steel. The data for a horizontal Monel tube supersede data presented in reference (50).

As indicated in Appendix A, the test section and steam space thermocouples were calibrated in place under actual test conditions by comparison with the bulk water thermocouple as a secondary standard. The result of this calibration is applied to the $T_o - T_{sat}$ column but not to the Avg T_i, Avg T_o, and T_s columns. It is shown in Appendix A that with no electrical current passing through the test section the temperature difference between the water and test section is negligible. Both the steam space temperature, T_s, and the bulk water temperature, T_B, were held constant at the water saturation temperature during the tests, therefore either of these could be used as the secondary standard.

The tabulated value of $T_o - T_{sat}$ at all values of heat flux is established as follows:

$$T_o - T_{sat} = T_o + (T_B - T_o)_{i=o} - \left[T_s + (T_B - T_s)_{i=o} \right] \qquad (21)$$

which is zero for zero electrical current.

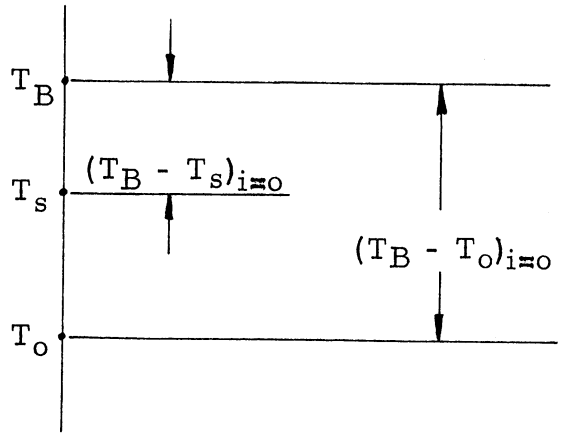

Since $T_o - T_B$ is the appropriate temperature difference for non-boiling natural and forced convection heat transfer, it is determined by the following equation:

$$T_o - T_B = T_o + (T_B - T_o)_{i=o} - T_B . \qquad (22)$$

As long as both T_s and T_B remain constant at the water saturation temperature equations (21) and (22) give identical results. Slight deviations in actual operating conditions allow a small difference between the two values, however, this difference very rarely was as large as 0.1^{o} F.

Date Run No.	Time	q/A Btu/hr-ft^2	Temperatures - ^oF Avg T_i	ΔT Wall	Avg T_o	T_s	T_B	$T_o - T_{sat}$
7-30-63	1330	0	472.65	0	472.65	473.1		0
	1410	696	474.25	0.16	474.10	473.1		1.5
HI1-2	1430	1,390	474.45	0.33	475.1	473.1		2.5
P = 535 psia	1450	3,120	477.30	0.73	476.6	473.1		4.0
Pool	1515	7,520	479.45	1.76	477.7	473.1		5.1
	1535	15,450	482.62	3.62	479.0	473.1		6.4
	1600	39,020	490.20	9.14	481.1	473.1		8.5
	1635	83,370	502.72	19.53	483.2	473.1		10.6
	1700	38,580	488.90	9.04	479.9	473.1		7.3
	1720	14,290	480.87	3.35	477.5	473.1		4.9
	1740	5,320	477.12	1.25	475.9	473.1		3.3
	1800	2,470	475.50	0.58	474.9	473.1		2.3
	1820	1,210	474.55	0.28	474.3	473.1		1.7
	1830	0	472.57	0	472.57	473.1		0
8-14-63	1145	0	472.85	0	472.85	473.2		0
	1215	703	473.27	0.16	473.1	473.1		0.3
HI1-3	1240	1,430	473.72	0.34	473.4	473.1		0.6
P = 535 psia	1305	3,310	474.97	0.77	474.2	473.1		1.4
V = 4.7 ft/sec	1325	7,660	477.30	1.79	475.5	473.1		2.7
	1350	16,370	480.90	3.83	477.1	473.1		4.3
	1410	32,050	486.50	7.51	479.0	473.1		6.2
	1435	63,780	496.45	14.9	481.5	473.1		8.7
	1505	114,300	510.42	26.8	483.6	473.1		10.8
	1550	113,400	510.02	26.6	483.4	473.1		10.6
	1610	64,350	495.90	15.1	480.8	473.1		8.0
	1630	28,630	484.50	6.71	477.8	473.1		5.0
	1655	15,520	479.85	3.64	476.2	473.1		3.4
	1715	5,160	475.52	1.21	474.3	473.1		1.5
	1737	2,500	474.22	0.58	473.6	473.1		0.8
	1755	1,230	473.55	0.29	473.3	473.1		0.5
	1815	0	472.80	0	472.8	473.1		0
11-27-63	1130	90,490	505.80	21.2	484.6	473.8	474.1	11.0
	1205	89,980	505.10	21.1	484.0	473.8	474.1	10.4
HI1-9	1250	42,420	490.15	9.94	480.21	473.8	474.1	6.61
P = 535 psia	1315	15,380	480.55	3.60	476.95	473.8	474.1	3.35
V = 4.7 ft/sec	1347	5,380	476.43	1.26	475.17	473.85	474.0	1.67
	1408	2,020	474.80	0.47	474.33	473.85	474.0	0.83
	1427	756	474.13	0.18	473.95	473.85	474.1	0.35
	1443	0	473.60	0	473.6	474.0	474.1	0

Date Run No.	Time	q/A Btu/hr-ft^2	Temperatures - ^oF Avg T_i	ΔT Wall	Avg T_o	T_s	T_B	$T_o - T_{sat}$
11-28-63	1117	89,050	506.67	20.24	486.4	474.0	474.0	13.0
	1145	88,720	506.30	20.16	486.14	474.02	474.0	12.7
HI1-10	1210	42,730	491.90	9.71	482.2	474.1	474.0	8.80
P = 535 psia	1230	15,520	482.57	3.53	479.05	474.1	474.0	5.65
Pool	1250	5,680	478.40	1.29	477.1	474.0	474.1	3.60
	1310	1,760	476.17	0.40	475.77	474.1	474.0	2.37
	1330	729	474.90	0.16	474.74	474.0	473.9	1.44
	1347	0	473.30	0	473.3	474.0	473.9	0
12-2-63	1350	85,330	507.79	20.0	487.8	474.0		14.3
	1420	82,720	506.44	19.4	487.06	474.0		13.6
HI1-14	1450	41,960	491.33	9.83	481.5	474.0		8.0
P = 535 psia	1515	15,380	480.86	3.60	477.26	474.05		3.7
V = 4.7 ft/sec	1549	6,350	476.94	1.49	475.45	474.0	474.3	1.85
	1610	2,200	474.98	0.51	474.47	474.05	474.3	0.87
	1630	819	474.09	0.19	473.9	474.05	474.3	0.3
	1650	293	473.77	0.07	473.7	474.0	474.3	0.1
	1705	0	473.59	0	473.59	474.1	474.3	0
1-17-64	1510	99,300	508.71	23.26	485.45	474.0	474.35	11.9
	1540	45,600	491.84	10.68	481.16	474.0	474.35	7.65
HI1-16	1615	17,540	481.66	4.11	477.55	474.0	474.35	4.04
P = 535 psia	1642	6,310	477.14	1.48	475.66	474.05	474.35	2.15
V = 4.7 ft/sec	1705	2,020	474.71	0.47	474.24	473.95	474.35	0.73
	1735	1,330	474.31	0.31	474.0	473.9	474.35	0.51
	1750	479	473.88	0.11	473.77	474.0	474.35	0.26
	1805	0	473.56	0	473.56	474.0	474.4	0
1-18-64	1135	99,300	510.14	23.26	486.9	474.0	474.1	13.6
	1210	43,820	493.10	10.26	482.84	474.0	474.1	9.54
HI1-17	1240	17,390	484.07	4.07	480.0	474.0	474.1	6.70
P = 535 psia	1307	5,660	479.11	1.32	477.8	474.0	474.1	4.50
Pool	1340	2,170	476.90	0.51	476.4	474.0	474.1	3.1
	1420	1,250	475.94	0.29	475.65	473.95	474.1	2.35
	1445	437	474.30	0.10	474.2	474.0	474.1	0.9
	1505	0	473.20	0	473.2	474.0	474.0	0
1-22-64	1350	100,180	512.78	23.47	489.3	474.0	474.2	15.9
	1420	45,240	495.18	10.60	484.6	474.0	474.1	11.3
HI1-21	1450	16,520	485.05	3.87	481.2	474.0	474.1	7.92
P = 535 psia	1515	6,760	480.74	1.58	479.16	474.0	474.2	5.78
Pool	1540	2,410	477.70	0.56	477.14	474.0	474.2	3.76
	1608	1,080	475.97	0.25	475.22	474.0	474.2	1.84
	1632	343	474.14	0.08	474.06	474.0	474.1	0.78
	1652	0	473.28	0	473.28	474.0	474.1	0

Date Run No.	Time	q/A Btu/hr-ft^2	Temperatures - ^oF Avg T_i	ΔT Wall	Avg T_o	T_s	T_B	$T_o - T_{sat}$
2-1-64	1235	101,800	514.22	23.85	490.37	474.0	474.2	16.9
	1307	43,470	495.23	10.18	485.05	474.0	474.15	11.6
HI1-23	1332	16,520	485.8	3.87	481.93	474.0	474.2	8.47
P = 535 psia	1354	6,530	481.11	1.53	479.58	473.95	474.2	6.12
Pool	1420	2,580	478.33	0.60	477.73	474.0	474.2	4.27
	1445	1,210	476.28	0.28	476.0	474.0	474.2	2.54
	1510	414	474.47	0.1	474.37	474.0	474.15	0.96
	1535	0	473.41	0	473.41	474.0	474.15	0
2-19-64	1238	100,540	510.19	23.55	486.64	474.1	474.4	13.0
	1314	43,460	491.81	10.18	481.63	474.0	474.3	8.1
HI1-25	1343	15,240	480.92	3.57	477.35	474.0	474.3	3.81
P = 535 psia	1412	6,460	477.17	1.51	475.66	474.0	474.3	2.12
V = 4.7 ft/sec	1440	2,360	474.93	0.55	474.38	473.9	474.3	0.86
	1508	1,010	474.28	0.24	474.04	474.0	474.3	0.50
	1538	364	473.81	0.09	473.72	474.0	474.3	0.18
	1600	0	473.54	0	473.54	474.0	474.3	0
2-20-64	1330	97,360	510.47	22.81	487.66	474.0	474.2	14.3
	1400	43,470	493.17	10.18	482.99	474.0	474.2	9.59
HI1-26	1430	15,870	483.71	3.72	479.99	474.0	474.2	6.59
P = 535 psia	1505	6,400	479.56	1.49	478.07	474.0	474.2	4.67
Pool	1530	2,500	477.09	0.58	476.51	474.0	474.3	3.01
	1600	1,020	475.45	0.24	475.21	474.0	474.2	1.81
	1625	364	474.19	0.08	474.11	474.0	474.2	0.71
	1642	0	473.30	0	473.30	474.0	474.1	0
2-22-64	1330	100,900	515.26	23.64	492.62	473.95	474.2	19.2
	1410	43,590	495.94	10.21	485.73	474.0	474.2	12.3
HI1-29	1445	16,730	485.42	3.92	481.5	474.0	474.3	7.9
P = 535 psia	1515	6,760	481.04	1.58	479.46	474.0	474.3	5.9
Pool	1550	2,580	478.18	0.60	477.58	474.0	474.45	3.87
	1620	1,310	476.45	0.31	476.14	474.0	474.3	2.58
	1650	479	474.53	0.11	474.42	474.0	474.2	0.96
	1720	0	473.36	0	473.36	474.0	474.1	0
5-20-64	0905	102,900	514.37	24.09	490.28	474.0	474.4	16.7
	0945	43,230	494.12	10.13	483.82	474.0	474.4	10.3
HI2-3	1015	17,620	482.97	4.12	478.85	474.0	474.3	5.4
P = 535 psia	1045	6,130	477.12	1.43	475.69	473.9	474.3	2.24
V = 4.7 ft/sec	1105	2,250	474.96	0.53	474.43	474.0	474.4	0.88
	1120	397	473.85	0.09	473.76	474.0	474.4	0.21
	1140	62	473.62	0.014	473.61	474.0	474.4	0.056
	1150	0	473.55	0	473.55	474.0	474.4	0

Date Run No.	Time	q/A Btu/hr-ft[a]	Temperatures - °F Avg T_i	 ΔT Wall	 Avg T_o	 T_s	 T_B	 $T_o - T_{sat}$
5-20-64	1610	102,300	580.2	23.24	556.96	546.2	546.7	11.0
	1630	43,440	562.94	9.87	553.07	546.1	546.6	7.18
HI2-4	1700	19,000	554.55	4.32	550.24	546.2	546.6	4.35
P = 1015 psia	1725	6,510	549.2	1.48	547.72	546.1	546.6	1.83
V = 4.7 ft/sec	1750	2,340	547.3	0.53	546.77	546.15	546.65	0.88
	1800	743	546.41	0.17	546.24	546.1	546.7	0.25
	1815	239	546.1	0.054	546.046	546.1	546.7	0.056
	1825	0	545.99	0	545.99	546.1	546.7	0
5-20-64	1320	103,600	631.43	23.09	608.34	600.2	600.6	8.66
	1340	45,940	615.9	10.23	605.67	600.2	600.6	5.99
HI2-5	1402	17,750	606.84	3.95	602.89	600.1	600.6	3.21
P = 1550 psia	1425	6,720	602.71	1.49	601.22	600.2	600.6	1.54
V = 4.7 ft/sec	1446	2,660	600.99	0.59	600.4	600.1	600.6	0.72
	1506	809	600.08	0.18	599.9	600.2	600.6	0.22
	1521	267	599.83	0.06	599.77	600.2	600.6	0.09
	1540	0	599.68	0	599.68	600.2	600.6	0
5-24-64	1323	100,900	514.92	23.63	491.3	474.0	474.4	17.7
	1353	43,470	494.58	10.18	484.4	474.0	474.4	10.8
HI2-6	1415	17,540	482.9	4.11	478.8	474.0	474.4	5.2
P = 535 psia	1440	5,960	477.09	1.39	475.7	474.0	474.4	2.1
V = 4.7 ft/sec	1510	2,410	475.02	0.56	474.46	474.0	474.4	0.88
	1535	504	473.86	0.12	473.74	474.0	474.4	0.16
	1551	135	473.65	0.03	473.62	474.0	474.4	0.02
	1607	0	473.58	0	473.58	474.0	474.4	0
5-25-64	0935	101,900	581.03	23.16	557.8	546.2	546.6	12.2
	1000	43,790	563.73	9.95	553.8	546.2	546.6	8.2
HI2-7	1030	17,850	554.22	4.05	550.2	546.1	546.6	4.6
P = 1015 psia	1055	6,470	549.07	1.47	547.6	546.15	546.6	2.0
V = 4.7 ft/sec	1114	2,290	546.91	0.52	546.39	546.1	546.6	0.74
	1130	493	545.93	0.11	545.82	546.1	546.6	0.17
	1144	108	545.66	0.02	545.64	546.1	546.6	-
	1200	0	545.65	0	545.65	546.1	546.6	0
5-25-64	1605	100,400	630.95	22.37	608.6	600.2	600.7	8.9
	1635	44,030	615.66	9.81	605.9	600.2	600.7	6.2
HI2-8	1657	16,570	606.86	3.69	603.2	600.3	600.7	3.5
P = 1550 psia	1730	6,440	602.74	1.43	601.31	600.2	600.65	1.63
V = 4.7 ft/sec	1755	2,630	601.0	0.58	600.42	600.15	600.65	0.74
	1820	671	600.12	0.15	599.97	600.2	600.65	0.29
	1833	214	599.84	0.05	599.79	600.2	600.67	0.09
	1848	0	599.7	0	599.7	600.2	600.67	0

Date Run No.	Time	q/A Btu/hr-ft[a]	Temperatures - °F Avg T_i	ΔT Wall	Avg T_o	T_s	T_B	$T_o - T_{sat}$
5-26-64	1325	95,270	516.13	22.32	493.81	474.0	474.3	20.4
	1355	43,120	498.68	10.10	488.58	474.0	474.2	15.3
HI2-9	1430	16,370	487.37	3.83	483.54	474.1	474.2	10.2
P = 535 psia	1505	6,260	481.63	1.46	480.17	474.0	474.3	6.74
Pool	1547	2,380	478.17	0.56	477.61	474.0	474.2	4.28
	1615	431	474.30	0.10	474.2	474.0	474.1	0.97
	1640	62	473.42	0.01	473.41	474.0	474.1	0.18
	1700	0	473.23	0	473.23	474.0	474.1	0
5-27-64	1108	100,400	581.5	22.79	558.71	546.24	546.42	13.2
	1140	44,380	565.21	10.09	555.12	546.14	546.40	9.65
HI2-10	1207	18,760	556.62	4.26	552.36	546.14	546.32	6.97
P = 1015 psia	1227	6,880	551.8	1.56	550.24	546.22	546.4	4.77
Pool	1255	2,650	549.23	0.60	548.63	546.16	546.4	3.16
	1330	889	547.38	0.20	547.18	546.17	546.36	1.75
	1402	294	546.09	0.07	546.02	546.12	546.35	0.6
	1433	0	545.32	0	545.32	546.18	546.25	0
5-27-64	1700	99,940	581.35	22.71	558.64	546.13	546.4	13.2
	1727	44,260	565.29	10.06	555.23	546.12	546.4	9.81
HI2-11	1748	18,070	556.54	4.11	552.43	546.17	546.32	7.09
P = 1015 psia	1825	6,880	551.82	1.56	550.26	546.14	546.4	4.84
Pool	1855	2,620	549.32	0.60	548.72	546.14	546.4	3.3
	1920	766	547.07	0.02	547.05	546.1	546.32	1.71
	1955	239	545.95	0.01	545.94	546.2	546.3	0.62
	2015	0	545.32	0	545.32	546.2	546.3	0
5-28-64	1040	0	599.32	0	599.32	600.2	600.3	0.09
	1102	168	599.82	0.04	599.78	600.15	600.4	0.45
HI2-12	1125	560	600.93	0.12	600.81	600.2	600.4	1.48
P = 1550 psia	1145	2,480	604.2	0.55	603.65	600.2	600.5	4.22
Pool	1217	6,960	606.2	1.55	604.65	600.2	600.4	5.32
	1245	18,280	609.75	4.07	605.68	600.2	600.3	6.45
	1315	46,060	617.31	10.26	607.05	600.2	600.4	7.72
	1335	105,800	631.95	23.58	608.37	600.2	600.5	8.94
	1445	102,500	631.03	22.85	608.18	600.2	600.4	8.85
	1504	45,220	616.51	10.08	606.43	600.2	600.5	7.0
	1527	17,750	608.08	3.95	604.13	600.1	600.4	4.8
	1553	6,720	604.03	1.50	602.53	600.2	600.4	3.2
	1620	2,800	602.24	0.62	601.62	600.2	600.4	2.29
	1640	762	600.8	0.17	600.63	600.2	600.4	1.3
	1704	223	600.0	0.05	599.95	600.2	600.4	0.62
	1722	0	599.33	0	599.33	600.2	600.4	0

Date Run No.	Time	q/A Btu/hr-ft^2	Temperatures - ^oF Avg T_i	ΔT Wall	Avg T_o	T_s	T_B	$T_o - T_{sat}$
5-30-64	1030	98,000	581.93	22.27	559.66	546.1	546.4	14.3
	1056	48,860	566.02	10.19	555.83	546.1	546.36	10.5
HI2-13	1125	17,550	556.62	3.99	552.63	546.1	546.35	7.31
P = 1015 psia	1150	6,560	551.97	1.49	550.48	546.1	546.32	5.19
Pool	1220	2,510	549.36	0.57	548.79	546.15	546.4	3.42
	1244	737	547.08	0.17	546.91	546.1	546.3	1.64
	1314	233	545.95	0.05	545.90	546.2	546.3	0.63
	1340	0	545.27	0	545.27	546.2	546.3	0
6-5-64	0900	101,600	516.0	23.80	492.2	474.0	474.4	18.7
	0955	98,770	514.8	23.14	491.7	474.0	474.4	18.2
HI2-14	1030	43,590	495.38	10.21	485.17	474.0	474.4	11.7
P = 535 psia	1103	17,390	483.31	4.07	479.2	474.05	474.35	5.75
V = 4.7 ft/sec	1137	6,440	477.35	1.51	475.84	474.0	474.35	2.39
	1203	2,670	475.15	0.62	474.53	474.0	474.4	1.03
	1218	819	474.0	0.19	473.81	474.0	474.37	0.34
	1235	265	473.69	0.06	473.63	474.0	474.35	0.18
	1250	0	473.45	0	473.45	474.0	474.35	0
6-5-64	1555	100,900	518.0	23.63	494.37	474.0	474.25	21.1
	1630	99,120	517.11	23.22	493.89	474.0	474.27	20.6
HI2-15	1707	44,170	499.08	10.34	488.74	474.0	474.2	15.5
P = 535 psia	1740	17,990	489.16	4.21	484.95	474.0	474.2	11.7
Pool	1820	6,040	482.69	1.41	481.28	474.0	474.42	7.8
	1852	2,360	478.35	0.55	477.8	474.0	474.27	4.5
	1923	609	474.72	0.14	474.58	474.15	474.2	1.33
	1947	170	473.66	0.04	473.62	474.0	474.17	0.40
	2007	0	473.2	0	473.2	473.95	474.15	0
6-6-64	0925	102,700	515.64	24.06	491.6	474.05	474.5	18.0
	1017	99,120	514.29	23.22	491.1	474.0	474.47	17.5
HI2-16	1048	43,470	494.84	10.18	484.66	474.0	474.45	11.1
P = 535 psia	1127	17,650	483.39	4.14	479.25	474.0	474.47	5.64
V = 4.7 ft/sec	1152	6,080	477.1	1.43	475.67	473.95	474.42	2.11
	1219	2,500	475.15	0.58	474.57	474.0	474.47	0.96
	1237	425	473.83	0.10	473.73	474.0	475.45	0.14
	1252	0	473.61	0	473.61	473.95	474.47	0
6-6-64	1532	104,300	518.08	24.44	493.64	474.0	474.2	20.4
	1615	101,260	516.82	23.71	493.11	474.0	474.3	19.8
HI2-17	1650	43,120	497.99	10.10	487.89	473.95	474.25	14.6
P = 535 psia	1720	17,690	488.26	4.14	484.12	474.0	474.22	10.9
Pool	1813	5,950	482.39	1.39	481.0	474.0	474.37	7.6
	1847	2,490	478.46	0.58	477.88	474.0	474.25	4.6
	1915	454	474.38	0.11	474.27	474.0	474.2	1.04
	1945	91	473.43	0.02	473.41	473.95	474.2	0.18
	2000	0	473.18	0	473.18	474.0	474.15	0

Date Run No.	Time	q/A Btu/hr-ft^2	Temperatures - ^oF Avg T_i	ΔT Wall	Avg T_o	T_s	T_B	$T_o - T_{sat}$
6-8-64	1148	98,600	513.12	23.1	490.0	473.95	474.55	16.3
	1230	96,140	512.35	22.52	489.8	474.0	474.6	16.0
HI2-18	1300	43,350	494.35	10.16	484.2	474.0	474.6	10.4
P = 535 psia	1338	17,690	483.12	4.14	479.0	474.0	474.65	5.17
V = 4.7 ft/sec	1412	6,080	477.34	1.43	475.9	473.95	474.65	2.07
	1437	2,770	475.45	0.65	474.8	474.0	474.62	1.0
	1456	504	474.08	0.12	473.96	474.0	474.62	0.16
	1517	0	473.8	0	473.8	474.0	474.62	0
6-8-64	1737	102,690	516.75	24.05	492.7	474.1	474.3	19.3
	1830	99,120	515.41	23.22	492.19	473.95	474.3	18.8
HI2-19	1903	43,580	498.04	10.20	487.84	474.0	474.3	14.4
P = 535 psia	1930	17,990	488.3	4.21	484.09	474.0	474.22	10.8
Pool	2010	6,310	482.6	1.47	481.13	473.95	474.32	7.7
	2055	2,640	478.9	0.62	478.28	474.05	474.27	4.9
	2135	420	474.28	0.10	474.18	473.95	474.2	0.86
	2204	0	473.29	0	473.29	474.0	474.17	0
6-16-64	1325	99,090	494.41	8.28	486.13	474.0	474.4	12.8
	1400	51,600	485.43	4.31	481.12	473.96	474.35	7.85
HS-1	1434	21,680	479.36	1.81	477.55	474.0	474.3	4.33
P = 535 psia	1500	8,982	476.27	0.74	475.53	474.01	474.3	2.31
V = 4.7 ft/sec	1530	2,770	474.32	0.23	474.09	474.02	474.3	0.87
	1546	798	473.50	0.07	473.43	474.0	474.3	0.21
	1601	236	473.26	0.02	473.24	473.97	474.3	0.02
	1623	0	473.23	0	473.23	474.01	474.31	0
6-17-64	0924	106,530	562.57	8.97	553.6	546.15	546.64	8.1
	0956	62,020	556.04	5.22	550.82	546.16	546.64	5.28
HS-2	1022	23,400	550.42	1.97	548.45	546.20	546.64	2.91
P = 1015 psia	1045	9,130	547.83	0.77	547.06	546.18	546.55	1.61
V = 4.7 ft/sec	1107	2,523	546.39	0.21	546.18	546.16	546.64	0.64
	1129	716	545.67	0.06	545.61	546.12	546.52	0.19
	1153	0	545.45	0	545.45	546.14	546.55	0
6-17-64	1550	116,440	614.94	9.92	605.02	600.18	600.65	5.48
	1622	67,960	609.07	5.79	603.28	600.2	600.55	3.84
HS-3	1640	25,520	603.70	2.17	601.53	600.2	600.57	2.07
P = 1550 psia	1702	10,640	601.70	0.91	600.79	600.17	600.6	1.30
V = 4.7 ft/sec	1724	3,130	600.44	0.27	600.17	600.22	600.57	0.71
	1743	716	599.7	0.06	599.64	600.17	600.55	0.20
	1802	0	599.49	0	599.49	600.2	600.6	0

Date Run No.	Time	q/A Btu/hr-ft^2	Temperatures - ^oF Avg T_i	ΔT Wall	Avg T_o	T_s	T_B	$T_o - T_{sat}$
6-18-64	0927	99,580	494.33	8.33	486.0	474.01	474.48	12.4
	1001	52,680	485.7	4.40	481.3	474.07	474.48	7.73
HS-4	1043	20,800	479.21	1.74	477.47	474.4	474.45	3.93
P = 535 psia	1115	8,030	476.37	0.69	475.68	474.01	474.43	2.16
V = 4.7 ft/sec	1138	2,530	474.48	0.21	474.27	473.99	474.43	0.75
	1155	457	473.74	0.04	473.70	473.99	474.43	0.18
	1210	0	473.53	0	473.53	473.99	474.44	0
6-18-64	1542	111,000	564.1	9.35	554.75	546.18	546.57	9.15
	1610	61,280	556.48	5.16	551.32	546.15	546.55	5.74
HS-5	1635	23,610	550.73	1.99	548.74	546.17	546.57	3.14
P = 1015 psia	1654	9,380	548.15	0.79	547.36	546.11	546.45	1.88
V = 4.7 ft/sec	1722	2,720	546.61	0.23	546.38	546.18	546.52	0.83
	1741	574	545.76	0.05	545.71	546.15	546.52	0.16
	1800	0	545.55	0	545.55	546.15	546.52	0
6-19-64	0949	113,300	616.02	9.65	606.37	600.19	600.63	6.79
	1022	50,570	607.58	4.31	603.27	600.18	600.68	3.64
HS-6	1100	16,920	602.8	1.44	601.36	600.16	600.68	1.73
P = 1535 psia	1140	7,770	601.4	0.66	600.74	600.16	600.63	1.15
V = 4.7 ft/sec	1217	2,580	600.45	0.22	600.23	600.22	600.63	0.65
	1237	553	599.8	0.05	599.75	600.18	600.65	0.15
	1258	0	599.58	0	599.58	600.18	600.63	0
6-28-64	1650	102,480	496.5	8.57	487.93	473.99	474.57	14.2
	1730	53,480	486.96	4.47	482.49	473.98	474.55	8.77
HS-8	1806	19,840	479.71	1.66	478.05	473.96	474.52	4.4
P = 535 psia	1840	8,230	476.63	0.69	475.94	473.99	474.5	2.27
V = 4.7 ft/sec	1906	2,360	474.66	0.20	474.46	474.02	474.52	0.77
	1925	704	473.94	0.06	473.88	473.97	474.5	0.21
	1959	0	473.65	0	473.65	473.97	474.48	0
6-29-64	1133	113,000	616.56	9.62	606.94	600.20	600.7	7.24
	1204	52,200	608.07	4.44	603.63	600.17	600.7	3.93
HS-9	1234	17,010	603.12	1.45	601.67	600.20	600.7	1.97
P = 1550 psia	1258	7,950	601.66	0.68	600.98	600.19	600.72	1.27
V = 4.7 ft/sec	1345	2,180	600.55	0.19	600.36	600.34	600.66	0.70
	1410	645	599.93	0.06	599.87	600.18	600.67	0.20
	1423	0	599.70	0	599.70	600.21	600.70	0

Date Run No.	Time	q/A Btu/hr-ft^2	Temperatures - ^oF Avg T_i	ΔT Wall	Avg T_o	T_s	T_B	$T_o - T_{sat}$
6-30-64	1515	99,880	495.78	8.35	487.43	474.03	474.3	14.0
	1550	47,660	486.61	3.98	482.63	473.99	474.27	9.18
HS-10	1620	15,680	480.78	1.31	479.47	474.01	474.22	6.07
P = 535 psia	1648	6,370	478.19	0.53	477.66	474.02	474.22	4.26
Pool	1714	2,150	476.40	0.18	476.22	474.02	474.22	2.82
	1743	763	474.85	0.06	474.79	473.99	474.17	1.44
	1804	244	473.89	0.02	473.87	474.01	474.15	0.54
	1820	0	473.33	0	473.33	474.0	474.15	0
7-1-64	0906	107,800	564.4	9.08	555.32	546.18	546.42	9.79
	0930	50,330	555.67	4.24	551.43	546.13	546.37	5.95
HS-11	1001	17,240	550.74	1.45	549.29	546.19	546.37	3.81
P = 1015 psia	1030	9,570	549.32	0.81	548.51	546.15	546.32	3.08
Pool	1053	2,190	547.54	0.18	547.36	546.14	546.35	1.89
	1122	551	546.48	0.05	546.43	546.20	546.32	1.00
	1151	94	545.63	0.01	545.62	546.14	546.25	0.25
	1208	0	545.38	0	545.38	546.16	546.27	0
7-1-64	1610	118,600	616.47	10.10	606.37	600.20	600.45	6.93
	1633	59,770	609.05	5.09	603.96	600.21	600.46	4.51
HS-12	1653	19,640	603.6	1.67	601.93	600.20	600.42	2.52
P = 1550 psia	1715	6,750	601.7	0.58	601.12	600.21	600.42	1.71
Pool	1735	2,460	600.91	0.21	600.70	600.20	600.44	1.27
	1755	707	600.44	0.06	600.38	600.20	600.37	1.02
	1817	205	599.92	0.02	599.9	600.20	600.35	0.56
	1853	0	599.36	0	599.36	600.18	600.37	0
7-2-64	1042	108,600	564.44	9.14	555.30	546.18	546.35	9.82
	1114	52,720	556.14	4.44	551.70	546.18	546.35	6.22
HS-13	1145	17,720	550.75	1.49	549.26	546.16	546.35	3.76
P = 1015 psia	1217	5,460	548.56	0.46	548.10	546.15	546.35	2.62
Pool	1250	2,340	547.72	0.20	547.52	546.18	546.35	2.05
	1313	555	546.57	0.05	546.52	546.16	546.27	1.12
	1334	127	545.72	0.01	545.71	546.17	546.22	0.36
	1358	0	545.38	0	545.38	546.15	546.25	0
7-3-64	1105	98,990	495.82	8.28	487.54	473.99	474.25	14.0
	1135	46,640	486.9	3.90	483.0	474.0	474.25	9.5
HS-14	1204	16,080	481.31	1.34	479.97	473.99	474.27	6.45
P = 535 psia	1233	5,090	478.21	0.42	477.79	473.98	474.25	4.29
Pool	1303	2,190	476.66	0.18	476.48	473.99	474.27	2.96
	1336	492	474.43	0.04	474.39	474.02	474.22	0.92
	1403	91	473.58	0.01	473.57	474.01	474.15	0.18
	1430	0	473.37	0	473.37	473.99	474.12	0

Date Run No.	Time	q/A Btu/hr-ft^2[a]	Temperatures - ^oF Avg T_i	ΔT Wall	Avg T_o	T_s	T_B	$T_o - T_{sat}$
10-22-64	1325	101,500	564.79	14.00	550.79	545.85	545.95	4.9
	1355	38,560	555.36	5.32	550.04	545.90	545.92	4.2
HM2-6	1418	10,960	550.01	1.51	548.50	545.89	545.92	2.64
P = 1015 psia	1448	3,410	547.43	0.47	546.96	545.91	545.92	1.10
V = 4.7 ft/sec	1512	1,300	546.49	0.18	546.31	545.91	545.90	0.47
	1530	723	546.17	0.10	546.07	545.89	545.87	0.26
	1550	173	545.94	0.02	545.92	545.90	545.92	0.06
	1605	0	545.84	0	545.84	545.90	545.90	0
10-23-64	1200	102,700	616.18	13.77	602.41	599.88	599.75	2.60
	1230	38,240	607.41	5.13	602.28	599.91	599.75	2.42
HM2-7	1252	11,340	603.26	1.52	601.74	599.91	599.77	1.86
P = 1550 psia	1320	4,430	601.54	0.59	600.95	599.88	599.75	1.09
V = 4.7 ft/sec	1337	1,970	600.70	0.26	600.44	599.86	599.75	0.58
	1350	1,075	600.32	0.14	600.18	599.91	599.72	0.35
	1420	384	600.00	0.05	599.95	599.90	599.75	0.09
	1435	0	599.88	0	599.88	599.90	599.77	0
10-27-64	1200	101,100	497.5	14.53	482.97	473.91	473.96	8.94
	1230	38,120	485.51	5.48	480.03	473.91	473.98	5.95
HM2-8	1252	10,870	478.68	1.56	477.12	473.90	473.96	3.06
P = 535 psia	1320	3,500	475.74	0.50	475.24	473.90	473.96	1.20
V = 4.7 ft/sec	1335	1,730	474.89	0.25	474.64	473.90	473.94	0.60
	1352	586	474.34	0.08	474.26	473.91	473.96	0.20
	1422	0	474.06	0	474.06	473.92	473.96	0
10-28-64	1233	101,300	564.81	13.97	550.84	545.91	545.82	5.0
	1300	37,280	554.95	5.14	549.81	545.90	545.82	3.94
HM2-9	1324	10,000	549.48	1.38	548.10	545.90	545.82	2.23
P = 1015 psia	1345	3,810	547.51	0.52	546.99	545.89	545.82	1.13
V = 4.7 ft/sec	1403	1,560	546.58	0.21	546.37	545.90	545.82	0.50
	1421	352	546.0	0.05	545.95	545.90	545.82	0.08
	1438	0	545.87	0	545.87	545.91	545.82	0
10-29-64	1150	101,200	614.04	13.57	602.47	599.87	599.8	2.60
	1215	37,800	607.2	5.06	602.14	599.92	599.82	2.30
HM2-10	1240	10,220	602.77	1.37	601.40	599.90	599.8	1.60
P = 1550 psia	1257	4,580	601.54	0.61	600.93	599.89	599.8	1.09
V = 4.7 ft/sec	1315	1,770	600.56	0.24	600.32	599.89	599.75	0.53
	1330	431	600.02	0.06	599.96	599.90	599.78	0.14
	1345	0	599.84	0	599.84	599.92	599.8	0

Date Run No.	Time	q/A Btu/hr-ft^2	Temperatures - ^oF Avg T_i	ΔT Wall	Avg T_o	T_s	T_B	$T_o - T_{sat}$
10-31-64	1212	101,300	497.75	14.55	483.20	473.90	473.87	9.15
	1240	39,180	485.79	5.63	480.16	473.90	473.85	6.13
HM2-11	1315	11,360	478.65	1.63	477.02	473.90	473.82	3.02
P = 535 psia	1335	4,070	475.88	0.58	475.30	473.90	473.82	1.30
V = 4.7 ft/sec	1348	1,950	474.94	0.28	474.66	473.90	473.85	0.63
	1405	1,024	474.47	0.15	474.32	473.90	473.82	0.32
	1420	342	474.16	0.05	474.11	473.90	473.84	0.09
	1435	0	474.0	0	474.0	473.90	473.82	0
11-5-64	1010	100,400	567.55	13.85	553.70	545.90	545.6	8.04
	1040	36,090	556.72	4.98	551.74	545.90	545.6	6.08
HM2-15	1100	11,200	551.4	1.54	549.86	545.91	545.6	4.20
P = 1015 psia	1120	4,030	549.0	0.55	548.45	545.89	545.55	2.84
Pool	1143	1,880	547.87	0.26	547.61	545.90	545.5	2.05
	1200	787	547.0	0.11	546.89	545.84	545.38	1.45
	1226	251	546.1	0.03	546.07	545.91	545.42	0.59
	1245	0	545.46	0	545.46	545.91	545.4	0
11-6-64	1208	100,400	618.2	13.46	604.74	599.89	599.75	5.0
	1228	38,620	609.02	5.18	603.84	599.87	599.75	4.10
HM2-16	1245	11,060	604.38	1.48	602.90	599.89	599.75	3.16
P = 1550 psia	1305	3,950	602.58	0.53	602.05	599.90	599.65	2.41
Pool	1330	2,010	601.83	0.27	601.56	599.87	599.58	2.0
	1400	696	600.79	0.09	600.70	599.91	599.6	1.11
	1440	87	599.75	0.01	599.74	599.90	599.58	0.17
	1453	0	599.53	0	599.53	599.88	599.54	0
11-10-64	1126	99,310	501.61	14.27	487.34	473.85	473.7	13.6
	1150	38,050	489.81	5.47	484.34	473.90	473.75	10.6
HM2-17	1220	10,630	481.12	1.53	479.59	473.89	473.7	5.89
P = 535 psia	1250	3,780	478.03	0.54	477.49	473.90	473.65	3.84
Pool	1320	1,560	476.4	0.22	476.18	473.89	473.6	2.58
	1350	458	474.61	0.06	474.55	473.91	473.62	0.93
	1405	69	473.81	0.01	473.80	473.91	473.6	0.20
	1418	0	473.6	0	473.6	473.90	473.6	0
11-11-64	1200	103,400	568.21	14.26	553.95	545.89	545.62	8.24
	1217	38,790	557.68	5.35	552.13	545.89	545.62	6.42
HM2-18	1240	11,080	551.79	1.53	550.26	545.89	545.55	4.62
P = 1015 psia	1306	3,910	549.16	0.54	548.62	545.95	545.48	3.05
	1333	1,710	547.88	0.23	547.65	545.91	545.47	2.09
	1353	604	546.74	0.08	546.66	545.90	545.45	1.12
	1411	163	545.86	0.02	545.84	545.89	545.4	0.35
	1427	0	545.45	0	545.45	545.90	545.36	0

Date Run No.	Time	q/A Btu/hr-ft^2	Temperatures - ^oF Avg T_i	ΔT Wall	Avg T_o	T_s	T_B	$T_o - T_{sat}$
11-12-64	1113	101,500	618.14	13.61	604.53	599.90	599.62	4.81
	1132	35,710	608.61	4.79	603.82	599.90	599.6	4.12
HM2-19	1152	10,850	604.39	1.46	602.93	599.88	599.58	3.25
P = 1550 psia	1215	3,780	602.66	0.51	602.15	599.92	599.56	2.49
Pool	1235	1,660	601.7	0.22	601.48	599.90	599.52	1.86
	1304	399	600.39	0.05	600.34	599.85	599.42	0.82
	1330	0	599.52	0	599.52	599.92	599.42	0
11-13-64	1200	99,070	501.49	14.23	487.26	473.90	473.57	13.5
	1225	36,780	489.37	5.28	484.09	473.95	473.6	10.3
HM2-20	1258	10,280	481.06	1.47	479.59	473.90	473.58	5.80
P = 535 psia	1325	3,690	478.1	0.53	477.57	473.90	473.48	3.88
Pool	1352	1,760	476.71	0.25	476.46	473.90	473.48	2.77
	1413	441	474.49	0.06	474.43	473.88	473.42	0.80
	1435	0	473.63	0	473.63	473.93	473.42	0
8-17-64	1142	97,270	502.24	13.72	488.52	473.63	474.10	15.6
	1243	93,430	501.1	13.17	487.93	473.63	474.10	15.0
VM-3	1317	37,830	486.81	5.33	481.48	473.62	473.96	8.64
P = 535 psia	1351	12,140	478.45	1.71	476.74	473.6	473.82	3.86
V = 4.7 ft/sec	1415	2,800	474.36	0.39	473.97	473.56	473.72	1.17
	1434	1,053	473.43	0.14	473.29	473.61	473.65	0.44
Bottom TC	1452	440	473.05	0.06	472.99	473.62	473.60	0.15
Position	1508	73	472.86	0.01	472.85	473.62	473.67	-
	1528	0	472.85	0	472.85	473.61	473.70	0
	1142	97,270	500.86	13.72	487.14	473.63	474.10	14.1
VM-3	1243	93,430	499.77	13.17	486.60	473.63	474.10	13.6
	1317	37,830	486.32	5.33	480.99	473.62	473.96	7.97
Center TC	1351	12,140	478.56	1.71	476.85	473.6	473.82	3.79
Position	1415	2,800	474.55	0.39	474.16	473.56	473.72	1.19
	1434	1,053	473.61	0.14	473.47	473.61	473.65	0.45
	1452	440	473.17	0.06	473.11	473.62	473.60	0.10
	1508	73	473.02	0.01	473.01	473.62	473.67	-
	1528	0	473.02	0	473.02	473.61	473.70	0
	1142	97,270	499.75	13.72	486.03	473.63	474.10	13.1
VM-3	1243	93,430	498.62	13.17	485.45	473.63	474.10	12.6
	1317	37,830	485.87	5.33	480.54	473.62	473.96	7.58
Top TC	1351	12,140	478.45	1.71	476.74	473.6	473.82	3.80
Position	1415	2,800	474.44	0.39	474.05	473.56	473.72	1.19
	1434	1,053	473.46	0.14	473.32	473.61	473.65	0.41
	1452	440	473.06	0.06	473.0	473.62	473.60	0.1
	1508	73	472.91	0.01	472.9	473.62	473.67	-
	1528	0	472.91	0	472.91	473.61	473.70	0

Date Run No.	Time	q/A Btu/hr-ft^2	Temperatures - ^oF Avg T_i	ΔT Wall	Avg T_o	T_s	T_B	$T_o - T_{sat}$
8-18-64	1041	104,200	570.27	14.10	556.17	545.95	543.85	11.2
	1124	101,700	569.69	13.76	555.93	545.86	544.0	11.1
VM-4	1202	38,650	557.06	5.23	551.83	545.87	543.97	7.0
P = 1015 psia	1230	11,260	550.05	1.52	548.53	545.88	543.48	3.67
V = 4.7 ft/sec	1300	2,710	546.32	0.36	545.96	545.87	543.50	1.11
	1327	1,220	545.59	0.16	545.43	545.88	543.76	0.57
Bottom TC	1346	623	545.21	0.08	545.13	545.86	543.78	0.29
Position	1402	208	544.91	0.03	544.88	545.87	543.50	0.03
	1422	0	544.86	0	544.86	545.88	543.92	0
	1041	104,200	569.15	14.10	555.05	545.95	543.85	9.9
VM-4	1124	101,700	568.71	13.76	554.95	545.86	544.0	9.9
	1202	38,650	556.41	5.23	551.18	545.87	543.97	6.14
Center TC	1230	11,260	550.13	1.52	548.61	545.88	543.48	3.56
Position	1300	2,710	546.55	0.36	546.19	545.87	543.50	1.15
	1327	1,220	545.8	0.16	545.64	545.88	543.76	0.59
	1346	623	545.4	0.08	545.32	545.86	543.78	0.29
	1402	208	545.12	0.03	545.09	545.87	543.50	0.05
	1422	0	545.05	0	545.05	545.88	543.92	0
	1041	104,200	567.85	14.10	553.75	545.95	543.85	8.8
VM-4	1124	101,700	567.17	13.76	553.41	545.86	544.0	8.5
	1202	38,650	555.41	5.23	550.18	545.87	543.97	5.3
Top TC	1230	11,260	549.42	1.52	547.90	545.88	543.48	3.0
Position	1300	2,710	546.31	0.36	545.95	545.87	543.50	1.06
	1327	1,220	545.62	0.16	545.46	545.88	543.76	0.56
	1346	623	545.22	0.08	545.14	545.86	543.78	0.26
	1402	208	544.96	0.03	544.93	545.87	543.50	0.04
	1422	0	544.9	0	544.90	545.88	543.92	0
8-19-64	1140	105,500	622.74	13.88	608.86	599.91	596.67	9.84
	1223	101,900	621.93	13.40	608.53	599.90	596.62	9.52
VM-5	1257	38,940	609.92	5.12	604.80	599.89	596.57	5.80
P = 1550 psia	1334	10,870	603.5	1.43	602.07	599.87	596.35	3.10
V = 4.7 ft/sec	1400	2,890	600.61	0.38	600.23	599.87	596.35	1.25
	1433	1,440	599.84	0.19	599.65	599.88	596.35	0.66
Bottom TC	1455	569	599.44	0.07	599.37	599.88	596.25	0.38
Position	1514	161	599.07	0.02	599.05	599.86	596.22	0.08
	1532	0	598.98	0	598.98	599.87	596.22	0

Date Run No.	Time	q/A Btu/hr-ft^2	Temperatures - ^oF Avg T_i	ΔT Wall	Avg T_o	T_s	T_B	$T_o - T_{sat}$
	1140	105,500	622.8	13.88	608.92	599.91	596.67	9.7
VM-5	1223	101,900	622.06	13.40	608.66	599.90	596.62	9.4
	1257	38,940	610.08	5.12	604.96	599.89	596.57	5.8
Center TC	1334	10,870	603.57	1.43	602.14	599.87	596.35	2.97
Position	1400	2,890	600.85	0.38	600.47	599.87	596.35	1.30
	1433	1,440	599.99	0.19	599.80	599.88	596.35	0.62
	1455	569	599.56	0.07	599.49	599.88	596.25	0.31
	1514	161	599.25	0.02	599.23	599.86	596.22	0.07
	1532	0	599.17	0	599.17	599.87	596.22	0
	1140	105,500	620.69	13.88	606.81	599.91	596.67	7.7
VM-5	1223	101,900	619.88	13.40	606.48	599.90	596.62	7.4
	1257	38,940	609.21	5.12	604.09	599.89	596.57	5.0
Top TC	1334	10,870	603.21	1.43	601.78	599.87	596.35	2.72
Position	1400	2,890	600.63	0.38	600.25	599.87	596.35	1.20
	1433	1,440	599.82	0.19	599.63	599.88	596.35	0.56
	1455	569	599.39	0.07	599.32	599.88	596.25	0.25
	1514	161	599.11	0.02	599.09	599.86	596.22	0.04
	1532	0	599.06	0	599.06	599.87	596.22	0
8-21-64	1235	97,500	502.97	13.75	489.22	473.61	472.8	16.3
VM-6	1310	38,520	487.04	5.43	481.61	473.63	472.72	8.7
P = 535 psia	1340	10,810	478.14	1.52	476.62	473.57	472.92	3.7
V = 4.7 ft/sec	1414	2,650	474.26	0.37	473.89	473.57	472.87	1.03
	1437	1,330	473.58	0.19	473.39	473.62	472.72	0.48
Bottom TC	1459	432	473.07	0.06	473.01	473.60	472.8	0.12
Position	1520	0	472.92	0	472.92	473.63	472.9	0
	1235	97,500	503.08	13.75	489.33	473.61	472.8	16.3
VM-6	1310	38,520	487.19	5.43	481.76	473.63	472.72	8.6
	1340	10,810	478.32	1.52	476.80	473.57	472.92	3.8
Center TC	1414	2,650	474.46	0.37	474.09	473.57	472.87	1.1
Position	1437	1,330	473.70	0.19	473.51	473.62	472.72	0.47
	1459	432	473.16	0.06	473.10	473.60	472.8	0.08
	1520	0	473.05	0	473.05	473.63	472.9	0
	1235	97,500	501.46	13.75	487.71	473.61	472.8	14.8
VM-6	1310	38,520	486.44	5.43	481.01	473.63	472.72	8.1
	1340	10,810	477.99	1.52	476.47	473.57	472.92	3.6
Top TC	1414	2,650	474.27	0.37	473.90	473.57	472.87	1.02
Position	1437	1,330	473.58	0.19	473.39	473.62	472.72	0.48
	1459	432	473.04	0.06	472.98	473.60	472.8	0.07
	1520	0	472.94	0	472.94	473.63	472.9	0

Date Run No.	Time	q/A Btu/hr-ft^2	Temperatures - ^oF Avg T_i	 ΔT Wall	 Avg T_o	 T_s	 T_B	 $T_o - T_{sat}$
8-24-64	1311	100,400	571.5	13.60	557.9	545.82	546.25	13.3
	1353	38,800	557.7	5.25	552.54	545.8	546.25	7.84
VM-7	1425	11,300	549.95	1.53	548.42	545.8	545.85	3.72
P = 1015 psia	1457	2,840	546.39	0.38	546.01	545.81	545.75	1.30
V = 4.7 ft/sec	1520	1,580	545.73	0.21	545.52	545.81	545.7	0.81
Bottom TC	1537	556	545.09	0.07	545.06	545.81	545.6	0.35
Position	1600	0	544.7	0	544.7	545.8	545.55	0
	1311	100,400	571.6	13.60	558.0	545.82	546.25	13.1
VM-7	1353	38,800	557.8	5.25	552.55	545.8	546.25	7.68
	1425	11,300	550.13	1.53	548.6	545.8	545.85	3.73
Center TC	1457	2,840	546.59	0.38	546.21	545.81	545.75	1.33
Position	1520	1,580	545.91	0.21	545.7	545.81	545.7	0.82
	1537	556	545.23	0.07	545.2	545.81	545.6	0.32
	1600	0	544.87	0	544.87	545.8	545.55	0
	1311	100,400	568.78	13.60	555.18	545.82	546.25	10.4
VM-7	1353	38,800	556.5	5.25	551.25	545.8	546.25	6.5
	1425	11,300	549.6	1.53	548.07	545.8	545.85	3.33
Top TC	1457	2,840	546.3	0.38	545.92	545.81	545.75	1.17
Position	1520	1,580	545.65	0.21	545.44	545.81	545.7	0.69
	1537	556	545.03	0.07	544.96	545.81	545.6	0.21
	1600	0	544.74	0	544.74	545.8	545.55	0
8-25-64	1440	101,600	622.78	13.37	609.41	599.89	599.90	10.3
	1510	40,500	610.57	5.33	605.24	599.92	599.90	6.1
VM-8	1535	11,700	603.80	1.54	602.26	599.92	600.05	3.1
P = 1550 psia	1606	3,020	600.81	0.40	600.41	599.90	600.34	1.28
V = 4.7 ft/sec	1625	1,670	600.07	0.22	599.85	599.92	600.36	0.70
Bottom TC	1645	607	599.48	0.08	599.40	599.92	600.25	0.25
Position	1705	0	599.11	0	599.11	599.88	600.30	0
	1440	101,600	623.02	13.37	609.65	599.89	599.90	10.3
VM-8	1510	40,500	610.78	5.33	605.45	599.92	599.90	6.14
	1535	11,700	603.70	1.54	602.16	599.92	600.05	2.85
Center TC	1606	3,020	601.0	0.40	600.60	599.90	600.34	1.31
Position	1625	1,670	600.22	0.22	600.0	599.92	600.36	0.69
	1645	607	599.62	0.08	599.54	599.92	600.25	0.23
	1705	0	599.27	0	599.24	599.88	600.30	0

Date Run No.	Time	q/A Btu/hr-ft^2	Temperatures - ^oF Avg T_i	ΔT Wall	Avg T_o	T_s	T_B	$T_o - T_{sat}$
	1440	101,600	621.61	13.37	608.24	599.89	599.90	9.0
VM-8	1510	40,500	609.98	5.33	604.65	599.92	599.90	5.4
	1535	11,700	603.41	1.54	601.87	599.92	600.05	2.63
Top TC	1606	3,020	600.79	0.40	600.39	599.90	600.34	1.17
Position	1625	1,670	600.02	0.22	599.80	599.92	600.36	0.56
	1645	607	599.56	0.08	599.48	599.92	600.25	0.24
	1705	0	599.20	0	599.20	599.88	600.30	0
8-27-64	1303	102,500	508.73	14.46	494.27	473.56	473.52	21.3
	1355	39,130	490.36	5.52	484.84	473.57	473.67	11.9
VM-9	1437	11,840	481.05	1.67	479.38	473.57	473.70	6.41
P = 535 psia	1505	2,810	476.14	0.40	475.74	473.59	473.72	2.75
Pool	1528	931	474.77	0.13	474.64	473.60	473.67	1.64
Bottom TC	1550	473	474.57	0.07	474.50	473.60	473.65	1.50
Position	1607	0	473.01	0	473.01	473.61	473.60	0
	1303	102,500	507.52	14.46	493.06	473.56	473.52	20.0
VM-9	1355	39,130	489.97	5.52	484.45	473.57	473.67	11.3
	1437	11,840	481.03	1.67	479.36	473.57	473.70	6.24
Center TC	1505	2,810	476.47	0.40	476.07	473.59	473.72	2.93
Position	1528	931	475.02	0.13	474.89	473.60	473.67	1.74
	1550	473	474.61	0.07	474.54	473.60	473.65	1.39
	1607	0	473.16	0	473.16	473.61	473.60	0
	1303	102,500	503.22	14.46	488.76	473.56	473.52	15.8
VM-9	1355	39,130	488.17	5.52	482.65	473.57	473.67	9.63
	1437	11,840	480.25	1.67	478.58	473.57	473.70	5.56
Top TC	1505	2,810	476.05	0.40	475.65	473.59	473.72	2.56
Position	1528	931	474.77	0.13	474.64	473.60	473.67	1.59
	1550	473	474.35	0.07	474.28	473.60	473.65	1.23
	1607	0	473.06	0	473.06	473.61	473.60	0
8-28-64	1355	104,900	573.66	14.20	559.46	545.84		14.5
	1430	39,110	558.40	5.29	553.11	545.89		8.06
VM-10	1500	11,760	550.93	1.59	549.34	545.90		4.28
P = 1015 psia	1530	3,090	547.43	0.42	547.01	545.96		1.89
Pool	1550	1,510	546.62	0.20	546.42	545.87		1.39
Bottom TC	1607	548	546.15	0.07	546.08	545.89		1.03
Position	1620	0	545.06	0	545.06	545.90		0

Date Run No.	Time	q/A Btu/hr-ft^2	Temperatures - ^oF Avg T_i	ΔT Wall	Avg T_o	T_s	T_B	$T_o - T_{sat}$
	1355	104,900	573.41	14.20	559.21	545.84		14.0
VM-10	1430	39,110	557.91	5.29	552.62	545.89		7.35
	1500	11,760	551.12	1.59	549.53	545.90		4.25
Center TC	1530	3,090	547.57	0.42	547.15	545.96		1.87
Position	1550	1,510	546.78	0.20	546.58	545.87		1.33
	1607	548	546.30	0.07	546.23	545.89		0.96
	1620	0	545.28	0	545.28	545.90		0
	1355	104,900	570.42	14.20	556.22	545.84		11.1
VM-10	1430	39,110	556.54	5.29	551.25	545.89		6.09
	1500	11,760	550.74	1.59	549.15	545.90		3.98
Top TC	1530	3,090	547.49	0.42	547.07	545.96		1.84
Position	1550	1,510	546.62	0.20	546.42	545.87		1.25
	1607	548	546.12	0.07	546.05	545.89		0.89
	1620	0	545.17	0	545.17	545.90		0
8-31-64	1433	106,000	623.57	13.95	609.62	599.90		10.5
	1510	40,500	610.59	5.33	605.26	599.97		6.08
VM-11	1537	11,280	603.74	1.48	602.26	599.90		3.15
P = 1550 psia	1607	2,980	600.96	0.39	600.57	599.90		1.46
Pool	1620	2,060	600.58	0.27	600.31	599.91		1.19
Bottom TC	1632	617	599.93	0.08	599.85	599.90		0.74
Position	1645	0	599.11	0	599.11	599.90		0
	1433	106,000	623.60	13.95	609.65	599.90		10.2
VM-11	1510	40,500	610.53	5.33	605.20	599.97		5.77
	1537	11,280	603.90	1.48	602.42	599.90		3.06
Center TC	1607	2,980	601.17	0.39	600.78	599.90		1.34
Position	1620	2,060	600.76	0.27	600.49	599.91		1.12
	1632	617	600.11	0.08	600.03	599.90		0.67
	1645	0	599.36	0	599.36	599.90		0
	1433	106,000	621.71	13.95	607.76	599.90		8.39
VM-11	1510	40,500	609.27	5.33	603.94	599.97		4.55
	1537	11,280	603.47	1.48	601.99	599.90		2.71
Top TC	1607	2,980	600.98	0.39	600.59	599.90		1.31
Position	1620	2,060	600.55	0.27	600.28	599.91		0.99
	1632	617	599.93	0.08	599.85	599.90		0.57
	1645	0	599.28	0	599.28	599.90		0

Date Run No.	Time	q/A Btu/hr-ft^2	Temperatures - ^oF Avg T_i	ΔT Wall	Avg T_o	T_s	T_B	$T_o - T_{sat}$
9-1-64	1115	106,600	573.93	14.43	559.50	545.80		14.1
	1151	39,500	558.52	5.35	553.17	545.89		8.05
VM-12	1223	10,890	550.53	1.47	549.06	545.85		3.98
P = 1015 psia	1255	3,110	547.29	0.42	546.87	545.82		1.82
Pool	1315	1,730	546.71	0.23	546.58	545.89		1.46
Bottom TC	1330	613	546.14	0.08	546.06	545.89		0.94
Position	1350	0	545.06	0	545.06	545.83		0
	1115	106,600	573.44	14.43	559.01	545.80		13.8
VM-12	1151	39,500	558.21	5.35	552.86	545.89		7.53
	1223	10,890	550.84	1.47	549.37	545.85		4.08
Center TC	1255	3,110	547.51	0.42	547.09	545.82		1.83
Position	1315	1,730	546.90	0.23	546.67	545.89		1.34
	1330	613	546.28	0.08	546.20	545.89		0.87
	1350	0	545.27	0	545.27	545.83		0
	1115	106,600	570.57	14.43	556.14	545.80		11.0
VM-12	1151	39,500	556.75	5.35	551.40	545.89		6.17
	1223	10,890	550.44	1.47	548.97	545.85		3.78
Top TC	1255	3,110	547.38	0.42	546.96	545.82		1.80
Position	1315	1,730	546.73	0.23	546.50	545.89		1.27
	1330	613	546.12	0.08	546.04	545.89		0.81
	1350	0	545.17	0	545.17	545.83		0
9-3-64	1145	102,600	507.07	14.46	492.61	473.53		19.6
	1225	38,980	490.99	5.50	485.49	473.65		12.4
VM-13	1300	11,050	480.52	1.56	478.96	473.58		5.95
P = 535 psia	1345	2,730	476.26	0.38	475.88	473.59		2.86
Pool	1415	1,200	475.35	0.17	475.18	473.61		2.14
Bottom TC	1437	508	474.69	0.07	474.62	473.58		1.61
Position	1453	0	473.05	0	473.05	473.62		0
	1145	102,600	505.87	14.46	491.35	473.53		18.2
VM-13	1225	38,980	490.58	5.50	485.08	473.65		11.9
	1300	11,050	480.77	1.56	479.21	473.58		6.06
Center TC	1345	2,730	476.57	0.38	476.19	473.59		3.03
Position	1415	1,200	475.45	0.17	475.28	473.61		2.10
	1437	508	474.76	0.07	474.69	473.58		1.54
	1453	0	473.19	0	473.19	473.62		0

Date Run No.	Time	q/A Btu/hr-ft^2	Temperatures - ^oF Avg T_i	ΔT Wall	Avg T_o	T_s	T_B	$T_o - T_{sat}$
	1145	102,600	501.94	14.46	487.48	473.53		14.5
VM-13	1225	38,980	488.50	5.50	483.0	473.65		9.86
	1300	11,050	479.87	1.56	478.31	473.58		5.24
Top TC	1345	2,730	476.07	0.38	475.69	473.59		2.61
Position	1415	1,200	475.09	0.17	474.92	473.61		1.82
	1437	508	474.46	0.07	474.39	473.58		1.32
	1453	0	473.11	0	473.11	473.62		0

BIBLIOGRAPHY

1. Clark, J. A., Merte, H., Lady, E. R., Vander Veen, J., and Yang, W. J., Low Heat-Flux Boiling, University of Michigan ORA Report 04653-1-P, Ann Arbor, 1962.

2. Clark, J. A., Merte, H., Lady, E. R., Vander Veen, J., and Yang, W. J., Low Heat-Flux Boiling, University of Michigan ORA Report 04653-2-P, Ann Arbor, April, 1962.

3. Bankoff, S. G., "Ebullition from Solid Surfaces in the Absence of a Pre-Existing Gaseous Phase," Heat Transfer and Fluid Mechanics Institute, Stanford University Press, 1956.

4. Fisher, J. C., "Fracture of Liquids," Journal of Applied Physics, Vol. 19, No. 11, November, 1948.

5. Mead, B. R., Romie, F. E., and Guibert, A. G., "Liquid Superheat and Boiling Heat Transfer," Heat Transfer and Fluid Mechanics Institute, Stanford University Press, 1951.

6. Corty, C., Faust, A. S., "Surface Variable in Nucleate Boiling," Chemical Engineering Progress, Symposium Series, 51(1955).

7. Griffith, P., Wallis, J. D., "The Role of Surface Condition in Nucleate Boiling," Chemical Engineering Progress, Symposium Series, 56 (1960).

8. Lady, E. R., Low Heat Flux Boiling, PhD Thesis, University of Michigan, Ann Arbor, Michigan, 1963.

9. Clark, H. B., Strenge, P. S., Westwater, J. W., "Active Sites for Nucleate Boiling," Chemical Engineering Progress, Symposium Series, 55 (1959).

10. Jakob, M., "Local Temperature Differences as Occurring in Evaporation, Condensation and Catalytic Reaction," Temperature, Its Measurement and Control in Science and Industry, Reinhold Publishing Corp., New York, 1941.

11. Nishikawa, K., et al., "Heat Transfer in Nucleate Boiling," Mem. Fac. Eng., Kyushu University, 15 (1955) and 16 (1956).

12. Kurihara, H. M., and Meyers, J. E., "Fundamental Factors Affecting Boiling Coefficients," AIChE Journal, 6, No. 1 83 (1960).

13. Gaertner, R. F., and Westwater, J. W., "Population of Active Sites in Nucleate Boiling Heat Transfer," Chemical Engineering Progress, Symposium Series, 56 (1960).

14. Gaertner, R. F., "Distribution of Active Sites in the Nucleate Boiling of Liquids," Chemical Engineering Progress, Symposium Series, 59 (1963).

15. Rohsenow, W. M., and Clark, J. A., "A Study of the Mechanism of Boiling Heat Transfer," Trans. ASME, 73 (1951).

16. Jakob, M., Heat Transfer, Vol. I, John Wiley and Sons, New York, 1949.

17. Chang, Y. P. and Snyder, N. W., "Heat Transfer in Saturated Boiling," Chemical Engineering Progress, Symposium Series, 56 (1960).

18. Gunther, F. C. and Kreith, F., "Photographic Study of Bubble Formation in Heat Transfer to Subcooled Water," Heat Transfer and Fluid Mechanics Institute, Stanford University Press, 1949.

19. Moore, F. D. and Mesler, R. B., "The Measurement of Rapid Surface Temperature Fluctuations During Nucleate Boiling of Water," AIChE Journal, 7, 620 (1961).

20. Rallis, C. J., Greenland, R. V., Kok, A., S. African Mech. Eng., 10, 171 (1961).

21. Cichelli, M. T. and Bonilla, C. F., "Heat Transfer to Boiling Liquids under Pressure," Trans. AIChE, Vol. 41 (1945).

22. Insinger, T. H., Jr. and Bliss, H., "Transmission of Heat to Boiling Liquids," Trans. AIChE, Vol. 36 (1940).

23. Clark, J. A. and Rohsenow, W. M., "Local Boiling Heat Transfer to Water at Low Reynolds Numbers and High Pressures," Trans. ASME, Vol. 76 (1954).

24. Rohsenow, W. M., "Heat Transfer Associated with Nucleate Boiling," Heat Transfer and Fluid Mechanics Institute, Stanford University Press. (1953).

25. Jakob, M. and Fritz, W., Forschung a. d. Geb. d. Ingenieurwes. 2, 1931.

26. McAdams, W. H., Addoms, J. N., Rinaldo, P. M. and Day, R. S., "Heat Transfer from Single Horizontal Wires to Boiling Water," Chemical Engineering Progress, Vol. 44 (1948).

27. Betz Handbook of Industrial Water Conditioning, 5th Ed., Betz Laboratories, Inc.

28. King, W. C., "The Basic Laws and Data of Heat Transmission, Part IV - Evaporation and Condensation," Mechanical Engineering, Vol. 54, 1932.

29. Larsen, R. F., "Factors That Influence Heat Transfer in Boiling," Heat Transfer and Fluid Mechanics Institute, Stanford University Press. (1953).

30. Hamer, Jackson, Thurston, Industrial Water Treatment Practice, Butterworth and Co, London, 1961.

31. Pocock, Fred J., Personal Communication, Babcock and Wilcox Co., Research Division, Alliance, Ohio.

32. Kreith, F., Principles of Heat Transfer, International Textbook Co., Scranton

33. McAdams, W. H., Heat Transmission, 3rd Ed. McGraw-Hill Book Co., New York (1953).

34. Bankoff, S. G., "The Prediction of Surface Temperatures at Incipient Boiling," Chemical Engineering Progress, Symposium Series, No. 29, Vol. 55 (1959).

35. Addoms, J. N., ScD. Thesis, M.I.T., Cambridge (1948).

36. McAdams, W. H., Kennel, W. E., Minden, C. S., Carl, R., Picornell, P. M., and Dew, J., "Heat Transfer at High Rates to Water With Surface Boiling," Industrial and Engineering Chemistry, Vol. 41 (1949).

37. Cryder, D. S. and Finalbargo, A. C., "Heat Transmission from Metal Surfaces to Boiling Liquids: Effect of Temperature of the Liquid on the Liquid Film Coefficient," Trans. AIChE, Vol. 33 (1937).

38. Farber, E. A., and Scorah, R. L., "Heat Transfer to Water Boiling Under Pressure," Trans. ASME, Vol. 70, 1948.

39. Engelberg-Forster, K. and Greif, R., "Heat Transfer to a Boiling Liquid-Mechanism and Correlations," Journal of Heat Transfer, Trans. ASME, Series C, Vol. 81, 1959.

40. Roeser, W. F., "Thermoelectric Thermometry," National Bureau of Standards Handbook 77 - Vol. II (1961).

41. Roeser, W. F. and Lonberger, S. T., "Methods of Testing Thermocouples and Thermoelectric Materials," NBS Circular 590 (1958).

42. Clark, J. A., Merte, H., and Lady, E. R., Low Heat-Flux Boiling, University of Michigan ORA Report 04653-3-P, Ann Arbor, July, 1962.

43. Dahl, A. I., "Stability of Base-Metal Thermocouples in Air from 800 to 2200°F," NBS J. Research, 24 (1940), RP 1278.

44. Shenker, H. et al., "Reference Tables for Thermocouples," NBS Circular 561 (1955).

45. Goldstein, S., "Modern Developments in Fluid Dynamics," Vol. II, pp. 361-2, Oxford University Press, 1957.

46. Larson, R. F. "Factors Affecting Boiling in a Liquid," Industrial and Engineering Chemistry, Vol. 37 (1945).

47. Hyman, S. C., Bonilla, C. F. and Ehrlich, S. W., "Natural-Convection Transfer Processes: 1. Heat Transfer to Liquid Metals and Nonmetals at Horizontal Cylinders," Chemical Engineering Progress, Symposium Series, 49 (1953).

48. Hsu, Y. Y., "On the Size Range of Active Nucleation Cavities on a Heating Surface," ASME Trans., Series C, J. of Heat Transfer 84 (1962).

49. Jakob, M., "Heat Transfer in Evaporation and Condensation - I," Mechanical Engineering, Vol. 58, p. 643, 1936.

50. Clark, J. A., Lady, E. R., Merte, H., Elrod, W. C., Low Heat-Flux Boiling, Univ. of Mich. ORA Report 04653-5P, Ann Arbor, 1963.